Laser and other cleaning procedures for aerospace moulds and a study of mould release agents.

LASER AND OTHER CLEANING PROCEDURES FOR AEROSPACE MOULDS AND A STUDY OF MOULD RELEASE AGENTS

By

Robert E. Litchfield

A PhD Thesis

Submitted in partial fulfilment of the requirements for the award of Doctor of Philosophy at Loughborough University

December 2003

Institute of Polymer Technology and Materials Engineering

Supervisor: Dr.G.W.Critchlow, Institute of Surface Science Technology

ABSTRACT

A selection of cleaning procedures are discussed which may be used to remove epoxide resin flash contamination bonded on metal and carbon fibre reinforced composite mould tooling that is used in the aerospace industry.

Laser ablation, dry ice blasting and chemical cleaning using sodium hydride are three cleaning procedures studied in depth and have been used to treat a range of industrially sourced and model substrates, and contaminants. The effectiveness of the different cleaning regimes have been evaluated using Scanning Electron Microscopy, Atomic Force Microscopy, Auger Electron Spectroscopy, X-ray Photoelectron Spectroscopy and other analytical characterisation techniques.

The necessity to clean aerospace tooling arises when moulded parts cannot be easily released from mould tooling and this is associated with mould release residues that have built up over a number of moulding cycles and eventually cause the moulding to stick. A comprehensive literature review of non-stick coatings is given and alternative mould non-silicone based release coatings are evaluated using the above analytical techniques. Coatings investigated include; fluoroalkylsilane, fluoropolymers and metal-fluoropolymer composites and the problems and merits associated with each are discussed.

Acknowledgements

I would like to take this opportunity to thank all the people who have supported me and helped me in achieving this thesis.

Firstly, I would like to thank my supervisor Dr.G.W.Critchlow for giving me the opportunity to work for this degree. He was always available to help, support and to guide me through any difficulties I faced relating to the thesis.

Secondly I would like to thank Professor D.C.Emmony for finding the time to discuss different aspects of laser cleaning with me and for guiding me through some of the complexities of the subject.

My final thanks go to all the staff and students of the Institute of Surface Science for their support and encouragement during my work and also to the staff of the Institute of Polymer Technology and Materials Engineering, and especially, Mr.John Bates who greatly assisted me in respect of electron microscopy.

LASER AND OTHER CLEANING PROCEDURES FOR AEROSPACE MOULDS AND A STUDY OF MOULD RELEASE AGENTS

Contents

ABBREVIATIONS AND NOMENCLATURE

AES	Auger Electron Spectroscopy
AFM	Atomic Force Microscopy
CFC	Chloro Fluoro Carbon
CRT	Cathode Ray Tube
DSC	Differential Scanning Calorimetry
dp	Degree of polymerisation
EDX	Energy Dispersive X-ray analysis
FEP	Polyfluoroethylene/propylene copolymer
FTIR	Fourier Transform Infrared Spectroscopy
He-Ne	Helium Neon (laser)
Hz	Hertz
IR	Infrared (Spectroscopy)
J	Joules
L	Optical penetration depth
LIBS	Laser Induced Breakdown Spectroscopy
LBU	Laser Based Ultrasound
LDI	Laser Doppler Interferometry
MEK	Methyl Ethyl Ketone
MEMS	Micro-Electromechanical Systems
Nd:YAG	Neodynium:Yttrium Aluminium Garnet (laser)
Pa	Pascal
PDD	2,2,-bistrifluoromethyl – 4,5,-difluoro-1,3-dioxole
PET	Polyethyleneterepthalate
PDMS	Polymethylsiloxane
PFA	Polyfluoroalkoxyalkane
PMNFHS	Polymethylnonafluorohexylsiloxane
PSA	Pressure Sensitive Adhesive
PTFE	Polytetrafluoroethylene
R_a	Surface roughness value – departure of profile from mean
R_t	Surface roughness value – maximum peak to valley height
R_p	Fresnel reflection coefficient
R_s	Fresnel reflection coefficient
RTM	Resin Transfer Moulding (resin)
SAM	Self Assembled Monolayer
SEM	Scanning Electron Microscopy
SIMS	Secondary Ion Mass Spectroscopy
TBT	Tributyl Tin
TEA	Transverse Excited Atmospheric

Teflon AF®	Amorphous PTFE
TEFAL	Trademark – contraction of Teflon and aluminium
TFE	Tetrafluoroethylene
T_g	Glass Transition Temperature
TGA	Thermogravimetric Analysis
TPE	Thermoplastic Elastomer
XPS	X-Ray Photoelectron Spectroscopy

LIST OF FIGURES

LIST OF TABLES

Chapter 1. Introduction

1.1. Aims and outline of work

There are two broad aims of this thesis. Firstly, it seeks to investigate and evaluate mould-cleaning technologies that can quickly and completely remove fully bonded epoxide resin from both metal and composite tooling used in the aerospace industry. The second aim is to investigate and evaluate alternative external mould release agents applicable to such tooling, using a current, widely used release agent as a benchmark standard, and to determine what properties a mould release agent should possess for optimum performance. These two goals are intimately linked since the successful application and subsequent performance of a mould release agent requires that it be applied to a clean moulding surface.

These objectives are also linked by the need to develop solutions that are environmentally benign and so satisfy international legislation that now restricts the use of solvents that are both toxic and harmful to the environment.

Cleaning methods evaluated include: laser cleaning, dry ice blasting and chemical reduction cleaning using sodium hydride in a bath of molten sodium hydroxide.
Alternative fluorinated polymer mould releases and non-stick coatings have been evaluated as replacements for the current silicone based mould release that is used in the aerospace industry. Chronologically, research on mould cleaning technologies was undertaken first and followed by an investigation of mould release agents and it is easier to present the work using this broad division. This research is focussed on the aerospace industry where the practical problems associated with moulding hinder production. Bombardier Aerospace in Belfast have supported this work and supplied many of the materials required.

Bombardier Aerospace is the third largest civil airframe manufacturer in the world with a multi-billion pound annual turnover. Business aircraft and regional airliners make up the majority of this income. At present Bombardier's site in Belfast has facilities for the design, manufacture and support of aircraft fuselages, wing

components, and engine nacelles, for both Bombardier aircraft programs and other aircraft manufacturers. It also specialises in composites, metal bonding, and computer-aided design/manufacture. Composite materials are usually made up from two or more phases that are combined to provide properties that the individual constituents themselves cannot provide. The continuous phase in a composite is referred to as the matrix, while the other phase or phases provide reinforcement.

Metal moulds used to fabricate airframe components have a range of sizes from small tooling perhaps one square metre in total area for an intricate and complex shaped component such as an aircraft door to tooling that may be tens of square metres in surface area, weighing many metric tonnes, for part of an aeroplane fuselage. Mould tooling can be made from a variety of materials such as steel, nickel, or carbon-fibre composite, whose coefficient of thermal expansion is chosen to be compatible with the part to be moulded over the curing cycle to avoid stresses associated with differential expansion. Such tools are very expensive to manufacture. Despite the use of semi-permanent mould release agents, the drive for ever shorter moulding cycle times to reduce production costs can cause moulding residues to accumulate after many production cycles to a level where mould sticking or fouling can occur. Manually intensive rotary abrasive methods are currently used to clean contaminated metal tooling but damage it in the process and incur a significant cost in downtime when the moulding tool cannot be used.

Industrial cleaning processes, in general, concentrate on substrate degreasing and removal of oxide scale or strongly absorbed contaminant layers. Environmental, health and safety legislation are acting as driving forces to develop new cleaning methods. Solvent-based industrial scale cleaning solutions may involve hazardous methylene chloride or methyl ethyl ketone (MEK) and inevitably produce large volumes of toxic waste with requisite disposal problems.

The research undertaken here is differentiated from these cleaning methods because the requirement is to remove fully crosslinked and bonded epoxide resin from metal mould tooling by such means that the substrate tooling is undamaged. To completely remove such contamination quickly implies that an energetic cleaning process is required. The application is particularly challenging because any cleaning method has

to be cost effective and capable of cleaning both small and very large mould tooling. Some acceptable cleaning solutions developed for the metal finishing industry could be applied to small mould tooling examples such as that used to mould the aircraft door already mentioned but would be impractical and uneconomic for much larger aircraft fuselage tooling.

Mould cleaning for rubber tyre moulds dominates the relevant literature with dry ice pellet blasting or laser cleaning being preferred solutions and the latter can be fully automated but can this technology translate to aerospace tooling and would it be viable for composite tooling ? Both techniques are superior cleaning solutions in comparison to mechanical cleaning using abrasive grits.

The capital and running costs associated with fully automated cleaning systems are significant when large surfaces have to be cleaned. Safety in the workplace now places stringent requirements on employers and powerful laser cleaning solutions using invisible beams of infrared radiation such as CO_2 lasers require isolation cells with multiple safety measures to protect staff. Safe enclosures do not add substantial cost to laser systems used for cleaning small parts but escalate dramatically when large surface areas have to be cleaned. Difficulties are encountered in cleaning process automation if the contamination is worse in some areas than others and if the geometry of the tool varies. The ability of a human operative to judge how much effort is required to clean a given area and apply a hand held cleaning tool to that area offers a very substantial cost saving over a computer controlled robotic system. A robot is a poor substitute for an intelligent human operative. A laser less powerful than that of a CO_2 laser, however, would be safer to use and more flexible but this would compromise cleaning speed. In evaluating cleaning options, pragmatism has to be married to the rigour required for an academic research dissertation and this is particularly challenging. Some very diverse topics are discussed and the scope and breadth of the research means that only some topics such as laser cleaning can be explored in detail in the time available. Also it is significant that the existing published literature covering some aspects of the research is very limited.

A systematic research approach might appraise a potential cleaning solution against a range of real aerospace tooling samples, examining areas where mould sticking was

severe, characterising the contamination present and then optimising the cleaning process variables. For a variety of commercial reasons it was only possible to obtain a few examples of contaminated tooling from Bombardier and it was agreed that a "worse case" sample should be prepared and used as a benchmark against which to assess a cleaning technology. For this reason it was decided to use a fully cured epoxide resin as representative of the contamination. This was bonded on steel, nickel and composite substrates. On mould tooling other contaminants such as degraded silicone release agents would also be present but the scenario is not unrealistic since tool cleaning invariably includes the scraping of the tool surface to remove resin flash.

The need to clean a mould in the first place arises because of mould fouling or sticking in which difficulty is experienced in removing a moulded part from the tool after a number of successful moulding cycles. Production imperatives again drive the need to maximise the number of moulding cycles that can be achieved before the moulding tool surface has to be reconditioned and fresh mould release agent applied to the cleaned surface. As with cleaning solvents, environmental legislation now impedes the use of chlorofluorocarbon (CFC) propellants traditionally used for the application of mould release by aerosol spray and the aerospace industry is reviewing the potential for water-based semi-permanent mould releases. Economic and legislative influences thus make it prudent to evaluate different chemistries that show promise of producing surface coatings possessing low surface energy and low coefficients of friction. Research into these and determining the optimum properties required by a mould release constitutes the second part of this research.

Chapter 2. Surface Cleaning Technologies

2.1 Introduction to Cleaning Methods

The cleaning of epoxide resin bonded onto metal and composite surfaces presents a challenging problem for any particular cleaning technique. The cleaning requirements for aerospace mould tooling were introduced earlier and it was identified that a chosen cleaning solution needs to satisfy the following criteria:

(i) capable of removing cured epoxide resin chemically and mechanically bonded to a surface
(ii) produce little or no damage to the substrate
(iii) no volatile and toxic organic solvents used
(iv) rapid cleaning of both small and large surface areas possible
(v) competitive and cost effective solution

Many different cleaning technologies are used in the metal finishing industry and some are appropriate in this application. Since aggressive chemicals would either damage the tooling or pose environmental pollution threats, a review of the literature has identified the following appropriate cleaning technologies:

(i) Laser ablation
(ii) Dry ice pellet blasting
(iii) Dry ice blasting and ultra-violet light
(iv) Cleaning using a fused alkali bath
(v) Ultrasonic cleaning
(vi) Plasma cleaning
(vii) High pressure water jet cleaning

The blasting techniques listed use dry ice and water but other media can be used depending on the application. Plastic media particles can be used dry and accelerated using compressed gas to impact with the surface and remove contamination. Alternatively the plastic media can be dispersed in water to form slurry and this used in a high pressure blasting system.

The first technology, laser ablation, has been studied in detail and its main commercial rival is dry ice blasting. Both have advantages and disadvantages as will

be discussed but one of the disadvantages they both share is that they are line-of-sight cleaning procedures unsuitable for complex shapes with re-entrant angles. The third cleaning solution combines the merits of cryogenic blasting to remove gross contamination with a photonic process, which removes any residual contamination to produce a very clean surface. The fourth cleaning technique uses a molten salt bath and is used for metal finishing of castings. Very few references to this technique occur in the literature. It can also be used to clean complex shaped products such as engine blocks but for practical reasons it would be limited to comparatively small examples of metal mould tooling since these have to be lowered into a treatment bath. The same size restriction is true of ultrasonic cleaning in which parts are immersed in baths containing either aqueous detergent solutions or organic degreasing chemicals. Radio frequency plasma cleaning using oxygen at low pressure can be an effective cleaning technology but traditionally has been extremely slow in comparison to the other cleaning techniques listed. High pressure water jets are often used industrially to decontaminate surfaces such as ships hulls but the large volumes of water used would probably be incompatible with aerospace mould tooling and that production environment.

2.2 Introduction to Laser Cleaning

Lasers were developed in the 1960's, the He-Ne laser being the first laser to emit a continuous beam and the lasing action could be initiated by an electric discharge rather than the intense discharge of photons from a flash lamp.

The light emitted by a laser is remarkable for being coherent. It is composed of regular and continuous waves, like those emitted at much lower frequencies by radio transmitters, and in this respect it differs from the incoherent light emitted by other sources of light such as stars, candle or electric lamps. The development of laser technology has been phenomenal and this growth has accelerated in the last decade spurred by great advances in telecommunication technology. Even for those scientists working in the laser industry, it is almost impossible to keep pace with the technology since its applications permeate into most aspects of everyday life.

High power gas and solid-state lasers are widely used in industry for materials processing applications [1] such as cutting, drilling, welding and marking. The requirements for these applications are very different to those for laser cleaning as discussed in section 2.2.2. Laser cleaning is a specialised laser application, but, in common with all laser interactions with materials, it is a complex process to describe and the present study has to restrict itself to the basic principles involved since laser cleaning is only one of several mould cleaning methods that are discussed.

The greatest growth area for laser technology has been in semiconductor lasers whose output power is generally considerably lower than lasers that have been used for cleaning purposes. Semiconductor based lasers find most frequent application in telecommunications. Only relatively recently are more powerful lasers being constructed using semiconductor materials. At one time lasers were only available that operated at certain output wavelengths but the situation today is such that the user can specify the output wavelength (or frequency) required and be almost certain that a laser type can be found which will operate at the required frequency or can be modified to operate at it by frequency doubling or tripling techniques.

Figure 1. Laser cleaning of stone gargoyle (After Agapaki [7])

The use of lasers for cleaning applications in conservation and art restoration was pioneered by John Asmus in 1972 [2 - 5] and over the last thirty years has become a mature technology and many publications cover the subject in depth [6]. Aspects of laser cleaning for art conservation are also relevant in this work since the removal of lacquers and resins has been studied using different types of laser although the

substrates are invariably non-metallic. Cleaning of stonework by sandblasting on ancient buildings is undesirable as it is destructive and this makes laser cleaning attractive.

Laser cleaning offers the advantage that it is both non-abrasive and dispenses with the need to use aggressive chemicals that damage artefacts. Pulsed lasers are almost exclusively used in this application as the energy supplied to a surface by a very short intense laser pulse cannot dissipate and so blasts off any contaminant layer. Part of the irradiated surface may vaporize and induced stress waves may pulverize the remainder such that it can be suctioned away as a particulate dust and collected in a filtration system. Figure 1 shows the removal of black encrustation from a stone grotesque at Lincoln Cathedral using a Neodynium Yttrium Aluminium Garnet (Nd:YAG) laser.

Laser cleaning has also made an impact in the semiconductor industry and within the last decade has emerged as a viable solution to problems encountered in the manufacture of integrated circuits, where removal of very fine particulate material is required from semiconductor materials and where other cleaning methods are unsuitable [8], [9]. A huge amount of research has been published and continues to be published in these areas [10].

In laser cleaning, size scales up the capital and infrastructure costs disproportionately and in a cost driven production environment, such as the aerospace industry, the economics do not favour a high cost technology over a lower cost solution. In contrast, the market for small portable or robotically controlled laser cleaning systems, particularly in rubber mould manufacture and medium scale industrial cleaning applications is already satisfied by laser manufacturers, and the technology competes with other physical cleaning methods such as dry-ice blasting. The research undertaken in this thesis presents evidence to suggest that laser cleaning can be a viable and competitive solution for large area industrial cleaning also.

The specific requirement to clean large surface areas quickly using a laser simplifies the types of laser that need to be considered. Lasers can be classified according to the type of material used for the active medium and the temporal characteristics of the

output. It was envisaged at the commencement of the present study that carbon dioxide lasers offered the best potential for laser cleaning of aerospace moulds but it was quickly realised that other types of lasers are used for cleaning applications. In total we are concerned with three laser types:

(i) the **Excimer** laser whose output radiation is in the ultraviolet region of the electromagnetic spectrum, typically 248nm;
(ii) the **Nd:YAG** laser whose output is in the near infra-red, typically at 1064nm, and;
(iii) the **Carbon dioxide** laser with output in the far infra-red between 9000nm and 11000nm, typically 10600nm.

When the output of these lasers is pulsed rather than continuous, all three can be used for laser cleaning. The selection of laser type for a particular laser cleaning application depends on the properties of the materials being cleaned. Each of the laser types will be discussed separately in section 2.2.2.

2.2.1 Laser Paint Stripping

The use of lasers for large scale cleaning applications is almost exclusively concerned with the stripping of paint from Airbus and similar size aircraft fuselages and several manufacturing companies have developed laser-cleaning systems. Stripping of paint from aircraft is periodically necessary to allow metallurgical inspection for metal fatigue and is a mandatory safety procedure for passenger carrying aircraft. The literature contains many references to aircraft paint stripping. Three technologies are used: -

(i) Tranverse Excited Atmospheric (TEA) CO_2 pulsed lasers
(ii) Nd:YAG lasers
(iii) High intensity ultra-violet flashlamps

Manz [11] discusses laser ablation using a 2KW TEA CO_2 Pulsed laser that was developed for cleaning the Airbus A320 and states that the system is most efficient at removing layers of paint up to 500 micrometres thickness at rates of up to 8 square

metres per hour (22 square centimetres per second). Capital and infrastructure costs dominate the process. Schulz [12], working with Lufthansa also describes a similar application. At present these systems are bespoke and capital costs upwards of one million pounds are not unrealistic. Tsunemi [13] and, separately, Schweizer [14] describe different 2kW TEA CO_2 pulsed laser systems developed for such paint stripping applications. Powerful multi-kilowatt carbon dioxide laser systems have been built by the United States military and have been applied to the paint stripping of aircraft, achieving reported stripping rates as high as 30 to 60 square metres per hour (83 to 166 square centimetres per second). Walters [15] comprehensively reviews the different laser cleaning technologies and shows how Nd:YAG lasers are also effective for laser cleaning. Patel [16] has also evaluated the use of Nd:YAG laser technology for paint stripping and it has been shown to be effective for removing paint from metal substrates but reported that paint removal from composite structures poses greater difficulties.

Successful paint stripping applications are also claimed for high intensity ultra-violet flash lamps and capital costs for these systems are considerably less than for the laser-based cleaning technologies. Slife [17] describes the successful stripping of Radomes and composites using a combination of xenon flash lamps and dry-ice pellet cleaning. A similar patented ultra-violet flash lamp technology is more fully described by Engelsberg [18]. Removal of paint or other contamination from composites presents special problems particularly for laser cleaning as discussed by Zafiropulos [19].

It is useful to briefly consider how the requirements of this application are satisfied using lasers and then contrast this against the requirements for large scale cleaning of contaminants from mould tooling.

Aircraft bodies are painted to provide protection from corrosion and to add decorative appeal. The paint is applied in layers with the total thickness of the coatings being, typically, several hundred micrometres. The substrate is often metal, though could be a polymer composite material. The paint layers are applied so that the final thickness is uniform over the area painted. The presence of pigmentation in the paint greatly enhances the absorptive properties of the paint for incident laser radiation.

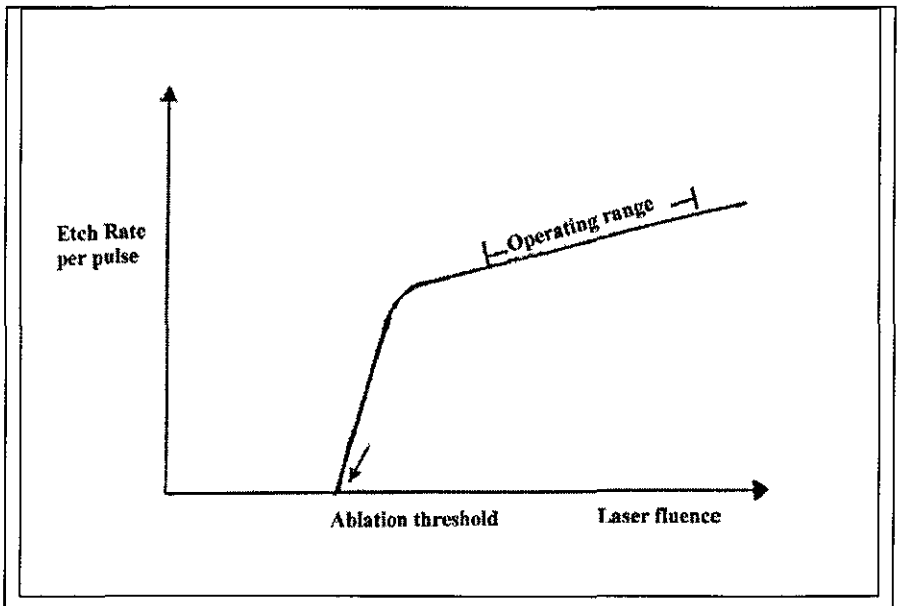

Figure 2. Typical laser ablation curve.

Generally, there will exist a particular threshold radiant energy density (fluence) for any given material below which no laser ablation will occur (figure 2). The threshold fluence is a function of the laser absorption of the material.

Laser stripping requires precise control over thickness of paint that is removed during one or more passes of the laser over the area to be stripped. Lasers with output wavelengths in the ultra-violet region of the electromagnetic spectrum are able to offer ten times the precision at removing distinct paint layers than is possible with laser output wavelengths in the infra-red or far infra-red. Lasers with ultra-violet output wavelengths do not, however, possess high enough fluences to strip hundreds of micrometres of paint covering large areas in a reasonable length of time. These lasers are more suited to medical and electronic laser ablation applications than heavy industrial use though they can be very effectively used in cutting plastics. The power density requirements for large area paint stripping are only satisfied with lasers that operate at infrared wavelengths and precision at removing defined layers of paint is achieved by using very short nanosecond laser pulses of high intensity. In the case of cleaning paint from carbon fibre or Kevlar composite substrates, these materials react to the laser in a similar way to the paint and so process control is difficult though not impossible. Pantelakis *et al* [20] have shown that paint stripping from graphite-epoxide and kevlar-epoxide aerospace composites using excimer lasers also results in significant degradation of flexural strength as measured by four-point bending tests. It

must be remembered though, that the composites concerned in paint stripping are those parts that have been moulded using a tool with the consequence that any degradation of flexural strength becomes serious. The same consideration does not necessarily apply to a composite tool that is used to mould a composite part because the former is not subjected to appreciable loading in a situation where failure would have catastrophic consequences. Some degree of surface damage may be acceptable to the aerospace manufacturer provided it is less than would be obtained using other cleaning technologies and commensurate with that level of damage that occurs as the tool is used and becomes worn.

It is apparent that in such paint stripping applications, the laser ablation process must be carefully controlled and this will significantly reduce cleaning rates to the extent that the laser cleaning technology may not be the most cost effective solution.

The contamination to be removed from large areas of metal mould tooling is invariably non-uniform in thickness and patchy so that some areas are relatively clean whilst others are contaminated. The texture of the contamination may also be variable and it is unlikely to possess any strong pigmentation. Removal of the contamination does not, however, have to be precisely controlled except perhaps where it is present on composite tooling substrates. Because very short duration pulsed lasers are used for cleaning, there is no opportunity for heat to be conducted to a metal substrate and thus the high reflectivity of metals at room temperature tooling substrates means that the process is self-limiting with ablation ceasing once the organic contamination had been removed.

The ablation of epoxide resin coatings bonded to metal substrates is of primary interest in the present study and requires that the optical absorption of epoxide resin be considered as well as that of the metal substrate. The requirement exists that substrate damage must be avoided and so it is necessary to also consider what surface temperatures are likely to be generated during laser ablation. Finally laser ablation generates very high surface pressures which assist in the removal of bonded contamination and it is also necessary to consider these kinetic effects.

2.2.2 Laser ablation processes

Laser ablation is the ejection of material from a surface as a result of intense irradiation. Interactions between lasers and materials are complex, often with several processes occurring together or within a very short period of time. Explanations of these interactions are inevitably simplifications and it is necessary to use assumptions to separate out the multiple dependent variables.

Generally, laser ablation is due to photochemical or thermal processes or a combination of the two. Photochemical processes are dominant where ultra-violet wavelength lasers impinge on materials since these are energetic enough to induce molecular dissociation. Because the products of such dissociation possess a larger specific volume, detonation of the material occurs with a micro-explosion at the point of impact. Where the laser output is in the near or far infrared, a thermal process dominates the ablation since the incident energy is only sufficient to excite molecular vibrational modes, which cause localised heating. Since the laser pulse is very intense and very short, the material can instantaneously vaporise which also gives rise to a micro-explosion. These localised volume explosions generate an acoustic pulse audible as a "snapping sound". These acoustic pulses can be used to monitor the laser ablation process since the amplitude of the pulses decreases as a highly reflecting substrate is approached. Ultrasound can be produced by focussed high power pulsed lasers due to the recoil force exerted by the ejected matter and the high pressure from the rapidly expanding vaporised material. At the very high power densities occurring when a focussed beam is used, the vapour cloud is ionised and forms a plasma. Stratoudaki [21] discusses how this forms the basis of a new non-destructive technique, laser based ultrasound (LBU), for the rapid detection of flaws and defects in carbon fibre reinforced composite components used in the aerospace industry. The technique combines the advantage of a non-contact optical technique with the ability of ultrasonics to detect flaws deep inside thick structures by virtue of the shock waves associated with pulsed lasers [22].

Excimer lasers operating at ultra-violet wavelengths are successful at processing many organic polymers [23] and are effective in laser cleaning but the relatively high absorptivity of metals at ultra-violet wavelengths is a problem where effects on a

metal substrate have to be considered. Excimer gas lasers are also popular in laser eye surgery for correcting myopia (near sightedness). The short ultra-violet wavelength output from these lasers can reshape the cornea by ablating its surface and the ablation rate is an almost linear function of the number of pulses applied for biological tissue. This allows the ablation process to be precisely applied. The term excimer is a contraction of "excited dimmer" and refers to a molecule composed of two identical atoms that exists only in its excited state. A nitrogen laser would be an example of this. Excimer lasers in contrast use exciplexes that are the same as excimers but where the atoms can be different. Examples of excimer lasers are KrF and XeCl. Atoms with high electro-affinity such as fluorine and chlorine readily strip the outer orbital electrons from noble gas atoms (Kr, Xe) to form the excited dimmer.

The excimer laser also finds wide application in plastics processing. In plastics the molecular structures possess absorption bands that match the ultra-violet output of excimer lasers so that coupling is efficient and the materials strongly absorb the incident radiation causing dissociation. The predominant laser interaction mode is thus photochemical in nature. Strong absorption gives rise to heating in a material for long duration laser pulses or pulses that are applied more or less continuously and because the radiation is so readily absorbed, very little penetrates deeper into the surface. The penetration depth of excimer lasers for plastics are typically 1-10 micrometres per pulse and therefore a high pulse repetition frequency is used for plastics processing. In such applications the laser beam is highly focussed and shaped so that the beam profile is optimised for drilling and cutting. Lasers with only moderate power outputs have sufficient energy to drill and cut through plastic materials when used in this way. The requirement for laser cleaning, however, is that the laser beam is greatly defocused to facilitate the cleaning of large surface areas quickly and this means that much higher laser power outputs are required. The output powers of excimer laser are insufficient to satisfy this requirement and this restricts their application to less demanding material processing applications.

The situation would be different if organic material needed to be removed from a composite tooling surface. Cleaning composite tools in the aerospace industry is particularly difficult and much slower cleaning rates are accepted to avoid substrate damage. Given that the requirement for rapid cleaning of large areas is relaxed, more

focussed beams can be used and the ability of excimer lasers to control the amount of material removed quite precisely means that, although absorption coefficients would be similar for both contaminant and composite tooling, the process could be stopped at the resin rich gel coat layer and the laser would have insufficient power per pulse to expose the carbon fibres below. This could be effective in applications where the contaminant layer was uniformly thin and homogeneous, such that the process could be automated and stopped after a fixed number of laser pulses. However, if contamination were patchy and less uniform, then automation would be more difficult. On-line techniques to spectroscopically analyse the ablated material provide a means of controlling the cleaning process. These will be discussed in section 5.3.1.

Laser cleaning of vulcanising residues from rubber tyre moulds is the most commonly encountered commercial application of laser cleaning and it has proved to be successful and competitive and utilizes Nd:YAG laser technology. Robotically controlled solid-state lasers can clean approximately one square metre surface area within an hour (2.8 square centimetres per second) [24]. This is approximately one order of magnitude slower at best than the cleaning rates associated with TEA CO_2 lasers developed for paint stripping (section 2.2.1). However, the capital cost of Nd:YAG lasers is much less than TEA CO_2 lasers.

A recent novel and successful application of laser cleaning utilizing a Nd:YAG laser has been to clean leaves from railway tracks [25]. Although lasers can be used to harden metals by introducing compressive surface stresses, this does not occur under the typical operating conditions used for laser cleaning.

Reflection of wavelengths for Nd:YAG lasers from metal surfaces is greater and their ability to ablate greater depths per pulse is increased compared to the excimer laser. Both types of laser energy can be transmitted using glass fibre optics and this has significant cost advantages in system design since the laser output can be coupled to the cleaning head or gun using a flexible hose which allows a trained operative to scan a tool surface with the laser cleaning head, and recognize where contamination is especially bad, making several passes over that area. Alternatively the laser output is fixed and the work piece is robotically moved but this system could not be used for very large areas and heavy mould tooling.

Standard glass fibres have a damage threshold for high power laser pulses and this limits the pulse width that they can transmit. Typically this is about 60ns for a Nd:YAG laser operating at 1064nm (1.06×10^{-6}m) wavelength whereas the optimum pulse duration for a cleaning application is around 10ns. The introduction of new fibre optic materials is reducing the gap between these two values but it is still significant at the present time. Transmission of the laser energy using fibres degrades the output intensity profile, which is modulated by strong interference between modes excited in the carrying fibres. This has implications in materials processing where precise cutting requires a Gaussian shaped beam profile. For laser cleaning, however, the output intensity requires a "top-hat" shaped profile since uniform intensity over the output beam diameter is required. This can be achieved with Nd:YAG lasers.

The third laser type mentioned was carbon dioxide, which is the workhorse of materials processing and is used to cut and drill metals. Its key properties are that it can produce a very high radiant flux density and operate at high power output levels continuously. Once again the requirements for optimum laser cleaning are very different than those required for metal processing. The output wavelength range is strongly absorbed by glass fibres and so these cannot be used as a wave-guide to couple the laser source to the work piece. For large area surface cleaning, there are significant cost implications not least because gas lasers suitable for cleaning are physically large. Such a laser would have to be accommodated on an overhead gantry and complex optics used to scan a tool surface. Automation would be required and stringent safety protocols implemented.

2.2.3 Interactions of lasers with materials

It is necessary to consider the principal types of interaction that occur when a pulse of laser energy impinges on a target material. Six interaction mechanisms have been identified to date [26]. These are:

(i) photon pressure
(ii) selective vaporisation
(iii) plasma detonation (spallation) evaporation pressure
(iv) shock waves produced by rapid heating and cooling

(v) evaporation pressure

(vi) photochemical (bond breaking)

Photon pressure

This effect is easily demonstrated by holding a thin steel foil at the focus point of a TEA CO_2 laser. When the laser is fired, the recoil of the foil can be felt and the energy is sufficient to deform the metal foil. The effect occurs because such lasers produce a very high flux of photons and although the momentum carried by each photon is tiny, the cumulative effect is noticeable. Stein [27] used the equation

$$p=h/\lambda \quad \ldots\ldots\ldots\ldots\ldots\ldots (1)$$

(where p is the photon pressure, h is Planck's constant and λ is the laser wavelength) to calculate the photon pressure exerted by a 1 KW CO_2 laser focussed to a spot of 0.1 mm diameter and found the photo pressure was 760 $N.m^{-2}$. This is a relatively small pressure though significant in laser cleaning application where sub-micrometre particles need to be removed from semiconductor materials.

Selective vaporisation

According to Asmus [5], the laser cleaning of dark encrusted contaminants from stone or marble artefacts is largely due to selective absorption in which the colour of the contaminant results in stronger absorption relative to the white underlying stone that does not absorb. This selective absorption leads to high, localised temperatures favouring vaporization and the process occurs using laser pulses in the range 1 x 10^{-6}s to 1 x 10^{-3}s and relatively low intensity ($10^3 - 10^5$ $W.cm^{-2}$). Cleaning that makes use of selective vaporization is very slow, however.

Spallation

It has been found that shorter pulses delivered by Q-switched Nd:YAG lasers (section 2.3.6.) induce less substrate heating than that generated by longer laser pulses and offered faster rates of contaminant removal. Here, the pulse duration is between 5 and 20 ns with typical flux densities between $10^7 - 10^{10}$ $W.cm^{-2}$. At these high flux levels surfaces readily absorb sufficient energy to vaporise and high temperatures ($10^4 - 10^5$ K) are created in the vapour that becomes partially ionised (forming a plasma) and

then absorbs the laser energy strongly. The initial surface vaporisation ceases as the target area is now shielded from the laser by the plasma. As the laser pulse continues, the plasma absorbs more energy and high pressures are generated in the range 1-100Kbar (101.3MPa – 10.13GPa). This results in a shock wave that compresses the surface. When the laser pulse ceases, the plasma dissipates and the surface relaxes ejecting a thin surface layer and this process is referred to as spallation. When spallation occurs using short laser pulses the effect is described as plasma detonation.

Shock waves produced by rapid heating and cooling

Spallation is associated with the creation of a plasma but shock waves can be produced that manifest themselves in a cleaning action in the absence of a plasma and this is explained as resulting from very rapid heating and cooling of a surface irradiated by a short laser pulse that is of insufficient fluence to create a plasma.

Evaporation pressure

Where absorption of laser energy at a surface causes vaporisation but is insufficient to generate a plasma the high momentum of the evaporating material will compress air between the vapour and the uncompressed ambient air. This will give rise to a shock front at the air/ambient air interface [28], [29] and an associated recoil wave that will propagate into the surface [30]. Very high pressures can be generated by such a mechanism, which are sufficient to remove organic contaminants.

Photochemical (bond-breaking)

In the photochemical mechanism the laser energy couples directly to the molecular absorption of surface species causing bond scission and in which little or no heating effect occurs. Excimer lasers, already discussed possess this capability by virtue of operating at ultra-violet wavelengths.

Schematically the events occurring when short laser pulses are applied to a target surface is depicted in Figure 3.

Although the synopsis of the principal mechanisms given above describes the current understanding of the processes by which material is removed during laser cleaning, the laser interactions with surfaces are considerably more complex. One or more of

the processes can occur in a very short space of time (nanoseconds) making analysis difficult. Absorption and reflection at surfaces, thermal diffusivity and thermal conductivity are all material properties that influence the type of interaction and rate of removal. Many of these properties are temperature dependent and this adds further complexity. These factors, together with a more detailed explanation of thermomechanical effects, are now presented.

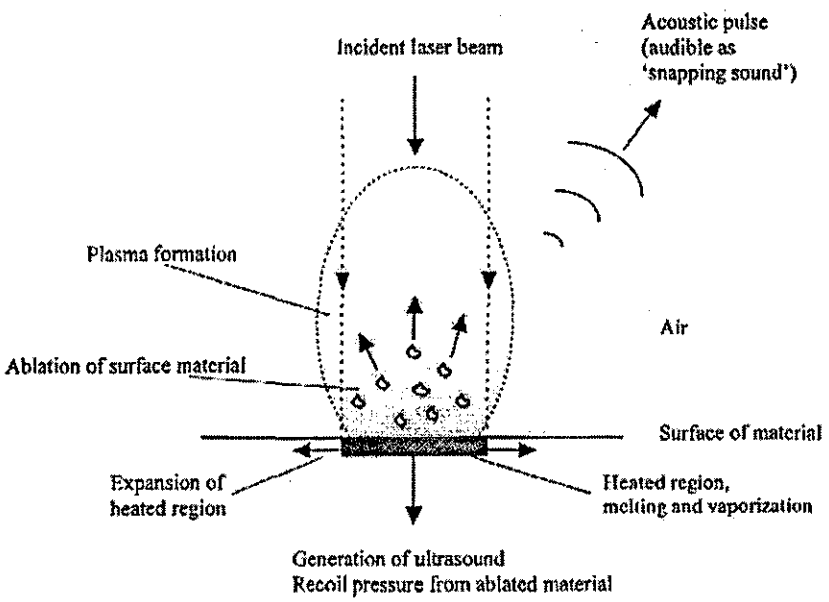

Figure 3. Laser ablation processes. (After Cooper [6]).

2.2.3.1 Refraction, Reflection and Absorption

The refraction of light waves at the surface separating two media of different refractive indices (n_1 and n_2 where $n_2 > n_1$) is expressed by Snell's law for refraction:

$$n_1 \sin i = n_2 \sin r \quad \text{.....(2)}$$

where "i" and "r" are the angles of incidence and refraction for a beam of light.

In order to obtain the amplitudes of the reflected and refracted beams it is necessary to consider the amplitudes of the tangential components of the electric and magnetic fields on the two sides of the boundary. The state of polarization of the beams is thus addressed and any phases changes that occur. Such an analysis results in expressions of the form:

$$A'/A = (n_2 \cos i - n_1 \cos r)/(n_2 \cos i + n_1 \cos r) \ldots.(3)\ [32]$$

where A is the amplitude of the incident beam and A' the amplitude of the reflected beam. And for the refracted beam of amplitude A",

$$A''/A = (2 n_2 \cos i)/(n_2 \cos i + n_1 \cos r) \ldots\ldots\ldots\ldots(4)\ [32]$$

In the present analysis it is the reflectance of surfaces which is of most interest and for normal incidence equation (3) reduces to

$$A'/A = (n_2 - n_1)/(n_2 + n_1) \ldots\ldots\ldots\ldots\ldots\ldots \quad (5)$$

and the reflective power R (proportional to the square of the amplitude) is

$$R = [(n_2 - n_1)/(n_2 + n_1)]^2 \ldots\ldots\ldots\ldots\ldots\ldots\ldots\ldots\ldots\ldots (6)^{[53]}$$

In many cases n_1 is the refractive index of air (approximately equal to unity) so

$$R = [(n_2 - 1)/(n_2 + 1)]^2 \quad \ldots\ldots\ldots\ldots\ldots\ldots\ldots\ldots \quad (7)$$

The equations are only valid really for normal incidence, which simplifies the algebra by removing the angle dependent terms. This would be very limiting for ordinary light but the nature of laser light and the fact that it is highly directional renders the assumption of normal incidence more plausible.

The above equations apply to media that transmit light energy and these are usually insulators such as glass or dielectric coatings. Metals are conductive however, and since radiation is electromagnetic in nature, the conductivity leads to a power loss since energy is absorbed through Joule heating. Because metals have low emissivity, the absorbed heat is not re-radiated which is why shiny metal surfaces such as wrenches can get hot when they are left out in the sun. However, metal surfaces reflect most radiation at optical and infrared wavelengths that are incident on them. Absorption and reflection in such cases occur within a surface layer or skin and which is typically between 5 – 10nm in thickness. In metals, conduction band electrons are present in this skin and free electrons, which oscillate and reradiate energy without disturbing the solid atomic structure, absorb electromagnetic energy. The skin thus

shields the interior of the metal and the skin depth depends on the wavelength of the incident radiation and the electrical conductivity and permeability of the metal. The skin depth δ for a wavelength of 1064nm (Nd:YAG laser output) is approximately 5nm.

The reflectivity of a metal surface is defined not only by refractive index n but also by an extinction coefficient k that takes account of the skin effect. This impedance to the propagation of radiation is defined in terms of a complex refractive index equal to n(1+ik) . Substituting n(1+ik) for n_2 in equation (7) gives:

$$R = [\{(n(1+ik) - 1\}/\{n(n+ik) + 1\}]^2$$

$$= (n^2(1+ik^2) + 1 - 2n)/(n^2(1+ik^2) + 1 + 2n) \ldots\ldots (8)^{[53]}$$

Jenkins and White [197] describe how techniques of ellipsometry (see section 3.8.4) enable values of n and k for a metal to be measured from the phase of reflected radiation.

Metal	Refractive index n (for 589nm wavelength)	Extinction coefficient k	Reflective power %
Steel	2.485	1.381	61.6
Copper	2.120	1.900	67.3
Aluminium	1.44	5.230	90.0
Gold	0.37	7.62	94.1
Silver	0.177	20.554	99.3

Table 1. Reflective power of metals calculated using equation (8) using data published by Jenkins and White [197](ignoring imaginary number i).

It is seen from Table 1, above, that strong absorbance (high values of k) accompanies high reflectance. Steen [27] gives values of n and k for radiation of wavelength 1064nm (the main lasing wavelength for Nd:YAG lasers). For copper n = 0.15 and k = 6.93 giving R = 99% and this trend of reflectance being higher for infra-red and far infrared wavelengths is common to many other metals which has obvious implications when laser cleaning employs such wavelengths. Kaye and Laby [34] have

published experimental values of reflectance for different wavelengths and this allows plots of reflectance against wavelength to be constructed, as shown in figure 4.

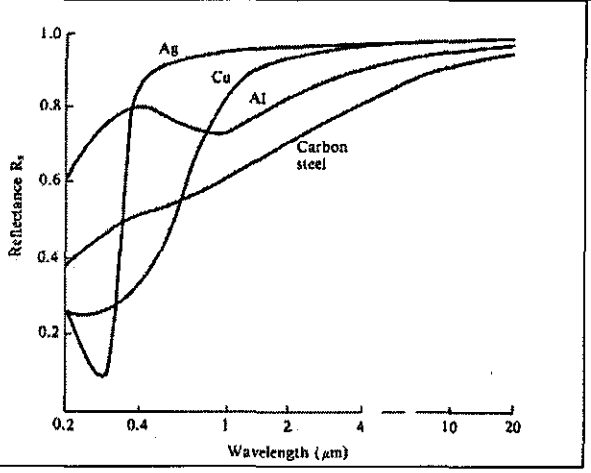

Figure 4. Reflectance of metals as a function of laser wavelength. (After Wilson [33])

Maxwell's equations describing the propagation of electromagnetic radiation can be used to derive an expression for the skin depth δ in nanometres [32]:

$$\delta = (\pi\sigma\mu_r\ \mu_o\ \nu)^{-1/2} \quad \text{.....(9)}$$

where σ and μ_r are the respective conductivity and relative permeability of the metal, μ_o is the permeability of free space and ν the frequency of the incident radiation.
The skin effect contributes greatly to the absorption of electromagnetic radiation incident on metals, as discussed, and since $\nu = c/\lambda$ it can be seen that the absorption is inversely proportional to the square root of the wavelength of the incident radiation. Thus the absorption is less for longer wavelengths than shorter ones.

The effect of surface roughness is to increase the effective surface area over which the incident flux can be absorbed. Surface roughness is usually expressed in terms of the international parameter of roughness, R_a. This is the arithmetic mean of the absolute departures of the roughness profile from the mean line of the profile measured over an assessment length. Another useful parameter is R_t, which is the maximum peak to valley height of the profile in the assessment length.

If the wavelength of the incident radiation (λ) is such that $\lambda >> R_a$ then the effect of the surface roughness will be slight and absorption due to multiple reflections or

interference will not occur [27], and this is generally satisfied for infrared and far infrared wavelengths.

Another important factor is the fact that the reflectivity of metals decreases as an approximately linear function of increasing temperature, as determined by the Drude model [35]. For example, the absorptivity (1-R) may as much as double from a temperature increase of a few hundred degrees or with a change of state from solid to liquid. It is this fact that makes it possible to use lasers for the cutting and drilling of metals. As the temperature of a metal surface rises there will be an increase in the phonon population causing more phonon-electron energy exchanges. Electron interaction with the structure thus increases and the efficiency with which free electrons oscillate and re-radiate incident energy is reduced. If the duration of an applied and focussed laser pulse is great enough or the repetition frequency high enough, a cycle is entered whereby absorption leads to more heating which leads to further absorption and eventually a melt zone is formed which is referred to a "keyhole". When lasers are used for cutting metals, a coaxial assist gas is used to blow out this molten material and allow the laser to cut deeper into the material. Only in the case of copper, silver or gold is the reflectivity sufficiently high enough to cause difficulties for laser cutting. These metals also possess high thermal conductivities and the combination of these properties prevents the establishment of a melt zone.

The skin effect is absent in non-metallic materials and so radiation penetrates deeper into the sample, to a depth of the order of micrometres.

A practical measure of attenuation in insulators and transparent materials is the optical penetration depth (L) which can be defined as the reciprocal of the absorption, i.e. $L = \alpha^{-1}$. The absorption coefficient for a material that absorbs strongly has values in the order of 10^6 cm^{-1} and so the penetration depth is very small (a few nanometres). Conversely a weak absorber has $\alpha \sim 10$ cm^{-1} and so the penetration depth is five orders of magnitude greater than for a strong absorber.

Unlike metals where radiation is absorbed in the skin depth at the surface, absorption in insulators and most semiconductors occurs over the attenuation length, L, which

can be much larger than typical skin depths. In the infrared $L > 10^{-4}$ cm and thus, in many instances, heating must be considered to be a volume effect. This is particularly valid for heating of thin films where L may exceed the film thickness.

Stratoudaki [21] has measured the optical absorption depths for Araldite LY 5052 epoxide resin irradiated using laser pulses from TEA CO_2 and Nd:YAG lasers and found that $\alpha^{-1} \sim 100$ micrometres at 10600nm but is 4mm at 1064nm. Comparable values were also obtained by Roberts [36] so there is good evidence that the removal of epoxide resin coatings on metals using Nd:YAG lasers cannot be due to heating and photothermal vaporization.

2.2.3.2 Heat flow theory

The literature shows [25] that thermal damage to metal surfaces as a consequence of laser cleaning is slight or negligible since by using high energy laser pulses of very short duration the penetration depth of the laser is very small and confined only to the surface layer of the substrate. It is pertinent to discuss some of the underlying heat flow theory.

Considering a block of material of cross-sectional area A, length L and specific heat capacity C that is subjected to a heat flux at one end. The heat is conducted through the material to emerge at the other end of the block. In equilibrium, the heat input is equal to the heat output but the temperature within the block has risen in response to the transfer of heat. If dQ/dt is the power input then from Fourier's first law

$$dQ/dt = KA (T_o - T_1)/L \quad \ldots\ldots\ldots\ldots\ldots\ldots\ldots\ldots\ldots\ldots (10)$$

The thermal conductivity, K, determines the temperature rise $(T_o - T_1)$ in equilibrium in response to dQ/dt. Since $(T_o - T_1)$ is proportional to K^{-1}, a material with a low thermal conductivity exhibits a higher temperature rise than one possessing a larger thermal conductivity, in response to the same dQ/dt.

The energy ΔE stored by a material of mass m that has undergone a temperature rise ΔT is

$$\Delta E = C\, m\, \Delta T \quad \text{.....(11)}$$

If this incremental expression is integrated over the entire sample, then the excess heat stored in the material can be calculated. The magnitudes of C and K determine the rate at which thermal equilibrium is achieved in response to the application of the heat source. For transient thermal effects in particular it is useful to introduce another parameter called the thermal diffusivity, κ, defined as

$$\kappa = K/\rho C \quad \text{.....(12)}$$

κ has the units $cm^{-1}\ s^{-1}$ and ρ is the sample density ($g.cm^{-3}$). For most metals thermal conductivity and diffusivity decrease as an approximately linear function of temperature increase (brass and bronze alloys are exceptions). Specific heat and density are also temperature dependent.

Ready [200] discusses the concept of a thermal time constant representing the time at which the rear surface of a metal plate of thickness D and thermal diffusivity κ reaches a temperature of the same order of magnitude as the front surface where heat is absorbed from an applied laser pulse. The thermal time constant τ is expressed as:

$$\tau = D^2/4\kappa \quad \text{.....(13)}$$

Using this equation Ready calculated the thermal time constants (msec) for plates of different thickness and some values are given in Table 2 below.

Metal	Thickness D 0.125mm	Thickness D 0.625mm	Thickness D 2.5mm
Stainless steel	1.0 msec	25 msec	400 msec
Nickel	0.26 msec	6.5 msec	104 msec

Table 2 .Thermal time constants for selected metals.

The significance of this data is that if the laser pulse length is shorter than the thermal time constant then the laser will not melt through the given sheet thickness. It has to be remembered that the majority of applications for high power lasers are for welding and cutting where it is desirable to form a melt pool on the surface by laser irradiation. To melt thick plates it is necessary to stretch the laser pulse length so that it is as long as possible or to repeat the pulses with a very short time delay between each pulse so that the laser is applied almost continuously. This is easily achieved with CO_2 lasers. In contrast the optimum time duration of Q-switched lasers used for laser cleaning is about 15nsec and it can thus be readily appreciated that the resultant depth of heating is very small.

These simple heat flow equations are limited in their application and a greater degree of mathematical rigour is required to analyse the complex thermodynamics associated with the heat flow arising from laser irradiation of a surface. In the present work it is important to be able to demonstrate that the temperature rise at the surface of a substrate, irradiated under laser cleaning conditions, is not great enough to cause significant thermal damage. In applications where lasers are used for cleaning, the irradiated area is much greater than the depth (z) to which heat is conducted for the duration of the pulse. This simplifies the analysis required so that it is only necessary to consider a one-dimensional linear heat flow for a semi-infinite solid.

This can be expressed by the following differential equation [22]:

$$\partial^2 T(z,t)/\partial z^2 - \partial T/\kappa\, \partial t = -A(z,t)/K \ldots\ldots\ldots (14)$$

where T(z,t) is the temperature distribution for a boundary plane z (initially z=0), A(z,t) is the heat production per unit volume per unit time, κ is the thermal diffusivity and K the thermal conductivity. Here the power density of the laser pulse is assumed to be sufficient to raise the surface temperature of the irradiated material to its vaporisation point in a time shorter than the pulse duration but the latter is great enough to allow the vaporised material to move away from the surface creating a retreating surface boundary.

The solution of this differential equation is discussed by Carslaw and Jaeger [37] in their mathematical treatise on the conduction of heat in solids and also by Stein[27].

In general analytical solutions to these and similar heat flow equations for different models depend on choice of boundary conditions and assumptions made. For the above equation an analytical solution can be found if it is assumed that the thermal properties of the material are independent of temperature, and that the absorbed laser flux is uniformly distributed over the irradiated surface with negligible losses. The solution to the temperature distribution equation then reduces to the following form in which the temperature rise at the surface of the sample (z=0) is defined as

$$T(0,t) = \frac{2F_0(\kappa t)^{1/2}}{\sqrt{\pi}.\,K} \quad \ldots\ldots\ldots\ldots\ldots\ldots\ldots\ldots(15)$$

where $F_0 = \alpha\, I_0$ is the absorbed power density arising from the incident laser intensity I_0 and α is the absorptivity of the surface.

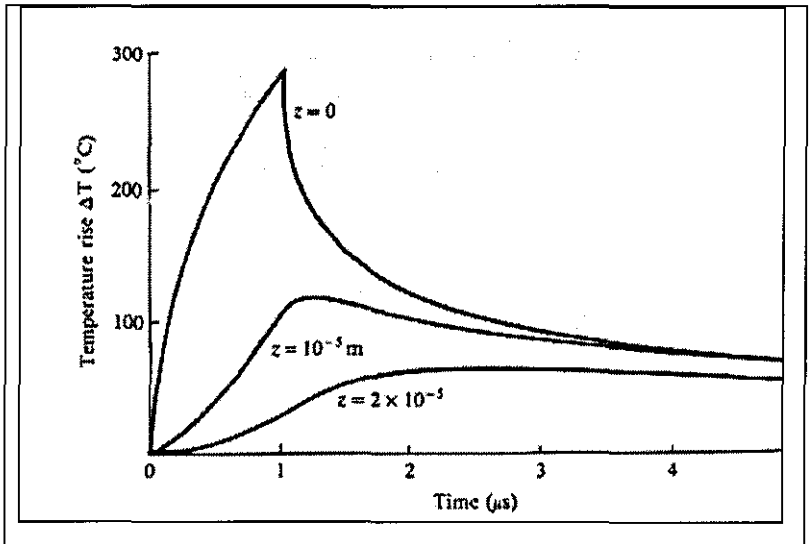

Figure 5. Theoretical surface temperature rise against time for aluminium (After Wilson [33]).

When the heat source is removed (at the end of a laser pulse where $t>t_0$) a second term has to be added to the equation to allow for the fact that the surface temperature will fall as heat is conducted into the bulk. The temperature rise at different depths from the surface (z=0) as a function of time after cessation of the laser pulse can be calculated from the previous equation and are shown in figure 5. Using the solution to

the given equation Scruby [22] similarly plotted the theoretical surface temperature rise on aluminium against time for different depths below the surface. For a 20ns pulse with $F_0 = 1.9 \times 10^{10}$ W.m^{-2} the temperature rise at the surface is approximately 140°C and reduces to 40°C at a depth of 2 micrometres. In non-metals the surface temperature was found to decay exponentially with depth. The importance of these calculations is that the heating even at the surface is not great and insufficient to cause any microstructural changes, a fact inferred from the concept of the thermal time constant discussed previously.

Power densities close to 10^{10} W.m^{-2} are typical with laser sources, which possess phenomenal brightness. Unfortunately, the temporal beam profiles of real lasers (Nd:YAG and CO_2) comprise spikes and tails rather than being constant flux sources and taking account of these factors in the theory adds another layer of complexity.

A recent paper by Zhou *et al* [38] compares the computer simulation of laser ablation with experiment and takes into account the further complication that in laser cleaning, the source heat energy is moving.

Of equal practical importance to pulse duration is the time between pulses. The ablation process creates a cloud of ablated material. This has to be removed from the work piece using a vacuum line mounted adjacent to the beam delivery head. This is essential for health and safety considerations as the contamination may well be toxic. More importantly, from the perspective of process efficiency, the next laser pulse must not occur before this cloud of ablated material is removed as it will defocus the incoming pulse and dissipate its energy. Again optimum pulse duration has to be found such that the cleaning process is not too slow. The area irradiated by the laser must also be large enough to give reasonable cleaning rates when it is scanned across the target.

2.2.3.3 Thermomechanical effects

Very short, intense bursts of laser energy impinging on materials can also create shock waves [39]. The magnitude of shock waves generated by laser cleaning depends strongly on the energy density of the radiation, duration of the laser pulse, and

substrate properties. Two effects can be separated depending on whether the shock wave originates from either rapid expansion of vaporised material or due to rapid expansion of a substrate layer. Both effects can occur together but the latter effect appears to dominate in circumstances when the radiation impinges first on a surface coating surface that is a weak absorber.

Considering the first case, when a layer of surface contamination strongly absorbs a high intensity laser pulse of a few nanoseconds duration, it is vaporised and this occurs so quickly that a high pressure wave is generated which lowers the boiling point of the surface which becomes superheated. The temperature can rise high enough for the heat of vaporisation to be reduced to zero and the effect is that of an explosive detonation over the area irradiated. Under these conditions the vaporised material is easily ionised to form an opaque plasma. Although high temperatures can be generated, these are confined to the surface and heat is not conducted to the substrate when energetic short pulses are used. High compressive stresses can also be generated in this operating regime and in certain applications, such as laser peening [40], are used to permanently harden the surface.

When the laser pulse is less energetic and its duration is longer, in the order of microseconds, material is still vaporised but the rate of vaporisation is less and the vaporised material retreats from the surface. Under these conditions the vaporised material is transparent and does not ionise or form a visible plume.

For laser cleaning laser pulse lengths are chosen to minimise thermal damage to the substrate whereby the heat energy imparted to the surface cannot be transferred to the substrate through conduction. This requires nanosecond pulses but the operating parameters have to be chosen to avoid the vaporised material forming an unstable plasma. Generally, this requires the radiation to be defocused thereby spreading its high energy over a larger area.

The thermoelastic wave generated through laser interaction with a metal substrate, assumed to possess isotropic properties, can be considered as equivalent to the insertion of a small extra volume of material dV at the irradiated region [22] where:

$$dV = 3\,\alpha/\rho C\,.dE \quad \ldots\ldots\ldots\ldots\ldots\ldots\ldots\ldots\ldots\ldots(16)$$

where α is the coefficient of linear thermal expansion, ρ is the density, C is the specific heat capacity of the metal and dE the energy absorbed from the laser pulse. Substituting material constants for aluminium and assuming the metal absorbs 1mJ of energy uniformly over an area of $10mm^2$, it is found that $dV = 3 \times 10^{-14} m^3$. In aluminium most of the temperature rise occurs within a thickness of 2 micrometres and this generates thermoelastic stresses ~ 10^8 Pa per mJ of absorbed energy. The yield stress of aluminium is highly variable, depending on heat treatment, but for Al 2024, used for aerospace applications, values can be several hundred MPa and such values are comparable to the thermoelastic stresses calculated above. This demonstrates the magnitude of the effects that are possible if high laser cleaning fluences are used without due care. The same magnitude of stress occurs in steel but is less serious since the yield stress in steel is an order of magnitude higher. The reflectivity of steel is also higher so that less energy is absorbed in the first instance. Current cleaning applications where Nd:YAG lasers are used to clean steel railway tracks have found no metallurgical evidence of damage even after millions of cleaning pulses [25]. At the cessation of the laser pulse, the surface relaxes and this can assist in the ejection of material.

Considering the second case where the incident radiant flux does not encounter a strong absorber, let us assume the poorly absorbing coating covers a metal substrate and speculate on some possible interactions that are pertinent to the case of an epoxide resin coating bonded to a metal substrate. The metal will possess an oxide layer and absorption at this interface may well be much stronger. It is assumed that the incident radiation is Q-switched Nd:YAG at 1064nm but defocused to treat a larger area. The pulse is very short (~ nanoseconds) and possesses high energy but is not as intense as would occur when the beam were focussed. The forces created could be more than sufficient to break any adhesive bonding over the area irradiated and this could cause failure at the oxide/resin interface.

In the case of an oxide layer several micrometres thick the laser might induce rapid thermal expansion that would generate a compressive shock wave. Reflected back from the much harder and denser metal substrate, the shockwave could further weaken and disrupt the oxide interface (figure 6).

The cohesive strength within the epoxide coating and its strong adhesion to the oxide outside the irradiated area would prevent it being "blown off " but in treated areas the epoxide could easily be detached by mechanical means without offering any significant resistance.

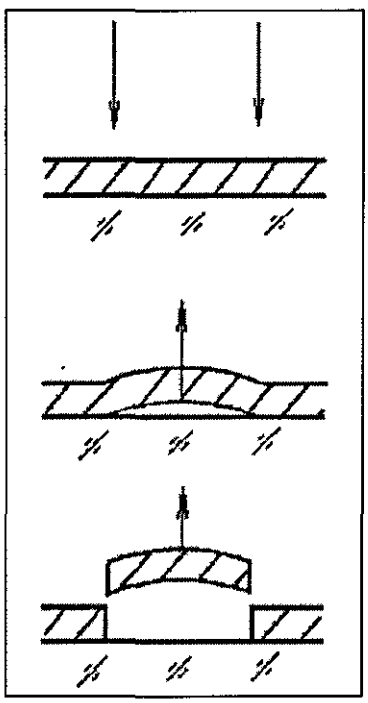

Figure 6. Shockwave propagation (After Lukyanchuk[9]).

This process has similarities to laser peening since in this process a substrate is coated with two overlays, one opaque and one transparent to the laser wavelength used. In laser peening the opaque layer might be black paint chosen to absorb the laser pulse and the transparent layer might be water. In this case, the laser pulse vaporizes a thin layer of the black paint and this is trapped momentarily between the underlying metal substrate and the water layer which causes the pressure to rise to much higher levels than if the water layer were not present. This creates a shock wave, which propagates into the metal, and providing the peak stress of the shock wave exceeds the dynamic yield strength of the metal, the metal will yield and plastically deform. This gives rise to strain hardening and compressive residual stresses at the surface of the metal, which are desirable effects in laser peening.

There is a mechanistic analogy between the metal oxide (in the laser cleaning example referred to above) and the black paint layer in the laser peening process. Similarly an analogy can be drawn between the non-absorbing epoxide resin and the water overlay used in laser peening. The difference between the processes is one of magnitude. In the laser cleaning case, defocused laser pulses are used and shock waves generated are not believed to be sufficiently powerful enough to result in any strain hardening. Clearly it would be undesirable to alter the metallurgy of a substrate

subjected to laser cleaning. X-ray diffraction is commonly used to measure minute changes in lattice spacings resulting from residual surface stresses and to determine phase transitions (notably austenite to martensite in steel). No such measurements were undertaken in this study but evidence exists from published literature [25] that no metallurgical changes accompany the laser cleaning operations on steel when Nd:YAG lasers are used.

2.2.3.4 Laser shock waves

The generation of concussive shockwaves has been developed into a technique to measure the interfacial strength of coatings on substrates. Gupta *et al* [41] has developed this technique and use Doppler interferometry to determine the interfacial strength of the coating and relates this to the interfacial fracture energy through a Griffith-type relationship. These experiments have similarities to the laser ultrasonics research of Stratoudaki [21] reported earlier since this also uses interferometry to determine transient displacements. Gupta's research uses the phenomenon of laser shock wave generation as the basis of an experimental technique in the same way that laser ultrasonics uses laser interactions with materials to determine structural information. It is worthwhile briefly describing Gupta's experiments since they have a bearing on the present research.

In this technique, illustrated schematically in Figure 7, a compressive stress pulse is generated by absorption of a Nd:YAG pulsed laser which irradiates a thin gold film sandwiched between a constraining block and the substrate. The substrate possesses a surface coating of thickness between 1 and 3 micrometres. On reflection of the transmitted compressive pulse from this coating's free surface, a tension pulse is created which detaches the coating at its interface with the substrate. Laser Doppler Interferometry (LDI) is used to measure the transient displacement and velocity of the coating as it separates and the interfacial strength can be determined from these measurements.

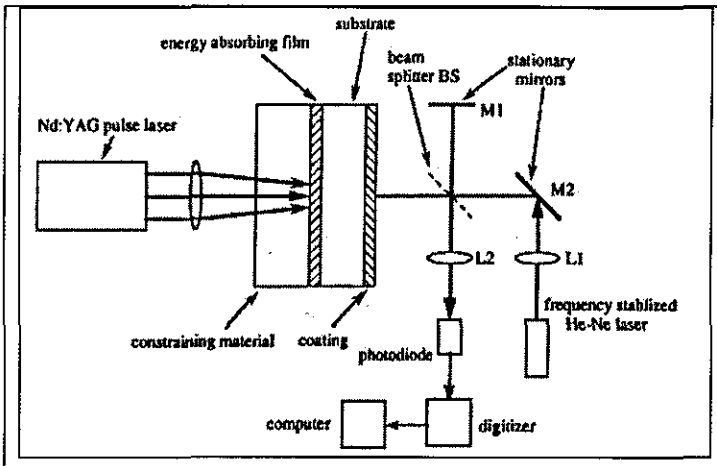

Figure 7. Experimental arrangement for using concussive shockwaves to measure interfacial strength of coatings (After Gupta [41]).

2.2.4 Laser cleaning of particulate surface contamination

The previous discussion has concentrated on the removal of continuous layers of contamination by laser irradiation. However, the contamination texture can take different forms and laser cleaning solutions are very popular in the semiconductor industry where the need arises to remove micrometre and sub-micrometre size particles from silicon wafers that would otherwise interfere with microchip production [42 - 44]. Such particles adhere extremely tenaciously to silicon surfaces and laser methods have been developed over the last fifteen years to cope with these intractable cleaning problems.

2.2.4.1 Interaction Forces in Interfacial Systems

Electrostatic forces are strong, long-range forces that are encountered in everyday life. At the molecular level other forces are encountered. The strong forces are associated with the covalent and ionic bonds between molecules and in addition much shorter-range of secondary forces exist that arise from molecular interactions. A total intermolecular potential energy defines the summation of all the possible interactions that can occur. These separate interactions depend on the type of charged bodies involved and these could be between two ions, two dipolar molecules or between a dipole and an ion. The interactions lead to molecules possessing dipole moments arising from uneven charge distributions. The interactions can be attractive or

repulsive depending on the system and involve induction of charge on one body by another.

For simple molecules a total intermolecular potential energy can be defined comprising the sum of five contributions:

(i) the charge transfer interaction

(ii) the interaction between two electrical multipole species

(iii) the interaction between two species where one is an electrical multipole and induces a charge on another species

(iv) the dispersion interaction

(v) the overlap interaction

The first contribution is the charge transfer interaction is associated with electron donation or sharing between two molecules and is more important in the interfaces between crystalline solids than in fluid systems.

The second contribution can be redefined as the Keesom potential that is always attractive and is obtained by averaging all the possible Coulomb interactions for all angles and orientational permutations between two dipolar molecules. This contribution has strong temperature dependence.

Similarly the third contribution, also attractive, is known as the Debye potential and occurs where one molecule possessing a permanent multipole induces a dipole in another molecular. This will depend on the polarizability of that molecule.

The fourth contribution, also attractive, is known as the London potential and can only be fully described using quantum mechanics but is associated with frequency dependent vibrations which perturb the electron distribution in one molecule causing an induced dipole and this in turn induces a dipole in another molecule. The attraction in fact acts between all atoms and molecules and the London potential gives rise to London Dispersion forces where the term dispersion relates to the dispersion of refractive index since this material property is used to determine the frequency dependent vibration which causes the interaction.

The fifth contribution, which is repulsive, arises directly from the Pauli exclusion principle and occurs when the electron clouds of two closed shell molecules overlap.

Hydrogen bonding is a special type of interaction that is sometimes included as a sixth term for the total intermolecular potential.

Forces arising from Keesom, Debye and London potentials all vary with the sixth power of the distance between molecules and are attractive forces. Collectively these are known as the van der Waals forces and apply to atoms as well as molecules.
Stokes and Evans [45] have derived mathematical expression for the potentials discussed and show how combining expressions for interaction potentials comprising the van der Waals forces arrives at the Lennard-Jones potential.

In the same way that the total interaction between molecules can be described by the summation of separate interactions, so can the interaction forces existing between two particles or macroscopic bodies, each comprising many atoms. The same microscopic forces are involved but the power law they obey is modified by translation to the macro scale and the interaction potentials are those associated with the geometries of the respective particles. There are two major interaction forces that operate in all particle systems. These are the London dispersion forces and that associated with repulsive overlap potential arises from the Pauli principle. Stokes and Evans [45] derive expressions for these forces acting in the macro size domain and introduce a material constant that measures the attraction between two particles in a vacuum. This constant is known as the Hamaker constant [46] and depends on the chemical and physical nature of the bodies involved [47]. This constant is encountered frequently in analytical descriptions of interaction forces occurring on the macro scale. The constant can be measured from the bulk properties of materials such as dielectric constant and refractive index and is expressed in units of 10^{-20} J or sometimes as electron volts.

The forces between particles are of concern when problems of adhesion of particles to surfaces are addressed. When capillary forces are present, it can be shown that adhesive forces are linearly proportional to particle radius whereas a cleaning force required to expel the particle from a surface is proportional to the weight of the

particle and hence to its volume and the cube of its radius. This means that it becomes harder to clean surfaces as the particle size reduces. The discussion now returns to how effective laser cleaning can be in removing very small particulate contamination adhering to smooth surfaces.

In the case of dry adhesion, van der Waals forces dominate the adhesion of sub micrometre particles whereas electrostatic force more important for particles larger than 50 micrometres. Conventional cleaning methods such as ultrasonic cleaning, wiping or etching all affect the substrate and so removal of the particles by lasers is an alternative solution. It is useful to quantify the magnitude of this force of attraction.

Considering the particle as a deformed sphere, Hamaker [46] states that the attractive force is given by

$$F=Aa/6h^2[1 + r_c^2/ah] \quad \text{.....(17)}$$

where 'a' is the radius of the particle; h ~ 0.4nm and is the equilibrium separation between the sphere and surface arising from the opposing attractive and repulsive molecular forces that act on the particle, and r_c is the radius of contact. The constant A is the Hamaker constant. The equation approximates to

$$F=Aa/6h^2 \quad \text{.....(18)}$$

since $r_c^2/ah >> 1$.

Assuming a particle diameter of 1 micrometre, substituting these values the attractive force is ~0.01 dyne (0.1×10^{-6}N) using an appropriate value for the Hamaker constant. However, condensation of liquid from ambient air can occur and create a liquid bridge at the particle surface interface. This results in an additional capilliary adhesion force that can increase particle bonding greatly. It has been found that if vapour from a liquid (water-isopropanol often used) is allowed to condense and form a micrometre thin film on a contaminated surface prior to laser cleaning, the liquid will completely cover sub-micrometre particles eliminating any capillary adhesion force. When irradiated by a sufficiently energetic laser pulse, the liquid can absorb so much energy that it explosively evaporates imparting enough momentum to particles to completely overcome particulate-substrate adhesion and eject them.

KrF excimer lasers, operating at ultra-violet wavelengths (248nm), have been found to be effective at removing fine particulate contamination [48]. Near infrared wavelengths provided by Nd:YAG lasers are also effective and incidence of the laser beam at angles lower than normal to the surface are found to enhance the cleaning effect.

In dry laser cleaning effective particle removal occurs when the incident radiation has sufficiently high fluence and acts for a very short time. Under these circumstances large inertial forces are applied to contaminant particles present on the irradiated surface.

To quantify the magnitude of these forces it is necessary to consider the thermal expansion of a surface due to laser heating.

The heat affected zone can be defined as $\beta . d_{th}.\Delta T$, where β the volume expansion coefficient of the material, d_{th} the thermal penetration depth and ΔT the temperature increase. To a first approximation the thermal depth of penetration d_{th} can be expressed as

$$d_{th} = (k\tau)^{-1/2} \quad \text{.....(19)} \ [48]$$

where k is thermal diffusivity and τ is laser pulse duration.

Assuming a particle sitting on the surface is spherical of radius r and density ρ, then it follows from Newton's law that the inertial force (equal to the product of mass and acceleration) experienced by the particle is

$$F_I \sim (4/3\pi r^3 . \rho).[(\beta . d_{th}.\Delta T/\tau)/\tau] \quad \text{.....(20)}$$

$$\text{or } F_I \sim 4/3\pi r^3 \rho\beta . d_{th}.\Delta T/\tau^2 \quad \text{.....(21)}$$

Using this equation it can be calculated that thermoelastic force values $\sim 10^{-6}$ or 10^{-7} N act on a 1 micrometre particle using a Nd:YAG laser with ΔT values between 100 and

500K. In other words the acceleration experienced by such small particles can exceed one million times the force of gravity. This tremendous acceleration makes it easy to appreciate the utility of laser cleaning in such circumstances.

2.2.5 Operation and characteristics of Transverse Excited Atmospheric (TEA) CO_2 lasers

A study of the effects of TEA CO_2 lasers on resin coated nickel tooling was performed using a Laserbrand L450 TEA CO_2 laser, emitting 10.6×10^{-6} m radiation in a 100ns pulse of 2J total output energy. The design of this laser was optimised for laser marking rather than laser cleaning applications. The unfocussed beam has an area of approximately $10cm^2$ and can be focussed down to $1cm^2$ using a plano convex ZnSe lens of focal length 30cm (figure 8).

Other materials such as NaCl could be used to focus the beam but these materials are all hygroscopic. The ZnSe glass used is stable but expensive. TEA CO_2 lasers require separate gas supplies to operate. The Laserbrand laser uses a typical gas mixture of 82% He, 8% N_2, 8%CO_2 and also contains 2% CO formed by dissociation of the CO_2. The gas pressure was approximately 40 psi (275.8kPa). Although this is more than twice atmospheric pressure, the laser is still referred to as "Atmospheric". The basic design of the laser is a gas filled cavity with electrodes placed between a pair of gold or copper coated mirrors. The gas mixture is pumped using a thyratron switch to discharge a potential of 40KV stored in a capacitor, across electrodes in the resonant cavity, thereby creating an electrical discharge, which partially ionises the gas exciting the carbon dioxide and nitrogen gas molecules.

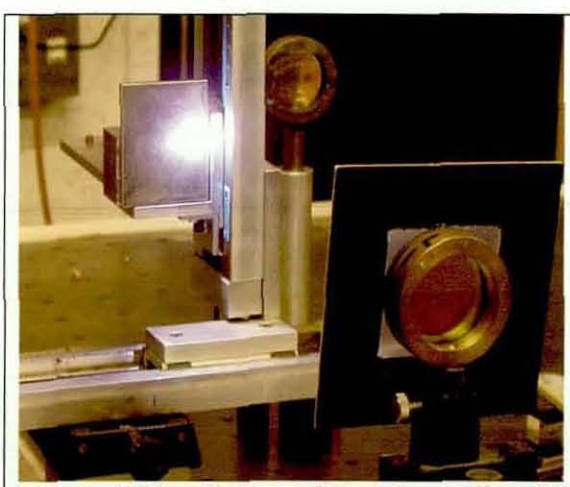

Figure 8. Irradiation of metal sample with TEA CO_2 laser.

Lasing of the CO_2 is assisted by the other gases present in the mixture with nitrogen transferring its vibrational energy to excite the carbon dioxide to the upper lasing level. Collisions of the carbon dioxide molecules with the helium molecules aids de-excitation once lasing has begun and contributes to the stability of the electrical discharge. As in any laser, a population inversion is created allowing many electron transitions to occur between a metastable and ground state energy level for the active lasing medium (figure 9).This gives rise to two principal emission lines for a CO_2 laser, these being at 10600 and 9600 nm respectively.

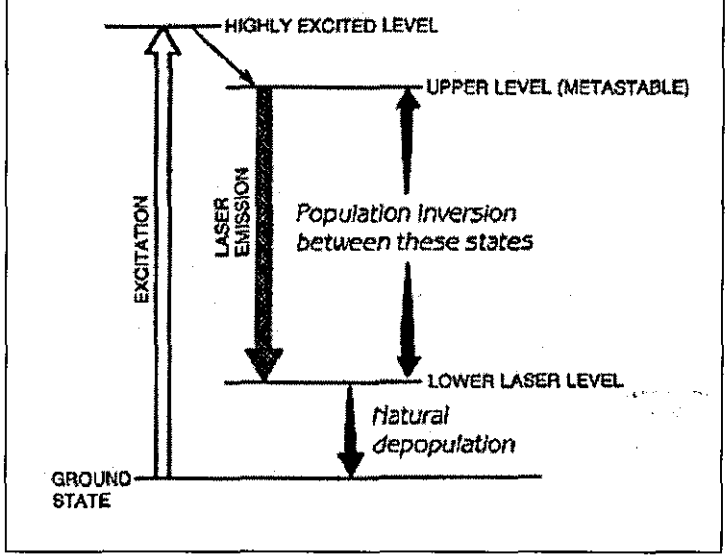

Figure 9. Energy level diagram for a laser (After Hecht[195])

There are many other weaker emission lines so it is possible to obtain an output between 9000 and 11000 nm depending on design. Carbon monoxide is present in the gas mixture to neutralise any 'free oxygen' produced by the breakdown of the CO_2 by the electrical discharge. A constant supply of fresh gas is required to replenish gas lost through breakdown.

The gas needs to flow through the lasing cavity since the power output falls off when the mixture gets too hot and a water cooled heat exchanger is used to stabilise temperatures within the resonant cavity to below 420K. Gas flow rates of 2 litres per minute ensure that the gas between the electrodes is effectively changed after each

discharge. Rather than flowing along the axis of the resonant cavity, higher power outputs are obtained by transverse gas flow. The temporal profile of the output beam typically comprises a 100 ns pulse or spike, this is followed by a 1 microsecond tail that contains approximately two thirds of the total output energy. By reducing the nitrogen concentration in the gas mixture, the tail can be shortened or made to disappear but the total energy of the pulse is reduced. Also the duration of the high intensity spike is a function of the resonant cavity length and with shorter cavities, 50 ns pulses can be obtained.

The arrangement of the electrodes and shape of the cavity mean that the output beam possesses a rectangular cross section that exhibits an intensity variation across the spatial profile of the beam. This beam inhomogeniety produces variations in the rate of ablation across an irradiated target area and "hot-spots" which may favour the formation of a plasma, which is undesirable and cannot be corrected using beam homogenisers available for most other low and medium power lasers.

Leakage of helium is another problem in TEA CO_2 lasers and the need for a flowing gas mixture creates practical difficulties for industrial applications. For this reason, sealed radio frequency excited CO_2 lasers were developed as an alternative since these do not require gas supplies and their reduced physical size makes them more suitable for robotic mounting. These systems though are not, however, as powerful as TEA CO_2 lasers and the intended market for them is biased towards materials processing rather than cleaning applications.

When the output beam of the Laserbrand model is focussed down to an area of $1cm^2$ the fluence is great enough to readily vaporise organic coatings. Coated metal samples can then be positioned at various distances from the focus to receive differing fluences. The samples studied in the present research undertaken were all mounted such that the laser beam was incident normal to the surface of the coated samples. This was done to eliminate angle of incidence as a variable and simplify evaluation. The number of pulses required to produce a visible effect on the coating for a given fluence was noted. With smaller, much lighter samples a sensitive mass balance could be used to monitor weight loss as the coating was removed but this was considered to be impractical in this study.

Cottam [49] reported that cleaning fluences for this laser range from 1 to 4J.cm $^{-2}$ depending on the absorption characteristics of the coating and studied the absorption of opaque inorganic pigments and compounds associated with metal corrosion products, reporting that strong absorption occurred in many instances. Higher fluences may be required for weakly absorbing materials although air breakdown occurs at fluences of 10 J.cm^{-2} or more, and this situation is avoided to prevent the formation of a plasma which produces many undesirable secondary effects. Sometimes these plasmas are triggered by the non-removal or ineffective removal of ablated material. Since very high temperatures are a characteristic of plasmas these can radiate sufficient energy to the substrate and induce thermal damage.

In common with other TEA CO_2 lasers the Laserbrand laser has very few operational parameters that can be altered easily without incurring considerable expense or loss of power output. Effectively only the fluence and angle of incidence of the radiation can be altered. The output wavelength and pulse duration are fixed and repetition rates exceeding a few Hertz cause unstable operation. Taken in combination, this makes it difficult to optimise lasing cleaning effects for a specific coating.

Most applications of continuous wave CO_2 lasers designed for cutting and welding utilize computer controlled platforms to move the work piece requiring cleaning with the laser being static or else mount the laser on a robot arm and control this to scan the laser over an area to be cleaned. Where the cleaning of very large moulding tools is contemplated, the workpiece cannot be moved and some form of automation is required to scan the laser over the area to be cleaned. The physical size of a TEA CO_2 laser and the gas, water and electrical requirements would suggest that this option would be costly to implement and not very flexible. Aside from the cost issues involved in realising an industrial scale laser cleaning solution with TEA CO_2 lasers, the technology has some other drawbacks. At present there exist few stable materials that will transmit this wavelength without significant absorption. Exceptions are zinc selenide, as mentioned, or germanium and focussing optics have to be produced from these rather exotic materials. Highly polished mirrors made from gold or copper also have to be used because of the very high reflectivity of the metals at 10600 nm. All these optics have to be kept clean and mounted components must be free from vibration in use that will degrade alignment. Unlike carbon dioxide lasers used for

cutting and welding processes, where optics focus the laser light down to very small spot sizes, laser cleaning requires defocused beams covering an area of a few square centimetres. Ideally, the energy distribution across such beams should be uniform but this is difficult to achieve because of the way high power CO_2 lasers are designed and the output consists of a series of lines over which the intensity varies.

Measurements of laser fluences are required to optimise cleaning conditions but for intense pulsed lasers this poses experimental problems. High-energy pulses very easily damage conventional power meters, used for most other laser lower power measurements. Other critical factors are the pulse duration and repetition rate.

2.2.6 Operation and characteristics of Nd-YAG lasers

The laser cleaning effects obtainable from 1060 nm wavelength radiation from Nd:YAG lasers were investigated experimentally using a Spectron SL456 pulsed Nd:YAG laser (figure 10). This laser utilizes a temperature stabilised Pockels cell to effect Q-switching, enabling the laser to produce a short, intense pulse of energy (duration 13ns). Output power level and repetition rate were adjustable to give a maximum output of 850mJ up to 10Hz. Repetition rates up to 5Hz were used giving pulse energies ~600mJ, this value being interpolated from the laser's power output calibration measurement.

Figure 10 .The Spectron Nd:YAG Laser

The Nd:YAG laser can be operated in two modes where the output consists either of fixed Q pulses or the output power can be boosted to produce short intense pulses by a process called Q-switching. Q-switched laser pulses deliver energy so quickly to a surface that there is little energy conducted away during the duration of very short pulse. The Q factor of a laser resonator is basically a measure of how good the resonant cavity is at keeping light in it. With a normal pulsed laser, a pumping source of intense light (flash lamp) raises the electrons of the active atoms of the lasing medium to an upper energy state. In this laser the ions from the rare earth metal Neodymium (Nd^{3+}) are used to dope a Yttrium Aluminium Garnet ($Y_3Al_5O_{12}$) crystal. The Nd^{3+} ions, present at about 1% concentration, usually displace Yttrium atoms in the crystal lattice and provide suitable energy levels for the lasing transitions. Lasing materials must have at least three energy levels comprising a ground state (lowest energy), an excited state and an intermediate or metastable state. Occupancy times for electrons in the metastable state are much longer than for excited states and to achieve stimulated emission of light, electrons have to be excited in such a way that they decay to the metastable state before de-exciting finally to the ground state. In nature the equilibrium state of systems coincides with minimal energy content so most electrons initially excited to high energy states in a material would randomly decay to the lowest energy state. By coaxing electrons to occupy an intermediate state, the occupancy of that state is described as a "population inversion". During the pumping cycle high frequency radiant energy is supplied to the lasing material to create such a population inversion. Spontaneous emission occurs from the highest energy level and is a random process. An electron decaying to a lower energy by this means emits a photon and if this is emitted in a direction such that it can be reflected back and forth between mirrors at each end of the resonant cavity, the energy of the photon can then trigger other electron transitions from the metastable state. Its energy must exactly match the transition energy from that state. The photons emitted by these electrons falling to the ground state energy will be emitted in the same direction as the parent photon. They will also possess the same frequency ($h\nu = \Delta E$ where ΔE is the energy difference between the upper excited state and the ground state, h is Planck's constant and ν the photon frequency).

This stimulated emission is thus coherent and monochromatic and is amplified by travel along the length of the lasing crystal. The photons are confined within this resonant cavity, their exit being prevented by mirrors at each end of the cavity, and the amplitude of the stimulated emission increases during the pumping cycle. The mirrors constitute a feedback mechanism that amplifies the gain per unit length for the resonant cavity. Standing waves are thus created within the optical cavity and when their amplitude reaches a saturation value, the output end mirror (which is only partially reflective) allows some of the light to escape. Since millions of such bursts of light are emitted during the pumping cycle a laser beam is created.

Lasing materials can possess more than three energy levels and the Nd:YAG laser is a four level laser. In practical terms this makes it easier to obtain a population inversion although the physics describing the radiative and non-radiative transistions is more complex.

The efficiency of the cavity defines its Q factor. If the light energy could be confined between the mirrors until very near the end of the pumping cycle, when the population inversion was as complete as possible, the output intensity would be greatly boosted. This can be achieved by spoiling the Q-factor of the cavity through the use of a high-speed electrically controlled optical shutter called a Pockel's cell. This effectively disables one of the mirrors so that the cavity cannot resonate properly. Very close to the end of the pumping cycle, the optical shutter is closed and the laser action commences but because there exists a very near total population inversion, a very intense short pulse of laser light is passed. The average power output for the Nd:YAG laser may be low compared to a CO_2 laser but the peak power when Q-switched can be in the kilowatt range which is desirable when the beam is defocused to cover a larger area for a cleaning application.

Different laser interactions occur depending on whether the Nd:YAG laser is operated in fixed Q mode or is Q-switched to boost its peak power. For the studies reported here Q-switching was used. This affects the thermodynamics of the surface interaction because the Q-switched pulse is very short (nanoseconds) and can be optimised for laser cleaning applications.

Without Q-switching the laser output pulses are in the order of millisecond duration and when sharply focussed, it was observed that the laser beam was powerful enough to bore tiny deep holes into nickel-plate . Noting the focus position at which this damage occurred, samples requiring cleaning were again positioned at varying distances back from this point and the coating removal effects noted until an optimum distance was found. This proved to be approximately 50mm from laser focus. The laser-operating mode was then changed to activate Q-switching since short pulses with high peak power are optimum for laser cleaning. With the same degree of defocus (diameter was about 10mm) a single pulse was sufficient to detach cured resin from the metal substrate to which it was bonded. Ideally, the laser beam used for a cleaning application should be spatially homogeneous with a "top-hat" shaped intensity distribution. Laboratory lasers generally do not meet this requirement and in the case of the Nd:YAG laser used, the beam output is multi-mode where the energy profile resembles a random collection of dots in a circular pattern. With excessive defocus the output was noted to become very "spotty" and unsuitable for cleaning. This energy distribution factor is particularly severe with TEA CO_2 lasers where the beam is never homogeneous and there exists a distribution of fluence over its area. This problem makes it difficult to correlate microstructure observed on treated samples with an accurately known fluence. In the case of Nd:YAG lasers, the manufacturers of a commercial Nd:YAG laser designed for cleaning applications (and possessing a homogenised beam) were approached and some resin coated samples submitted for laser cleaning. These samples were cleaned at a rate of $10cm^2$ per second using a fluence of 1 $J.cm^{-2}$ with normal incidence of the beam. The microstructural topography was found to be comparable to those obtained with the Spectron laser.

The effects observed during the interaction of a laser pulse from a Q-switched Nd:YAG laser with a coated metal will depend on whether the coating or substrate or both absorb energy at the lasing wavelength of 1064nm. In all real samples the metal will possess an oxide layer and so it is the absorption of this oxide layer will also influence the results. In the present study nickel and steel substrates were examined and these posses good reflection properties at 1064nm. In contrast, aluminium can strongly absorb at this wavelength and would thus not be a suitable substrate for a laser cleaning application. Walters and Campbell discuss the application of such

Nd:YAG lasers to clean oil and grease contamination from stainless steel, aluminium and titanium [50].

Despite a greater propensity to cause thermal damage on metal substrates due to the reduced reflectivity, the use of Nd:YAG lasers, operating at an output wavelength of 1060 nm, offers some real practical advantages. Glass fibre optic beam delivery from the laser source to the work piece is possible because there is very little absorption by the glass at this wavelength. This greatly enhances the flexibility of the cleaning process since a skilled operator can now manoeuvre a hand held laser cleaning head over the area to be cleaned and, if necessary, simply increase the fluence to remove stubborn contamination. Removal of patchy contamination from large areas would be difficult to control by an automated process. The use of a solid-state laser also makes the laser inherently more reliable and free from operating faults. The technology of these lasers is well developed and several European companies now market competitively priced laser-cleaning systems for industrial applications. Unlike TEA CO_2 lasers, which are physically bulky systems requiring gas and three phase electrical power supplies, the size of Nd:YAG systems has been steadily reduced and current small footprint units are marketed. These advantages are made at the sacrifice of cleaning rates which are slower than using CO_2 lasers but still competitive with other non-laser cleaning methods. In most other respects Nd:YAG lasers offer the most cost effective laser cleaning solution.

2. 3 Mould Cleaning by Dry-ice pellet blast cleaning

Contaminated composite tooling, in particular, poses significant problems when laser cleaning methods are applied because of chemical similarities between the substrate and the contaminant. The use of solid CO_2 pellet blasting was considered as a viable technology for the removal of resin contamination from both metal and composite tools and the potential of this cleaning technology was therefore evaluated. There are many small companies trading today that specialise in dry ice cleaning and these have appeared only within the last twenty years or so.

Figure 11.Dry ice blasting

Prior to the 1970s the use of dry ice for blast cleaning application was pioneered by relatively few researchers and the first commercial companies developed from this early work. The aircraft manufacturers Lockheed developed the technology for paint stripping applications but did not pursue commercial applications.

Dry ice blasting is one of the most effective means for removing loosely bound organic contaminants [51 - 53] and the blasting process is illustrated in figure 11. The cleaning process can be gentle enough to clean delicate electrical components or aggressive enough to remove bonded coatings. A popular application is the cleaning of printing presses. Dry ice does not erode or wear away the targeted surface upon impact as traditional grit media and even wire brushes do. This means that surface integrity and critical tolerances are preserved and equipment will not have to be replaced because of the surface erosion.

Paint, oil, grease, asphalt, tar, soot, dirt, ink, resins, and adhesives are some of the materials removed by this procedure. Since dry ice evaporates completely to a gas at atmospheric pressure without going through a liquid phase it disperses in the atmosphere and is environmentally benign since it is not an ozone-depleting compound. Carbon dioxide gas is also virtually inert and non-flammable. Only the material being removed must be disposed of. When dry ice cleaning replaces hazardous chemical cleaners the disposal cost of that chemical is thus eliminated. Another advantage is that carbon dioxide is not electrically conductive and it is possible to clean equipment that is running.

The shelf life of dry ice is reasonable if suitable storage facilities are used. Under these conditions blocks can last for up to two weeks. Utilisation of these blocks depends on equipment design but generally involves shaving the block into sugar grain-sized granules by rotating blades inside the unit. Shaved ice machines deliver a particle blast with a high flux density due to the small size of the particles and are more effective on thin coatings. Other dry ice blasting machines only accept carbon dioxide pellets and the storage life of this form is typically three days because of the larger surface area. Hydraulic rams squeeze these pellets through die plates to produce a much greater density pellet for maximum impact energy.

2.3.1 Principles of Carbon Dioxide Cleaning Processes

The process is similar to sandblasting whereby the media is accelerated in a compressed air stream and impacts on the contaminated surface that requires cleaning.

Figure 12. Dry ice blasted sample

One unique aspect of using dry-ice particles as a blast media is that the particles sublimate upon impact with the surface. The size of the particles of dry ice can be varied though are often a few cubic millimetres in volume (about the size of a grain of rice). Solid carbon dioxide pellets are relatively soft and when they impact on a surface they are compressed and mushroom out. The combined impact energy dissipation and rapid heat transfer between the pellet and the surface cause an almost instantaneous change of phase from the solid to carbon dioxide vapour and this creates a flushing action which first weakens and embrittles contamination as it is

rapidly cooled and then the vapour assists in lifting off fragments from the adherend. The ice formation on a cleaned sample is shown in figure 12. The volume change occurring due to sublimation of the carbon dioxide pellet is large with the vapour occupying a volume approximately eight hundred times that of the solid pellet. The sublimation occurs within a few milliseconds so that each pellet effectively detonates when it impacts with the surface creating a micro-explosion. Abrasive additives such as sodium bicarbonate are sometimes added to increase the scouring action of the cleaning process.

As with other blasting methods, the cleaning action is driven by the kinetic energy of the accelerated media. This is a function of the impacting particle's mass and hence density and the impact velocity. Carbon dioxide pellets possess a relatively low density so that blast cleaning relies on accelerating the pellets to subsonic or even supersonic velocities using compressed air jets to achieve the required impact energy. Therefore three distinct mechanisms are associated with such a cleaning procedure:

(i) Kinetic Energy

The principle cleaning effect is produced by those solid particles of dry ice colliding with the surface to be cleaned. Kinetic energy is transferred to the surface thereby "chipping" away the contaminant from the substrate. The effect can be described by the equation

$$K.E = 1/2\ mv^2 \qquad \text{.......................................(22)}$$

where KE = Kinetic Energy (Joules)

m = the mass of the CO_2 particle (kg)

v = the velocity of the particle($m.s^{-1}$)

The density of solid carbon dioxide is low (1565 kgm^{-3}) so that its mass per unit volume is also low and hence it can therefore be assumed that changes in the velocity produce large changes to the degree of kinetic energy transferred to the object to be cleaned. Since velocity is related to air pressure, it follows that changes in air pressure affect the degree of kinetic energy that is transferred to the object to be cleaned in proportion to the square of velocity, whereas a change in the particle's mass has proportionally less effect. Particle velocities are typically 100 to 300 $m.s^{-1}$ [54].

Compressed air supplies up to 150 psi (1034kPa) are typically required and these must be grease and water free. Kinetic energy is then largely converted to heat, which raises the temperature of the solid CO_2 forcing it to vaporize, on impact.

Although compressed air pressure is the most effective processing parameter that can be varied, enhanced removal rates can be achieved by mixing the dry ice with abrasive powder. An example of such is sodium bicarbonate, used in the present study. This can be used as a blast media in its own right [55] but can lead to increased rates of chemical corrosion with some metal substrates. Cleaning rates for dry ice systems are very variable and depend on the application and equipment but can be as high as 120 square metres per hour (3.3×10^{-2} $m^2.s^{-1}$) [55].

(ii) Thermal Differentials

The second effect is the production of a thermal shock and is associated with the low temperature of the solid CO_2 particles (-78.5°C), which endothermically removes heat from the surface to be cleaned producing a pronounced cooling effect of $628kJ.kg^{-1}$. In cases where significant thermodynamic differences exist between the contaminant and the substrate, this can have the effect of contracting and or solidifying the contaminant. As the temperature of the contaminant decreases, it becomes embrittled and cracks are formed, enabling the particle impact to break up or dislodge and fracture the coating still further and possibly to sever the chemical bonds already weakened by the lower temperature. This is, however, most likely to cause cohesive failure of the coating. This thermal shock is most evident when blasting a non-metallic contaminant bonded to a metal substrate and consequently was considered potentially effective at removing cured epoxide resin when this is stuck to a metal moulding tool. A liquid contaminant such as oil or grease can become more viscous or may partially solidify in this process and this can assist in its removal.

(iii) Reverse Fracturing

This effect is a direct result of the solid particles of CO_2 subliming to a vapour. In ambient air pressures, CO_2 cannot exist as a liquid, only as a solid or vapour. One kilogram of solid CO_2 becomes 540 litres($0.54m^3$) of CO_2 vapour upon sublimation.

CO_2 vapour is also more "fluid" than the blasting air, which has transported the pellets to the surface. Sublimation therefore assists in the removal process through gaseous CO_2 expansion at the surface, which has been observed to penetrate and lubricate the surface. This can have the effect of forcing away the contaminant from behind and is termed flushing.

The dry ice cleaning process employs a mechanical means to prepare the dry ice and as a delivery system to accelerate dry ice particles which are accelerated at subsonic or supersonic speeds under compressed air and exiting to atmosphere via a operator hand held nozzle.

Operating variables are the jet pressure, dry-ice particle size, jet angle of incidence and working distance and it is necessary to optimise these parameters for a given application. Spur *et al* [56] discuss process optimisation for the removal of paint from metal sheets and silicone seals from aluminium.

2.3.2 Advantages and Disadvantages of the process

Using the cryogenic system operated in the present study, the following advantages and disadvantages of the process can be identified:

Advantages

(i) The cleaning process does not use any chemical solvents and the only waste that needs consideration is that removed from the tool by the blasting process. The cleaning technique is thus environmentally benign.

(ii) Carbon dioxide is a solvent itself for some materials (see section 2.4.4.2).

(iii) The cleaning apparatus is portable and this facilitates in-situ cleaning and can be done when the tooling is hot to minimise downtime.

(iv) The cleaning process is non-abrasive for metal tooling and can offer a very gentle cleaning action on more easily damaged materials such as composites.

Disadvantages

(i) Solid 27 kgm standard blocks of carbon dioxide are required as a consumable. Typically block ice is consumed at a rate of about 1 kilogram a minute and pellets at about twice that rate. Consumables have to be factored into an analysis of likely running costs.

(ii) The loud noise produced by impact of the particles on a substrate requires that operators protective earphones and may cause irritation to other people nearby. Noise levels typically > 100 decibels.

(iii) Effective cleaning can only occur in a straight line-of-sight from an automated dry ice jet nozzle. Manual application allows the nozzle to be angled relative to the work piece.

(iv) Large amounts of carbon dioxide are released which are harmful if one is in a closed space without ventilation since oxygen levels are depleted. The surfaces of metal moulding can get very cold and cause burns as can contact with dry ice pellets. The cold metal surfaces also attract moisture from the surrounding air and this can pose a corrosion problem for steel tooling unless post drying is carried out.

(v) In some applications an electrostatic charge can build up on an insulating substrate as a result of the process and a means of safely discharging this has to be considered.

2.3.3 Mould Metallurgy and Temperature Effects

Dry ice cleaning is frequently used in the rubber industry to clean moulds and very often the moulds are hot after use. Initial concerns over use of the technology were principally that the temperature differential created by dry ice blasting might induce changes in the metallurgy of the heat-treated and hardened metal moulds or promote micro-cracking. Manufacturers of dry ice blasting equipment subsequently funded research to investigate these concerns. The reports were unpublished and, in general, it is very difficult to track down any non-trade publications relating to dry ice cleaning using academic databases. The findings of the aforementioned metallurgical studies have been reported in trade literature. These claim that no metallurgical changes were evident on tool steel moulds or in precipitation hardened aluminium alloys. The

widespread use of the cleaning technology within the industry appears to validate these claims [54].

2.3.4 Other carbon dioxide and related blasting technologies

2.3.4.1 Carbon dioxide "Snow" cleaning

For completeness it is appropriate to mention this technique that also uses dry ice to clean surfaces. In this case high purity (99.999%) carbon dioxide gas is expanded through a small orifice in a cleaning nozzle and is cooled by the Joule-Kelvin effect to produce a snow of tiny dry ice particles and gaseous carbon dioxide. Using compressed gas the dry ice particles can be used to clean surfaces in much the same way as with the cleaning techniques already discussed, the difference here being that the dry ice particles are much smaller and consequently the cleaning action is much gentler. Typically, CO_2 snow cleaning is used for friable materials that are easily damaged and an obvious example would be the cleaning of semiconductor wafers where it is effective for removing very small particles. It will not, however, remove substances that are chemically bonded to surfaces such as paints and resins and its application to industrial large scale cleaning is limited as a result. Kimura and Kim evaluated both laser and using CO_2 snow cleaning applied to astronomical mirror samples[57]. In this application the presence of particulate material degrades the performance of aluminium coated mirrors but these are too fragile and expensive to risk more aggressive cleaning methods. It was found that excimer laser cleaning and CO_2 snow cleaning gave comparable results in terms of cleaning quality.

2.3.4.2 Solvent Properties of Supercritical Carbon dioxide

The most commonly known application for supercritical carbon dioxide is for the extraction of caffine from coffee and tea but it is an effective solvent for many non-polar materials including oils, organic contaminants and some polymers. It can thus be used as a replacement for hydrocarbon solvents. In carbon dioxide the supercritical state is most accurately described as that of a dense gas rather than a liquid though it possesses many properties similar to those of a liquid phase. A comprehensive review of the fundaments, applications and technology of supercritical carbon dioxide is provided by McHardy and Swan [58].The pressure/temperature phase diagram for

carbon dioxide (figure 13) defines the range of pressures and temperatures that allow carbon dioxide to exist as a supercritical fluid.

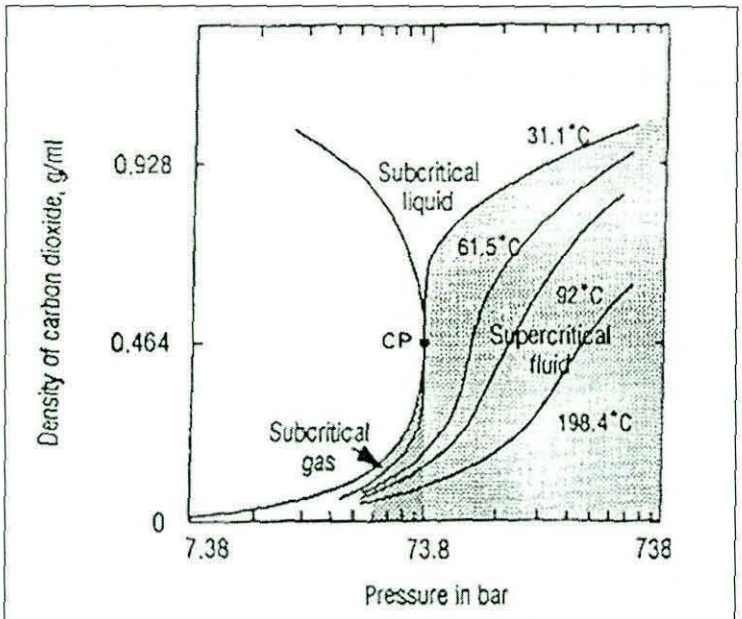

Figure 13 Carbon dioxide phase diagram (After McHardy and Swan [58]).

The critical pressure is 1070 psi (7377kPa) and the critical temperature is about 31.1°C. Supercritical applications typically operate at temperatures between 32°C and 49°C and pressures between 1070 and 3500 psi. (7377 and 24134kPa). The supercritical fluid has a lower surface tension than many ordinary liquids and this gives it the property of being very searching. Combined with its solvent abilities this means that the process is suited to the cleaning of intricate geometries that cannot be cleaned by more conventional cleaning technologies.

In practical applications, the object requiring cleaning has to be placed in a reaction in a pressurized chamber and this obviously limits the size. Closed loop recycling is engineered so that only a small proportion of the cleaning solution is lost over time. A separation process is used to remove dissolved contaminants. When the cleaned object is removed from the chamber no drying or rinsing is required and this is ideally suited to the cleaning of precision components where exacting standards of surface

cleanliness are desired. It is not suggested that this technique would be viable for industrial scale mould cleaning but its inclusion is pertinent to a full appraisal of the cleaning potential afforded by carbon dioxide.

2.3.4.3 Blast cleaning using ordinary ice

A variation of dry ice blasting has been developed which uses ordinary water in the form of tiny ice crystals as a blast media. Most of the technology has been developed from snow making machines and the small ice particles (a few micrometres in diameter) are actually created in the blasting nozzle. An aerosol of atomised water droplets is created and a stream of compressed gas, chilled using liquid nitrogen, which rapidly freezes the droplets into roughly spherical shaped ice and propels them towards a contaminated surface. The particles created can be easily accelerated to speeds in excess of Mach 1 (approximately 224 $m.s^{-1}$). Significant advances over the use of high pressure water jets in cleaning operations are that in most blasting applications the small size of the ice particles means that the heat generated at the surface of a contaminant layer by kinetic energy conversion is sufficient to cause evaporation. At worse only a small amount of water may be present in dislodged contamination. Successful applications claimed include paint stripping from aluminium surfaces. It is claimed the process is best suited to soft metals and composites [54]. Obviously, the process might not be suitable for cleaning where rust corrosion is an issue but the technology brings together some of the advantages from dry ice blasting with the negligible consumable cost.

2.4 Dry ice and ultra-violet light cleaning method

A recent publication by Deffeyes *et al* [59] discusses the removal of surface contamination from substrates using a combination of dry ice and ultra-violet light. In the context of cleaning procedures for the aerospace industry, finding a single cleaning method to replace CFC solvents is difficult. A combined approach might be suitable in some circumstances. In this method gross contamination is removed by dry ice blasting. Any small amounts of residual organic contamination are then oxidized at low temperature using ultra-violet light. This light source is not a laser but rather a quartz-mercury vapour lamp. This emits strong ultra-violet light at wavelengths of

254nm and 185nm. The lower wavelength light stimulates ozone creation through the photo-dissociation of oxygen in the air above the target surface and it is postulated that the ozone reacts with surface hydrocarbons to enhance cleaning. The higher wavelength causes photochemical breakdown of the bonds of many organic compounds evolving carbon dioxide and water as molecular fragments. The pre-cleaning step using dry ice is necessary because ultra-violet light can only remove thin layers of contamination. Thick layers of organic contamination tend to crosslink under ultra-violet irradiation rather than oxidise. The generation of toxic ozone poses safety issues for workers that would need to be addressed. Alternatively the light source could be modified to minimise ozone production though this would reduce cleaning efficiency.

Another publication by Rich *et al* [60] discusses the use of ultra-violet light alone to remove external mould release compounds from metals and non-metallic surfaces. This application proved successful in removing mould releases from the surfaces of aluminium, steel and glass fibre/vinyl ester composite samples as measured using water contact angles before and after irradiation of a few minutes duration. Whilst successful for the removal of standard micrometre thicknesses of these release agents, the process would not remove thick layers of contamination.

2.5 Mould Cleaning by immersion in fused alkali bath

As discussed, one drawback of laser cleaning is that it is largely a line-of-sight technique and therefore has difficulty in cleaning very complex shaped tooling. Other physical cleaning technologies such as dry-ice pellet blasting, high-pressure water jet cleaning and possibly plasma cleaning all share this difficulty to a greater or lesser extent. In such cases there is little alternative but to resort to a wet chemical cleaning method, which would involve lowering the mould into a bath of the cleaning agent. In these applications it is also desirable that the cleaning chemistry employed removes silicones arising from degraded mould release agents as well as crosslinked resin. The chemical inertness of silicones requires aggressive and very searching cleaning solutions that will not, however, damage the metal substrate. Solvents for fully crosslinked resin are either acidic and would damage metal tooling, possibly causing pitting which might aggravate mould release, or else are strong and volatile organic

solvents which are environmentally unfriendly. Therefore, the use of these in conjunction with a large ultrasonic bath would be inappropriate. One technology that will fulfil these requirements is the use of a fused alkali bath that will chemically reduce all such contamination and has found application in the destruction of hazardous chemical waste [61]. No other solvents are involved and so the waste is kept to a minimum. A cleaning solution based upon a high temperature bath of molten alkali is obviously hazardous to operate but does not damage the environment. Immersion of the tool into a bath of this material imposes a practical size limitation on what can be cleaned. For reasons that will be discussed the process is also best suited to nickel or non-ferrous metals that are not susceptible to rapid corrosion once a clean surface has been obtained.

DuPont developed the sodium hydride treatment in 1942 [62] as a method for removing oxide scale and casting sand residues from metal castings using a fused alkali bath, which would not cause any damage to the casting. The process has been described in detail by Lightfoot [61] where it was applied to the destruction of toxic chlorinated organic compounds. The use of fused alkali baths is not a common cleaning technique and is used predominantly in the metal finishing industry to clean complex shaped parts such as engine blocks. This process has not, however, been used for mould cleaning applications. Literature searches have failed to find any academic studies of its use for mould cleaning and very few trade descriptions appear to have been published. The two references given are the only ones found relating to the cleaning process generally.

The process itself requires the part to be immersed in a molten bath of anhydrous sodium hydroxide maintained at 360°C. Hydrogen is passed through the melt to create a relatively dilute 2% solution of sodium hydride. This hydride is a very powerful reducing agent that is capable of reducing many metal oxides to the bare metal. Refractory oxides such as those of aluminium, titanium or silicon are not reduced directly but are removed by conversion to the corresponding hydroxides by the highly basic hydrous component in the melt. The hydroxide is then soluble in the sodium hydroxide and is therefore removed. Unlike conventional acid pickling solutions the substrate metal is not attacked by this highly basic medium provided the metal is immediately quenched in a large excess of clean water upon removal from the melt.

Lightfoot [61] states that stainless steel corrodes rapidly, however, under these circumstances unless the drying can be carried out very quickly following washing. Because of the susceptibility of steel to rust it is thought that the process shows greater promise for cleaning of nickel tooling.

The very low surface tension of the melt renders the treatment extremely searching penetrating into any hairline cracks or the interfacial regions between any coating and the metal. Combined with the high temperature of the melt, the net action on any organic coatings such as resins would be to "carbonise" them and pressure washing is necessary to remove carbonised organic residues from the metal surface.

Sodium hydride cleaning has the advantage of being one of very few methods that will remove any silicone contamination from a metal surface. Cleaning time is relatively quick, typically an hour.

2.6 Ultrasonic Cleaning of mould tooling

This method requires immersion of the contaminated part into a treatment bath and uses high frequency vibration (between 40kHz and 400 kHz) to improve the cleaning efficiency of aqueous and semi-aqueous cleaners that often incorporate a surfactant to reduce surface tension of the solvent. There is no restriction on the solvent used provided it does not chemically attack the bath containing it. Ultrasonic transducers are externally bonded to the bath, usually underneath the base of the bath. When activated these transducers create intense waves of compression and rarefaction in the cleaning solution. The resulting alternating zones of high and low pressure impose powerful shearing forces on the molecules of the solution and literally tear them apart creating microscopic vacuum bubbles that implode when the sound waves move and the zone changes from negative to positive pressure. The phenomenon is known as cavitation and the millions of tiny bubbles break against the surface of any object immersed in the bath. The interaction of cavitation with a layer of surface contamination is analogous to abrasion with molecular sized grit. This allows the solvent to penetrate the contaminant layer and the reduced surface tension allows it to work its way between the substrate and the contamination enhancing the cleaning process. A similar technique called Megasonics uses yet higher frequencies in the

range 700 kHz to 1.2 MHz. The higher frequencies result in smaller cavitation bubbles and produce a gentler cleaning action. This technology is favoured for cleaning delicate precision parts such as semiconductor wafers [63].

2.7 Plasma Cleaning

Plasma cleaning is really an application of plasma etching and this technique has been used for many years to chemically modify the surfaces of materials, particularly fluoropolymers, to make them chemically reactive, enhance their wetting ability to wet or improve adhesion. It is thus a surface chemistry tool but the same physical process can be used to etch away surface contamination, eventually producing an exceptionally clean surface. Typically, for a cleaning application, the object requiring cleaning is placed in a reactor chamber that is evacuated using a rotary pump to a low pressure. Oxygen is then bled into the chamber and the gas excited using radio frequency energy (typically 13.5MHz at 1kW power) and this is ionised to form a plasma. The object is surrounded by this plasma, which reacts with organic contamination producing only water and carbon dioxide as the reaction by-products so that the cleaning process is environmentally friendly. The plasma is characterised by an equilibrium or near equilibrium discharge which exists, once stable operation has been established, wherein electrons, ions and neutral species in the plasma are in thermal equilibrium. The electrons present have negligible heat capacity since their masses are tiny and so most of the heat generated in this cleaning process is that transferred by bombardment with ions of much greater mass. The object cleaned is usually quite hot when removed from the reactor.

Used in this way etching rates are very slow and typically ~0.5 micrometres per hour and the technique described is essentially that which would be used for a surface chemistry application. The cleaning effect is strongly dependent on surface roughness and smooth surfaces tend to clean faster than rough surfaces. Paciej *et al* [64] conducted an evaluation of plasma cleaning for the removal of lubricants from metallic surfaces and compared cleaning efficiencies against identical samples treated with CO_2 snow cleaning and cleaning using detergents. They found that plasma cleaning reduced contamination to the lowest levels but was relatively slow in

comparison to the other techniques. The detergent cleaning methods were more effective in reducing gross contamination. This research was published in 1993 and since then new developments in plasma cleaning technology have dramatically increased cleaning rates.

Until relatively recently the use of plasmas for surface engineering in industry have not been adopted because of the constraints imposed by the need for low pressure environments, the slow cleaning rates and the initial set up costs for the technology. What has now changed is that non-equilibrium plasma processes have been developed that can operate at atmospheric pressure [65]. Also by adding reactive gases such as sulphur hexaflouride to oxygen, plasma etch rates can be increased by several orders of magnitude to levels in excess of 250 micrometres per hour for the etching of polymethlymethacrylate (PMMA) [66].

The same technology can be applied to metals that are difficult to clean such as aluminium and can produce exceptionally clean surfaces as measured by X-ray Photoelectron Spectroscopy (XPS) and water contact angles [67]. In a study by Hicks [68] on the cleaning of radioactively contaminated surfaces where tantalum was used as a surrogate material for plutonium, it was claimed that etch rates of 360 micrometres per hour can be achieved by introducing a low concentration of carbon tetrafluoride into the oxygen whereby the plasma generates a large flux of reactive fluorine atoms.

In the new technology available the atmospheric plasma is produced using a torch electrode design called a plasma jet (figure 14). This can be used to scan over an area requiring cleaning. This non-equilibrium plasma is characterised by a much lower temperature typically between 50° and 300°C so potential thermal damage is reduced. The design can be modified so that, instead of being cylindrically shaped, flat parallel and planar electrodes can be used and these have the potential to clean larger surface areas. This emerging technology merits a feasibility study for a mould cleaning application provided it can be shown that high etching rates are achievable without introducing adverse substrate reactions which compromise tooling chemistry or metallurgy. However, at the moment it suffers from the disadvantage that helium gas is required to stabilise the non-thermal plasma and to efficiently cool the electrodes on account of its high thermal conductivity.

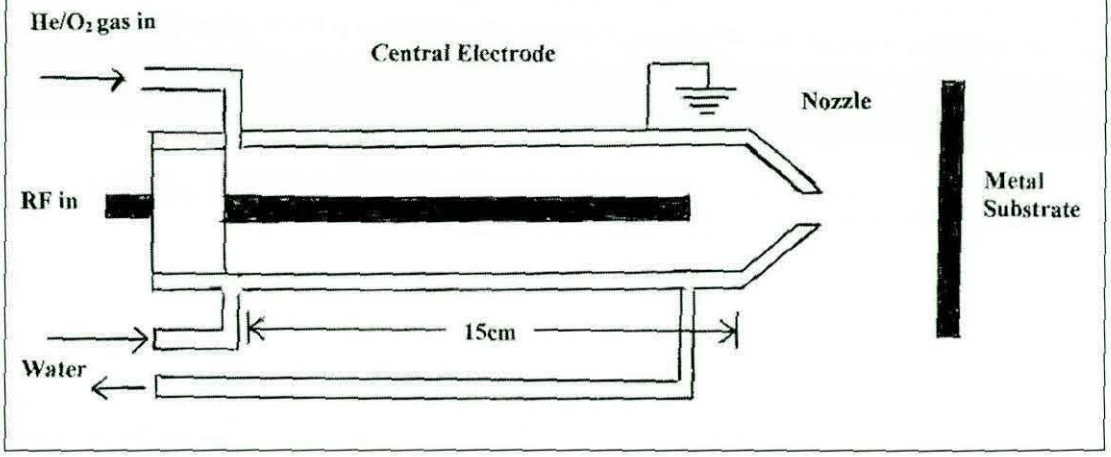

Figure 14 Plasma jet electrode design.

2.8 High Pressure Water Jet Cleaning

Of all the cleaning technologies discussed, the use high-pressure water jets are the one most commonly encountered in everyday life. They have been used in industry for many years and can operate at pressures as high as 55 000 psi (379MPa) and can be used in fully automated cleaning operations. Applications are found in almost every industry from stripping of paints, rust and epoxide resins from metal parts to cleaning marine fouling on ships hulls. Abrasive materials can be added allowing water jets to be used for cutting or for simply more aggressive cleaning. The major drawbacks of the method are that very large volumes of water waste are produced and legislation requires industrial users filter the solid waste before discharge into sewers is allowed. Also in many industrial processes involving unprotected iron and steel, rusting would result from use of water jet cleaning unless parts were very quickly dried and drying is thus an added complication.

2.9 Summary of Surface Cleaning Technologies

The need to clean the large surface areas of aerospace tooling is a fundamental requirement in the present research and influences the choice of appropriate cleaning

technology. The most appropriate technologies considered worthy of study were identified as follows:

2.9.1 Laser Cleaning

- The literature shows there are many successful aerospace applications of laser cleaning and that the technology is a viable cleaning solution that does not damage metal substrates.
- The optical absorption characteristics of the contaminant coating and the underlying substrate determine the laser interactions that occur.
- For a contaminant modelled on epoxide resin bonded to metal tooling, the literature states that absorption is strong using high power pulsed carbon dioxide lasers and coating removal is largely photothermal. For Nd:YAG lasers, absorption by the resin appears to be weak but concussive shockwaves generated by treatment result in a thermomechanical effect that constitutes an equally effective cleaning mechanism and which recommends the technology over the more expensive pulsed carbon dioxide lasers.
- The literature suggests that there are many difficulties associated with the laser cleaning of composite tooling. These may not be insurmountable but they would significantly compromise the rate at which large surface areas could be cleaned.

2.9.2 Dry ice blasting

- The literature suggests this is the main competitor for laser cleaning. Dry ice blasting is already used for mould cleaning in the rubber industry. The essentially physical nature of the cleaning means it can be applied to both contaminated metal and composite substrates. Some disadvantages are higher consumable and running costs.

2.9.3 Sodium hydride cleaning

- This cleaning procedure is efficient at removing organic contamination quickly and could be applied to contoured moulding geometries that would be difficult to clean by line-of-sight techniques. Its limitations arise from the hazardous nature of the cleaning chemicals and practical size of the moulds that could be treated.

2.9.4 Other Cleaning Procedures

These were identified in sections 2.7 – 2.9 but were not considered worthy of further study. The cleaning technologies that do not produce large volumes of waste are limited to cleaning of relatively small moulds that can be lowered into a treatment bath or placed within a reaction chamber. It is not thought that these are capable of removing large areas of crosslinked epoxide resin in reasonable time scales from metal or composite surfaces.

Chapter 3 Mould Release Agents and Non-Stick Polymers

3.1 Introduction

The discovery of polytetrafluoroethylene (PTFE) some 60 years ago marked the start of an era when the term "non-stick" entered into the common vocabulary. Stickiness (adhesion) and non-stickiness (abhesion) are related surface properties in the sense that the properties of a surface that make it non-stick are for the most part the opposite of those needed to allow other materials to stick to it or adhere. Scientists first became interested in adhesion in the nineteenth century and many theories explaining the mechanisms of adhesion have been proposed in the twentieth century, so that today adhesion can be referred to as a mature science.

Abhesion, a term first used by Zisman [69], is a term used increasingly in research publications. It is used as a surrogate for the opposite of adhesion and conveying the idea of non-stickiness. Briscoe has described abhesion as a "Cinderella subject" [70] because most of the knowledge and expertise in the subject resides in thousands of patents held by large and small companies trading in non-stick products around the world. Academic research has been erratic and has been pioneered by only a few researchers, so in comparison to information on adhesion, relatively few systematic studies have been published. Mould release agents comprise another specialised type of non-stick material.

3.2 Mould Release Agents

Mould release agents are used in many different industries and problems of mould fouling are rife. Rapra [71] has recently produced a compilation of abstracts relating to mould fouling and the majority of research publications listed therein are associated with proprietary trade formulations claiming superior releasing performance, though invariably with sparse factual detail. Patent abstracts are also included in the Rapra publication.

Relatively few systematic and scientific investigations relating to mould release, functional chemistry and performance exist in the literature, a fact commented upon

in a recent comprehensive review "Mould Fouling and Cleaning" by Packham [72], and so it is difficult to give a historical perspective in any literature review.

Legislation designed to reduce environmental pollutants and in particular, the Montreal Protocol of 1987, required the makers of mould release agents to develop products that could be applied using harmless solvents. In response there was renewed effort to develop semi-permanent mould releases and water-based releases.

The semi-permanent releases comprised, in large part, either cured resin systems that coat the mould or fluoropolymer films applied to the mould. These were developed for the moulding of rubber, thermoplastics elastomers (TPEs), urethanes, epoxies, and polyesters. Some releases cure at room temperature whilst others require moulds to be heated to complete crosslinking. They are best suited to moulding very large parts where relatively low numbers of moulding cycles are required rather than in high output mouldings where a part is made every few minutes.

Water based releases represent a later product development and now offer equal or in some cases better performance than semi-permanent releases. Industry has been reluctant to accept these because of the need to fully evaporate all the water solvent once the release agent is applied to the mould. The products have been reported to work best on hot moulds such as those for cast urethanes that are pre-heated [73]. There are still problems in some applications arising from poor wetting, slow evaporation, chemical reactions and wetting agents used in the formulation. In a separate technology [73], a mould release agent was developed that was solvent free being applied as an atomised cloud of the solid release agent.

Companies in the U.S.A. largely dominate manufacture of mould release agents. There are literally hundreds of different types of mould releases made and this testifies to the fact that the market for good mould release agents is very profitable as demand is high. Product selection is difficult because of the number of different types. Applications in the rubber and polymer processing industries predominate. Despite the high incidence of mould fouling problems in these industries, the science of mould release agents is poorly understood. Proprietary formulations are developed by trial and error and contact with a leading manufacturer of mould release agents in the

U.S.A. suggests that formal test methods are rarely used to evaluate release performance in practice. This is because every customer has a different set of fabrication requirements and mould tooling geometry and moulding chemistries are such that no single laboratory test is deemed relevant [74].

It is important in the context of the present research to emphasise the fact that fibre reinforced composite moulding processes in the aerospace industry almost exclusively uses external mould release agents and these tend to be semi-permanent formulations which allow multiple moulding cycles to be performed before the release agent has to be re-applied. This distinction is necessary because much of the literature that is published concerning mould releases is biased towards their use either as internal release agents, where they are mixed with polymers that are injection moulded, or for rubber moulding applications [75]. Although many external release agents are used to prevent mould sticking in the rubber industry, additives in the rubber formulations can lead to very specific chemical reactions with the mould substrate during vulcanisation of moulded rubber products. Examples are reactions between sulphur additives used in rubber compounds with nickel mould tooling and, in the case of halogen-based rubbers, reactions between chlorine and steel mould tooling, particularly where the steel has a high chromium content [75], [76]. In such cases adhesion leading to mould sticking is enhanced by interfacial chemical reactions, which are influenced by the surface structure and acid resistant properties of the metal moulds [77], [78]. In contrast, the chemistry occurring between thermosetting epoxide resins, which may be monocomponent systems, and metal tooling is markedly different with the consequence that a significant proportion of the limited information published on mould fouling research is of limited value to the present research. It is, however, useful to broadly categorise the different types of mould release products that are available.

3.2.1 Internal Mould Releases

These are added to a polymer formulation that is intended to be injection or compression moulded. Proprietary formulations are used which may be fatty acid esters, metal stearates (often zinc or calcium) and waxes and which are believed to migrate to the surface during the moulding process presenting a weak boundary layer

between the moulding and the tool which allows ejection of the part with minimal force [79]. According to Comyn [80], one internal mould release agent based on oleamide operates not by forming a thin, uniform weak boundary layer on the surface, but by forming microcrystals, which increase interfacial stresses.

3.2.2 External Mould Releases

Injection and compression moulding are relatively new processes and historically the first mould release agents used were applied externally to moulds. These agents were mineral or ester oils and waxes such as paraffin and provided a cohesively weak boundary layer between the moulded part and the moulding tool. Multiple coatings of waxes had to be used and these were buffed to a high gloss, which was very time consuming and there were several other disadvantages [81]. Once a moulding was removed, the mould release had to be reapplied. These were thus termed sacrificial release agents. These release agents were generally only economic for small-scale production runs because their use was labour intensive. Since rubbers have a much longer history than plastics the association of mould releases with that industry is intimate. It was found that moulded rubber parts could absorb the oils and waxes during curing processes and this was undesirable. Also it was difficult to obtain a uniform thickness of mould release agent and this lead to the use of release agents dissolved in organic solvents that allowed conformal coatings to be applied.

In the middle of the last century when silicones became available, these were attractive because of their unique properties and thermal stability and the dominance of waxes as other lubricants as mould release agents was eroded. Silicones, especially poly(dimethyl siloxane), are amongst the most inert and chemically stable materials known. Because silicones will not react with most things they are prone to migration and this leads to serious problems where adhesion to a moulded part is required or where the part has to be painted. Silicones generally can be classified as fluids, rubbers or resins. The ability to make silicones is based on the fact that carbon atoms can be replaced with silicon atoms that are also tetravalent and can form up to four bonds with neighbouring atoms. Oxygen is usually bound to at least one of the atoms. An organic group can be attached to one or more bonds, which differentiates silicones in terms of the functionality of the organic radicals attached to the silicon. These are

methyl groups, methylvinyl groups, phenyldimethyl groups and fluorodimethyl groups.

Release agents and lubricants can be formulated from silicone emulsions whilst sealants are the best-known example of silicone rubbers. Semi-permanent mould releases and a wide range of silicone masonry water repellents can be formulated using silicone resins. Semi-permanent releases can themselves be sub-divided into products where the resin is present in low concentration, typically 2-5%, in an organic solvent such as an aliphatic hydrocarbon, and products where high-pressure homogenisation in the presence of a surfactant allows a micro-emulsion of the resin in water to occur. Environmental legislation was the driving force for the development of these water-based release agents. Organic solvent-based semi-permanent releases are preferred in industry because drying times are shorter. Water-based releases work well on composite tooling (that is itself used to mould other composite structures) but cleaning procedures on metal tooling render them prone to rapid rusting when water based releases are used, though this fact is rarely mentioned by the manufacturers. On a separate theme, Boeing is developing organically modified ceramic coatings called "ormocers" for the high temperature processing of advanced composite materials where conventional release agents are thermally unstable. These combine the thermochemical stability of a glass with the surface chemistry of a fluoropolymer [82]. Other commercially available coatings comprise dry films (usually based on fluoropolymers) that are applied to the mould tooling to effect good release.
The key to success of a mould release is a marriage of its properties to the intended application, thus ensuring that the release agent is compatible with the chemistry of the moulded material and environment in which it will be used. These qualities are usually arrived at empirically by trial and error and through close liaisons between a release agent manufacturer and a customer.

A very successful commercial mould release agent used in the aerospace industry is called Frekote™ (hereafter referred to as Frekote) and was formally marketed by the Dexter Corporation in the U.S.A. The Loctite Group today markets this product. A logical starting point for this research is to consider what is known about Frekote.

As has been mentioned, the chemistry of mould release formulations is only ever discussed in general terms in the literature. One noteworthy exception is a publication by Clarke *et al* [83] , which provides some insight into the functional mechanisms of the release polymers. Utz, Hensel and Sprenger [84], employed by the same company, separately published another article on the subject though the content is very similar.

In common with many other semi-permanent mould release agents, it is believed that the Frekote product comprises two resin-based reactive polymers. The manufacturers suggest a thoroughly cleaned moulding is first primed with two light coats of a sealing formulation. The first coating is allowed to dry for 30 minutes at ambient temperature and then the second sealing coat is applied allowing another 30 minutes drying period but this time at 125°C. This is followed by an application of "at least" two further coats of the mould-releasing agent. Again, the first coat is allowed to dry at ambient temperature and then another coat added.

It is believed that the first sealing component polymerises on contact with air, when applied to a clean metal mould surface, and seals surface pits and porosities in the mould. Heating can accelerate the crosslinking reaction and an open sponge-like structure is created. The second chemically compatible mould release polymer is now applied and it is this polymer that reduces friction between the moulding and the mould. Catalysts can be added to the component formulations to change the curing conditions though as a general rule the durability of the release coating is improved by a higher temperature cure. The one requirement shared by all release agents is that they must be applied to a clean substrate and the manufacturers include proprietary cleaning products with their release agents. Other key properties for release agents used in high volume industries are that the number of moulding cycles per application is maximised and that the release coating is durable and can withstand abrasive scratching or be easily reapplied to touch up damaged areas.

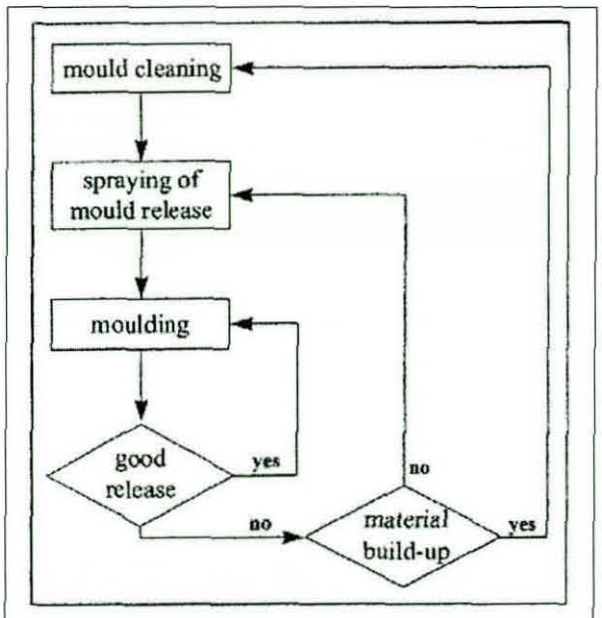

Figure 15. Mould cleaning decision tree (After Clarke [83]).

Mould users use a decision tree such as that shown in figure 15 to determine the frequency of reapplication of a release agent and of mould cleaning. This in turn relates to the number of moulding cycles that can be carried out without problems of mould sticking.

Clarke [83] used Atomic Force Microscopy to show that application of a semi-permanent release fills grooves and holes in a metal mould surface and levels the surface topography but does not create a perfectly smooth surface. The single coating thickness is estimated to be approximately 300nm. The point is made that if the release coating is too thick and the surface too smooth, it becomes unstable due to the high shear forces encountered in moulding and demoulding operations. An optimum thickness works best, which reduces frictional contact with the mould substrate and provides a lubricating effect. Which of these effects is more important is not known but Clarke believes that both effects contribute to the performance of a good release coating by some form of synergistic mechanism. Clarke contrasts a coated and uncoated substrate using frictional mode Atomic Force Microscopy (AFM) and this clearly illustrates the effectiveness of the release coating. Substrate surface roughness is an important factor in achieving a good release and will be discussed more fully

later. Briscoe and Panesar [85] have studied the effect of surface roughness on the adhesion of polyurethane to metal substrates.

Some years ago Blanchard [86] did some valuable research on mould releases associated with injection moulding of thermosets and in particular studied the build up of Frekote 700 NC on electroformed nickel tooling. Blanchard's work is the only research the author has found that has any relevance to the Frekote system. Using Secondary Ion Mass Spectroscopy (SIMS), Blanchard was able to identify PDMS from the SIMS spectra of residues built up on nickel tooling and concluded that this material must be a major constituent in the formulation of the Frekote. Further evidence in support of this was found in the present research and it is probable that other competitive products are also based on a similar chemistry.

Both the sealing component and the release component in the Frekote system comprise resins dissolved in an aliphatic hydrocarbon such as dibutylether. The solvent is present in concentrations up to 98% and readily evaporates at room temperature to leave a rubbery residue. This residue is suggestive of a material with a low, sub-ambient glass transition temperature consistent with what might be expected for PDMS. With the Frekote system two resin based polymers are used together, one to seal mould porosities and the second to provide a slippery non-stick surface with low surface energy.

The trade literature published by most of the manufacturers of semi-permanent releases now shares the consensus that thin coatings often outperform thick coatings although, with the exception of Clarke [83], quantitative measurements of coating thickness are never quoted. There is ambiguity as to whether these manufacturers are referring to the thickness of one coat or that of the total coats applied, since most of them suggest a minimum of four coatings per application of release onto a cleaned mould; these coatings comprising mould sealing agent and release agent collectively. This vagueness may not be intentional since the total thickness of four or more coatings may only be a few micrometres at most and this is very thin by the standards involved in industrial applications, as opposed to surface science investigations that look at the effects of nanometre thicknesses at surfaces.

One or two manufacturers suggest monolayer thicknesses of their coatings are effective implying a thickness in the order of a few nanometres and it is likely that these few products utilise different chemistries to silicone resins, possibly fluoropolymers or fluorosilanes. Unfortunately, it is not always easy to obtain samples to test and determine composition by independent analysis. The author has encountered reluctance on the part of some manufacturers to supply small quantities for study. There can be many reasons for this. Usually their customers order large volumes and there is no demand for small quantities and the solvents involved would pose shipping difficulties since many of the companies making release agents are based in the U.S.A. It is conjectured though, that the degree of secrecy surrounding many proprietary formulations implies they broadly possess very similar chemistries although each naturally claim superior performance, and the absence of published literature, in part, supports this view.

Werner [87] proposed the use of perfluorinated polyethers as mould release agents for high temperature thermosetting resins. These satisfy the properties that good release agents should possess but are only soluble in highly fluorinated solvents and as such are inappropriate for a pollution conscious industry.

3.3 Mould Fouling

Within the rubber industry this is also referred to as mould sticking or 'scumming' and collectively these terms refer to moulds where residues, from chemically or thermally degraded release agents and contaminants arsing from the moulded parts, have accumulated on the mould surface to such an extent that the release performance has been impaired.

As has been mentioned previously, the causes of mould fouling are very complex and specific to a particular moulding process and reactions occurring between the moulded part and the mould substrate. The mould release is not usually considered since release agents are by their nature usually chemically inert. Excessive over use of a release agent can, however, aggravate mould sticking particularly if it has been

applied as uneven coatings. In practice applying an even coating on a large area mould is no easy matter because, irrespective of the release agent used, the coating is transparent so that when cured and dry it is largely invisible unless it is applied so thickly that interference colours arise when light reflects off the coated substrate. From the customers' point of view, applying an even coating would be easier if the release agent incorporated a dye so that an operative might easily assess coating thickness. Equally, the customer would not want this dye to transfer to the moulding which may be one reason release agents with dyes in them are not offered. Spraying or wiping are preferred methods of mould release application since brushing can produce a streaky coating.

3.4 Theories of Adhesion

Anyone pursuing research in abhesion seeks an answer to the fundamental question: What makes a surface non-stick? An attempt to answer this question might reasonably take as its starting point an examination of the theories that have been proposed to explain why surfaces do stick together and then invert the arguments for the case of abhesion.

The theories propounded to explain the mechanisms involved in adhesion have been developed over many years and occur frequently in the literature [88], [89]. Four main theories have evolved:

(i) the absorption theory (attributing adhesion to intimate molecular contact between an adherend and adhesive with interfacial van der Waals forces, hydrogen bonding and possible chemical primary bonding occurring).

(ii) the diffusion theory, advanced and developed by Voyutskii and Vasenin [90],[91], whereby molecules from adherend and adhesive are assumed to migrate across an interface. This assumes molecular mobility and chemical compatibility between the surfaces in contact as occurs in some rubbers.

(iii) the mechanical interlocking theory where adhesion is said to arise from the interlocking of the adhesive into pores or cavities in the substrate, whereupon it hardens and anchors itself into the surface. There is evidence from many

workers such as Venables [92] that mechanical interlocking plays a significant role in adhesion.

(iv) the electrostatic theory, proposed and supported Deryaguin [93], which is based on phenomena that occur on the close contact of two dielectric materials or between a metal and a dielectric. It considers the adhesion of a pressure sensitive tape to a smooth surface and treats the two components as equivalent to the two plates of an electrostatic condenser and relates the energy of this condenser to the work of adhesion. When such a pressure sensitive adhesive tape is peeled rapidly from a substrate, a weak glow discharge has been observed and this implies there is some validity in the theory.

Adhesives can have three principal components:

(i) A surface conditioner that etches or otherwise roughens and cleans the surface providing more points for mechanical retention,

(ii) A wetting agent or carrier solvent that causes the adhesive to spread well over the surface,

(iii) A thermosetting or crosslinkable resin, which conforms the surface intimately and cures to provide mechanical retention and a cohesively rigid material.

The reactivity of the surfaces being bonded is a critical factor in determining whether an adhesive will be able to spread over the surface and wet it completely. The chemical reactivity of a surface is related to its surface energy measured in units of energy (millijoules) per unit area. Contact angle measurements, using a polar liquid such as water and a non-polar liquid such as diiodomethane (DIM), are frequently used to assess the surface energy of a material. Many metals, especially after vigorous cleaning, possess relatively high-energy surfaces and will wet with water very easily.

The term 'water-break' is used to describe the wetting achieved with water on cleaned substrates. Surface energy is also the driving force for polymer surface kinetics such that a system will always try to minimise its interfacial energy and move towards a thermodynamic state of equilibrium. Non-stick materials such as polytetrafluoroethylene (PTFE) have exceptionally low surface energies ~ 16 $mJ.m^{-2}$,

are very unreactive, and water will not spread over their surfaces. Some materials are not reactive with water but may be reactive with other fluids so some caution must be exercised in the interpretation of high water contact angles when used in isolation as an indicator of low surface energy.

The mechanisms of adhesion outlined can be inverted to develop indicators of good release behaviour. From the discussion of contact angle theory in section 3.8.8, an ideal non-stick surface requires a zero work of adhesion and a very low surface energy such that its water contact angle would be very high but these properties alone are not sufficient to guarantee that nothing will stick to it as will be discussed.

3.5 Non-stick Polymers

The best known non-stick polymers are PTFE and PDMS and it is pertinent to discuss the properties of these materials. One of the aims of this research was to evaluate some novel coatings that might offer promise as better performing mould release agents. Some insights into potentially useful chemistries are found from research into non-stick surfaces and this bridges many diverse industries. Application examples include non-stick bakeware which predominantly use fluoropolymers, pressure sensitive adhesive tapes where a silicone backing paper allows easy use of the tape, antifouling paints for immersed marine structures, ice-repellent surfaces for aircraft wings, biomedical implants and robot part fabrication on the nanoscale level.

In many applications the non-stick coating can be applied from solvents by brushing onto a surface or from an aerosol spray onto a substrate and this is the most convenient method of surface preparation for a moulding tool application. Selection of the type of moulding tool for the aerospace industry is made with regard to matching the coefficient of thermal expansion of the tool to the product being moulded. Any polymer coating should have a minimal effect on this and so needs to be effective when applied as a thin coating from a solvent.

3.5.1 Polytetrafluoroethylene

Polytetrafluoroethylene was discovered in 1938 by Roy Plunkett [94] and first became commercially available as Teflon™ marketed by DuPont. Thesis dissertations concerning fluorpolymers often start with the description of the discovery of PTFE as a "serendipitous event" without explaining the circumstances that may be unfamiliar to non-chemists.

Reputedly the discovery of PTFE occurred when Plunkett opened up a brand new cylinder of tetrafluoroethylene gas one day in his laboratory only to find that nothing

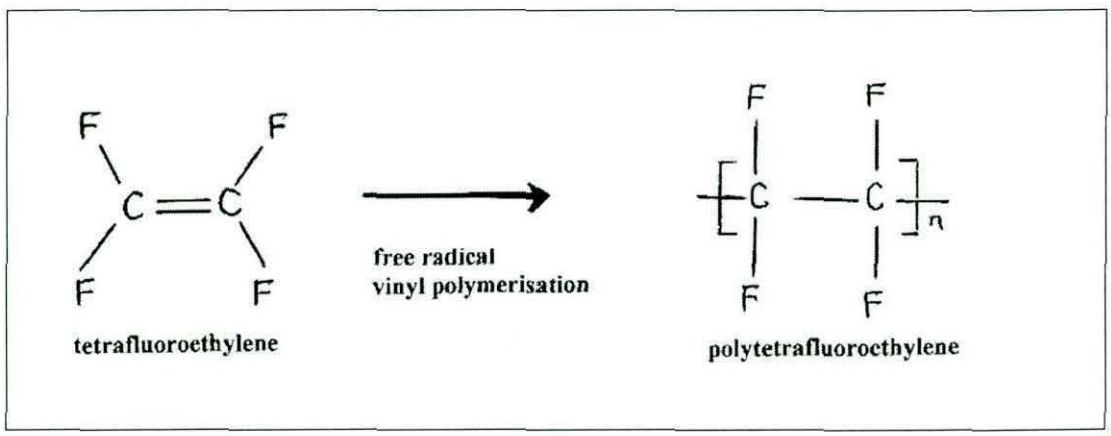

Figure 16 Conversion of TFE to PTFE.

came out! He subsequently found a solid white powder where the gas should have been which was PTFE, polymerised from the gas [95] (figure 16). PTFE was the first commercial perfluoropolymer and is a solid semi-crystalline polymer with a high melting point (327°C) that consists of long chains of carbon atoms fully saturated by fluorine atoms. When all the hydrogen atoms attached to carbon atoms in an organic polymer are replaced by fluorine atoms, the resulting polymer is known as a perfluoropolymer. Many different perfluoropolymers have been synthesized to date.

Fluorine is the most electronegative of the elements and in fluorine-carbon bonds the electrons are closely held around the nucleus as compared to those in a hydrogen-carbon bond where the electron distribution allows for interactions with contaminating materials. The carbon-fluorine bonds are extremely strong and the shielding of the carbon bonds by the fluorine atoms is responsible for the chemical

resistance of the material. The PTFE chain forms a slightly twisted helix as shown in figure 17 due to mutual repulsion of adjacent fluorine atoms. The helical conformation of PTFE molecules thus comprise of carbon atoms in the core shielded by a sheath of large fluorine atoms and the molecules pack together like parallel rods in the crystalline domains.

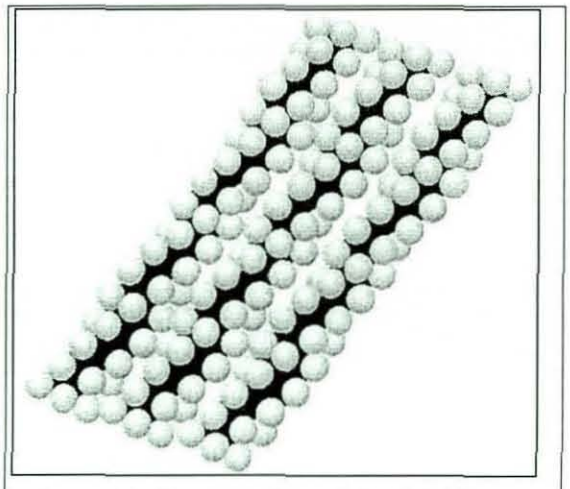

Figure 17. Structural model of PTFE depicting a sheath of fluorine atoms (light coloured spheres) shielding a core of carbon atoms (dark coloured backbone) (After Herber & Reucker[111]).

The properties of the closely packed fluorine atoms (figure 17) on the outside contribute to exceptional physical properties of PTFE, which include a very low surface energy, and one of the lowest coefficients of friction of any known material (0.04 – 0.09) [96]. Unfortunately, PTFE is insoluble in almost all solvents and is difficult to mould or extrude since it has a very high melt viscosity (10^{11}-10^{13} Pascal.sec). It is most frequently encountered in non-stick coating formulation as a dispersed solid phase or emulsion or can be processed in granular form by sintering. Melt processing is possible by modifying PTFE with the introduction of hexafluoropropylene and perfluoroalkylvinyl ether into the polymer chain to give Teflon FEP and Teflon PFA respectively, both possessing lower crystallinity and molecular weight [97].

There are some materials that have a lower surface tension than PTFE and these are frequently characterised by possession of CF_3 functional groups rather than the CF_2

groups of PTFE. Zisman [69] found that the surface tension depends on the constituent groups in polymers which decrease in the order of :

CH_2 (36mN.m^{-1}) > CH_3 (30 mN.m^{-1}) > CF_2 (23 mN.m^{-1}) > CF_3 (15 mN.m^{-1}).

The surface interface in a coating dominates its interaction with other materials and this interaction occurs at a molecular level so that the properties of coatings depend not only on the complete chemical coverage of a substrate by a polymer coating molecule but also on how the polymer is packed or oriented on the surface. An optimum configuration of polymers with CF_3 groups can lower the surface tension to as little as 6 mN.m^{-1} [69]. The surfaces of such materials strongly repel most liquids. Examples of fluorinated polymers possessing low-surface-energy have been reported in the literature and include perfluoroacrylates [98], [99], which are used to increase stain and soil resistance of textiles, perfluoromethacrylates [100],[101] and polysiloxanes [102],[103].

Perfluorosiloxanes are used as mould release agents for casting polymethylmethacrylate (PMMA) and fluorochemical elastomer additives are used as release agents for ethylene-propylene, nitrile and fluoroelastomers. They also prevent melt fracturing in film blowing of linear low density polyethylene [80]. Fluorinated groups in such coatings preferentially migrate to the upper surface since this is favoured thermodynamically because it minimises the free energy at the interface between the surface and air.

3.5.1.1 Teflon AF

DuPont have recently introduced a range of completely amorphous fluoropolymers based on copolymers of 2,2-bistrifluoromethyl-4,5-difluoro-1,3-dioxole (PDD) and market the products under the trade name Teflon AF [97] (figure 18). These materials possess all the desirable properties of PTFE and additionally can be melt processed and are soluble in fluorinated solvents. Processing can be performed from solution, casting, spraying, painting, vacuum pyrolysis and even laser ablation [104] and this versatility makes them potentially attractive for release applications and it is being used as a low energy non-stick coating for photomasks in contact lithography in the semiconductor industry [105], [106]. This application requires a release coating that is

optically transparent and Teflon AF satisfies this since it is completely amorphous. At present Teflon AF is quite expensive and this limits applications. Scheirs [107] give full details of the properties of these unusual fluoropolymers.

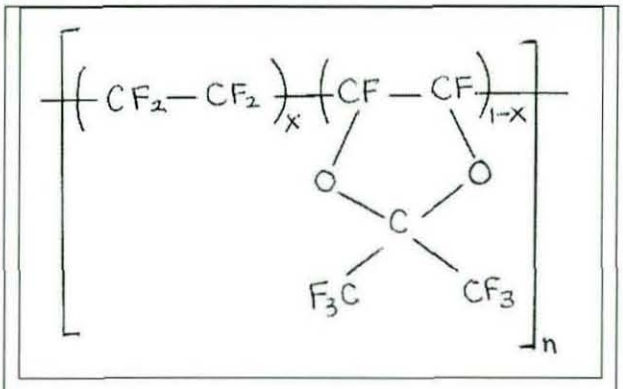

Figure 18. Molecular structure of Teflon AF

3.5.2 Polydimethylsiloxane (PDMS)

PDMS was discovered in 1912 by Frederick S. Kipping [108] but was only manufactured by Dow Corning in 1943. It is more commonly known as silicone oil but comprises materials possessing different viscosities depending on the degree of polymeriszation (dp).

At a dp of 1000 or less, PDMS is a fluid but at dp's of several thousand, PDMS

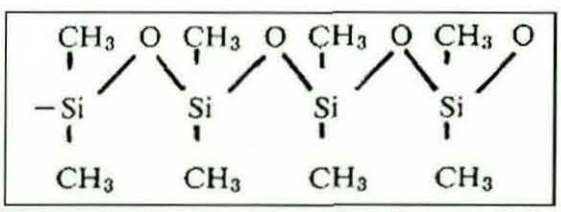

Figure 19.Repeating units of dimethylsiloxane (After Bey[53]).

can be a gum. It consists of an inorganic silica backbone as shown in figure 19. Silicon is tetravalent like carbon and in PDMS it forms two bonds with methyl groups.

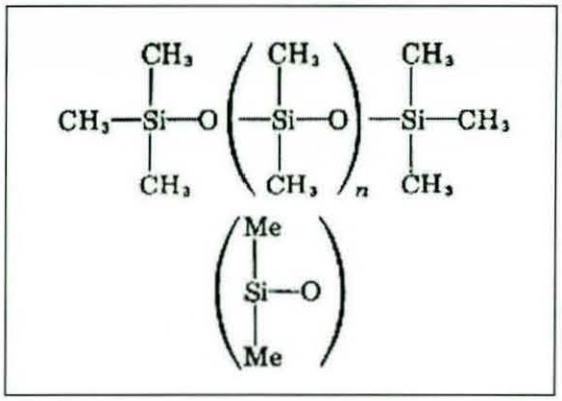

Figure 20 Structure of PDMS (After Arkles [109])

This structure defines the repeat unit and the polymer thus comprises a long, very flexible inorganic backbone terminated by methyl groups. As a consequence of the long silicon-oxygen bond and flatter bond angles of the backbone, there is no barrier to the rotation of the methyl groups about the backbone. Thus the backbone is very efficient in presenting the methyl groups to an air interface and adopts this molecular conformation since it minimises its surface energy. PDMS can be modified depending on the terminal end groups. Figure 20 shows termination by a trimethylsiloxy (Me_3SiO) group. These pendant groups effectively shield the strongly polar backbone and since the carbon atoms are fully saturated by hydrogen atoms, intermolecular forces between adjacent polymer chains are very low. This means that they slide over one another easily without any steric hindrance. Measurements of surface free energies are in the range 20 – 23mJ.m^{-2}. In solution the polymer readily migrates to an air/liquid interface and if used in a coating formulation, thus confers lubrication properties.

As a surface layer PDMS presents a weak boundary layer that has poor wetting properties and low compatibility with non-silicone materials. If a linear polysiloxane is used as a release coating it will probably divide on debonding and would contaminate the moulded part. This is avoided by crosslinking the polymer using a condensation reaction that may involve silicon hydroxide groups. Alternatively an

addition reaction might be used involving vinyl silanes [80]. Silicones form the basis of whole families of solid polymers such as silicone elastomers much used in DIY and building applications and silicon resins that make excellent water repellent coatings for masonry protection. The thermal stability as well as structure related properties of polysiloxanes in general are dependent on the nature of the pendant groups bonded to the silicon atoms. Although PDMS is inert other groups or atoms can replace the methyl pendant groups. For example, if hydrogen atoms are substituted for one of the methyl groups, the resulting polymer is polymethylsiloxane and this can be reactive in certain conditions. Figures 21 and Table 1 below, suggest how different functionality can be conferred to PDMS by substituting different groups at branch points on the molecular backbone.

Functional Groups

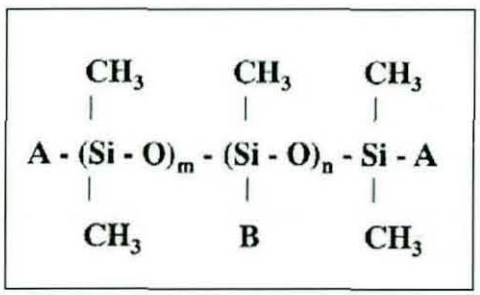

Figure 21 Functionality added to PDMS by group substitution (After Dow Corning [199]).

Group	Position	Function Added
Phenyl	B	Thermal stability
Alkyl	B	Lubrication
Fluoroalkyl	B	Hydrophobicity
Amino	A or B	Softening
Methoxy	A	Durability
Polyether	A or B	Surfactant/lubricant
Acetoxy/Hydroxy	A	Crosslinking RTV
Vinyl	A	Crosslinking LSR
Hydrogen	B	Crosslinking

Table 3 Functionality added to PDMS by group substitution (After Dow Corning [199]).

3.5.3 Non-Stick Coatings for Cooking and Baking

One of the earliest applications for PTFE in the 1950's was as a non-stick coating for frying pans and non-stick coatings are universally associated with cookware by members of the public. The problem encountered with PTFE for this application has always been to find ways to bond the polymer to the metal base of a cooking utensil. Thomas [110] and Herber [111] describe how this seemingly intractable problem was overcome and how subsequent modifications to the chemistry of PTFE and introduction of copolymers have aided its future processing and use. The means by which bonding is achieved is worthy of brief mention.

One of the theories of adhesion emphasises the importance of achieving mechanical interlocking between adhesive and adherend and this effect is very important in getting PTFE to stick to a metal. The metal surface, first degreased using solvents, is grit-blasted to create a rough surface. It is then etched in a mixture of chromic and phosphoric acids and an aqueous dispersion of PTFE granules mixed with a binding agent is applied to the surface and heated at 430°C. At this temperature all the solvents evaporate and the PTFE melts although it does not flow very well because of its very high melt viscosity. This binder component (often polyamideimide) promotes adhesion to the metal substrate and helps anchor particles of PTFE to the roughened metal surface; the slippery molecules of the PTFE effectively bracing themselves against pits and cavities in the surface. The heating process sinters the PTFE and helps it to flow. This first PTFE coating acts as a primer (a term borrowed from painting technology). The primer contains thermally stable pigments and other additives. Other fluoropolymers such as PFA and FEP may be present in the formulation.

Once the primer is applied and has been cured, successive coats of PTFE rich polymer are added, building up the total coating thickness as stratified layers. During the sintering the fluoropolymer tends to migrate towards the surface and the stratification occurs to minimise the surface energy of the system since PTFE has a lower surface energy than the binder. Once a small amount of PTFE has been anchored to the metal substrate in the primer application, further PTFE added in subsequent coatings will

stick well to itself. The quality of the end product is related to the total thickness of the coatings.

TEFAL frying pans, a tradename belong to a French cookware company founded in the mid 1950's, were one of the first non-stick range of pans to be marketed in Europe. TEFAL is a contraction of TEFlon and Aluminium since this was the substrate metal used. Anyone that has used non-stick pans knows that one should not stir the heated contents with a metal spoon but instead use only wooden utensils. This is because PTFE is very soft, especially when heated and the coating can easily be damaged especially if the pan was inexpensive since the coating may then be very thin. Another problem arises from the crystallinity of PTFE because after sintering and cooling to room temperature a pan coating will re-crystallize and form a film with a high microporosity. The main advancements in the technology of making non-stick cooking and bakeware have been in the range of fluoropolymers that can be used and finding more efficient ways to make them stick to metals.

3.5.4 Non-stick coatings to prevent marine fouling

Marine fouling has long been a problem for immersed marine structures and ships hulls and paint manufacturers have struggled to find suitable protective coating. The Paint Research Association and the paint industry in general have been active in publicising new technological improvements, particularly those that utilise the properties of fluorinated polymers. In shipping, barnacles, tube worms, algae and other marine organisms attach themselves to exposed surfaces causing large area encrustations and this can slow down a ship by approximately 5% in serious cases and increase fuel consumption by 40% and necessitates increased frequency of cleaning in dry docks. The worldwide economic consequences are not trivial and runs into billions of pounds each year. Conventional solutions used comprised antifouling paints containing tributyl tin (TBT), copper, arsenic or mercury which act as biocides. These toxic metals leach out from the paint and cause marine pollution that is especially severe in harbour and coastal waters where the ships move slowly and where the water temperatures may be higher which aggravates the problem. Unchecked, these biocides can harm other salt-water shellfish such as oysters together with fish stocks. A new generation of environmentally friendlier coatings use other

biodegradable biocide paint additives or other paints containing Teflon dispersions that inhibit fouling by a presenting a low energy surface to which adhesion is more difficult. These coatings resist adhesion by molluscs but are at their most effective as anti-foulants when under hydrodynamic shear, and exceptionally so on high-speed craft. Fouling can still occur when a ship is laid up for any period. The ship getting underway usually washes off this fouling. Early research on the anti-fouling potential of Teflon found that, despite its exceptionally low surface energy ($18mJ.m^{-2}$), the biopolymeric adhesive secretions from marine organisms were somehow able to stick tenaciously to pure Teflon sheeting in static flow tests even though such adhesion occurred underwater. These sticky secretions comprise amino acid proteins and rapidly bond to surfaces on contact. Understanding this bioadhesion is important in many other areas such as medical implants where moving surfaces of artificial joints must resist protein adsorption and cell adhesion. The ability of marine organisms to stick to PTFE and other low energy surfaces is still not fully understood but it is apparent that no simple relationship exists between surface free energy and adhesion. In the case of PTFE, it is known that this is quite porous and it is thought that marine organisms inject their adhesive into porosities and achieve a mechanical interlock. This might explain the adhesion for PTFE but generally the adhesion mechanism is thought to be chemically complex and only recent publications provide insights into its nature [112] though it does appears to be chemical in origin rather than associated with intermolecular forces. Unlike the sticky feet of gecko lizards, that can walk upside down on polished glass surfaces due to the fact that the soles of their feet are covered by billions of sub-micro keratin hairs [113], [114], van der Waals forces are not responsible for the stickiness of barnacles. Even geckos can't stick to Teflon!

Many antifouling marine paints are based on polyurethane coatings. Research has shown [115] that, for fluorinated urethanes, the adhesion of marine organisms is a minimum for coatings with surface energies ~$25mJ.m^{-2}$ and actually increases gradually for surfaces with lower energies. The smoothness of a coating is also known to influence its ability to resist fouling. Bonafede and Brady [116] suggest that the adhesive from marine organisms initially penetrates surface cavities and surface porosities in PTFE and then after chemical bonding has occurred, mechanical interlocking of the crosslinked adhesive contributes to the tenacious attachment of the organism to the surface.

Andrade [117] reports a correlation between surface molecular mobility and ability to form permanent adhesive bonds whereby increased polymer surface mobility of the molecules comprising the coating reduces the possibility for adhesive bonding. Brady [118] describes such a molecularly mobile surface as providing "a moving target", making it difficult for a compatible adsorbate functional group to latch onto and bind to a specific site on the mobile molecule bound to the surface. Bonafede and Brady [116] in studying fluorinated urethanes with different levels of PTFE fillers conclude that supple, soft polymers with low glass transition temperatures may be more effective as antifouling materials. The suggestion is that surface roughness and molecular mobility play an important part in the success of a non-stick coating. According to Comyn[80], the viscoelastic properties of a non-stick coating are more important than the surface chemistry .

Silicone polymers are another ecological solution, which utilise the low surface energy of silicone binders in formulated paints. However, the natural salt-water environment in harbours comprises a combination of chemicals that can swell and chemically degrade the performance of these materials over time making them less effective than their toxic predecessors.

Perfluoropolyether based coatings have also been shown to be effective as anti-fouling agents for marine applications, although since the ban on the use of CFC's by the Montreal Protocol, finding convenient and effective solvents has proved difficult rendering these polymers rather intractable materials to process although one effective solvent that could be used is compressed carbon dioxide. Perfluoropolyether possesses high thermal and chemical stability, low surface energy and a very low glass transition temperature. Different functional groups (alcohols, isocyanates, epoxies and methacrylates) can be added to produce a wide range of materials.

3.5.5 Silicone Release Coatings

These types of coatings are frequently used to make release liners to carry and protect pressure-sensitive adhesives (PSAs) until they are applied to a surface when the liner is peeled away and good release properties are required to effect this removal. The

liner is usually some form of paper substrate impregnated or coated with a release formulation. The coating is very thin ~ 1 micrometre or less and typical surface free energies can range from 10 - 20mJ.m^{-2} depending on formulation. The development of faster curing and more aggressive adhesives for ever more demanding applications has spurred the development of release liners that will be effective for all product ranges. A combination of bulk and surface properties are required including inertness to at least one of the separating surfaces at the temperature of the release process and low surface energy. Release in this application is a complex interaction of the bulk and surface effects including adhesive and release coating thickness, viscoelasticity, delaminating speed, angle of peel, humidity and temperature. Only the surface properties of these types of coating are of relevance to the present research on mould release agents. Release performance for mould release agents is most often assessed qualitatively by performing an automated peel test using a strip of adhesive tape and measuring the force required to detach it. Similar tests are performed manually in mould release applications where the ease of release of adhesive tape to a treated mould surface indicates the effectiveness of the release coating. Essentially PSA release formulations must ensure a weak interface exists between the adhesive and liner itself and additionally should possess a low coefficient of friction. These requirements are most often satisfied with polydimethyl siloxanes though some fluorosilicones such as polymethylnonafluorohexylsiloxane (PMNFHS) [107] are useful when exceptionally low surface energies are required. Surface energies lower than PDMS are engineered by lengthening the pendent fluorocarbon sidechains, which has an enhanced shielding effect in fluorosiloxanes.

Some authors such as Owen [119] believe a definite correlation exists between polymers possessing a low glass transition temperature (T_g) and those making good PSA release agents since low T_g is associated with good molecular chain mobility and by implication low surface energy. Ho [120] in his study of minimally adhesive surfaces stated that a low T_g was desirable to minimise mechanical interlocking of adherents. It is interesting that other authors such as Andrade [117] engaged in marine antifouling research make similar assertions. It is perhaps not surprising then that many good release coatings essentially comprise a cured rubbery silicone.

Bey [121] states that silicones that are potentially useful for release applications should possess:

(i) low polarity to minimise intermolecular attractive forces
(ii) low surface energy to prevent wetting by adhesives
(iii) high polymer chain flexibility to allow surface mobility
(iv) molecular incompatibility with other organic polymers and adhesives

The ability to form a weak boundary layer can be added to this list.
Bey [121] describes how such compounds can be synthesized by taking a silicone with reactive end groups and combining it, using a metal catalyst, with another siloxane that can function as a crosslinker (figure 22). Curing of the polymer occurs by a condensation reaction.

Contact angle measurements have been the principal method of calculating surface free energies for many years and their use in comparing different PSAs was pioneered by Gordon and Colquhoun [122], amongst others. Packham [123] discusses how a different analysis independent of contact angles and based on the work by Johnson, Kendall and Roberts [124] can be used to calculate surface energies.

The peel force of the adhesive from the paper however, often does not correlate with contact angle measurements or with surface analysis by X-ray photoelectron spectroscopy but instead correlates with rheological properties [80].

An important relationship that was first used in 1926 to understanding adhesion and release behaviour is expressed by Harkins' equation [125]:

$$S = W_a - W_c \quad \text{.....(23)}$$

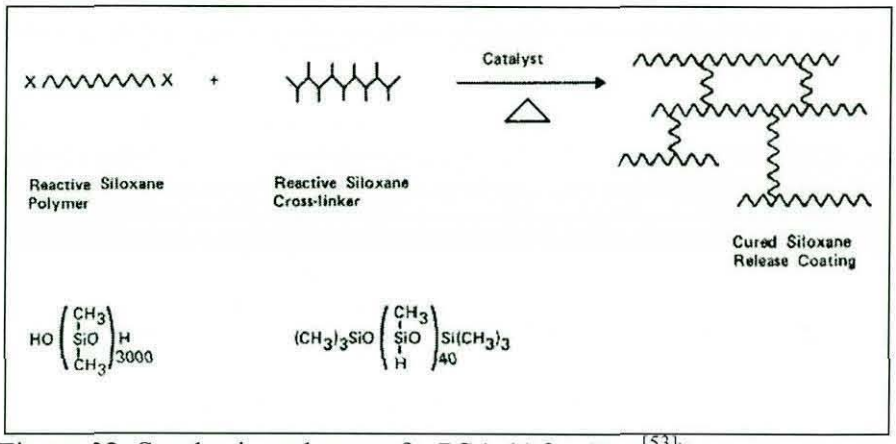

Figure 22. Synthesis and cure of a PSA (After Bey[53]).

where S is the spreading coefficient of the adhesive on the release coating, W_a, the work of adhesion, i.e. the change in energy per unit surface area when two surfaces come into contact, and W_c is the work of cohesion of the adhesive. This is twice the surface energy of the adhesive, as two surfaces would be produced by cohesive cleavage.

For a good adhesive we would want the bond between two surfaces to be strong such that failure does not occur at the bonding interface between the surfaces but through cohesive failure in the bonding material itself (or through cohesive failure in one of the parts being joined). A positive spreading coefficient is thus required with the work of adhesion being higher than the work of cohesion.

For a good release agent we require the exact opposite. In this case the release agent is analogous to a very poorly performing adhesive bonding two surfaces. We want the adhesive to separate at the interface (interfacial failure). Thus we want the spreading coefficient to be negative (i.e. the "adhesive" will not wet either surface) and this requires the work of cohesion (the energy necessary to cause failure within the bulk of the "adhesive") to be greater than the work of adhesion.

The Harkins relationship is obeyed for a wide range of PSAs and release coatings. Packham [123] makes the point that it is necessary to distinguish the work of adhesion from the fracture energy G which is a measurable parameter independent of surface energies calculated by contact angles measurement. Andrews and Kinloch [126] have shown that in the case of a simple adhesive

$$G = W_a \times \varphi \quad \text{.....(24)}$$

where φ is a temperature and rate dependent viscoelastic term which acts as a multiplying factor. Measured fracture energies are several orders of magnitude higher than works of adhesion and the above equation is one attempt at formulating a quantitative relationship between work of adhesion and practical bond strengths manifest in the measured fracture energy.

3.5.6 Hydrophobic Coatings

Hydrophobic materials find very wide applications from waterproof clothing and masonry protection to high technology examples such as ice-phobic surfaces for shipping and aviation. Hydrophobic surfaces have mainly nonpolar groups, like hydrocarbon chains. While there is relatively strong hydrogen bonding and dipole-dipole interactions in hydrophilic liquids, weaker van der Waals interactions are present in hydrophobic materials. As a consequence, hydrophobic materials typically have very low surface energies. Meyer [127], [128] describes the application of hydrophobic coatings in masonry protection and typical coating formulations comprise silanes, siloxanes and silicone resins. A requirement in masonry protection is that ingress of water from outside a building is prevented whilst ensuring that pores in the building materials are not obstructed so that they remain permeable to water vapour. Coatings must possess the ability to wet the pores and capillaries without clogging them. Pocius [129] discusses the kinetics of pore penetration and refers to research published by Packham [130].which is reproduced below. Packham argues that the penetration of a liquid into a capillary (considered here as a pore) is given by Poiseulle's Law:

$$x.\, dx/dt = r^2 P / 8\eta \quad \text{.....(25)}$$

Where x is the pore penetration distance; η the viscosity of the adhesive; P is the capillary pressure; t is the time an r is the radius of the pore. The capillary pressure is given by:

$$P = 2\gamma_{LV} \cos\theta / r \quad \text{.....(26)}$$

where θ is the contact angle and γ_{LV} is the surface free energy of the adhesive.

Schonhorn, Frisch and Kwei [131] studied the wetting of a surface by a polymer and Newman [132] derived the following expression that describes the change in contact angle with time as a surface is wetted:

$$\cos\theta(t) = \cos\theta_{\infty}(1 - a\exp(-ct)).....(27)$$

where θ_{∞} is the contact angle at infinite times, θ(t) is the time dependent contact angle and 'a' and 'c' are adjustable parameters. Combining the above three equations gives:

$$x^2(t) = r\gamma_{LV}\cos\theta_{\infty}/2\eta\ [(t - a/c) + a\exp(-ct)/c]\ .....(28)$$

and this describes the distance a pore is penetrated by an adhesive. Packham [130] used this equation to consider the wetting of different pore sizes by polyethylene in air at 200°C for which γ_{LV} =23.5 $mJ.m^{-2}$ and over a timescale of 20 minutes. The following results were obtained (Table 4):

Pore radius (micrometres)	Distance penetrated (micrometres)
1000	220
10	22
1	7
0.1	2.2
0.01	0.7

Table 4.Penetration depth for different pore radii [129].

These calculations show that only very small pores are completely filled by an adhesive with the consequence that to engineer good adhesion between two surfaces we should ensure that a fine morphology is present and that the adhesive has a sufficiently low viscosity. Conversely a fine morphology will be detrimental for abhesion and we would need to ensure that any fine morphology present on a surface should be filled by a mould release compound. Good adhesion is required , however, between the release agent and the metal to which it is applied. Clearly the substrate

must be clean but its ability to wet the surface is a function of its microstructural roughness.

In building materials, coatings have been formulated that are able to wet the small pores in building materials without blocking them and these formulations often contain molecules that act like the bristles of a molecular brush where one end of the bristle is bound onto the surface that is coated and the other end is free to push away a water molecule. Silicone resins are used in these coatings and bind to the masonry by a crosslinking condensation reaction to form a three-dimensional stable structure resembling quartz. Unlike quartz though where each silicon atom is bonded to four oxygen atoms, in these resins one of the oxygen atoms is replaced by an organic group such as a methyl which imparts a water repellent property. Applied to a glass substrate such coatings would yield a transparent, tack-free water repellent surface.

The interest of these coatings in relation to release agents is two fold. Firstly, to reiterate the point already made that a low energy surface is only one desirable property of a release agent. Clearly a masonry coating is not optimised for application as a release agent. Secondly, the modified quartz structure has the property of binding to many different types of substrate and if a different organic group was substituted that would confer different properties, then the basic advantages of a silicone resin might be used to engineer a good non-stick coating or release. In fact silicone resins are used in many commercial release agents.

3.5.7 Fluoroalkylsilanes

The properties that make water repellents successful on a molecular scale have been identified in the case of hydrophobic masonry coatings discussed above. What is required is a molecule that possesses a duality of behaviour where one end reacts in with a surface and the other end possesses non-wetting functionality. Fluoroalkylsilanes are one group of compounds that possess such characteristics. The fluoroalkylsilane molecule is thus bifunctional with a silane termination which will bond to many different types of substrates whilst a highly fluorinated chain is terminated with a CF_3 group at the other end. After molecular bonding with the substrate, the fluorinated chain, with its tendency to orient itself away from the

surface, forms a tightly packed comb-like structure and provides a low-energy release surface. Such molecules form self assembled monolayers (SAMs) on substrates [133], [134].

Fluoroalkylsilanes are relatively new materials that have been used for hydrophobic textile coatings [135] but are finding new applications in niche areas such as ice phobic coating applications [136] and in particular, the semiconductor industry and there is great interest in their application in Japan in particular. Several recent publications suggested the potential of fluoroalkylsilanes. Mayer *et al* [137] discuss their use for adhesion control in micro-electromechanical systems (MEMS) and this appears to be a key application area with many papers appearing in the literature. Burns *et al* [138] discuss their application as model lubricants in studies of nano-scale friction investigated using the latest scanning probe technologies. Tadanaga [139] has described a lithographic masking application whereby the hydrophobicity of fluoroalkylsilane coatings can be destroyed by depositing the coating over a thin layer of titanium dioxide. Irradiation of the mask by ultra-violet light then causes a catalytic reaction between the titania and the fluoroalkylsilane which breaks the bonds between the molecule and the surface.

Fluoroalkysilanes have many interesting tribological properties as non-stick coatings and have been investigated and reported by several authors such as Shanahan *et al* [140], [141]. It was envisaged that these compounds might be used singly or in combination with similar bisfunctional chemistries to engineer a suitable barrier between a metal moulding tool substrate and a resin rich moulded part but it is noted that their performance could be impaired in the relatively aggressive environment encountered in industrial composite moulding where contact with thermosetting epoxide resins at high temperatures and under elevated pressures occurs.

One particular commercially available fluoroalkylsilane is tridecafluoro-1,1,2,2-tetrahydrooctyl) triethoxysilane $C_{14}H_{19}F_{13}O_3Si$. (figure 23). This is marketed by ABCR-Gelest (UK) under the trade name Dynasylan F8261. It is used at concentrations of approx 1% by weight in a solvent such as hexane and is a fluoroalkyl functional silane that can be applied to a wide variety of substrates. Samples are dip or spray coated and the coatings cured in an over at 110°C for

30mins. Gelest produce several types of Dynasylan. That specified above is used in waterproofing and oil-proofing applications. Other products are intended as hydrophobic and oleophobic coatings for porous and non-porous ceramic substrates. Use of Dynasylan F8261 as part of a mould release formulation applied to a metal is a potential new application.

The properties of fluoroalkylsilanes can be summarised as: -

- Coated surfaces are hydrophobic
- Coatings possess low adhesion energy
- Coating thicknesses are typically only a few monolayers
- Coatings will bond to clean metal substrates
- Coatings are easily applied and thermally stable
- Use non-toxic solvents

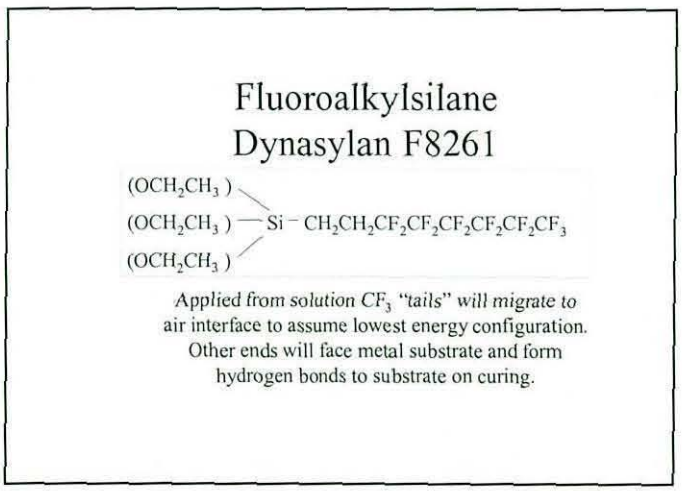

Figure 23. Dynasylan molecular structure.

Dynasylan bonds to the substrate via a hydrolysis and condensation reaction. Covalent bonding then occurs at the substrate surface. The application of heat cures the coating allowing crosslinking to occur with the elimination of water (figure 24).

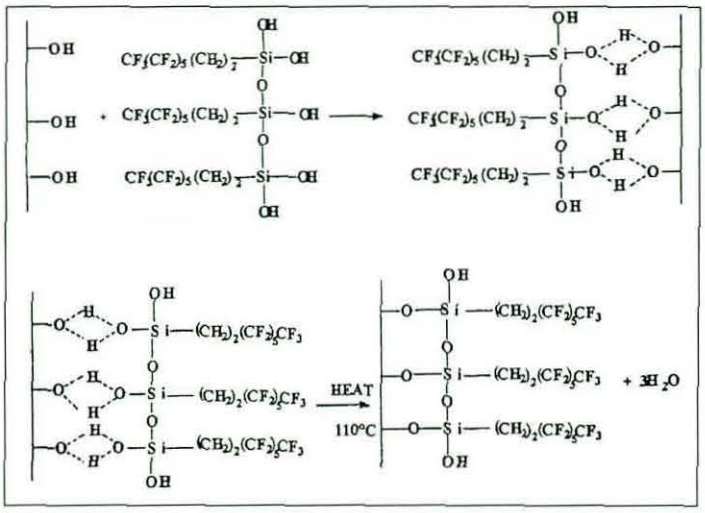

Figure 24. Reaction and cure of Dynasylan (After Shanahan [141])

Materials were coated with this fluoroalkylsilane and their performances as a mould release agent were evaluated.

3.6 Electroless Nickel/PTFE Composite Non-stick Coatings

Nickel/PTFE composite alloys having excellent tribological properties and durability were developed in the 1990's and a number of publications in the literature have evaluated their application as a mould coating material [142], [143].

The process of incorporating non-metallic species into a metallic coating developed from the electroplating industry. Electroless composite coating technology was patented by Metzger [144], gaining popularity from the early 1970's, and was based on a nickel-phosphorus matrix [145].

These coatings are produced by the chemical reaction of metal salts and a reducing agent. Electroless coatings can be applied to many substrate types, such as metals, alloys, or non-conductors with excellent thickness uniformity, typically ranging from 10 to 25 micrometres, and are suitable for coating complex moulding tools provided they could be lowered into a treatment bath. Different types of particles can be added to the matrix phase depending on what final properties are required for the coating and careful process control is required to deposit these particles uniformly within the matrix. For the mould release applications of this study, the inclusion of very fine particles of PTFE is of interest. These particles can be in the range of 0.4 to 1.0 micrometres and the low frictional properties of this fluoropolymer are transferred to

the coating. The nickel-phosphorus matrix provides hardness and durability in the coating and this is influenced by the volume percentage of phosphorus in the alloy, typically between 4% and 12%. The particle loading also affects the hardness and volume percentages in the range 15% to 25% are typical. A compromise in final properties of the coating has to be established between lubricity, hardness and wear resistance. Once deposited the coating can be heat-treated to promote the development of hard nickel phosphorus phases and sinter the PTFE to enhance its adhesion to the substrate. The performance of the material at elevated temperatures is limited by the thermal stability of PTFE and this limits its use in practice to 400°C. For applications requiring higher temperatures, molybdenum disulphide might be used to provide lubricity though the beneficial properties of PTFE would be lost.

The first commercial electroless nickel/PTFE composite coating system was developed by Ebdon [146] in conjuction with Fothergill Engineering Surfaces. Apticote® electroless nickel/PTFE coatings have been developed by Poeton Engineering (amongst other companies) and the company claims that these coatings outperform hard chrome coatings in dry running conditions. Poeton claim that their Apticote 450 coating has low wear properties at low loading and a bulk hardness of about 250VPN although this can be increased after heat treatment at 300°C to 400VPN. The exceptional properties of the Apticote coating are believed to originate from the high concentration of the PTFE dispersed phase comprising very tiny beads of PTFE with approximate diameter ~ 200 nanometres. Stevens [147] discusses the application of Apticote coatings in the moulding of thermoplastic trays and extols their properties as replacements for conventional mould release agents.

3.7 Mechanical Tests for Non-stick polymers

The close relationship between mould fouling and adhesion has been established in the previous discussions and, in the development of release agents in particular, it is desirable to have some means of testing how good a coating is in preventing adhesion and hence in reducing mould fouling.

Established and well-documented testing methods used for adhesive bonding cannot be used to test mould releases. The problem of devising test methods for releases is

not trivial because if the release agent is any good at all, the release forces will be very small, particularly in the case of a laboratory test where samples usually possess small or modest surface areas. In industry, release performance is most frequently assessed qualitatively by performing a peel test using a layer of adhesive tape. The absence of a standard quantitative method of release agent evaluation has stunted progress in the characterisation of mould releases and prompted research to redress this issue. Many of the methods proposed are associated with internal release agents and on the measurement of ejection forces for a thermoplastic moulding operation.

Percell [148] measured ejection force by mounting a piezo-electric device to the ejector rod. Such methods are, however, specific to the moulding equipment used and cannot be generally applied to external releasants. Another approach first adopted by Wilkomm [149] was to use a modified rheometer to measure the shear force required to separate a moulded part from a substrate coated with a release agent.

Reeves and Packham [75] used a similar test apparatus to examine the adhesion of rubber to steel substrates. The use of a tapered double cantilever beam by Clayfield and Berry [150] was one of the earliest methods proposed to measure the adhesion of external semi-permanent mould releases.

3.7.1 The "blister" test method

Dannenburg [151] first developed the blister test in 1961 and used it to measure adhesive fracture energies. Parry & Wronski [152] and Kinloch [153] further developed this method and a body of literature and results accumulated over the last twenty years testify to its usefulness in quantifying adhesive fracture energies. The principles of the test are described in section 4.6.2. The following gives an account of the theory.

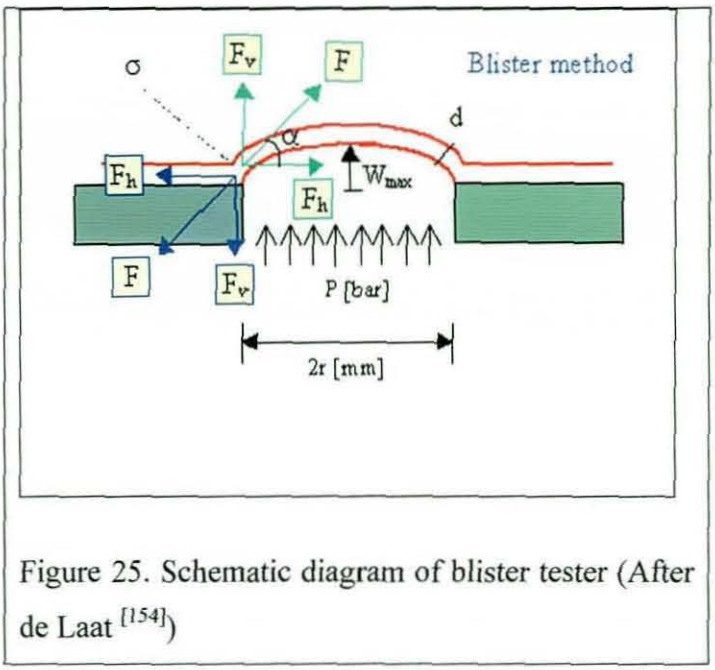

Figure 25. Schematic diagram of blister tester (After de Laat [154])

Figure 25 shows a schematic diagram of the blister test geometry. It is assumed that the blister is circular and that the circumference at the start of the measurement is equal to the circumference of the drilled hole (2π r). The total vertical force depends on the surface area of the hole (πr^2) and the pressure (P). Before delamination takes place, the stresses induced by the liquid or gas pressure should not exceed the maximum tensile stress of the coating (σ_{max}). Therefore the coating thickness (d) is significant. Besides the adhesion energy, the detachment pressure (P_d) and the angle (α) of the coating layer, are also dependent on the viscoelastic behaviour of the coating, which is neglected in this model.

The forces acting on the system can be resolved into their vertical and horizontal components F_v and F_h. Delamination only takes place when simultaneously the following conditions are fulfilled:

1. F_v > Adhesive strength
2. $\sigma < \sigma_{max}$

As soon as the induced stress (σ) exceeds the maximum tensile stress of the coating (σ_{max}) the coating will fail. If the area of the hole is too large, then σ exceeds σ_{max} before F_v exceeds the adhesive strength, which implies that there will be no

delamination, but just failure of the coating. So it should be clear that, when using this method, the dimensions of the "hole" must be chosen very carefully

Following the analysis given by Parry & Wronski [152] the adhesive fracture energy

$$G_c=P^2a/E\ f(h/a) \quad \ldots\ldots\ldots\ldots\ldots\ldots(29)$$

where E is the modulus of the adherent plate and f(h/a) is a dimensionless geometric factor dependent upon the adherent plate thickness, h, and crack radius, a. Finite analysis by Bennet [155] showed that for a thick plate,

$$f(h/a) \sim 2 \text{ and so } G_c=P^2a/2E \quad \ldots\ldots\ldots\ldots\ldots\ldots(30)$$

Since E is a constant G_c can be found by determining the radius of the blister delamination for a given pressure P.

Briscoe and Panesar [156] proposed a method of measuring the release force using the 'blister test' originally developed for measuring low adhesion interfaces. An apparatus based on this test was constructed for this research and further details are given in section 4.6.2. Although this method proved very successful for Briscoe it was used to study the effects of external releasants on the adhesion of elastomeric materials such as polyurethane [157], whereas this research is concerned with thermosetting composites possessing a much higher elastic modulus when cured. Blanchard [86] appraised the blister test and concluded that it was unsuitable for thermosetting compounds. Even in relatively recent publications [82], quantitative measurements of release force seem to be avoided because of the experimental difficulties and qualitative assessments of performance are given instead. New methods of evaluating mould releases continue to be developed [158] which testify to the fact that no single method has yet been accepted as being universally applicable

Adhesion is one of the most complex and important parameters that determine the quality of coating systems. The theoretical adhesion strength is a result of all interfacial and intermolecular forces. However, the practical adhesion strength, which is the force or energy needed for detachment of the coating, never reaches this

theoretical value. The difference is caused by the hollow spaces and defects at the interface of substrate and coating. It is assumed that the delamination process develops from the weakest point.

Due to the fact that the applied force or energy is not only used for delamination but also for plastic deformation of the coating, the concept is even more complicated. Environmental parameters (temperature, diffusion of water, oxygen, etc.) contribute substantially to the adhesive strength of a system.

3.8 Analytical Techniques

A wide variety of analytical techniques can generate useful information in satisfying goals of the present research. Contact angle analysis gives information pertaining to surface cleanliness and surface energies and both are important aspects of this research.

Microstructural studies of cleaned substrates give data about surface roughness and the scanning electron microscope (SEM) is the technique of choice in providing this information since it can image over a wide range of magnification and provide bulk analysis in combination with the energy dispersive X-ray microanalysis (EDX) facility built into modern microscopes.

Development of a good release agent requires a means of studying interfacial surface chemistry and X-ray photoelectron spectroscopy (XPS) and Auger electron spectroscopy (AES) are ideal techniques to provide this information. Chemical information is also complimented using infrared (IR) spectroscopy.

Other important measurements relate to the thickness determinations whether these are associated with residual contamination following cleaning or the thickness of an applied low energy coating. AES, ellipsometry and interference microscopy can all provide this information.

Finally Atomic Force Microscopy (AFM) has the ability to provide qualitative comparative information on frictional forces present on treated surfaces, correlating these with surface relief and this is useful in the study of low energy surfaces. Some of these techniques will now be discussed in detail.

3.8.1 Scanning Electron Microscopy & X-ray Microanalysis

Scanning electron microscopy is such a widespread analytical technique that a detailed explanation of its operation is unnecessary. Where topographic images are required, a primary electron beam is focussed onto a sample (mounted in the vacuum chamber of the microscope) and scanned using deflection coils that raster the electron beam over a small area on the sample surface (figure 26 overside). The sample surface, frequently sputter coated with a few nanometres of gold to render it electrically conducting, emits secondary, inelastically scattered, lower energy electrons that are detected by a positively biased collector.

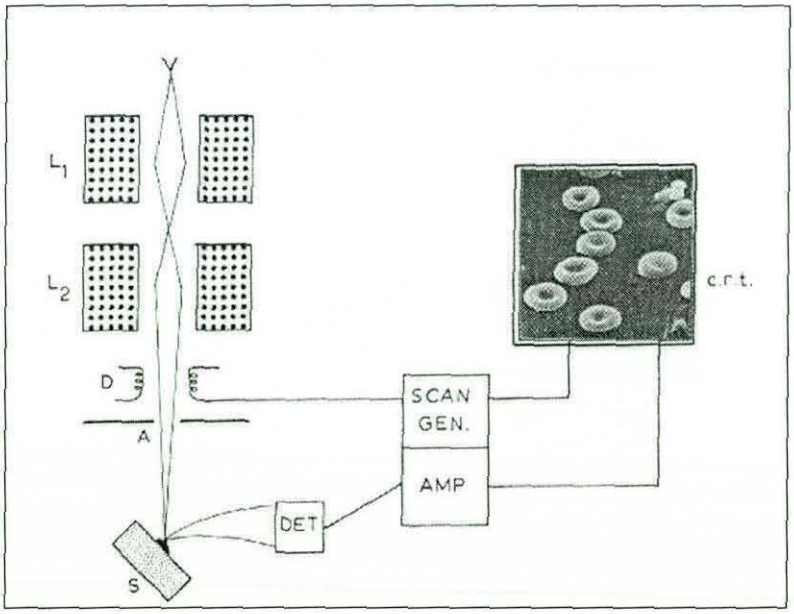

Figure 26. Schematic diagram showing the operating principles of an SEM. An electron beam is focussed on to the specimen (S) using condenser lenses (L_1 and L_2) and it scanned across the specimen surface by deflector coils (D). Secondary electrons are then emitted from the specimen surface and these are converted into a current by the detector; this current is amplified and used to modulate the brightness of a cathode ray tube (c.r.t.) which is scanned in synchronism with the area scanned on the specimen surface.(After Goodhew [205]).

The electrons strike a scintillator that emits photons of light. A photomultiplier tube amplifies these and the resulting electrical signal is used to modulate the brightness of a cathode ray tube (CRT). The raster on the CRT is synchronized with that traced on the sample surface by the primary electron beam. An image magnification is obtained which is simply the ratio of the area scanned on the CRT to that scanned on the sample. Different contrast mechanisms can be invoked depending on the type of electron detectors used. High-energy electrons from the primary beam penetrate a few micrometres into the sample surface and can excite X-ray photons characteristic of the atoms comprising the sample. This is the basis of EDX analysis. These can also be detected and used to provide elemental information, which compliments topographic data.

3.8.2 Atomic Force Microscopy (AFM)

AFM is one of many scanning probe techniques that share a common general operating principle (figure 27). An atomically fine tip often made from silicon or silicon nitride is mounted on the end of a cantilever, which is mechanically scanned in a raster pattern over a surface of interest using piezo-electric transducers.

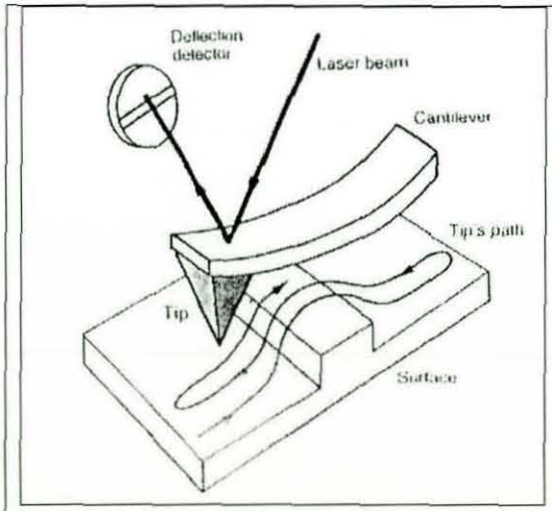

Figure 27. Schematic diagram of an AFM (After Feast, Munro & Richards[159])

These permit very precise and accurate control of its movement. As the tip is brought close to the surface to be scanned it is influenced by interaction between atoms in the tip and those in the surface. Theoretically this is described by the Lennard-Jones potential [160] (figure 28) :

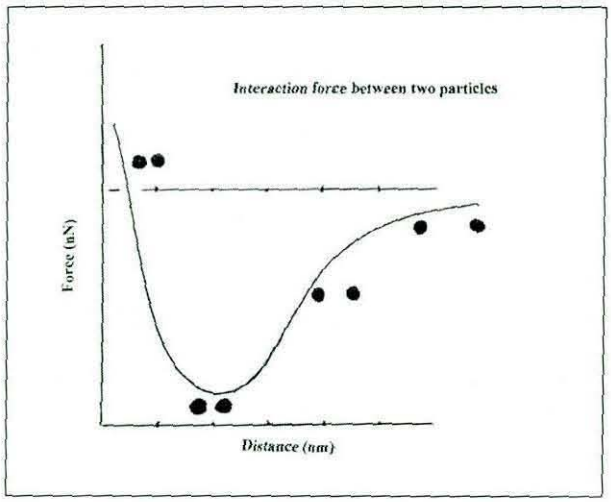

Figure 28. The Leonard-Jones Potential

$$V(r) = - A/r^6 + B/r^{12} \quad \text{.....(31)}$$

where V(r) is the potential and A and B are interaction constants for a separation value of r. The interaction force is

$$F = -dV(r)/dr = -6A/r^7 + 12B/r^{13} \quad \text{..... (32)}$$

At separations of about 0.4 nm a net attractive force exists but as the separation is reduced and the outermost atoms of the tip begin to touch those of the surface, strong electron-electron repulsive forces become dominant. Figure 29 shows the typical tip pull off force-distance curves for NiP, Ge and Si semiconductor substrates. The different pull off forces reflects different Hamaker constants of these substrates [9].

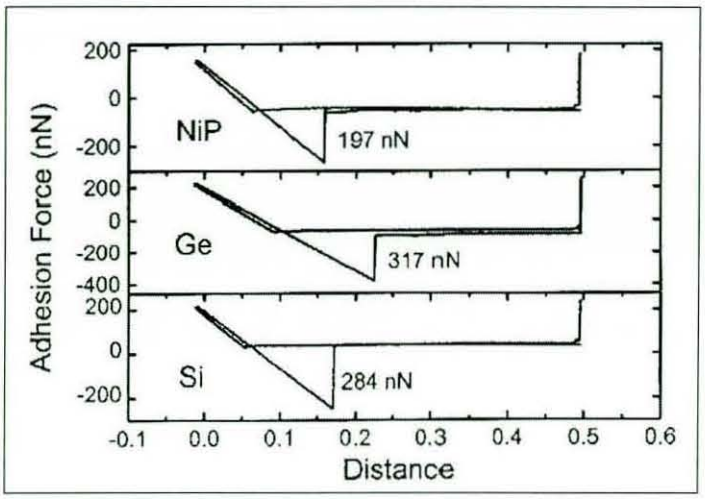

Figure 29 AFM pull-off force distance curves (After Luk'yanchuk [10])

The cantilever to which the tip is attached has a low spring constant and is deflected as the tip tracks the surface contours. A diode laser is focussed onto the back of the cantilever close to the tip and reflected light detected by a two or four quadrant photodetector which converts the minute perturbations of the cantilever into an electrical signal. Using feedback controls either the separation between the tip and surface can be kept constant and the varying force measured or conversely the force can be kept constant and the separation varied. By assigning an arbitrary colour scale to the parameter measured three-dimensional maps of the scanned surfaces can be displayed. The technique possesses atomic resolution provided the tip is not damaged and areas scanned can be as small a few micrometres square up to about 100 micrometres square. Lateral resolution can be less than 5nm with height resolution of 0.01nm. The force-distance curve is critical to the operation of the microscope.

The contact mode of operation in which the tip is mechanically contacted with the surface and then retracted is the mode most likely to result in damage to the tips since water or other contaminants absorbed onto the surface can cause the probe to stick to the surface. Increased retraction force amplitude then has to be applied to the cantilever to remove the tip and during the time taken for this action, the tip can be dragged along the surface as scanning continues.

AFM was unable to provide much useful topographical information relating to the cleaning of tooling samples studied in this thesis because the surface roughness of the

samples was largely incompatible with the sensitivity and resolution of the technique. Scanning electron microscopy was more useful in this context.

AFM did, however, prove itself to be very useful in providing qualitative comparisons of the "stickiness" of surfaces treated with different mould release agents. This information was obtained by operating the AFM in such a way that the cantilever was excited into resonance oscillation (at about 300kHz with an amplitude of about 60nm) with a piezoelectric driver. This is called the "tapping mode" since the tip is made to strike the sample surface during the downward cycle of each oscillation. Once the tip is attracted to the surface it is tracking, the oscillating cantilever experiences a damping force if the surface is adhesive which tries to keep the tip in contact with the surface. The amplitude of oscillation is such that it will be sufficient to overcome this and then carries information about the pull-off force required. Effectively the sinusoidal response of the cantilever will lag behind that of the oscillation impressed upon it and this phase lag can be extracted by operating software and the resulting signal used to modulate an image contrast.

Such phase images can provide information concerning the viscoelastic properties of the sample and adhesion forces. Since the resonant frequency of the cantilever is very high several thousand pull-off force measurements may be made for a very small area scanned. To use this technique effectively to qualitatively compare the stickiness of different surfaces (resulting from application of different mould release agents) it is necessary to largely eliminate large differences in surface height on a microscopic scale and hence substrates need to be polished to a mirror finish. Quantitative data by this means is very difficult to obtain, relying on precise knowledge of the spring constant of the cantilever used, a means of calibrating a microscope and a thorough understanding of the complex interactions between tip and surface within the size domain of the technique. Adhesive force measurements can be related to the AFM pull-off force via the Johnson, Kendall and Roberts (JKR) theory of adhesion mechanics [161]. This theory provides a means of calculating the surface energy of a solid directly in terms of the interactions between solid surfaces rather than through the use of contact angle measurements [129]. The theory can be used to derive the following equation:

$$F_{ad} = 3/2\pi \; RW_{SMT} \quad \ldots\ldots\ldots\ldots\ldots\ldots\ldots\ldots\ldots (33)$$

where $$W_{SMT} = \gamma_{SM} + \gamma_{TM} - \gamma_{ST} \text{ (after Dupré)} \ldots\ldots\ldots\ldots (34)$$

W_{SMT} is the thermodynamic work of adhesion for separating the sample and tip with associated surface free energies of the sample (S) and tip (T) in contact with the medium (M) and where γ is the interfacial surface free energy of the two interacting solid surfaces ; F_{ad} is the pull-off force required to separate an AFM tip of radius R from a planar surface. If the two materials in contact are the same then the work of adhesion is equal to the work of cohesion. This is rather limited since it is only possible to directly measure the surface free energy for a material which is the same composition as that which the AFM tip is made from but the principle is valid.

3.8.3 Interference Microscopy

A number of publications discuss the techniques and applications of interference microscopy [162 - 164]. In this particular application a Mirau interference objective was used with a Zeiss Polarizing Microscope to determine the thickness of organic films coated onto glass microscope slides. This special objective functions as a two-beam interferometer. This divides originally coherent light into two beams of equal intensity, directing one beam onto a reference mirror and the other onto the specimen, and measuring the optical path difference (the difference in optical distances) between the resulting two reflected light waves.

The principle of the Mirau objective (figure 30) relies on placing a reflection reference mirror in the centre of the objective lens, and interposing a half mirror between the objective lens and the specimen. These components are so arranged that an interference pattern will appear if the system is focused upon the specimen.

If the specimen is inclined, localized interference fringes will appear. Fringes will also appear if there is a step change in vertical height and this can be used to measure the thickness of a coating by carefully removing part of the coating from the glass-supporting slide using a very sharp razor blade (figure 31).

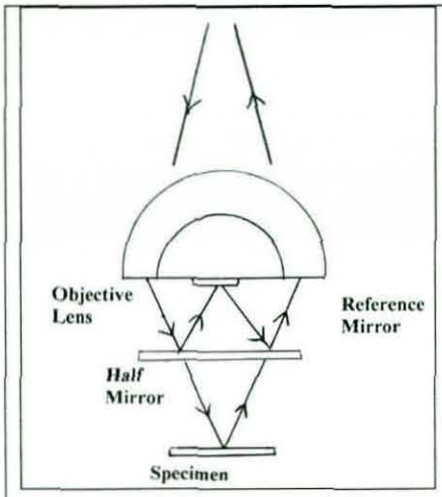

Figure 30. Mirau objective schematic and in use on a Zeiss microscope

In use, adjustments are made to bring the interference pattern to the centre of the field of view, which aligns it with the optical axis, since the centre of the reference mirror coincides with the optical axis. A monochromatic filter passing a wavelength of 546nm may be used to view the fringe pattern.

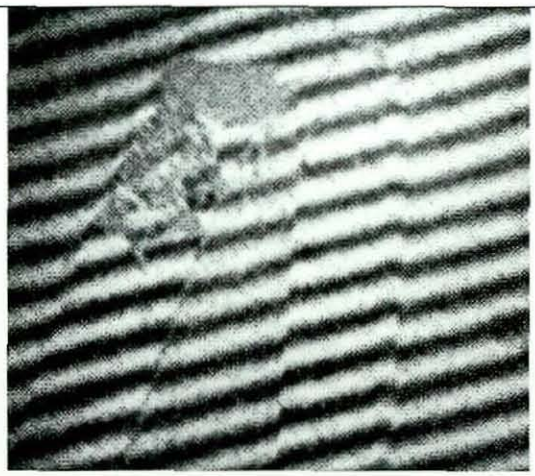

Figure 31. Interference fringes

The distance between the fringes is given $N\lambda = 2nt.\cos\theta$ .....(35)

where N is an integer, λ the wavelength of light used (546nm if a mercury green filter used), n is the refractive index of the medium (in this case air so that n=1), t is

thickness and θ the angle of incidence of the light (perpendicular to the sample in this case so that cosθ = 1). Hence t=N. λ/2 where N=1,2,3,...etc. Consequently each time the thickness changes by λ/2, another interference fringe is seen. Referring to figure 40, the distance between the fringes is thus equal to 546/2 = 273 nm. Fractions of this thickness can then be determined by the displacement of adjacent fringes at a discontinuity such as that shown in figure 31.

3.8.4 Ellipsometry

Ellipsometry is an optical technique that uses polarised light to probe the dielectric properties of a sample. The most common application of ellipsometry is the analysis of very thin films. Through the analysis of the state of polarisation of the light that is reflected from the sample, ellipsometry can yield information about layers that are thinner than the wavelength of the light itself, down to a single atomic layer or less.

Ellipsometry measures the change in polarisation state of light after reflection from the surface of the sample. This is characterised by two angles: iΔ, a phase change term, and ψ, the tangent of which describes the amplitude change. These experimental values are measured and are related to the optical constants of the reflective surface, expressed by the Fresnel reflection coefficients R_p and R_s, by the equation:

$$\rho = \frac{R_p}{R_s} = \tan\Psi e^{i\Delta} \qquad \text{.....(36)}$$

These two coefficients contain information related to material optical properties and physical dimensions. Spectroscopic ellipsometry measures this complex ratio as a function of wavelength.

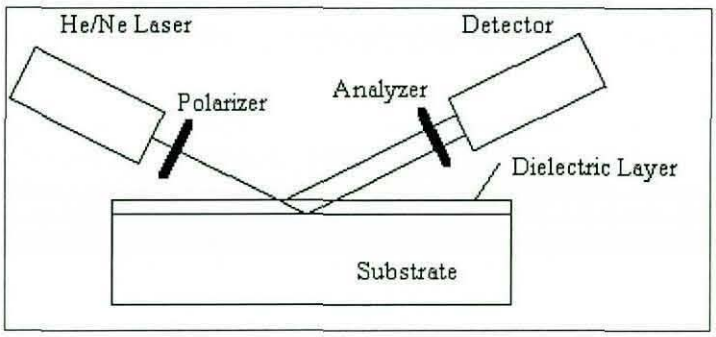

Figure 32. Schematic diagram of a simple ellipsometer (After Van Zeghbroeck [202]).

The basic experimental configuration is shown in figure 32 above and the fundamentals of the technique are described in standard texts such as Riedling [165] and Tompkins [166].

The polarization state of the incident light is known whilst that of the reflected light is determined, often using a nulling technique whereby the polarizing elements are rotated until the measured signal is extinguished. Early ellipsometers required that the user knew either the refractive index of the reflective coating or its thickness. One or the other could be determined. However, modern computers allow models to be used for which both quantities can be determined. In other words the technique is now model dependent such that you cannot access directly to the physical quantities you wish to determine (dielectric functions, refractive indices, material compositions, film thicknesses etc). A mathematical model that described the sample structure is required to determine them. Data fitting is then used to match the experimentally measured data to the theoretical model. The data fitting is usually performed using the Levenberg-Marquardt nonlinear regression algorithm [167] to find the minimum in the mean square error between the experimental data and the best fit to the data. The process is complex and the user largely relies on developed computer software to obtain the best fit of a model to the experimental data.

Ellipsometry is mainly used in semiconductor research and fabrication to determine properties of layer stacks of thin films and the interfaces between the layers. The technique works well in such materials because they are usually well defined and homogeneous. In the present research, ellipsometry was required principally to supply film thickness measurements of coatings deposited onto glass slides from solution, which were expected to be smaller than the wavelength of visible light. Unfortunately,

these were not entirely homogeneous and it proved difficult to fit the measured data although measurements were obtained which agreed reasonably well with measurements made using light interference microscopy.

3.8.5 Auger Electron Spectroscopy (AES)

This analytical technique is based on the Auger electron emission process discovered by Pierre Auger in the last century. In this process the sample to be studied is irradiated by primary beam high-energy electrons typically between 1KeV and 10KeV.

The sample atoms contain electrons occupying both inner and outer electron orbitals. If a sufficiently energetic electron strikes an atom in the sample, there is a probability that it will eject an electron from the inner or core level in that atom. The ejected secondary electron can be collected and used to form an image of the sample in exactly the same manner as occurs in SEM. In fact AES operates in a similar fashion to an SEM except that the vacuum is much higher and instrumentation exists to detect the Auger signal.

When the atom has this electron ejected, it is left in an excited state and one method by which it can relax is to allow another of its electrons from a nearby orbital to fall into the core vacancy with the remaining energy imbalance being used a eject a third electron, possessing a relatively low kinetic energy (typically 40 to 2500ev). This is called an Auger electron and its energy is characteristic of its parent atom and also the chemical environment in which that atom occurs in the sample.

Unless the parent atom is very close to the surface of the sample, intense inelastic or elastic scattering will further reduce the kinetic energy of the Auger electron by collisions as it finds its way to the surface and effectively it will be detected only as part of the general background signal as opposed to part of a discrete AES peak. In AES, the kinetic energy spectrum of emitted Auger electrons is collected and then amplified and the signal differentiated to enhance the peaks giving a characteristic spectrum similar to that illustrated in figure 33 overside.

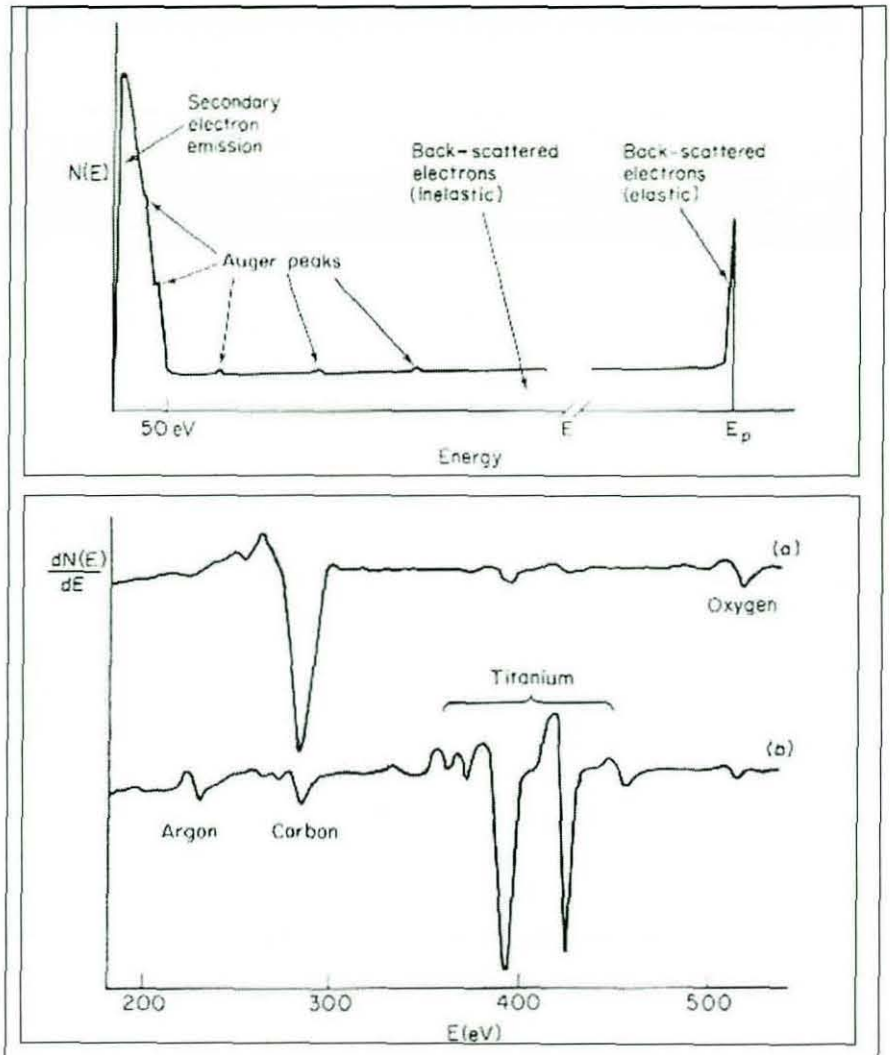

Figure 33. The top diagram shows the energy spectrum of electrons emitted from a sample being irradiated with electrons of primary energy E_p. The bottom diagram shows Auger spectra from a sample containing titanium (a) as received with surface contamination and (b) after ion etch cleaning. The energy distribution is differentiated to enhance the small Auger peaks seen in the top diagram. This gives the Auger peaks in the bottom diagram a characteristic maxima and minima as shown (After Southworth [203]).

Since these can only be detected if originating from atoms very close to the surface, within a few monolayers, the technique is very surface specific with a sampling depth between 5 and 10nm.

It is possible to plot attenuation lengths against Auger electron energies for different elements as shown in Figure 34, after Briggs [168].

A curve can be fitted to this data and a numerical expression found for attenuation lengths within a defined range of energies. In general this equation takes the form:

$$\lambda = 0.41.\, a^{0.5}\, E^{1.5} \quad \ldots\ldots\ldots\ldots\ldots\ldots\ldots\ldots (37)$$

where λ is the attenuation length for Auger electrons, a is the lattice spacing for the material irradiated and E is the energy of the Auger electron (eV).

As the sample is irradiated with high-energy electrons, many of these will not contribute to Auger emission and unless a conduction path to earth exists, these will create a net charge at the surface and this will repel ejected Auger electrons. Thus AES encounters severe difficulties for insulating samples. Unlike SEM, sputter coatings of gold or carbon cannot be used to render samples electrically conducting since the thickness of such coating would greatly exceed the attenuation length for Auger electrons. With conducting samples this problem does not arise unless there is excessive hydrocarbon surface contamination or an insulating oxide layer.

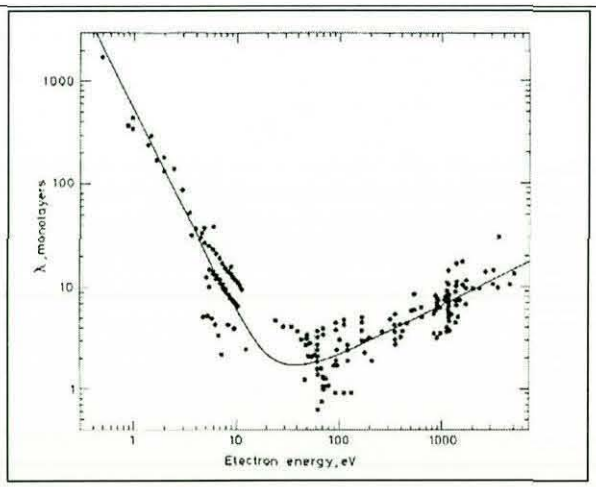

Figure 34. Attenuation lengths (After Briggs & Seah [168]).

As with most spectroscopic techniques, quantification requires the use of reference standards and calculation of sensitivity factors that take into account different elemental properties such as density, which affect the Auger electron yield. Peak shifts in the Auger spectrum can give important information of the oxidative state of atoms. Elements can be detected to concentrations between 0.1 and 1%. In common with other high vacuum surface science techniques such as X-ray Photoelectron Spectroscopy (XPS), argon ion sputtering enables surface layers to be etched away in-situ enabling depth profiling up to a couple of micrometres into the sample surface. Theoretically, an etching rate can be defined by the following equation [168]:

$$Z_a = (M_a \,.\, S_a \,.\, j_a) \,/\, (D_a \,.\, Na, e) \quad \ldots\ldots\ldots\ldots (38)$$

Where Z_a is the etch rate ($m.s^{-1}$), M_a is the mole mass of target material ($kg.mol^{-1}$), S_a is the sputter yield ($atom.ion^{-1}$ – how many surface atoms removed for each incident ion), j_a is the primary ion current density ($A.m^{-2}$), D_a is the surface density ($kg.m^{-3}$), Na is Avogadro's number and e is the charge on the electron.

Many metallic samples are studied using AES and oxide layers are generally present at the surfaces. Thus although the bulk densities for the metals are known, the largest unknown in the above equation is the density of such surface layers D_a since oxides are present on most metals and these are not homogeneous and the density is very variable locally. The term j_a has been calculated for the Auger spectrometer used (JEOL 7100) used in this research and was found to be 75×10^{-6} $A.m^{-2}$, measured using a Faraday cup. The sputter yield is a function of angle of incidence of the ions and their kinetic energy so both are this usually kept constant. Argon or Xenon is most usually used for ion etching and the sputter yields for most solid elements have been measured experimentally with the data usually supplied by manufacturers of surface science instruments. In practice a combination of instrument specific data and experimentally derived rates are used to determine empirical etch rates. For the instrument used in the present study the etch rate for steel is known to be 12nm/minute assuming Argon ions are accelerated using a potential of 3kV and this can be used as an empirical guide to likely etching rates for an unknown etched under the same experimental conditions. The value of this knowledge is that it enables the

thickness of surface coatings to be determined by measuring the intensity of an Auger peak as a function of etching time. By this means one is able to quantify the cleanliness of a surface by etching through a hydrocarbon contamination layer and if this is thin the underlying metal substrate will be detected. AES was thus used in combination with contact angle analysis to determine surface cleanliness.

3.8.6. Secondary Ion Mass Spectroscopy (SIMS)

This is another surface analysis technique in which a sample is bombarded with an energetic ion beam. Fragments of the surface are thus sputtered and these fragments comprise single atoms to large molecules. A small percentage of these fragments are secondary ions, which can be either positively or negatively charged, and these ions can be collected and their masses analysed using a spectrometer [168]. As with conventional mass spectroscopy, a secondary ion mass spectrum provides a chemical fingerprint of the sample being bombarded. When the ion dose used to acquire the spectrum is kept very low the technique is termed static SIMS and the entire analysis can consume less than a tenth of an atomic monolayer with the consequence that the technique can be very sensitive. Identification of an unknown compound relies on the availability of very large searchable databases and accurate interpretation of the spectra is often a skilled process.

3.8.7 X-Ray Photoelectron Spectroscopy

This is an ultra high vacuum surface sensitive technique in which the electron energy distribution of ejected electrons is measured but in this case ejection results from the photoelectric effect whereby atoms in the sample to be analysed absorb soft X-ray photons which are focussed on the sample by the instrumentation. These excited atoms then relax by the emission of a photoelectron from a core level according to the Einstein photoelectric equation:

$$B.E = h\nu - K.E. - \varphi \quad \text{.....(39)}$$

where $h\nu$ is the energy of the incident X-ray photon, φ the sample work function, K.E. the kinetic energy of the photoelectron and B.E. its binding energy.

The photoelectrons are characteristic of the parent atoms and are collected by an ion lens system and focussed into an energy analyser as depicted in figure 35.

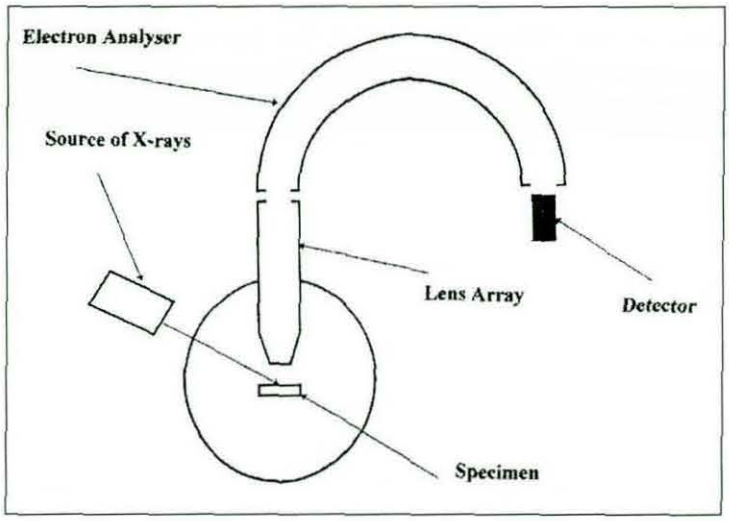

Figure 35. Essential elements of an XPS (After Mathieson [204]).

This effectively counts the number of electrons within a given kinetic energy. Since photoelectrons have similar kinetic energies to AES electrons they too can only be detected if they arise from atoms very close to the surface. XPS is, like AES, a very surface sensitive technique with a similar depth resolution of a few monolayers.

Inelastic scattering processes influence the sampling depth and a mean free path length can be determined for different samples. Generally it is accepted [169] that 95% of the photoelectron signal originates from 3 times the inelastic mean free path (λ) so that the sampling depth is given by:

$$\text{Sampling depth} = 3\lambda \cos\theta \quad \ldots\ldots\ldots\ldots\ldots (40)$$

where θ is the angle between the energy detector and the sample surface normal [168] (figure 36).

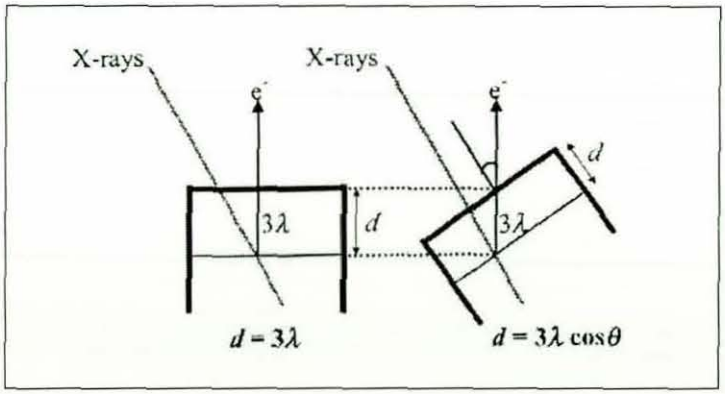

Figure 36. XPS sampling depth (After Briggs & Seah [168]).

By setting θ to increasing angles the sampling depth is reduced and this angular sensitivity forms the basis of angle-resolved XPS whereby it is possible to determine the orientation of some organic polymers present on the surface. Such polymers are easily damaged by X-ray irradiation and, in particular, defluorination can occur with fluoropolymers such that data acquisition times must be minimised to prevent polymer degradation.

By allowing the analyser to sweep across a wide energy scale, a survey spectrum (usually binding energy plotted against counts per second) is obtained which gives data about the elements present on the surface of the sample. Figure 37 shows an example of a typical spectrum obtained from a fluoropolymer. The relative intensity ratios of the detected elements are proportional to the concentrations of the surface atoms.

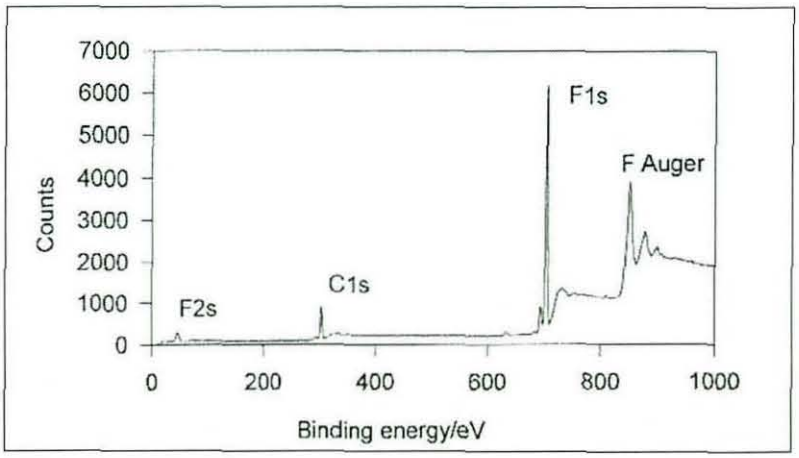

Figure 37. Typical XPS survey spectrum for a fluoropolymer (After Mathieson [204]).

The main strength of the technique is its ability for elucidating surface chemical bonding. The presence of adjacent atoms in a molecule causes atoms to exhibit a small shift in their binding energies (chemical shifts) due to perturbations induced by chemical bonding within the valence electrons of an atom. These chemical shifts are well documented in the literature [170]. Instrumental sensitivity factors allow collected spectra to be quantified to yield an atomic percentage concentration of each type of atom present (detection limit typically 0.1 – 1 atomic%). In practice, after a survey

spectrum has been collected the instrument is set up to perform high-resolution scans of narrower ranges of binding energies for all or some of the elements present.
In combination with the chemical shift data, this makes XPS extremely useful in understanding the chemical state of any surface and functional groups present. Because X-rays cannot be focussed easily the spatial resolution of the technique is inferior to AES, which uses an electron beam as the source of primary excitation. AES has the additional advantage that the higher current densities obtainable using focussed electron excitation results in greater signal to noise ratios. However, problems associated with charging of insulators are easier to compensate for in XPS than in AES. The two techniques are largely complimentary.

As with AES, argon ion etching is possible to prepare depth profile information but the area etched must be coincident with the area from which the XPS spectrum was obtained and since this area can be 1000 times larger than that analysed on a similar sample using AES, the overall etching rates are considerably slower. Because of this there is a much greater probability that surface information will be degraded by absorption of contaminants from within the vacuum chamber during the course of an etching experiment and results need to be interpreted with care.

3.8.8 Contact Angle Analysis

When a single drop of water is gently dispensed from a syringe onto a surface, it will either spread over the surface or sit passively on top of the surface as a bead depending on which process is energetically most favoured (figure 38). All natural systems move towards a thermodynamic state that minimises their total energy content. They are then in equilibrium with their surroundings.

Pure water has one of the highest surface tensions of any liquid, measured as 72.8 $mN.m^{-1}$ [1], and its polar molecules have a high affinity for each other. This means that water molecules at the surface of a drop have a surplus of attractive energy and so nature wants to keep that surface area to a minimum. The smallest surface area to volume ratio in nature is that for a sphere and so in the absence of other forces, a water droplet would assume a spherical shape.

Before such a drop is placed on the surface, the atoms of the substrate at the surface may also possess a higher energy than those in the bulk, particularly if the substrate is a metal and if it has just been cleaned. Pure clean metals have exceptionally high surface energies, typically, 400 –1000 $mJ.m^{-2}$ [171]. When the drop rests on such a surface, the affinity of the water molecules for the surface atoms of the metal will exceed the attraction of the water molecules for each other and the drop will spread completely over the surface exhibiting a very low contact angle potentially down to zero degrees.

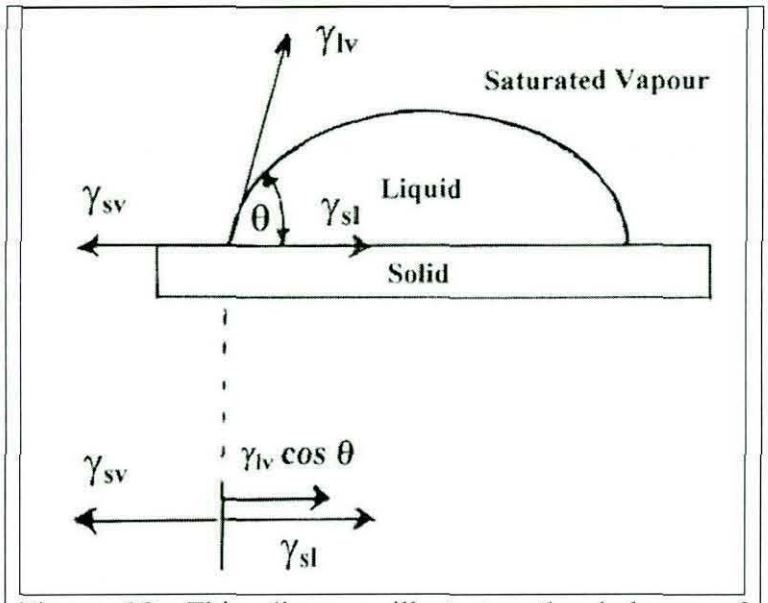

Figure 38. This diagram illustrates the balance of interfacial surface tension forces that exist at equilibrium for a liquid droplet on a solid surface. The liquid surface tension in the presence of its own saturated vapour γ_{lv} is resolved into its horizontal component γ_{lv} cos θ which combines with the interfacial tension between the solid surface and the liquid γ_{sl}. These surface tension forces are counterbalanced by that between the solid in the presence of the saturated vapour of the liquid.

The attractiveness of a clean metal surface is such that many other molecules would like to cover it and the surface rapidly becomes contaminated and is particularly attractive to hydrocarbons present in the atmosphere. If these molecules form a thin

layer on the metal surface before a water contact angle measurement is made, the attraction of the water molecules in the drop for those on the new surface may not be so great and the drop may not wet the surface completely. The drop will then define a different higher contact angle. The degree of spreading can be measured by the contact angle and is defined as the angle included between the tangent plane to the surface of the liquid and the tangent plane to the surface of the solid, at any point of contact (figures 38 and 39).

The spreading or lack of spreading results from a balance of interfacial surface tension forces that are defined by defined from Young's equation [172], first proposed in 1805, according to which

$$\gamma_{lv} \cos \theta + \gamma_{sl} = \gamma_{sv} \quad \text{.....(41)}$$

where γ_{lv}, γ_{sl}, and γ_{sv} are the surface tensions at the boundaries between liquid (l),solid (s) and vapour(v). Only θ, the contact angle, and γ_{lv} are directly measurable.

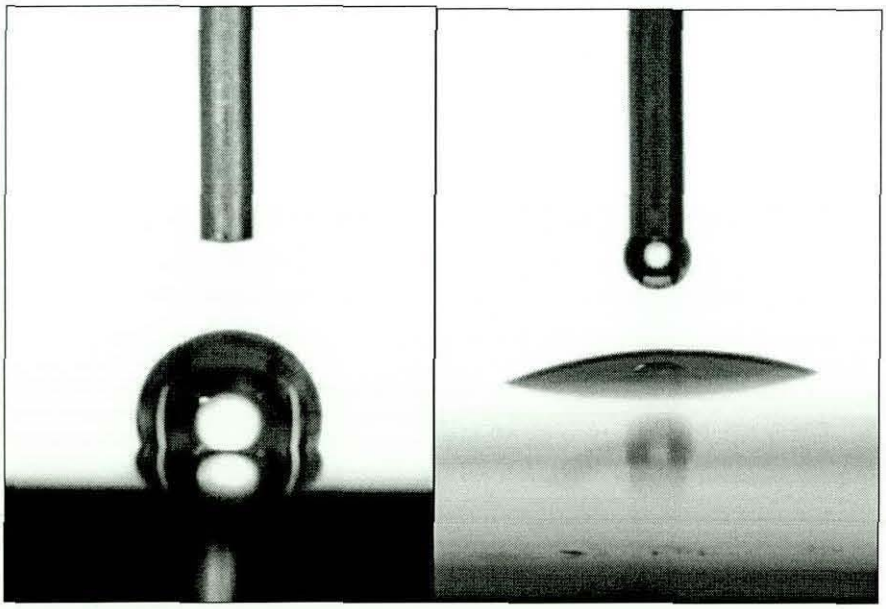

Figure 39. Photograph of a water droplet on a non-wetting surface (left) and photograph of a water droplet on a surface it wets (right).

As with many natural phenomena that are seemingly simple at first sight, explanations of contact angle behaviour can be exceedingly complex and subject to many variables

such as surface roughness, chemical heterogeneity of the surface and surface sorption layers to mention but a few. The thermodynamics of surfaces are a function of their chemistry and so polymer surfaces are very different from metals. The bonding in polymers is such that there are few free electrons at a surface and this makes them unreactive chemically and they are said to possess a low surface free energy.

Wettability is commonly used to predict intrinsic adhesion since the spreading of an adhesive onto a substrate is intimately related to surface energetics that favour this. When describing adhesive spreading, the term "work of adhesion" is used and since all forms of work are associated with energy, surface free energies are used synonymously with surface tensions in much published literature though thermodynamically they are different. As its name implies, surface tension is a tangential stress in a surface layer. A mathematical description follows which describes how surface energy can be calculated from contact angle measurements.

3.8.8.1 Quantitative Contact Angle Analysis

Surface tensions dictate whether an applied liquid will wet and spread over or retract from a solid surface [69]. Different theories have been proposed over the last fifty years to enable the surface energy of solids to be measured from contact angle data for two or more liquids that are applied to the solid. Successive researchers have refined and modified previous theories over this time period but there does not exist one universally accepted theory at present. These theories are expounded in numerous publications [173 - 175] of which that by Rance[174] is particularly informative. The development of these theories will be briefly outlined.

Imagine a liquid adhesive wets the surface of a substrate. Let the substrate have a surface energy γ_{Sv} , the liquid adhesive have a surface energy γ_{lv} and that of the interface be γ_{Sl}, then the work of adhesion W_A, first proposed by Dupré in 1869 [176], represents the energy that would be needed to separate a unit area of the liquid adhesive from the substrate completely, and this is given by the following equation:

$$W_A = \gamma_{Sv} + \gamma_{lv} - \gamma_{Sl} \quad \text{.....(42)}$$

From Young's equation $$\gamma_{Sl} = \gamma_{Sv} - \gamma_{lv}\cos\theta \quad \text{.....(43)}$$

and combining gives $$W_A = \gamma_{lv}(1 + \cos\theta \quad \text{.....(44)}$$

Equation (44) known as the Young-Dupré equation.

Thus for good adhesion, a high work of adhesion is required and this can only occur if the contact angle θ is low (for θ = 0°, cos θ = 1 and decreases to 0 when θ = 90°). Conversely mould releases must coat the substrate such that the work of adhesion is very low and hence a high contact angle is required. Since contact angles as high as 180° have never been measured (when cosθ = -1 and W_A=0), then every liquid must wet every solid to some extent.

By plotting cos θ against γ_{lv} for a homologous series of liquids on a solid, Fox and Zisman [177] found that a straight line could be drawn where:

$$\cos\theta = 1 + b(\gamma_{lv} - \theta_c) \quad \text{.....(45)}$$

where θ_c is defined as the critical surface tension for wetting and b is a constant. In this equation θ_c is the value of γ_{lv} at which the liquid just wets a surface with zero contact angle.

Fowkes [187] then suggested that the surface energy of a solid γ_s or of a liquid could be described as the sum of components that arise from different intermolecular forces ,principally dispersion and polar forces. The surface energy of a solid is thus:

$$\gamma_s = \gamma_s^{\,d} + \gamma_s^{\,p} \quad \text{.....(46)}$$

where $\gamma_s^{\,d}$ and $\gamma_s^{\,p}$ are the dispersion and polar contributions (similarly $\gamma_l = \gamma_l^{\,d} + \gamma_l^{\,p}$ for a liquid).

Fowkes then proposed that the interfacial interaction was due to the interaction of like forces. Unlike forces were assumed to not interact. Using a geometric mean approximation to describe the interaction, he proposed the interfacial tension between a saturated hydrocarbon, where only dispersive forces may operate (i.e. $\gamma_l^p = 0$ so $\gamma_l = \gamma_l^d$), and a solid surface can be expressed as:

$$\gamma_{sl} = \gamma_s + \gamma_l - 2\sqrt{(\gamma_s^d \gamma_l^d)} \quad \text{.....(47)}$$

Owens,Wendt, Kaelble & Uy [179] extended this concept by considering both dispersive and polar forces and, also using a geometric mean approximation, proposed :

$$\gamma_{sl} = \gamma_s + \gamma_l - 2\sqrt{(\gamma_s^d \gamma_l^d)} - 2\sqrt{(\gamma_s^p \gamma_l^p)} \quad \text{.....(48)}$$

Owens,Wendt, Kaelble & Uy then combined this with Young's equation and after algebraic manipulation showed that

$$(1 + \cos\theta)\,\gamma_l / (2\sqrt{(\gamma_l^d)} = \sqrt{(\gamma_s^p)} \cdot \sqrt{(\gamma_l^p / \gamma_l^d)} + \sqrt{(\gamma_s^d)}$$

$$\text{Setting } X = \sqrt{(\gamma_l^p / \gamma_l^d)},\ Y = (1 + \cos\theta)\,\gamma_l / (2\sqrt{(\gamma_l^d)}$$

$$Y = \sqrt{(\gamma_s^p)} \cdot X + \sqrt{(\gamma_s^d)} \quad \text{.....(49)}$$

γ_l , γ_l^d and γ_l^p have been measured for many liquids and can all be found in the literature [69] while θ can be measured by experiment. Thus, X and Y can be calculated for each liquid. A straight line can be drawn using a series of liquids. γ_s^p is then the square of the gradient, and γ_s^d is the square of the intercept of the line with the Y axis and then the surface energy of the solid is just the sum of these values in accordance with equation 46.

The approach used by Owen,Wendt, Kaelble & Uy [179] has been used extensively in the present study to calculate the surface energies of treated samples by measuring contact angles using two liquids. A polar liquid such as water and a non-polar liquid such as diiodomethane are often used.

The popularity of equation (49) belies the fact that there is much controversy about whether the geometric mean approximation, used by Owen,Wendt, Kaelble & Uy and by Fowkes earlier, is the best approach for finding the polar interactions at an interface.

Zettelmoyer [206] and Wu [207] separately discuss this approximation in detail. Wu states that it gives reasonable results in only a few cases where the interface is between high and low energy phases such as mercury on a polymer surface. In general though Wu ascerts that the geometric approximation gives rather poor results

for many organic liquids on organic polymers and that a harmonic mean approximation is preferable.

Despite these quite serious objections, equation (49) allows simple and quick measurements of surface free energy to be made on many surfaces using only a polar and non-polar liquid and this explains its popularity. Acknowledging the reservations of Wu and other authors, it is possibly prudent to consider the values obtained as being useful only for comparative studies where the differences between surfaces energies are of practical importance rather than when absolute values of surface energy are required.

Such is the importance of surface energy values for solids that numerous approximate models [180 - 182] have been developed and different approaches used to enable their calculation.

The theory discussed is based on the equilibrium contact angle of a sessile drop on a flat, horizontal, smooth, homogeneous, isotropic, and rigid solid. However, this is clearly an idealised situation and in practice it is found that a range of contact angles are measured on real surfaces that agree with each other within two degrees or so. Surface roughness, in particular, has a profound effect on contact angle measurements. As a consequence, practical experiments usually comprise at least twenty angles per sample measured over an area of a few square centimetres and a mean value calculated. The measurements should be taken in orthogonal directions if the surface possesses directionality. Hysteresis effects resulting in advancing or receding angles can occur on some polymer surfaces, which is an added complication. On metals, dissolved salts absorbed onto the surface can result in dynamic contact angles where the angle decreases rapidly with time as the drop is absorbed by the surface and spreads.

3.8.9. Infrared Spectroscopy

When exposed to infrared radiation (wavelengths between 2.5 and 25 x 10^{-6} m), molecules in solids, liquids and gases can selectively absorb radiation at frequencies that match those of their allowed vibrational modes. By convention absorption is

referred to in terms of wavenumber rather than wavelength (wavenumber is the inverse of the wavelength expressed in centimetres). The chemical bond between molecules can be thought of as springs oscillating at different frequencies depending on the molecules and type of bond (figure 40) [183], [184]. An analysis using Hooke's law can be used to estimate the wavenumber of light that will be absorbed by different types of chemical bonds.

$$\text{Wavenumber} = 4.12 * (K / \mu)^{1/2} \quad \text{.....(50)}$$

where K = force constant (in dynes / cm)

- for single bond: $K = 5 \times 10^5$ dynes/cm
- for double bond: $K = 10 \times 10^5$ dynes/cm
- for triple bond: $K = 15 \times 10^5$ dynes/cm

$$\mu = M_1M_2 / (M_1 + M_2) \text{.....(51)}$$

where M_1 and M_2 are molar masses of atoms involved in bond.

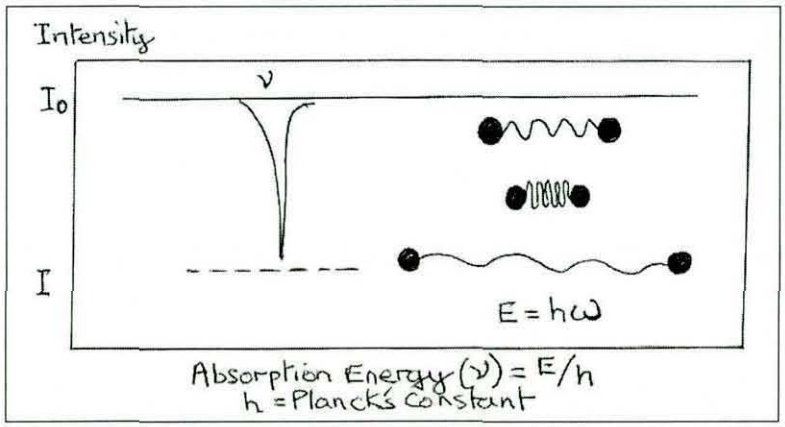

Figure 40 Diagram relating absorption to molecular bond stretching

Vibrations that do not yield a change in dipole moment do not absorb IR radiation. For example, O_2 and N_2 do not absorb IR radiation. Measurement of the absorption of IR radiation by the sample as a function of frequency produces a unique spectrum that can be used to identify functional groups and consequently structure. The spectrum can be shown as either absorption or as a transmittance. Figure 41 shows the transmission spectrum for a fluoroalkylsilane.

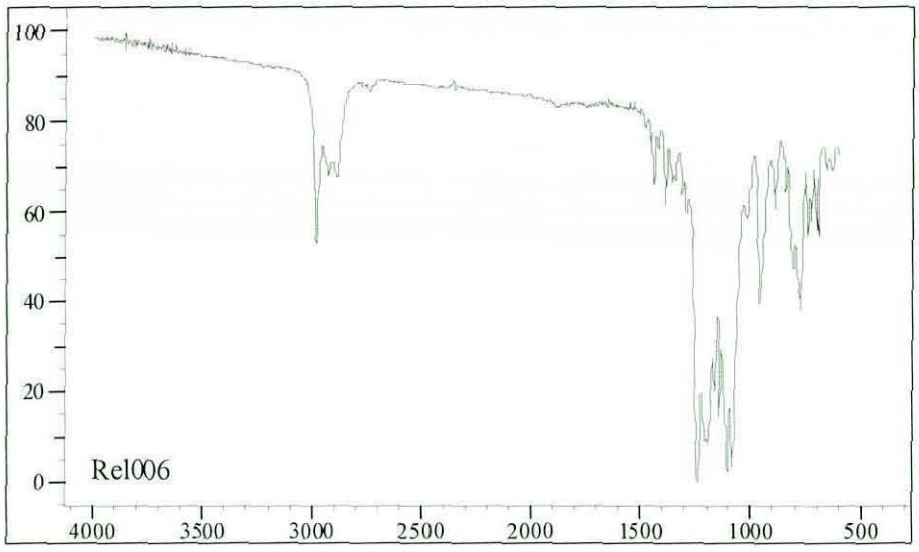

Figure 41 Transmission infrared spectra for Dynasylan F8621 fluoroalkylsilane (ordinate is transmittance; abscissae is the wavenumber(cm^{-1}).

Different chemical functional groups possess different ranges of absorption in wavenumbers depending on the type of molecular motion that is excited (bend or stretch). Experimentally, Fourier Transform IR instruments are almost exclusively used because all frequencies are observed by the detector simultaneously allowing for short data acquisition times and signal averaging of repeated scans.

3.8.10. Differential Scanning Calorimetry and Thermogravimetric Analysis

Differential scanning calorimetry (DSC) detects the difference in temperature between a sample and a reference (an empty sample holder) by means of thermocouples placed in contact with the sample and reference, as both are subjected to a controlled temperature program in a special furnace (figure 42) [185].

The electrical signal from the thermocouple is converted to a power difference using the calorimetric sensitivity of the cell, which is determined by calibration against a standard metal such as indium, which has an accurately known enthalpy of fusion. Exothermic (heat liberating) and endothermic (heat absorbing) events occurring in the sample as it is heated, and the enthalpy changes associated with such physical transitions can be calculated. Many factors can affect the results obtained such as heating rate, sample size, sample preparation, sample holder, thermal history of the sample and the gas used to purge the DSC cell.

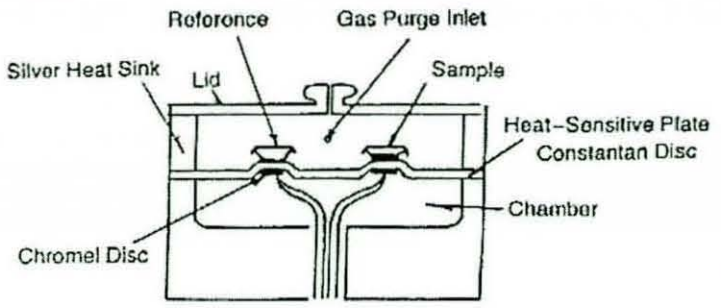

Figure 42. Schematic diagram of DSC furnace. After Hatakeyama [201].

The principle of the DSC can be expressed by the following heat flow equation:

$$dH/dt = Cp.\ dT/dt + f(T, t) \quad \text{.....(52)}$$

where dH/dt is the total heat flow measured by the calorimeter, Cp is the specific heat capacity, dT/dt is the heating rate and f(T, t) is the kinetic response of the sample.

The heat capacity term is associated with reversible thermal events such as glass transitions and melting whereas the time dependent term, associated with the kinetic response is in turn associated with irreversible thermal events such as cure, decomposition, crystallization and evaporation. In modern instruments it is possible to choose operating conditions to enhance data for either reversible or irreversible transitions.

Glass transitions are associated with time dependent relaxations in partially crystalline polymers that are subjected to controlled heating. The glass transition temperature (Tg) is associated with a change of physical state from a hard, glassy solid to a rubbery, flexible solid. Glass transition temperatures are associated with molecular mobility of polymers and hence to their molecular structure and are thus characteristic of the polymer. Different transitions are associated with the mobility of segments of a polymer molecule and these can shift to higher temperatures depending on the frequency of any applied deformation.

Thermogravimetric analysis (TGA) is a complimentary thermal analysis technique to DSC and measures changes in sample mass as a function of temperature and time. A TGA is in essence a very sensitive microbalance enclosed in a high temperature furnace where the atmosphere can be controlled. TGA is most often used to determine the thermal stability of polymers and other materials.

3.9 Summary

It is useful to summarise the literature reviewed in sections 3.1 to 3.7.

The detailed chemistry of external semi-permanent mould releases of primary interest in this work is largely based on proprietary formulations covered by patents but they are thought to comprise silicone resins in a hydrocarbon solvent. One of the most widely used commercial product is Frekote and comprises a surface sealant and a mould release agent.

The surface sealing agent has an important role and seals any micro-porosities in the surface to which it is applied prior to a coating of the release agent itself. The two chemistries are compatible. Using Frekote as a benchmark, a discussion of the functionality of this product was addressed. Similarly the functionality of other non-stick silane and fluoropolymer-based coatings were discussed with examples being found in a wide variety of applications from cooking and bakeware to marine biofouling and pressure sensitive adhesives. The experimental work detailed in Chapter 6 examines a number of different non-stick coatings and seeks to appraise the properties that make them successful in a given environment.

In seeking to find alternative mould release coatings that are not based on polydimethylsiloxane, the properties that make this material successful as the basis of external semi-permanent release agents have been identified from the literature. From the available literature on the topic of non-stick coatings it is possible to identify some properties that make each successful in a particular environment. These include:

- a low surface energy
- dissimilar solubility parameter to that of the surface applied to (to prevent interdiffusion)

- thermal stability (required for some applications)
- durability
- molecular mobility associated with low glass transition temperature
- ability to cover and fill in major surface asperities resulting from roughness but leave a degree of roughness to allow fracture stresses to concentrate at air pockets remaining on the surface
- ability to form a cohesively weak boundary layer with many flaws to concentrate interfacial stresses and reduce the release force

Fluoropolymer and fluorosilicone materials offer combinations of these properties and are thought to offer potential as mould release agents.

The PDMS-based mould releases, currently used in the aerospace industry are associated with the high temperature moulding of thermosetting resins. Resin impregnated carbon fibre and Kevlar laminates are laid up on moulding tools treated with release agent. Sheets of resin are interspersed with the prepregs. A copper mesh lightning conductor may also be added. The whole assembly is vacuum bagged and heated to 180°C in an autoclave pressurised with nitrogen at up to 10 atmospheres pressure (1.013MPa). This constitutes a complex multi-variable system that is difficult to model in a laboratory and it is likely that the chemistry of the resin systems themselves and unknown proprietary additives influences mould fouling. The wide scope of the present research allows insufficient time to study mould fouling in significant detail and instead concentrates on developing an understanding of the optimum properties of mould releases.

A review of techniques that have been used to measure the mechanical performance of mould releases in the laboratory has shown that no single method is widely accepted and that there are many real difficulties encountered in measuring the low forces involved. This chapter has also identified and provided details of the main analytical techniques used in the present study.

Chapter 4 Experimental

4.1. Introduction

This chapter details the materials sourced, the processes used and analytical procedures performed in the present study. A dichotomy exists between the principal areas investigated with the consequence that it is helpful to consider firstly, the substrates and contaminants associated with the cleaning procedures, and secondly, the investigation of mould release coatings.

4.2.Materials

4.2.1. Industrially sourced substrates

Bombardier supplied two contaminated nickel tooling plates (30cm x 20 cm) which had been obtained from a moulding tool that had reached the end of its service life.
The contamination present on the used nickel tooling was very slight, comprising a residue of resinous material giving it a light brown discolouration (figure 43).
The nickel plates were subdivided and some of the original parts were retained whilst the contamination was removed from one part using the same type and grade of abrasive as used by Bombardier. Smaller coupons (5cm x 6cm x 0.5cm) for testing were cut from this abrasively cleaned material.

One side of the nickel tooling plate as received was covered with exceptionally hard nodules from the electrolytic manufacturing process making it uneven. Attempts to grind down this face in laboratory workshops proved difficult and blunted tools. Also the plate as received had a slight overall curvature resulting from the mould geometry in which it was originally used. This was a serious problem because it meant that pressure applied during laboratory curing of resin samples could not be applied evenly, using laboratory hydraulic heated presses, even when small samples were used.

At Bombardiers curing is achieved using a combination of vacuum bagging of the moulding against the tool surface and autoclaving in a nitrogen atmosphere pressurised up to 10 atmospheres (1.013MPa). These conditions could not be easily reproduced in the laboratory.

Cytec Fiberite Ltd., of Wrexham, supplied FM300 epoxide resin sheets and a small, virgin carbon composite tool (Cyform 777 of dimension 50 cm x 50 cm x 8mm thickness) and a sample of the virgin composite material is shown in figure 44. The FM 300 resin is a high shear strength adhesive formulated for composite structure mouldings and is believed to be a diglycidyl ether of bisphenol A (DGEBA).
Bombardier also supplied some examples of used composite tooling (figure 45) and although some preliminary characterisation was performed on these, there proved to be insufficient time in the project to treat and further test the samples.

4.2.2. Model substrates

It was agreed with Bombardier that steel plate could be used as a substitute for an example of steel mould tooling, which Bombardier could not supply. Mild steel plate, supplied by Adey Steel Ltd., of Loughborough, was used, and this was cut into small coupons (figure 46).

With hindsight the choice of industrial grade mild steel was unsuitable for the project because of the presence of a relatively thick oxide layer (approximately 10 micrometres thickness measured from cross sections). This gave rise to artefacts in subsequent treatments that might not be present, or else present to a much lesser degree, on the stainless steel tooling used by Bombardier. No particular difficulties were otherwise encountered in material preparation.

It was decided that the aforementioned materials (nickel plate, mild steel, composite tooling) would be used to evaluate the effectiveness of different cleaning techniques and that scanning electron microscopy would be the main analytical technique used since this imposed no sample size restriction.

The situation for the proposed work on mould releases relied more heavily on analytical instrumentation and it was decided to supplement the materials used with a stainless steel foil of 150 micrometres thickness, type SS304 supplied by College Metals, Salford. This was chosen because it was readily available whereas the quantity of samples supplied by Bombardier was limited. The foil was also easy to cut and use for coating experiments and sample cleanliness could be easily controlled. Possessing a lower roughness value than the Bombardier samples, the stainless steel foil was also more suitable for microscopic studies. It is acknowledged that the surface chemistry and composition of the foil will be different to that of Bombardier tooling but at this stage it was considered necessary to conduct a preliminary study with idealised samples and then progress to treating Bombardier tooling once the viability of a coating system had been proven.

A surrogate material for nickel-tooling plate was used comprising nickel sputtered onto standard glass slides to a thickness of 1.1micrometres. These sputtered slides were supplied by Teer Coatings, Hartlebury, Worcestershire. Unfortunately, the cost of preparing such samples limited availability to ten slides so it was decided to use these sparingly and only for an angle resolved XPS experiment. Due to the delicate nature of these samples no surface roughness measurements were made. The surfaces of these sputtered nickel films were very smooth and no SEM or AFM characterisation of topography was made.

Again for the work on mould releases, it was decided to mill down a single coupon of nickel plate (sourced from Bombardier) to 3mm thickness and sub-divide this into $10mm^2$ squares, several of which were subsequently hand polished using a series of diamond pastes, finishing with a 1 micrometre particle size diamond paste.

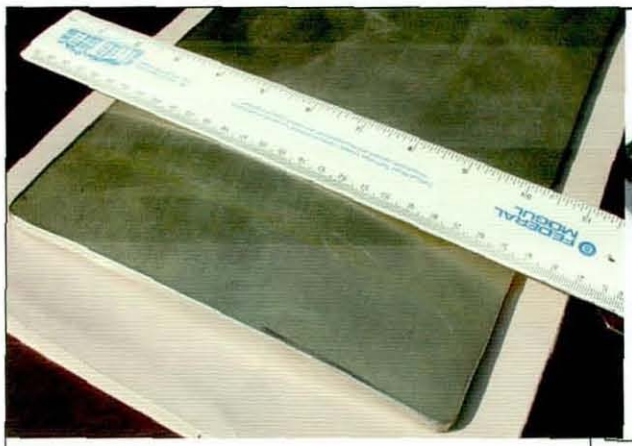

Figure 43. Example of contaminated nickel tooling

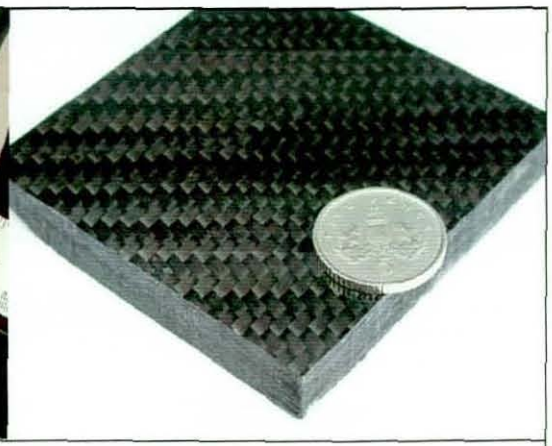

Figure 44. Example of virgin composite tooling

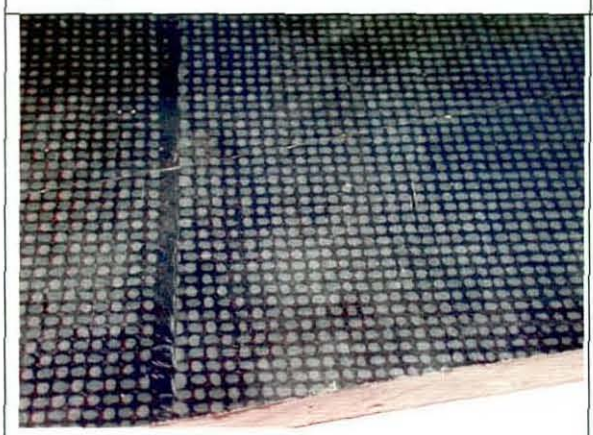

Figure 45. Example of used composite tooling

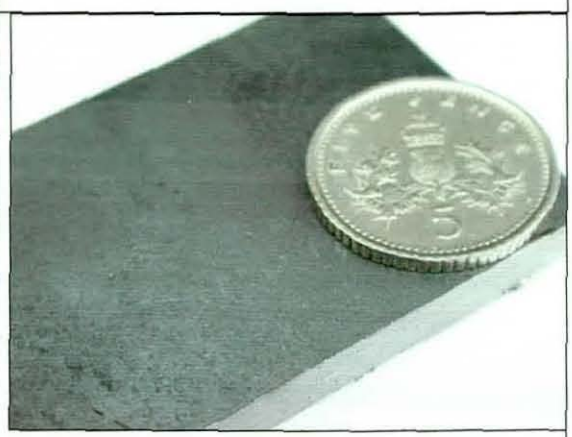

Figure 46. Example of mild steel plate

4.2.3. Model contaminants

It was also agreed with Bombardier that an epoxide resin, RTM6, supplied by Hexcel Composites, Duxford, would be used to treat nickel, steel and composite coupons and that different cleaning methods would be evaluated using these samples. RTM6 is a premixed, monocomponent transfer moulding epoxide resin containing tetraglycidyl methylene dianiline, 4,4'-methylenebis(2,6'-diethylaniline) and 4,4'-methylenebis(2-isopropyl-6-methylaniline).The advantage of this resin was that it could be easily applied to test coupons and contained no additives or pigments unlike the FM300 resin sheets supplied by Cytec Fiberite. Because the latter product was proprietary, no details concerning the additives were known or could be obtained and this introduced additional unknown variables into the cleaning evaluations. Particularly with laser cleaning, pigmentation and other additives have a very significant effect on absorption

characteristics. Details of application and cure conditions for both RTM6 and FM300 are given in section 4.2.3.2.

4.2.3.1 Pre-treatment cleaning

Cleaning is an essential part of the surface preparation and although rigorous cleaning regimes can be used on laboratory samples, the same degree of rigour is often not practical in the aerospace industry where very large tooling moulds have to be cleaned quickly. In assessing cleanliness levels for substrates it is necessary to remain focussed on this fact and be dissuaded from repeated cleaning procedures to obtain ever-cleaner surfaces since the same rigour could not be applied industrially.

The nickel and steel plate samples to be coated with RTM6 resin were cleaned according to the following regime. This same regime was also used subsequently to treat the steel foil used for mould release experiments.

Coupons were degreased ultrasonically in two changes of fresh acetone and then treated in a proprietary aqueous alkaline cleaner, Isoprep 44, supplied by Lea Manufacturing of Buxton, which was mixed with tap water and brought to the boil, and the samples were mechanically agitated in this hot solution for 30 minutes. Each sample was then rinse washed in running hot tap water and transferred to a fresh solution of the alkaline cleaner at room temperature. Each sample was then subjected to ultrasonic agitation for a further 30 minutes before being again rinse washed in hot tap water and thoroughly dried in an oven set at 120°C for 60 minutes. This drying time was doubled for the mild steel samples since rusting was a problem.

4.2.3.2 Application of resin

RTM6 resin was warmed to approximately 80°C for 15 minutes to reduce its viscosity and then a quantity thoroughly mixed with an equal volume of acetone, which was used as a thinning solvent. This was then brushed onto cleaned metal and composite coupons. This single application was cured for 4 hours in an oven at 180°C and ambient pressure. Thickness measurements of plates before application of the resin and after removal and cooling of the cured resin showed the resin thickness to be

within the range 100 - 150 micrometres, the greater thickness occurring towards the edge of the samples. Particularly difficulties were encountered with the nickel coupons because they were uneven as previously described.

Resin was only applied to the gloss face of virgin composite tooling coupons and these were first cleaned by ultrasonic agitation for 30 minutes in distilled water. After this cleaning, excess water was drained off and the coupons dried with clean paper towels and left overnight at room temperature before being treated.

The FM300 epoxide resin was supplied in sheet form impregnated into a polyethylene terepthalate (PET) membrane and comprises part of a typical moulding. A silicone release paper protected the resin. This was unfortunate because the resin was thus contaminated with silicon on receipt before it was brought into contact with any mould release agent. Consequently the transfer of release coating could not be easily investigated. The resin sheeting is applied to the metal mould tooling at Bombardier interleaved with alternating layers of carbon fibre or Kevlar resin impregnated cloth. The assembly is then vacuum bagged on the mould surface and cured in a large autoclave in a pressurised nitrogen atmosphere.

It was found through experimentation that the absorption properties of FM300 resin sheet, for incident laser energy, were considerably greater than those of an equivalent thickness of RTM6 resin. This was considered to be due to the fact that the former resin product is pigmented and contains inorganic fillers that absorb laser energy with greater efficiency than the resin matrix, as discussed in section 5.2.1. In terms of its absorption properties the FM300 resin sheet has similarities to a thick layer of paint and it is well known that TEA CO_2 lasers are particularly efficient at removing these by laser ablation. No pigmentation is, however, present in typical mould contamination. As a consequence, the use of FM300 resin was deemed inappropriate as a contaminant material and RTM6 was considered to be a more suitable model contaminant. The FM300 resin sheet was only used mould release studies discussed in section 6.3.1.

It is useful to briefly summarise both the industrially sourced substrates and contaminant samples that are characterised in this project.

Substrates

- Contaminated Ni tooling plate (ex-Bombardier)
- Mild steel plate
- Stainless steel 304 foil (150 micrometres thickness)
- Ni sputter coated glass slides
- Virgin composite tooling
-

Contaminants

- Particulate resinous material of unknown composition on Ni tooling plate (ex-Bombardier)
- Hexcel RTM6 resin bonded onto pre-cleaned Ni tooling plate (ex-Bombardier)
- Hexcel RTM6 resin bonded onto pre-cleaned mild steel plate
- Hexcel RTM6 resin bonded onto virgin Cytec composite tooling
- Used composite tooling (ex-Bombardier)
- Cytec FM 300 epoxide adhesive film applied to various substrates

4.3 Surface Cleaning Procedures

4.3.1. TEA CO_2 Laser cleaning

Details of the TEA CO_2 laser used in the present study and the operating parameters were given in section 2.2.5. The optimum fluence conditions were determined experimentally and the only variable was the number of pulses incident per unit area during the cleaning procedure, as detailed in section 5.2 1.

4.3.2 Nd:YAG Laser cleaning

Details of the operation of the Nd:YAG laser used in the present study are given in section 2.2.6. The Spectron Nd:YAG laser previously detailed was used independently to evaluate the efficacy of laser cleaning for removal of resin from the

prepared sample set. A lens in the final segment of the arm contains a focussing lens (figure 47).

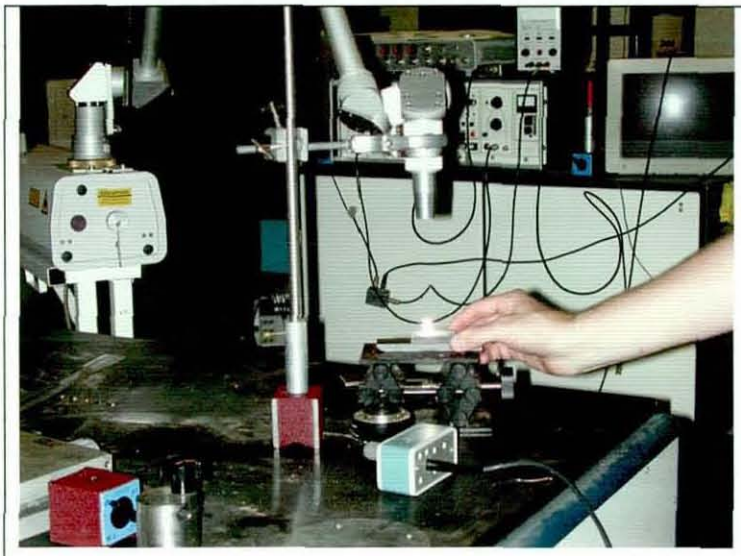

Figure 47. Nd:YAG experimental arrangement.

Although the pulse duration of this laser is fixed, the duration is within the range that is required for a laser cleaning application (10 – 50ns) and other laser parameters such as power output and frequency of applied pulses were more easily controlled. It was decided to use Q-switching (section 2.2.6) to boost the power output and conduct a series of experiments to determine the optimum distance of the sample from the focal point of the laser for normal incidence. At this optimum distance the beam is defocused for laser cleaning which spreads the energy over a larger area. The operating conditions were such that an effective cleaning mechanism occurred for samples placed at 25cm from the focal point of the laser. No substrate damage occurred at this distance and the beam diameter was approximately 8mm. It is not suggested that these conditions are suitable for large scale cleaning and were used merely to evaluate laser effects in the laboratory using this particular Nd:YAG laser. These results were then compared with those received from external laboratories.

4.3.3 Liaison with External Laser Laboratories

As discussed by Cottam [49], experimental work using the Laserbrand TEA CO_2 laser is largely limited to varying the laser fluence used and number of pulses applied to a target, and then assessing its effect. The instrumentation and expert instruction required to measure the laser fluence and temporal profile of this laser was no longer

available in the Department of Physics at Loughborough University at the time the present study was undertaken and assistance from external laboratories was sought. There are relatively few laboratories which possess expertise on the laser cleaning of resinous materials but fortunately the National Laser Centre in Pretoria, South Africa, very kindly agreed to treat submitted samples using both a TEA CO_2 laser and a Nd:YAG laser and a useful dialogue was established which was of great value.

Collaboration was also established with the European laser manufacturer Quantel and the facilities of their laboratories in Paris, France were made available. This contact provided some useful data on the rate of cleaning that was possible for contaminated nickel tooling received from Bombardier. The commercial system marketed by Quantel for laser cleaning combines the outputs from four standard 250W Nd:YAG lasers into a single cleaning head in which the spatial energy distribution of the output and area coverage are both optimised for quick automated cleaning. On the treated samples, the surfaces were characterised and the effects interpreted, as discussed in section 5.2.3.2. in which the experimental conditions used are given.

4.3.4.Dry ice Cleaning

The facilities and co-operation of CryoGenesis Ltd., Littlehampton, were enlisted for these evaluations and samples prepared as described were taken to their premises for treatment using a variety of operating conditions. The primary interest was to determine if the technique could effectively remove resin bonded to composite material without damaging the substrate. The parameters which were varied were time, pressure, particle size and the presence or otherwise of abrasive media.

The operating parameters used for manual cleaning were:

(i) Sample size 60 mm x 60 mm x 8 mm thickness

(ii) Stand Off Distance (nozzle tip to surface): 10 cm.

(iii) Nozzle inlet pressure varied in the range 3 – 10bar (304kPa – 1.013MPa)

(iv) Nozzle angle with respect to surface was either up to about 30° or else normal to the surface

(v) Duration of blasting was varied between 3 and 30 seconds.

Resin was also cleaned from metal substrates although these results were largely predictable. No detailed analytical analysis of the treated samples was conducted because the intervening time from treatment to return of the samples to the laboratory would have resulted in contamination invalidating any surface cleanliness measurements. Analysis was restricted to a visual assessment and photographic recording of results, which are presented in section 5.4.1.

4.3.5 Sodium hydride chemical cleaning

This high temperature chemical cleaning process, as previously described in section 2.5., can only be applied to the resin coated metal substrates. The facilities at Leicester Treatments Ltd were used to evaluate the cleaning potential of this technique. Samples were treated for approximately one hour at a bath operating temperature of 360°C. On the first occasion subsequently analysis of the samples showed that they had become contaminated after being treated. The treatment environment, typical of an industrial metal finishing enterprise, is very far removed from the levels of cleanliness required by surface analysis techniques. On the second occasion the samples were rinsed thoroughly, immediately after treatment using tap water, and then stored under absolute ethanol to minimise contamination. The results from this second analysis will be presented and discussed in section 5.5.1.

4.4 Application conditions for mould release coatings

4.4.1 Frekote

Frekote comprises a series of semi-permanent external mould release products that are widely used in the aerospace industry, as discussed in section 3.2.2. The release agent is dissolved in an aliphatic hydrocarbon solvent. It was agreed with Bombardier that this release agent would be used as a benchmark against which to assess the performance of alternative release coatings. Samples were treated according to the treatment regime specified in Bombardier documentation.

Starting from a clean surface prepared as detailed in section 4.3.2.1, the substrate surface was first treated with an application of Frekote B15 surface sealer. The B15 sealer is used to fill micro-porosities on the tooling substrate surface. It is important

that this product has not been contaminated with water, which renders it cloudy in appearance and unsuitable for use. The coating is normally applied to an industrial mould using a clean cotton cloth moistened with the chemical and an area of approximately one square metre is wiped over with the moistened cloth to produce a thin, uniform film. The small size of laboratory samples makes this procedure impractical and consequently samples were dipped into the chemical contained in a glass beaker and excess sealing agent removed by vertical drainage for a few moments. The samples were then placed horizontally onto a clean surface to dry. This procedure coats both sides of the sample but only one face is required for testing. Care is required to make sure the required face is uppermost as it dries. When samples had been coated the contents of the beaker were decanted into a separate screw top bottle and not returned to the can of B15 sealer. This first coat was left to dry for 30 minutes at room temperature. A second coating was then applied in the same manner. It is important that the drying time for the first coat is not reduced below 30 minutes, which will result in the second coat dissolving the first coat. Conversely poor bonding between the two coats may result if the drying time for the first coat is significantly increased from 30 minutes. The second coat was then dried for 30 minutes in an oven at 125°C. Alternatively the second coat can be dried at room temperature for 24 hours.

The samples are next coated with Frekote 710 NC mould release agent. Similar precautions are required to ensure that this chemical is not contaminated by water.

The aim is applying the release agent is to obtain a thin, uniform film and this is more easily achieved when preparing large surface areas. However, the same dip coating procedure described above was also used to coat the sealed substrate surfaces with mould release agent. The first coat is applied and allowed to dry for 15 minutes at room temperature. Similar considerations, as discussed above, apply if the drying time is shortened or increased substantially. The time between successive coats should never exceed 30 minutes as the manufacturers state that this will degrade the performance and durability of the treated surface. A second coat is applied which is also left to dry for 15 minutes at room temperature. Finally a third coat is applied and left to dry at room temperature for 20 minutes.

4.4.2.Zyvax

Zyvax Inc., in U.S.A. (www.zyvax.com), manufacture a range of water soluble crosslinking polymer resins which are marketed as a environmentally benign external release agents for aerospace applications. The products trading under the name Waterworks comprise a mould-cleaning agent (called "Fresh Start"), a mould sealer (called "PreFlight") and the mould release product (called "Departure") and the manufacturer specify how these components are used.

The cleaning agent comprises an alkaline paste that it applied in small amounts on a paper towel and used to rub the surface repeatedly until it is clean enough to "water break". This occurs when water applied to the cleaned surface forms a continuous sheet rather than coalescing into discrete droplets on the surface.

The specific chemistry of this proprietary cleaning agent was unknown and it was considered inappropriate to use it instead of the pre-treatment cleaning detailed in section 4.2.3.1.since comparison data was sought. The "PreFlight" component fulfils the same role as Frekote B15 sealer and is applied as four coats. The same coating conditions were used as for Frekote, with the interval between coats being 15 minutes. Zyvax recommend that second and subsequent coats are buffed off from the surface before they have dried. The final coat is then cured in an oven at 83°C for 15 minutes. The difference between the Frekote B15 and "PreFlight" coatings appears to be that the latter forms a thinner, uniform film. Zyvax recommend that their "Departure" mould release agent is either applied by wiping over the surface to be treated or by spraying using an appropriate spray applicator. The first coating is allowed to dry for 2 minutes and is then buffed off. Two subsequent coats are then applied allowing a drying time of 15 minutes between coats and neither coat is buff finished. This treatment regime was used only on polished nickel substrate (section 6.2.3) but because of the small sample size, the buffing treatment was replaced by rubbing the treated surface for approximately 5 seconds on the piece of clean paper towel.

Zyvax claim that better mould release performance is obtained by using thinner applications of their products and it is clear that this is the aim from the application regime detailed. Another factor maybe that the aqueous solvent has a very high latent

heat of vapourisation and buffing between coats may assist in its evaporation since it might otherwise promote rapid rusting on clean ferrous substrates. The performance of the Zyvax product appeared to be inferior to Frekote for reasons that will be discussed in section 6.2.3 and its use was subsequently discontinued.

4.4.3.Fluoroalkylsilane

Shanahan et al [140], [141] describe how a commercial fluoroalkylsilane was used to provide a non-stick coating on enamelled steel. On this particular smooth substrate it was found to form an effective non-stick coating. The fluoroalkylsilane used, Dynasylan F8621, as described in section 3.5.7, is sold for laboratory use in 100ml quantities and this chemical polymerises very quickly on exposure to laboratory air when the bottled is opened so it is necessary to use the whole volume at once and coat as many samples as possible. It is a relatively expensive chemical but is used in low concentrations in an ethanol/water solvent and consequently can coat large surface areas.

Different concentrations of Dynasylan solutions were prepared and used to coat samples of pre-cleaned stainless steel foil and also the set of samples of nickel sputtered onto glass slides. The manufacturers recommend preparing a working solution by first mixing absolute ethanol and water in the ratio 95:5. Then by adding 1 part of Dynasylan to 119 parts of the working solution, a final concentration of 0.5% Dynasylan is obtained. Stirring then produces a dispersion that has a shelf life of up to 24 hours. Acidification was recommended to accelerate polymerisation and it was recommended that acetic acid be used to adjust the solution to a pH between 4.5 and 5.5. Dipping of samples in this solution for periods of at least 1 minute allows sufficient material to react with a high surface energy substrate and produce a uniform coating. Heating in an oven at 110°C for 10 minutes can subsequently cure this hydrophobic coating.

Varying these mixing proportions and acidifying each to a pH of 5.0 produced metal samples coated with 0.1%, 0.5%, 1.0%, 2,0% and 5.0% Dynasylan. Although different immersion times were tried ranging from 1 to 60 minutes it was subsequently found reaction times in excess of 10 minutes did not result in higher

water contact angles implying that once the substrate surface had fully reacted with the fluoroalkylsilane, further treatment time did not produce a thicker coating or increase the hydrophobicity of the coating.

4.4.4 Oxsilan

Stainless steel foil samples were first treated with a silane primer before being dipped into the Dynasylan solution. It was thought that a weak boundary layer would be created at the interface between the two cured coatings that would enhance the ease of mould release. Chemetall of Bletchley, Milton Keynes supplied a proprietary organofunctional silane (Oxsilan AL-0501) for this purpose that was developed for use a pre-treatment for aluminium surfaces.

The theory associated with such coatings has been described by van Ooij [186] who describes their application as replacements for chromate pre-treatment of metals. The active silane component in Oxsilan AL-0501 is unknown but is believed to possess a similar chemistry to bis-[tri(m)ethoxysilyl]methane (BTSM) as described by van Ooij and is dispersed in a water\ethanol solution at a few percent concentration. Samples were dip coated in the solution, blow-dried and the coating cured at 80°C for 30 minutes.

4.4.5 Oxsilan and Fluoroalkylsilane coating

Stainless steel foil samples were dip coated with undiluted Oxsilan AL-0501 as received from the manufacturers and the coatings cured. Some of these coated samples were then immersed in a solution of 1% Dynasylan F8261 fluoroalkylsilane and left to react for 15 minutes. These samples were then removed and cured according to the conditions already mentioned.

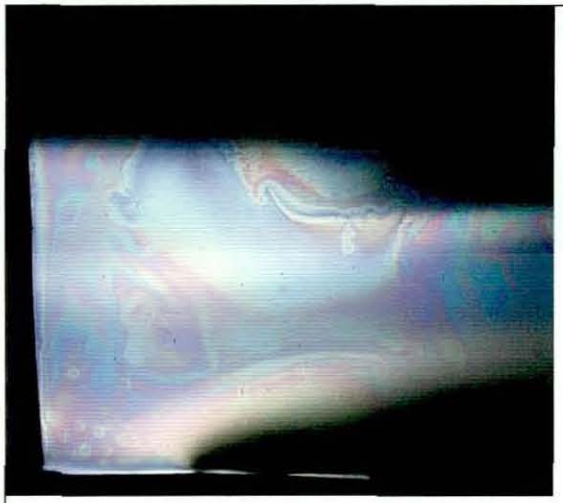

Figure 48 Interference colours from Oxsilan coating on stainless steel foil.

The Oxsilan treated samples displayed pronounced interference colours in reflected light (figure 48) implying the thickness of the coating was less than the average wavelength for visible light.

4.4.6 Fluoropolymers – Xylan 8080 & Xylar 2020

The use of fluoropolymers as non-stick coatings in the food processing industry was discussed in section 3.5.3. Whitford Plastics Ltd., Runcorn supplied two fluoropolymer coating formulations for experimental evaluation – Xylan 8080 and Xylar 2020. The principle difference between these coatings was that the latter contains a dispersion of PTFE in an aqueous solvent and could be cured at the lower temperature of 205°C compared to 400°C required for Xylan formulations. In terms of composition the Xylar formulation contains inorganic binding agents rather than organic resins which are present in Xylan coatings. Spray coating was the preferred method of application with typical coating thickness between 12 and 20 microns for a single coat of either formulation. Both coatings could be applied to most metals and although primers could be used, the coatings were reported to adhere well to cleaned substrates without using any primer. Standard cleaning procedures could be used. In the majority of evaluations, the coatings were sintered onto pre-cleaned stainless steel

foil. Grit blasting, a standard method of producing a grease free surface, was not used because experience showed that it strain hardened the foil.

Although spray coating was recommended the particle size in the coating was too large for the spray coater available and it was decided to apply coatings using a brush. The Xylan coatings were flash evaporated for 10 minutes in an oven set at 150°C and then removed. The oven was reset to 400°C and the coated samples replaced when the oven had reached this temperature and were left in the oven for a further 5 minutes.

The water based Xylar 2020 was heated in an oven set at 200°C for 15 minutes to effect full cure. The results of these preparations were quite variable. Sometimes boiling of the solvent during flashing or cure generated a rough surface and these samples were discarded. Only samples where the cured coating was smooth and blemish free were retained for testing and analysis. Two substrates comprising stainless steel plates for the blister tester (see section 4.6.2) were grit blasted and treated with the Xylar and Xylan coatings.

4.4.7 Ni/PTFE composite coating

It was decided to evaluate the potential of these type of low-friction coatings. Samples of Bombardier nickel tooling plate were treated with a proprietary coating, Apticote 450 applied by Poeton Industries Ltd., Gloucester. This is a self-lubricating nickel alloy composite coating comprising a micro dispersion of PTFE particles. The coating was deposited onto selected nickel substrates with an estimated thickness of 20 micrometres.

Mould Release Coatings	
Industrial sourced	Model
Frekote	Dynasylan fluoroalkylsilane
Zyvax	Oxsilan
	Xylar 2020 and Xylan 8080
	Apticote 450

Table 5 Release coatings.

4.5 Surface Analytical Procedures

The theory associated with these techniques was discussed in section 3.8.

4.5.1. SEM

The majority of images and spectra presented were obtained using a Leo Gemini 1530 SEM (figure 49) with field emission electron source was used in the present study. This was operated most frequently at 20 kV accelerating potential to obtain high quality X-ray spectra. Images were recorded using either 10 kV or 20 kV.

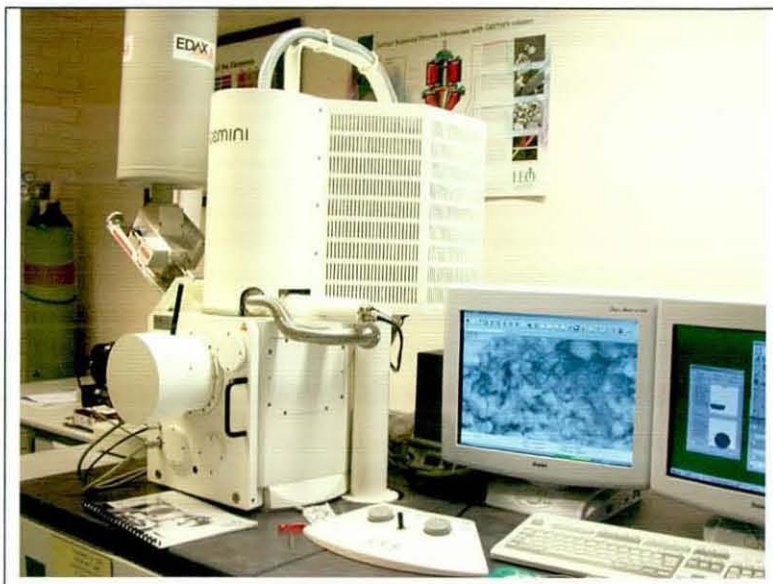

Figure 49. Leo Gemini FEGSEM.

Since most samples were conducting metals it was not necessary to sputter coat the samples to render them electrically conducting. When required gold sputter coated samples were examined.

A Cambridge Instruments Stereoscan 360 SEM operating at 20 kV accelerating voltage was also used and several images from this instrument are included.

4.5.2. AFM

Two AFM instruments were used in this study. Initial work was performed using a Burleigh Personal SPM instrument operated in contact mode using a silicon probe. This instrument provided only topographic information. To provide data on pull-off forces to quantify differences in adhesion between coatings it was necessary to use

another AFM instrument. This was a TA instruments 2990 Micro-Thermal Analyser shown below in figure 50. This instrument combines the surface imaging capabilities of AFM with the characterisation potential of a thermal analyser. This is achieved by using a probe that functions both as a programmable heat source and as a temperature sensor. Different probes can be used when non-thermal AFM information is sought and the instrument can be used in the tapping mode of operation.

Figure 50. TA Instruments 2990 AFM

4.5.3. Interference Microscopy

In this particular application a Mirau interference objective was used with a Zeiss Polarizing Microscope.

4.5.4. Ellipsometry

A Uvisel Ellipsometer was used to collect data pertaining to the thickness of mould release coatings. Facilities at Jobin Yvon Ltd, London were used to collect this data since no ellipsometers were available on campus at Loughborough University.

4.5.5. AES

A JEOL 7100Auger Spectrometer was used in this research for which the primary ion current density is 75 x 10^{-6} $A.m^{-2}$. Samples, approximately 10mm were de-magnetised prior to examination but received no other preparation. These were placed in the analysis chamber of the spectrometer that was pumped down to a residual pressure of approximately 10^{-6} Pa. The sample was then imaged using a beam accelerating voltage of 20kV and an area selected for Auger analysis.

After adjustment of the beam intensity to an appropriate analysis value, the analysis conditions were defined. These generally comprised survey scans from 20 eV to 1000 eV (sometimes to 1650 eV depending on elements to be detected) with step of 1.0 eV, dwell time of 100ms and pass energy set to low. Typically 3 to 5 scans were averaged. After collection of a survey spectrum, ion etching, in-situ, was usually performed to determine a coating thickness using a series of fixed etch durations. Auger spectra were collected after each ion etch and a selected peak height monitored until its intensity had fallen to within the background noise level or to a level where its intensity remained constant. Through a knowledge of the sputter yield for ion etching, the peak intensities for a series of Auger spectra collected for different etching times, can be used to calculate a concentration profile using appropriate elemental sensitivity factors. A coating thickness can then be estimated and this used as a measure of surface cleanliness.

4.5.6. XPS

XPS spectra were recorded on a VG Scientific Escalab Mk I vacuum generator with unmonochromatised Al Kα X-ray source (1486.6 eV) and operated in the constant analyser energy (CAE) mode.

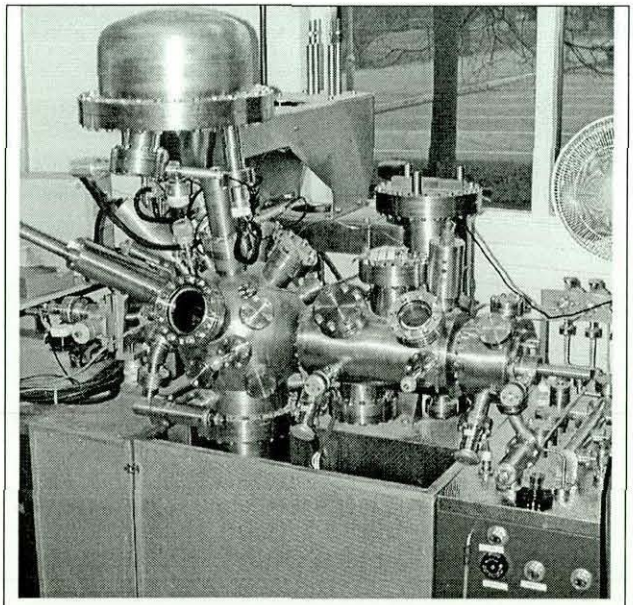

Figure 51. Escalab Mk I XPS

A potential of 9 kV was used at 20mA current. For later experiments this was reduced to 8.5kV at 20mA.The survey spectra were obtained at a pass energy of 100 eV and scan width of 1000 eV and the high resolution spectra using a 25 eV pass energy with summation of multiple scans to reduce noise. XPS spectra were calibrated by assuming a 285 eV binding energy for aromatic and aliphatic carbons. Quantification was achieved by measurement of peak area following subtraction of a Shirley type background.

4.5.7. SIMS

A Cameca 3F SIMS instrument was used to analyse the chemistry of Frekote mould release and prepare positive ion spectra for comparison with data obtained by Blanchard [86].

4.5.8. *Contact angles*

A Data Physics SCA20 Contact Angle Analyser was used to obtain experimental measurements of contact angles using the sessile drop method. Each droplet was imaged using a digital camera and interactive drop shape analysis software then allowed the user to set a baseline to the drop displayed on a monitor. The software then automatically fits a profile to the drop shape and draws a tangent from which a contact angle is computed. By this means it is relatively easy to make many measurements on a single sample and average the results. Using known dispersion values, contact angle measurements using two liquids allows the user to calculate surface energies using the same software.

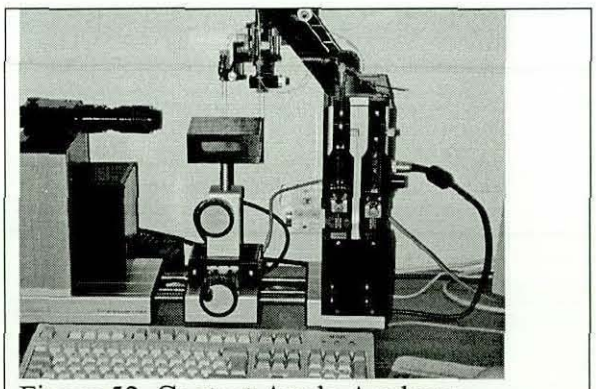

Figure 52. Contact Angle Analyser.

Triply distilled water and diiodomethane (DIM) were polar and non-polar liquids of known surface tensions [187] used to determine surface energies according to the method of Owens-Wendt-Rabel and Kaelble. DIM decomposes with prolonged exposure to daylight and must be stored in an amber coloured glass bottle. Fresh DIM was used to fill the micro syringe before any measurements were taken. A dosing volume of 3 microlitres was used in the majority of experiments and at least twenty contact angles were measured for each liquid and every sample analysed. The mean contact angle was then quoted. The water contact angles were always measured first to minimise substrate contamination.

On metals, dissolved salts absorbed onto the surface can result in dynamic contact angles where the angle decreases rapidly with time. Using the image capture facilities on the Data Physics Contact Angle Analyser, acquisition can be controlled whereby a fixed number of frames is collected in a set time period (typically 10 seconds) and a series of several hundred image frames stored. On playback the baseline for the frame when the drop first touches the surface is manually set and the software uses this reference to calculate the varying contact angles for the subsequent frames. This measures means dynamic contact angles and a plot of the contact angle variation with time is stored.

4.5.9. FTIR

Spectra were collected using a Mattson 3000 FTIR spectrometer. The majority of samples examined were liquids and these were prepared by preparing a film of the liquid onto a KBr disc and allowing to dry in air at ambient temperature. This disc was then placed in the spectrometer and spectra collected over the range 300 to 4000 wavenumbers using 64 scans. The same numbers of scans were used to record the background.

4.5.10. DSC and TGA

These techniques were used to determine the thermal properties of Frekote mould release. Frekote 710 NC mould release agent is a resin dissolved in dibutyl ether. A volume of 250ml of this liquid in a glass beaker was placed in an empty fume

cupboard and the solvent allowed to evaporate completely over a 48 hour period with the fume cupboard extraction left on for this period. After this period a rubbery solid remained at the bottom of the beaker. This material was used for subsequent thermal analysis experiments.

4.5.10.1.DSC

A mass of 11.05mg of solid Frekote was placed in an aluminium DSC sample pan, which was hermetically sealed, and then the lid of the pan was pricked to allow volatiles to escape. This was then subjected to a three stage controlled heating ramp in the furnace of a TA Instruments 2920 modulated DSC. A heating rate of 20°C per minute was used which is a standard heating rate for the determination of glass transition temperatures. The heating cycle consisted of a ramp from 30°C to 120°C using nitrogen purge gas to drive off excess solvent and the sample was held isothermally at the latter temperature for 5 minutes. The second segment of the heating program caused the sample to be cooled to –100°C using liquid nitrogen cooling. In the final segment the sample was heated from –80°C to 300°C.

To achieve the stated degree of cooling required the use of a whole dewar of liquid nitrogen and it was impractical to try to reduce the starting temperature further. At such low temperatures the heat flow signal in the DSC takes some time before it settles down and becomes steady, after about 20°C into the run. Thus the recorded data shows heat flow from –80°C to allow for this settling period.

4.5.10.2. TGA

The thermal stability of Frekote was determined using a TA Instruments TGA 2950HR. A mass of 10.011mg of solid Frekote was weighed into a platinum crucible, which was then positioned inside the TGA furnace. The furnace was purged with dry air at a suitable flow rate (typically 10ml per second). The sample was heated from 30°C to 300°C at a heating rate of approximately 3.5°C per minute. A slow heating rate was chosen to allow excess solvent to be released from the sample. This particular TGA allowed high resolution data to be obtained whereby the heating rate is reduced automatically when a significant mass change occurs.

4.6 Mechanical Tests

4.6.1 Axial butt test

Early in the research it was decided to fabricate a testing geometry made from stainless steel comprising two 60 mm diameter discs whose surfaces could be treated with Frekote products (applied as specified by the manufacturer). A water contact angle of 122° was measured following application of the Frekote. Cytec Fiberite supplied some carbon fibre fabric impregnated with FM300 resin. This material is known as "prepreg" and some of this was used in initial experiments. Three layers of carbon fibre prepreg cut to 57 mm diameter were then sandwiched centrally between the Frekote coated discs and the assembly weighted under 10 kgm load and placed in an over. The prepreg was then cured at 180°C for three hours. As shown in figure 53 below, the steel discs were constructed so that one end of each could be secured into a mounting arm and the assembly then mounted between the jaws of a tensile testing machine. The intention was to quantify the tensile force required to separate the discs thereby determining the quality of the release obtained.

With hindsight it was perhaps naive to suppose this means would be successful to measure the force involved because it was found that the cured prepreg separated so easily from the treated metal discs that it was never possible to mount the assembly in a tensometer without separation occurring first.

Figure 53. Axial butt test components. This figure shows two steel discs which each screw into the adjacent

Figure 54. Used axial butt test disc.This disc was coated with Frekote and achieved 20 releases of prepreg cured

(Legend Figure 53 continued) tensometer bolts. It was envisaged this assembly could be used to test the effectiveness of mould release coatings but in the event the forces were too small to measure using a standard tensometer.	(Legend Figure 54 continued) against it without any sticking.

This was because the release force was so small. Testing methods that can be used to quantify adhesion are generally inadequate to obtain meaningful data for very small release forces and a new testing methodology is required.

It was found that a single full application of Frekote to the steel discs allowed easy release for twenty separate cure cycles for the prepreg laminate. The only slight sticking that was noticeable after 20 cycles occurred at the periphery of the discs due to bleed out of the resin onto uncoated edges. As the number of moulding cycles increases an imprint of the prepreg weave appears on the tooling and a gradual brown staining becomes apparent (figure 54). This exactly mimics what is observed on real tooling used by Bombardier. It is possible that even more releases could have been obtained from the single application of the release agent but the experiments were discontinued after the twentieth cure cycle. A particular difficulty was encountered when mould release agents were applied to laboratory scale sample is achieving an even coating over such a small area. As shown in figure 54, puddling can occur during drying resulting in features known as "fish-eyes" where the coating is locally thicker than elsewhere. From these simple experiments, it was immediately apparent that finding an alternative coating as effective as the Frekote mould release product was not going to be an easy task. The cure conditions described were those that could be conveniently applied using standard laboratory equipment but it is acknowledged that they are very different from the industrial curing conditions previously described as used by Bombardier, particularly in terms of the much greater moulding pressures used industrially. The use of compression springs is one means of applying greater pressure during laboratory curing but even this means falls short of the real moulding pressures used.

4.6.2.Blister test

Most adhesion studies are directed at achieving better adhesion between two surfaces and measuring high fracture energies. In developing effective mould releases, very low fracture energies are desirable and it has proved an intractable problem to find a means of measuring mould release performance in any quantitative way. A design of the blister test was implemented (figures 55, 56 & 57) with the aim of using gas pressure to create a blister between a resin which had been cured onto a metal support treated with a release agent. The gas pressure could be measured initially using a regulator or if greater sensitivity was required, a pressure transducer could be installed in line. The adherent plate is 65mm diameter.

Figure 55. Blister test plate and cell

Figure 56.Blister test cell components

Figure 57 Assembled blister tester

The theory of the method was discussed in section 3.7.1, and in the method, a gas is forced between substrate and coating in such a way that the coating delaminates and

forms a blister. The gas pressure is supplied through a hole in the substrate. In this research a cylinder of compressed air was used in which the pressure could be varied up to approximately 6 atmospheres pressure (608KPa).

The adhesive bonding strength is proportional to the pressure at which delamination occurs. Mechanical properties of the coating, adhesion energy and layer thickness determine and restrict the size of the formed blister. Thicker and stronger coatings and low adhesion energies will give larger blisters before failure. The application of the blister test in this research will be discussed separately.

4.6.3. Friction coefficient and wear test comparisons

Friction coefficient and wear test measurements were made on the Apticote 450 and 460 coatings applied to Bombardier nickel tooling substrate. Both Apticote coatings were compared against cleaned but untreated nickel tooling and the same tooling that had been treated with Frekote mould release.

The four samples were tested for friction and wear using a bi-directional wear test. Each sample was tested at a load of 5N and 10N for 200 cycles against a 5mm tungsten carbide-cobalt (WC-Co) ball. The following conditions were used for each bi-directional wear test: 150mm $min.^{-1}$ table speed, 2mm displacement, 200 cycles.

4.6.4 Surface Roughness Measurements

Profilometry measurements of R_a and R_t were made using a Talysurf instrument.
R_a is defined as the arithmetic mean of the absolute departures of the roughness profile from the mean line. R_t is the maximum peak to vallaey height of the profile in a given assessment length.

4.7 Summary

The number and type of substrates used in this research generated a considerable amount of characterisation data relating to the cleanliness, roughness, chemistry and

topography of the surfaces. This chapter has detailed the preparation procedures, experimental configurations and testing techniques and these, which require no additional comments.

It is inevitable that the laboratory preparation of the substrates diverges from the conditions used industrially and this has obvious implications for the direct transfer of the research to that environment. The emphasis of this research is in evaluating the potential of cleaning technologies and mould release coatings.

Table 6 below lists the materials specified in this chapter and the principal characterisation techniques that have been applied (signified by a tick symbol ✔).

Sample	Principal Characterisation Technique											
	SEM	AFM	AES	XPS	θ_c	SIMS	DSC-TGA	FTIR	Ra/Rt	Friction	IntMic	Ellipse
Industrially Sourced Substrate												
Abraded Ni tooling	✔	✔	✔		✔				✔	✔		
Contaminated Ni tooling	✔		✔	✔	✔				✔			
Virgin Composite tooling	✔	✔			✔				✔			
Used Composite tooling	✔			✔	✔				✔			
Model Substrates												
SS 304 metal foil	✔	✔	✔		✔				✔			
Ni sputtered onto glass slides			✔	✔	✔							
Polished nickel tooling	✔	✔	✔		✔				✔			
Mild steel plate	✔		✔		✔				✔			
Model Contaminants cleaned												
RTM6 on nickel plate	✔				✔				✔			
RTM6 on mild steel plate	✔			✔	✔				✔			
RTM6 on virgin composite	✔				✔				✔			
Release Coatings												
Frekote	✔	✔	✔		✔	✔	✔	✔	✔	✔	✔	✔
Zyvax		✔			✔			✔				
Fluoroalkylsilane	✔	✔	✔		✔			✔				
Oxsilan	✔			✔	✔						✔	✔
Sintered fluoropolymer	✔				✔							
Electroless Ni/PTFE coating	✔	✔	✔	✔	✔				✔	✔		

Table 6 Experimental techniques used to characterise materials used in the present study.

Chapter 5 Results and Discussion of Mould Cleaning Technologies

This chapter details the surface characterisation carried out on both as-received and processed substrates along with the effectiveness of the various cleaning procedures identified.

In view of the number of materials involved and the differing nature of the cleaning procedures, it is helpful to divide this chapter into three separate sections:

Section 5.1 discusses the characterisation of the substrates and contamination,

Section 5.2 gives an account of the evaluation of laser cleaning procedures applied to contaminated metal substrates,

Section 5.3 presents an evaluation of laser cleaning applied to composite tooling, and,

Section 5.4 presents an evaluation of dry ice blasting, and,

Section 5.5 presents an evaluation of sodium hydride cleaning.

5.1 Characterisation of industrial and model substrates and contamination

5.1.1 Techniques

Samples as received were recorded photographically using a digital camera before any work was carried out. Microscopic characterisation of the industrially sourced and model substrates was mainly restricted to examination by SEM and AFM, where appropriate. Contact angle measurements were made to assess surface cleanliness and surface energy together with a limited amount of AES. The chemical composition of the surface contamination on the nickel tooling was characterised by XPS.

As discussed in section 2.2.3.1 clear, unpigmented epoxide resins are surprisingly weak absorbers of infrared laser energy such that the optical absorption depths range from 100 micrometres for laser wavelengths of 10600nm to several millimetres for a laser wavelength of 1064nm. The presence of inorganic pigments such as occurs in paint formulations greatly increases the absorption characteristics but these were only present in the Cytec Fiberite FM300 resin sheets, which were excluded from the model contaminants. As will be discussed more fully in section 5.2.4.2, an important conclusion of the present study is that one means for the efficient removal of bonded

resin from metal substrates is not wholly dependent on its absorption characteristics. For this reason it is not necessary to try to match absorption bands detected in infrared spectra to the optical output of a given laser.

5.1.1.1. Contact Angles

Water contact angle measurements were used as the principal technique in establishing the cleanliness of a surface following a preparation regime. Auger Electron Spectroscopy can be used to provide data on cleanliness but this requires a series of ion etching experiments to be made and cleanliness data is more easily obtained by water contact angle measurements. The use of AES was restricted to determining cleanliness after application of specific cleaning procedures to remove polymerised resin from samples.

Clean surfaces attract a thin layer of contamination very quickly and measured angles increase to from 0° to 50° or more, such is the sensitivity of the contact angle technique. Surface roughness is a factor affecting contact angles and may give rise to large angular differences on surfaces that possess the same chemistry but different degrees of roughness. Unfortunately, there is no simple relationship existing between surface roughness and contact angle. One of the main uses of the technique is in providing a relatively quick measurement of the degree of cleanliness of a metal since a water droplet will readily spread over a clean metal surface giving a low contact angle. Conversely a high contact angle would be expected for a surface coating that resists wetting. Beyond these simple trends, numerical differences in contact angles are difficult to interpret, especially when both surface chemistry and roughness vary for different materials.

In the experimental measurements of contact angles, triply distilled, deionised water was used together with diiodomethane to determine surface energies. Data on these two liquids from Fowkes [187] was used in the computer software calculations. Table 8 gives contact angle measurements (rounded to nearest degree) using two liquids for most of the samples studied.

An average water contact angle of 32° was measured for the nickel samples (ex Bombardier) following ultrasonic cleaning. This suggested the nickel samples were reasonably clean since contact angles for uncleaned metals can be higher than 50°. The cleaning process was repeated for one sample of the nickel plate to see if a lower contact angle could be obtained but no significant improvement occurred. These values could only be obtained if measurements were made immediately after cleaning. The same cleaning regime applied to a smoother stainless steel foil resulted in average angles ranging between 20-30° measured in two orthogonal directions to take account of differences in roughness from the steel rolling process. The measuring software on the Data Physics SCA20 Contact Angle Analyser, used in the present study, does not perform well when attempting to fit drop profiles to very low contact angles and the measurements increase in difficulty as the angle decreases. Consequently some of the data tabulated is incomplete because it was not possible to obtain reproducible measurements. A summary of mean contact angle data from both as-received, cleaned and coated substrates is given in Table 7. The raw contact angle data showed variations of about two degrees either side of the mean value.

Sample	Water	DIM	Surface Energy $mJ.m^{-2}$
Nickel tooling (contaminated)	107°	53°	32.5
Nickel tooling (abraded)	71°	41°	46.2
Nickel tooling (abraded & cleaned)	32°	-	-
Frekote 710 on nickel tooling	120°	95°	10.7
Stainless steel foil (SSF), cleaned.	21°	-	-
Clean SSF dipped in Frekote 710	105°	76°	20.4
Mild steel	96°	48°	35.8
Virgin composite	79°	40°	43.5
Frekote 710 on virgin composite	105°	76°	20.5
Used composite	60°	47°	49.7
1% Fluoralkylosilane on SSF	117°	99°	9.6
1% Fluoralkylosilane on nickel	119°	104°	7.9
Xylan 8080 Fluoropolymer on SSF	126°	99°	9.0
Xylar 2020 Fluoropolymer on SSF	118°	96°	10.8

Apticote 450 coating on nickel	116°	82°	16.5
PTFE sheet (standard control)	116°	82°	16.7

Table 7. Surface energies of substrates.

High water contact angles and very low surface energies were obtained for both the fluoroalkylsilane and fluoropolymer coatings on different substrates.

5.1.1.2. Surface Roughness and Hardness measurements

5.1.1.2.1. Metals

Bombardier finishes their metal tooling using Scotchbrite® fine abrasive pads. The surfaces of all the metal tooling used for testing was mechanically abraded using these pads prior to being cut into test coupons. Average roughness measurements were made on the abraded plate surfaces and R_a = 0.405 micrometres was obtained for the nickel plate and R_a =1.210 micrometres for the mild steel. The mild steel plate as received was oxidised with dull grey colouration and the abrasive finishing applied was not sufficient to remove the oxide. The hard nickel tooling in comparison was highly reflective and it is suggested that the relative hardness differences are reflected in the roughness measurements obtained.

5.1.1.2.2. Composites

A different cleaning regime has to be applied to the composite tooling used by Bombardier and this involves manual rubbing the surface with a very mildly abrasive proprietary compound called G3 Farecla that is readily available from many hardware retailers. A sample of the unused composite tool supplied by Cytec possessing a gloss finish was treated in this way and surface roughness measurements made and compared with those for the unused composite. Despite vigorous manual rubbing, the Farecla compound did not appear to noticeably roughen the gloss surface of the unused composite although the average R_a for the rubbed composite was 0.250 micrometres and that for the untreated virgin material was 0.177 micrometres. The corresponding values for used composite tooling received from Bombardier were R_a = 0.270 micrometres.

5.1.1.2.3. Electroless Ni/PTFE alloy

Talysurf roughness measurements were made on Apticote 450 coating which was deposited onto a piece of the ex Bombardier nickel tooling plate. The measured surface roughness parameter R_a = 1.498 micrometres for Apticote 450.

Table 9 summarises the average surface roughness values from measurements made in two orthogonal directions. Indentation hardness measurements, measured from the area for the indentation of a stylus or ball bearing under a specific loading, really measure the yield stress of the material, which is dependent on the plastic properties of the material [188].

Hardness measurements were made for selected samples using the Rockwell C scale and measured using an Indentec 8150 ACD tester, which applied a load of 150kg to a pyramidal shaped indenter for a dwell time of approximately 8 seconds. A conversion chart was used to convert the average of three separate readings into the Vickers hardness scale and these are shown in Table 8.

Substrate	R_a micrometres	Vickers Hardness
Nickel ex Bombardier	0.483	372H_V/150
Nickel ex Bombardier Scotchbrite abraded	0.405	
Hand polished Nickel Plate	0.0240	471H_V/150
S304 Stainless Steel Foil	0.1295	
Mild steel Scotchbite abraded	1.210	458H_V/150
Virgin Composite	0.177	
Composite ex Bombardier	0.270	
Composite Farecla rubbed	0.250	
Apticote 450	1.498	354H_V/150

Table 8 Roughness and hardness values of selected substrates

No hardness measurements were possible on the stainless steel foil (type SS304) or the composite material.

Since the Apticote 450 coating is applied to nickel plate substrate, it is not surprising that the hardness values are similar under this loading. Some microhardness measurements were made using a Buehler 2100 Microhardness Tester (which applies loads from 10g force to 1 kg force).

Difficulty was encountered in obtaining consistent results for the Apticote 450 sample because the indentations were poorly defined and due to the presence of the softer PTFE phase in the material. A Vickers hardness 364 $H_V/0.2$ was obtained (i.e. for a loading of 200 g). It is thought that penetration of the 20 micrometre Apticote coating occurred even at this low loading.

As the load is reduced further, the indentation becomes smaller and backlash errors associated with the curtain micrometer in the eyepiece reduce accuracy of measurement of the dimensions of the indentation. Using a 25 g force, the average of three readings gave a hardness of $222H_V/0.025$. The manufacturers quote a bulk hardness of $250H_V$ though no loading is specified.

5.1.1.3.Friction coefficient and wear test comparisons

Friction coefficient and wear test measurements were made on the Apticote 450 and 460 coatings applied to Bombardier nickel tooling substrate. Both Apticote coatings were compared against cleaned but untreated nickel tooling and the same tooling that had been treated with Frekote mould release.

Figures 58 and 59 show the friction coefficients for 5N and 10N loadings. Figure 60 shows combined images for the wear tests on the samples.

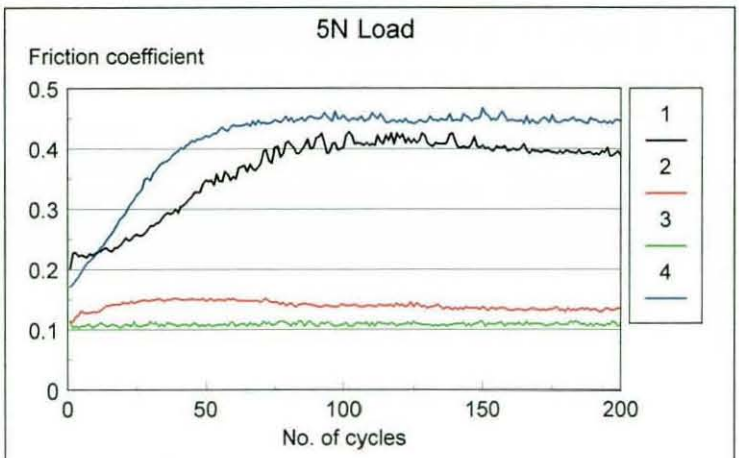

Figure 58. Friction coefficient for selected surfaces using a 5N loading. Sample legend as follows:

Sample 1 = Frekote on nickel

Sample 2 = Apticote 460

Sample 3 = Apticote 450

Sample 4 = untreated nickel

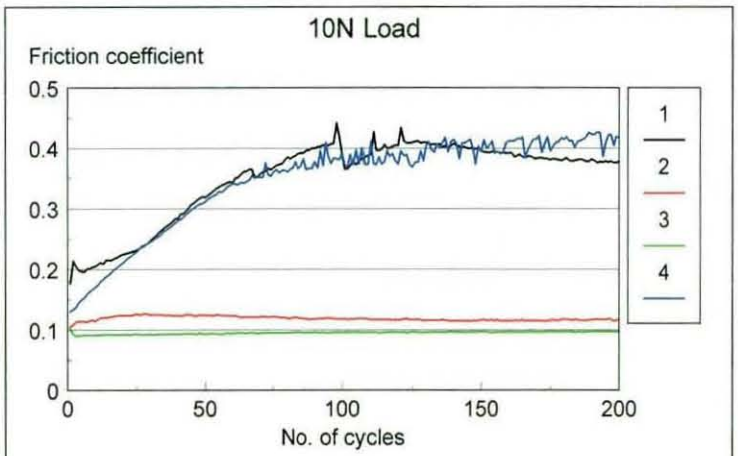

Figure 59. Friction coefficients for selected surfaces using 10N loading. Same legend as for figure 58.

From figures 58 and 59 it is clear that both Apticote coatings clearly have exceptionally low friction coefficients.

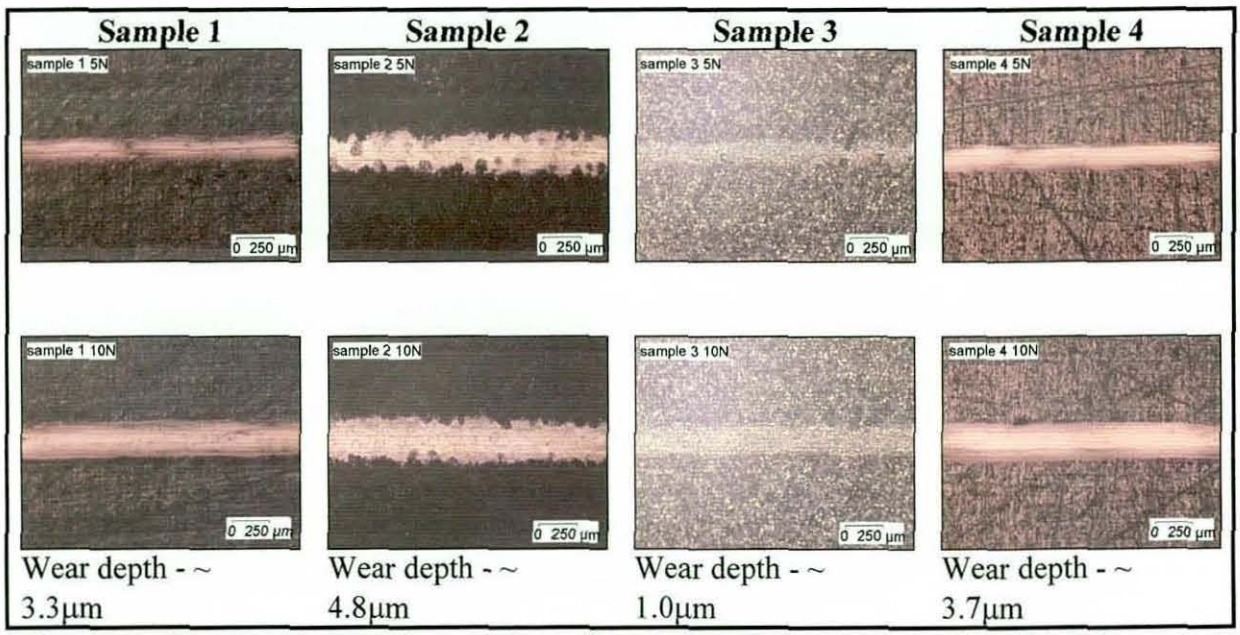

Figure 60. Wear test images for sample surfaces using 5N and 10N loadings.Sample legend as follows: Sample 1= Frekote on nickel, Sample 2= Apticote 460, Sample 3 = Apticote 450, Sample 4 = untreated nickel.

An approximate wear depth was measured for the 10N load tests. This depth would also include any deformation of the sample. The wear is greatest for the softer Apticote 460 coating. The Apticote 450 coating is heat treated to enhance its hardness. The Frekote makes little difference to the wear of the untreated tooling.

5.1.1.4. Surface topography

Scanning electron microscopy was the preferred method of surface characterisation because it can image both very rough and smooth surfaces at a wide range of magnifications. Atomic force microscopy is capable of greater spatial resolution but the areas imaged are smaller and the technique copes less easily with industrially rough or contaminated rough surfaces where large differences in surface relief can damage the mechanical probe or cause it to stick. The electron beam probe in an SEM does not suffer from this disadvantage. SEM images for some of the substrates are presented with corresponding AFM images where appropriate.

5.1.1.4.1. Industrially sourced substrates

Figures 61 to 65 shows the surface topography of the industrially sourced nickel substrate using SEM and AFM. Mechanical abrasive cleaning used by Bombardier results in scouring of the surface with many scratches as shown in figure 61. Such a rough surface is not conducive to obtaining good AFM images because the scratches give rise to deep furrows (figure 62) using the very high resolution obtainable with the technique. The brown contaminant layer on the nickel substrate is shown in figure 63. The contamination has a discontinuous texture as revealed by SEM (figure 64) and was estimated to be between 2 and 7 micrometres in thickness, as determined from SEM cross section (figure 65). It is difficult to measure the thickness of the contamination, as it does not form a uniform layer but instead forms discrete islands of contamination. Also cross section techniques require samples to be embedded in resin that is then subsequently mechanically ground down and the contrast between the contamination and embedding resin is poor. Since the resin interface is mechanically weak, good cross sections are also difficult to obtain and the reliability of the contamination thickness measurements is questionable.

It is apparent, however, from figures 63 and 64 that the contamination is very thin and likely to be of order of the thickness measurements quoted. The light brown coloured contamination on the nickel tooling was scraped off from a large area using a razor blade in an attempt to collect sufficient contaminant to dissolve up into a solution for infrared analysis. It was found that insufficient material could be collected this way and that it was in any case insoluble in common solvents. No further attempt at identification using infrared spectroscopy was attempted.

SEM examination of this contaminated composite tooling reveals a roughened surface (figure 68) rich in silicon as detected by EDX. This is consistent with mould release residue. By contrast the virgin composite (macro-photograph shown in figure 44, section 4.2.2) possesses a smooth, largely featureless, surface by SEM (figure 66) and by AFM (figure 67).

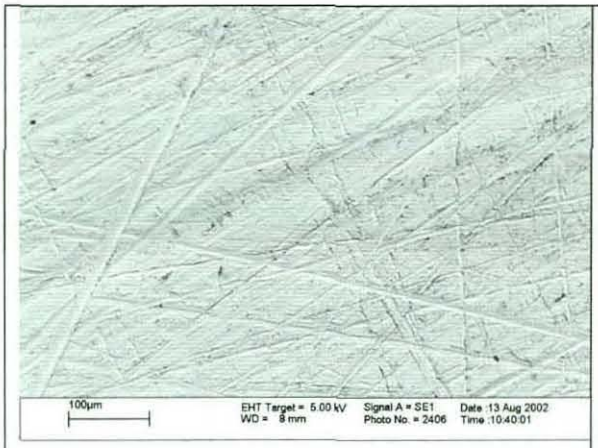

Figure 61. SEM image of abraded nickel tooling ex-Bombardier. Scale bar equivalent to 100 micrometres.

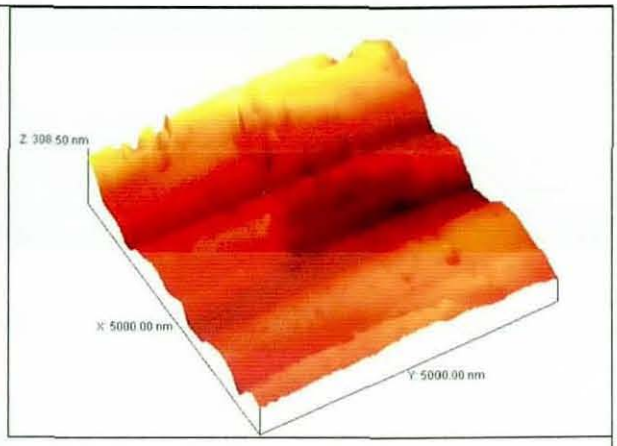

Figure 62. AFM image of abraded nickel tooling ex-Bombardier (5 x 5 micrometres area). Vertical scale 0.3 micrometres.

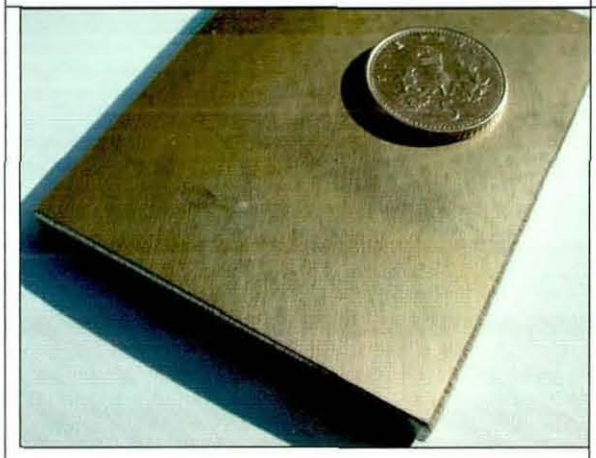

Figure 63. Macro-photograph of coupon of resinous contamination on nickel tooling ex Bombardier.

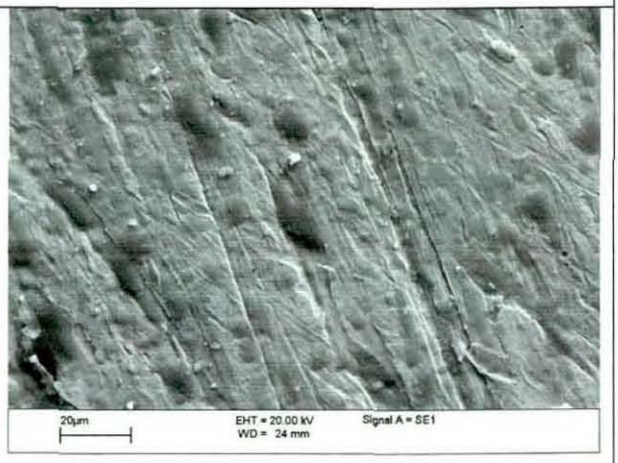

Figure 64. SEM image of resinous contamination. Scale bar equivalent to 20 micrometres.

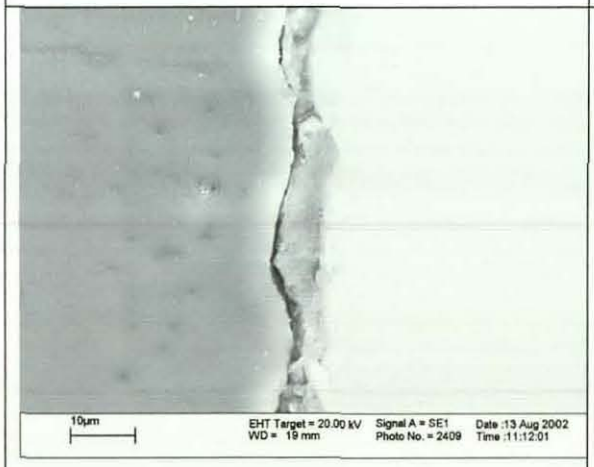

Fig 65. Cross-section of contamination on nickel tooling (ex Bombardier).

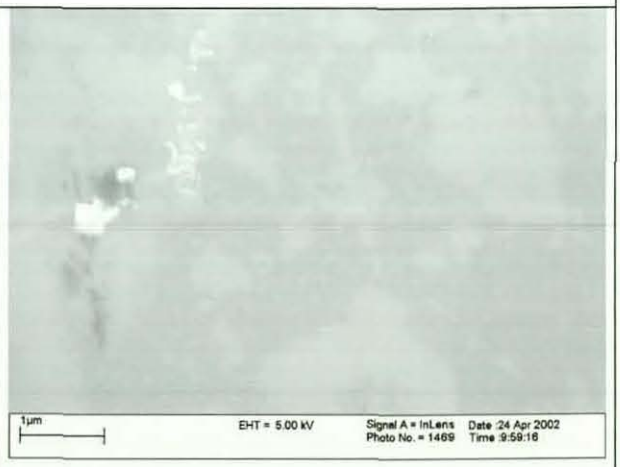

Figure 66. SEM image of virgin composite tooling . Scale bar equivalent to 1 micrometre.

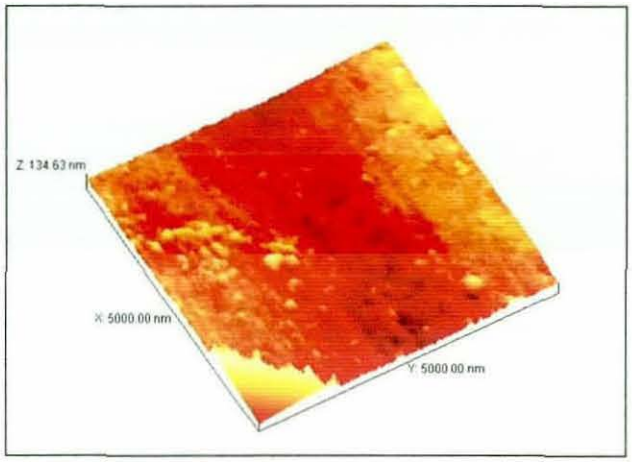

Figure 67. AFM image of virgin composite.
Area scanned 5 x 5 micrometres. Vertical scale 134 nm.

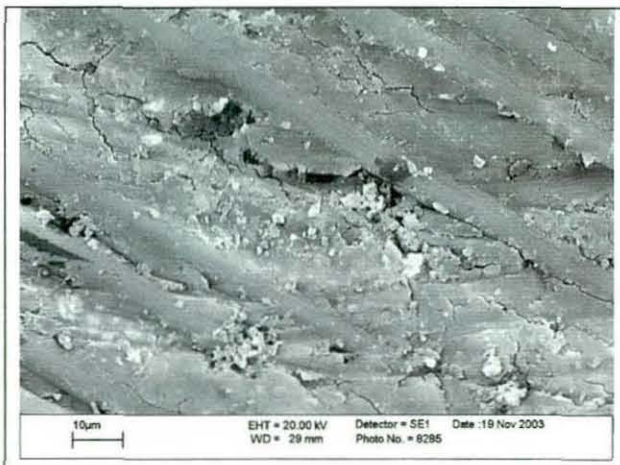

Figure 68. SEM of used composite tooling show what is believed to be degraded resin and residual Frekote contamination.
Scale bar = 10 micrometres

5.1.1.4.2 Model substrates

Figures 69 to 73 show SEM and AFM images of the model substrates discussed in section 4.2.2. The mild steel surface was characterised using SEM only since the oxide scale on the surface was very uneven (figures 69 and 70) and judged unsuitable for characterisation by AFM. The thickness of the oxide layer was determined from a cross section (figure 71) examined in the SEM.

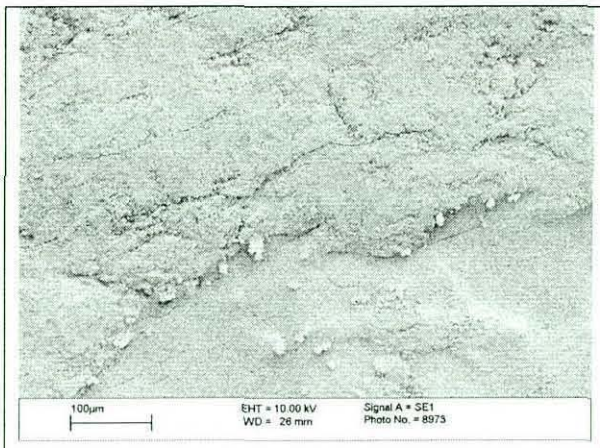

Figure 69. SEM image of oxide scale on mild steel substrate.

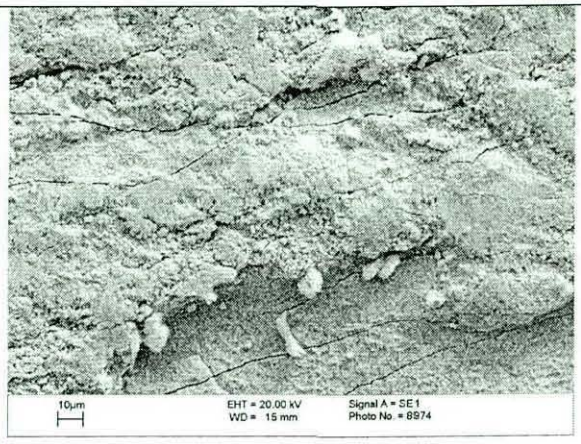

Figure 70. Higher magnification of figure 69.

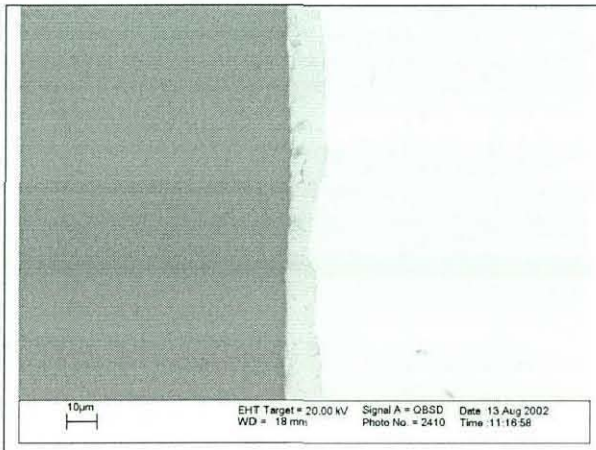

Figure 71. Cross-section of oxide scale (central region) on mild steel substrate.

The stainless steel foil substrate is generally smooth in comparison to the surface of the mild steel and shows only unidirectional fabrication features (see figure 72 for SEM image and figure 73 for AFM image).

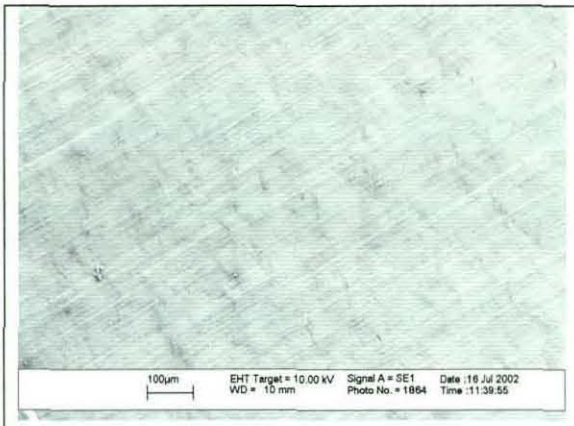

Figure 72. SEM image of surface of stainless steel foil substrate. Scale bar equivalent to 100 micrometres.

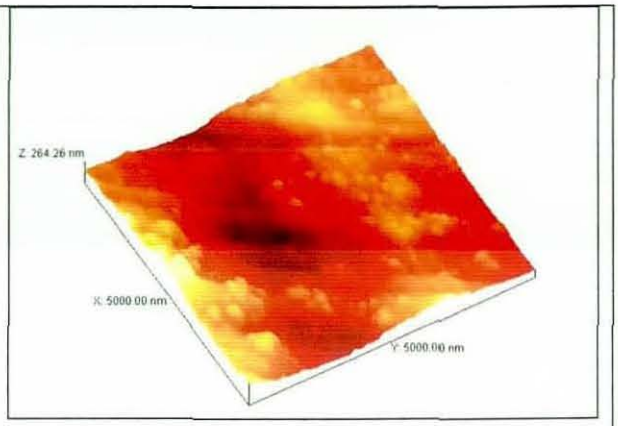

Figure 73. AFM image of stainless steel foil substrate (5 x 5 micrometres area). Vertical scale 264 nm.

The polished nickel 10mm x 10mm squares, referred to in section 4.2.2, were examined by SEM (figure 74) and AFM (figure 75) and are relatively smooth surfaces.

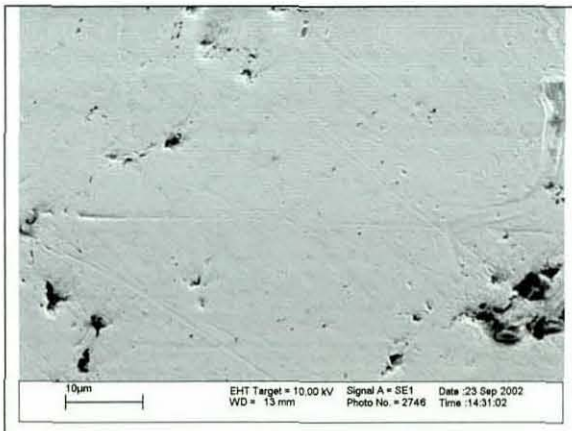

Figure 74. SEM image of hand polished nickel tooling. Scale bar equivalent to 10 micrometres.

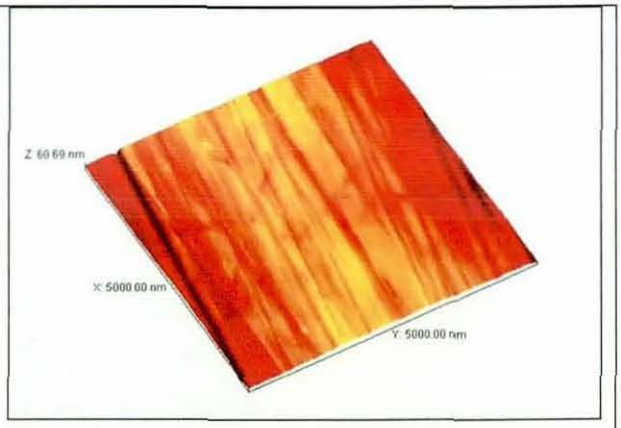

Figure 75. AFM image of hand polished nickel tooling (5 x 5 micrometres area). Vertical scale 60 nm.

5.1.1.4.3 Apticote 450 coating

Figure 76 shows a macro-photograph of the Apticote 450 coating applied to industrially sourced nickel plating. A five pence coin is used as a scale. The coating, as received, has a brown colouration thought to be due to heating which hardens the

coating. Figure 77 shows an SEM image of the coating and it is seen to possess a shallow dimpled appearance. Higher magnification (figures 78 and 79) reveals the dispersed PTFE phase that contributes to the enhanced release properties of the coating, discussed in section 4.4.7. The coating thickness, measured from a cross section, was found to be approximately 20 micrometres (figure 80).

Figure 76. Macro photograph of Apticote 450 coating on nickel tooling. A five pence piece used for scale.

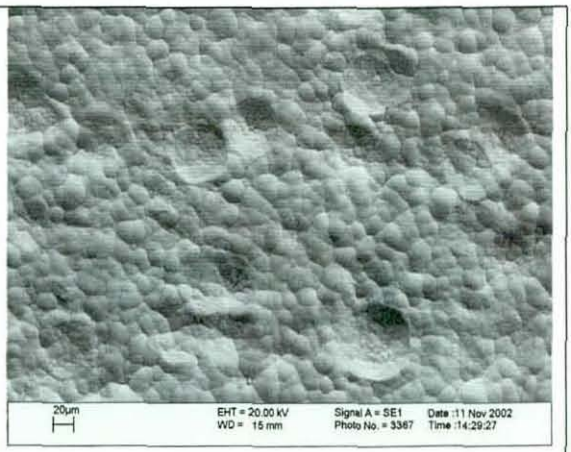

Figure 77. SEM image of Apticote 450 coating. Scale bar equivalent to 20 micrometres.

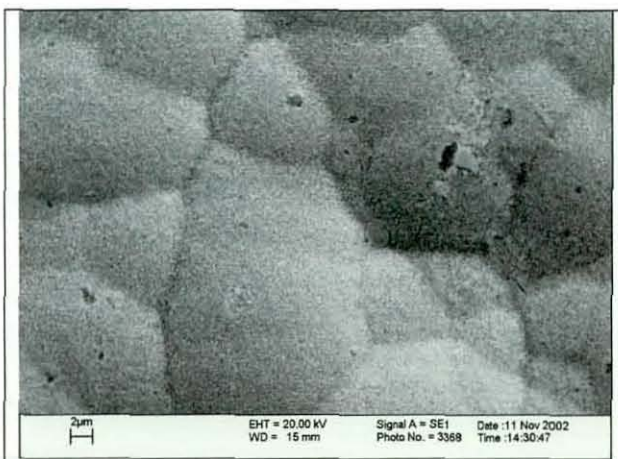

Figure 78. Higher magnification of figure 77. Scale bar equivalent to 2 micrometres.

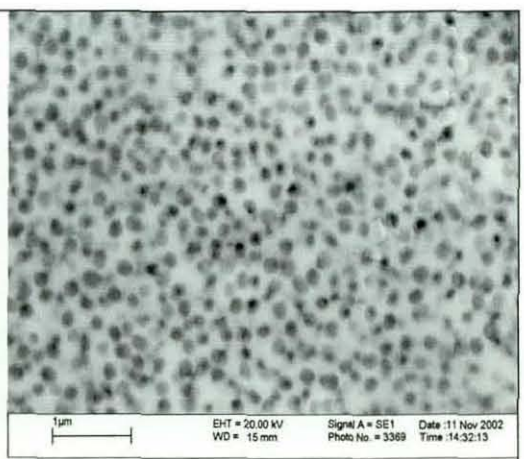

Figure 79. SEM image of PTFE particle phase. Scale bar equivalent to 1 micrometre.

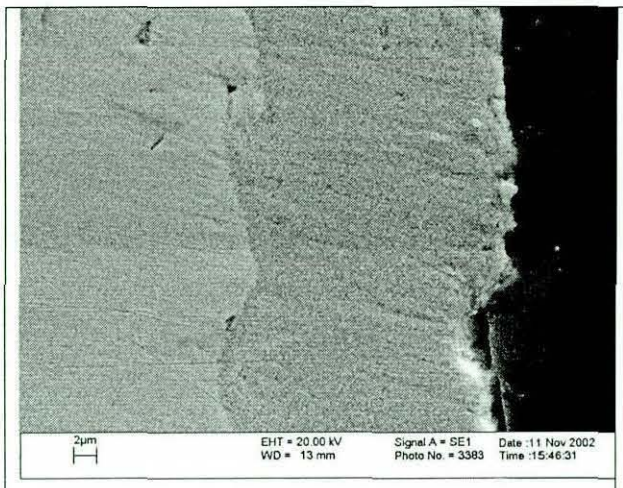

Figure 80. Cross-section of Apticote 450 coating

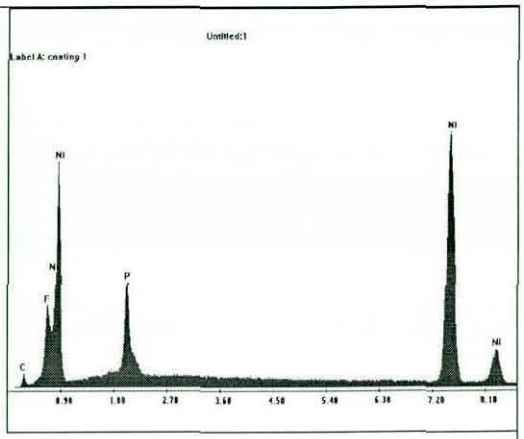

Figure 81. EDX spectrum of Apticote 450 coating.

Elemental analysis using EDX in the SEM identifies Ni, P and F as the major peaks (figure 81). The size of the PTFE particles is below the resolution limit for X-ray mapping and so it was not possible to produce a map to show the fluorine rich sites but it is reasonable to assume that the dark, roughly circular features in figure 79 are the PTFE phase. These particles have a diameter of approximately 200nm.

5.1.1.5.Surface Chemistry of Contaminants

X-ray photoelectron spectroscopy was used to characterise a sample of the contamination on the nickel metal tooling plate received from Bombardier. The results suggested that this contamination is a mixture of hydrocarbons from breakdown deposits of the resin and some silicon from Frekote residues. Table 9 gives the elemental quantification data. In all cases peak positions were energy referenced to C1s defined at 285eV.

Element & Peak	Binding Energy eV	Atomic % present
Carbon C1s	285	64.5
Oxygen O1s	532.5	23.7
Silicon Si2p	102.3	3.6
Sulphur S2p	168.1	1.6

Calcium Ca2p	348.1	1.2
Nitrogen N1s	399.8	3.3
Fluorine F1s	689.1	1.5
Nickel Ni2p3	855.9	0.3
Sodium Na1s	1071	0.4

Table 9. XPS composition of contaminated Nickel tooling (ex-Bombardier)

The surface of the used composite tooling (ex-Bombardier) was also examined using XPS . Table 10 shows the surface composition of the used composite and it is seen that higher levels of silicon are found on the used tooling surface. The surface composition of virgin unused composite tooling is included for reference.

Element & Peak	Binding Energy eV	Atomic % present
Carbon C1s	285	82.2
Oxygen O1s	525.8	17.8

Virgin composite tooling

Element & Peak	Binding Energy eV	Atomic % present
Carbon C1s	285	56.9
Oxygen O1s	532.6	23.9
Silicon Si2p	102.3	19.2

Used composite tooling

Table 10. Comparison of XPS surface composition of virgin and used composite tooling (ex-Bombardier).

The higher level of silicon on the used composite tooling may reflect the less abrasive cleaning that is commonly applied to such tooling (in comparison to the very abrasive cleaning applied to nickel tooling). Also mild abrasives polishes are used to clean the composite tooling and these likely contain silicon compounds which remain as a surface residue. The chemical nature of the residue on either type of tooling is complex and difficult to interpret.

5.1.1.6.Summary

It is useful to summarise the findings from the three principal characterisations as outlined above.

5.1.1.6.1.Contact angle data

This shows that reasonably clean metal surfaces can be prepared using the procedures described. When the cleaned surfaces are treated with mould release coatings, these exhibit the properties of low energy surfaces and the data shows that surfaces energies lower than that measured for PTFE can be obtained using fluoroalkylsilane treatments.

5.1.1.6.2.Substrate roughness

The different surface chemistries and roughness of the substrates makes correlation to contact angles very difficult. The main value of the surface roughness measurements is in comparison to similar measurements made following the application of cleaning technologies. For example, there exists the need to determine how laser cleaning affects the surface roughness of substrates.

5.1.1.6.3.Substrate topography

The surface topography of the substrates, revealed by SEM and AFM images as shown, contrasts the very rough surface of ex Bombardier nickel tooling to the smooth composite tooling. These images justify, in part, the choice to adopt the stainless steel foil material as a surrogate replacement for the nickel tooling. The foil has a roughness approximately intermediate between that of the metal and composite tooling and the use polished nickel samples supplements the foil for specific experiments.

5.1.1.6.4.Surface chemistry of contamination

The evidence from XPS suggests the contamination on the tooling received comprises organic material containing silicon but is of complex composition.

5.2. Laser Cleaning of Resin from Metal Mould Tooling

5.2.1. Initial investigation of laser cleaning using a TEA CO_2 laser

The use of a Laserbrand TEA CO_2 laser to clean inorganic contamination from a variety of metal substrates had been studied by Cottam[49] and the experimental characteristics of the laser such as the temporal beam profile and temperature rise at surfaces were determined as part of his PhD dissertation. A schematic diagram of the experimental set up used in this research is shown in figure 82. After initial trials the gold mirror was removed and the only optical elements used was a ZnSe focussing lens of focal length 30cm. The energy density (fluence) is one parameter that can be simply varied. This is a measure of how much energy is concentrated into the beam and is defined by:

Fluence ($J.cm^{-2}$) = Energy of laser per pulse (J)/ Area of laser beam on surface (cm^2).....(53)

It was found in the present study that the cleaning fluence was too great for samples when they were located at the focal point of the lens where the area irradiated was approximate 4mm x 5mm. Plasma formation occurred at the focus. Also for cleaning applications, the area irradiated needs to be larger whilst still possessing enough energy to remove contamination. By trial and error it was found that an optimum cleaning fluence occurred for samples located 15 cm in front of the focal point, or some 45 cm in total. Apart from this sample to source distance, the only other parameter that could be varied was the number of pulses applied to effect removal by laser ablation.

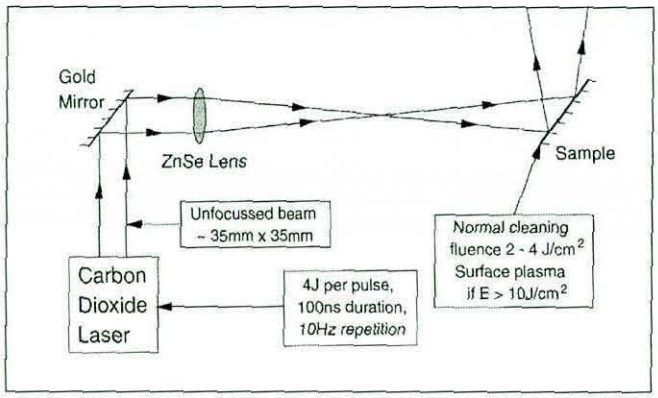

Figure 82. Initial experimental arrangement for Laserbrand TEA CO_2 laser (After Cottam[49]).

In the majority of investigations reported using the Laserbrand TEA CO_2 laser the fluence values given are estimates based on measurements made by Cottam. Unfortunately the laser manufacturers could not be contacted for advice on this and related topics since they ceased trading many years earlier. No efficient extraction facilities for the removal of ablated material were available in the laboratory and simple means had to be improvised to implement some rudimentary level of extraction. In practice the extraction nozzle could not be located close enough to the work piece without obscuring the line of sight from the laser. Poor extraction resulted in re-deposition of ablated material onto the area treated and because of this water contact angles were higher than expected on cleaned surface (usually 40° or 50°) unless a high fluence was used, when angles of approximately 20° could be measured.

One of the experimental difficulties in using high power lasers is in measuring laser energy per pulse. This measurement is relatively easy in the lower power laser systems that are frequently encountered in telecommunication applications and use solid-state area detectors. The output of such detectors is saturated by the energy from high power lasers and the energy is sufficient to permanently damage them.

Advice concerning fluence measurements was sought from Roberts [36] and his comments were particularly informative: "*There's no easy way to measure fluence for a TEA CO_2 laser! The higher the power, the more difficult it is. With an homogenised beam it should be relatively easy as the fluence is just the pulse energy divided by the area of the "footprint". We measure the pulse energy here (National*

Laser Centre, South Africa) with a Molectron detector but care must be taken to expand the beam over a large area and sample over a small number of pulses to avoid detector damage. We don't have an homogeniser with our TEA so we measure the fluence by scanning the beam area with a pinhole (0.5 to 1 mm diameter) and normalize the profile to the total energy. Even here the beam has to be expanded up from the pinhole to avoid detector damage. We have also measured beam profiles with an infra-red multichannel camera (Spiricon) but the intensity has to be massively attenuated to avoid damaging the camera. With a Gaussian or near Gaussian beam profile we measure the transmission of circular steel apertures of different sizes and find the best fit to F(r) = F(0)exp(-2r2/w2). In all cases to get absolute errors within 10% is quite difficult. Of course with non-homogenised beams one has to take account of the distribution of fluence and not just use an average fluence. While the beam centre may be efficiently removing the coating, the outer regions could be below threshold and remove nothing at all ".

The above extract gives some insight into the complexity of just one aspect of laser cleaning – the specification of a key operating parameter. The beam quality for a solid state Nd:YAG laser is much greater and approximates to a Gaussian energy distribution. However, for laser cleaning, as oppose to laser cutting, the beam profile needs modifying to approximate a "top-hat" distribution where the intensity is uniform over the beam area.

In the present study an initial investigation was made using FM 300 epoxide resin sheet of 150 micrometres thickness that was fastened to a steel supporting substrate with tape and the effects of only 5 pulses from the laser are shown in figure 83. The laser fluence was approximately 1 $J.cm^{-2}$ and a five pence coin was used as a scale. At the area shown, the absorption of the resin was large and the heating at this fluence was sufficient to cause the laser to ignite the resin.

A solution of the resin sheet was prepared by dissolving 30 square centimetres in a beaker containing 100ml of acetone. The insoluble PET supporting membrane was removed and the solution painted onto a steel substrate and allowed to drain vertically. This was then cured in an oven at 180°C for three hours and a thin film of resin approximately 20 micrometres thickness was obtained. Figure 84 shows the area

of this thin film that was irradiated by the laser. The area treated was the same size as shown in figure 83 except that the image has been enlarged to show the incomplete removal of the resin.Using the same fluence (1 $J.cm^{-2}$), 100 laser pulses were required to produce the effects shown in figure 84 which also illustrates the poor uniformity of the beam intensity comprising a series of lines. This means that laser ablation is much more efficient at removing thick coatings of strongly absorbing resin that much thinner layers of the same resin.

Figure 83. Photograph showing effect of 5 laser pulses from Laserbrand TEA CO_2 laser on a 150 micrometre thick sheet of strongly absorbing pigmented resin.

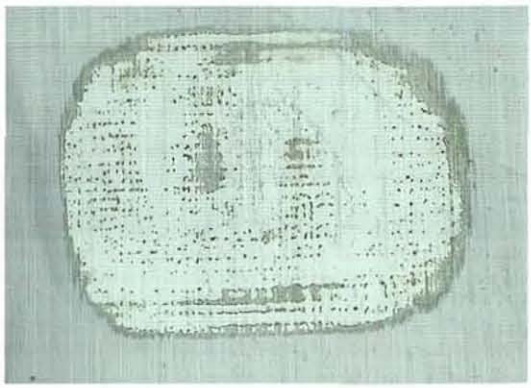

Figure 84. Photograph showing effect of 100 laser pulses from Laserbrand TEA CO_2 laser on a thin cast film of the same resin.

Irradiation of clean nickel substrates at fluences up to 2 Jcm^{-2} appeared to cause no microstructural damage at all when the surfaces were examined by SEM.

The radiation from the Laserbrand CO_2 TEA laser has a wavelength of 10.6 micrometres and because this is large compared to the scale of surface damage caused by mechanical abrasion cleaning on the sample, this level of surface roughness has a negligible influence on the reflective properties of the substrate. If laser treatment had damaged the surface, thermal effects would expect to be seen but none were resolved. The same was not true for the mild steel but in this case the presence of a thick oxide layer gave rise to artefacts. These observations will be developed later in section 5.3.2.2.

5.2.1.1. Roughness measurements on TEA CO_2 laser treated metal samples

Talysurf profilometry was used to measure the surface roughness R_a parameter (in micrometres) for the treated areas of the nickel and steel samples. Table 11 compares these to the corresponding roughness values on the untreated substrates.

	R_a Untreated	R_a Treated
Abraded nickel plate	0.2099	0.2871
Abraded mild steel	0.9049	1.3804

Table 11. Measured roughness values of laser cleaned metal tooling.

Comparing the SEM images for the CO_2 laser treated nickel plate; these suggest that not all the resin has been removed and that further passes of the laser would be required. This may be a consequence of photothermal ablation predominantly associated with high power pulsed TEA CO_2 lasers. The different in surface roughness before and after treatment is not great and probably simply represents sample-to-sample variation.

Although the SEM images for the laser cleaned steel suggest a much cleaner surface has been obtained, the creation of porosities in the surface associated with the proposed melting of the thick oxide layer are the most noticeable feature. Since these porosities are ~ 1 micrometre diameter or less and the Talysurf stylus tip is 2 micrometres diameter, it is unlikely that the difference in R_a is attributable to any change is surface topography resulting from laser cleaning, and again, the data may simply reflect sample-to-sample variation. In view of the above results roughness measurements were not made on the Nd:YAG treated samples.

5.2.2. TEA CO_2 laser irradiation of contaminated nickel tooling (ex Bombardier)

A sample of contaminated nickel tooling similar to that shown in figure 63 (section 5.1.1.4.1) was cleaned using a Laserbrand TEA CO_2 laser. The contamination is slight and, as discussed in section 5.2.1, this leads to inefficient cleaning with many pulses required to achieve a visibly clean surface. It was found that the fluence had to be increased to approximately $2J.cm^{-2}$ and 12 pulses applied to completely remove all visible traces of the contamination. The area irradiated was approximately $25mm^2$

and in order to attempt a measurement of contact angle the sample was moved manually to irradiate a target area of approximately $100mm^2$. It is likely that some fraction of the areas received more pulses than others since the sample was moved manually. Examination of the cleaned area using SEM showed (mostly) only the abrasion scratches from previous cleaning of the tooling (figure 85) with no apparent thermal damage to the nickel substrate at higher magnifications.

Figure 85. TEA CO_2 laser removal of contamination on nickel tooling. Scale bar = 200 micrometres.

Three water contact angles of 54°, 42° and 39° were measured on the small area cleaned by laser. These measurements had to be done sometime after the cleaning although the sample was wrapped in aluminium foil for protection after laser cleaning. It is likely that the surface picked up carbonaceous contamination that is reflected in the high contact angles. The extraction facilities to remove ablated materials were not efficient at the point of cleaning and although the SEM shows the sample is relatively clean, the level of cleanliness attained is relatively poor and consequently AES was not used to determine residual contamination levels. Overall the subjective impression obtained from several attempts at cleaning the type of contamination shown in figure 63 was that although the cleaning efficiency was poor, (resulting from the very thin, weakly absorbing contaminant layer), the contamination could be removed to produce a visibly cleaner, more reflective surface.

5.2.3. TEA CO_2 laser irradiation of RTM6 resin coated metal substrates

As discussed in section 4.3.3, the co-operation of external laser laboratories was sought to conduct some sample trials using measured fluences. Nickel and mild steel coupons coated with approximately 150 micrometres of RTM6 resin were laser cleaned and returned. The results are presented and interpreted. With reference to the macro-photographs of the laser cleaned samples, the following treatment conditions applied.

5.2.3.1 Resin coated nickel coupon

See Figures 86 to 91.

Treatment conditions : Larger removed area, laser fluence F= 8 $J.cm^{-2}$

Single line, F= 6.0 $J.cm^{-2}$

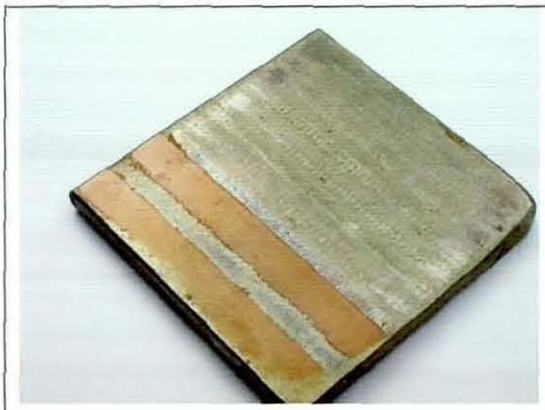

Figure 86. Effect of TEA CO_2 laser cleaning of epoxide resin from nickel tooling. Originally the epoxide resin covered the whole sample. The laser was then used to selectively remove the resin over most of the surface leaving two epoxide resin strips (depicted by the brown colouration) to contrast the areas cleaned against uncleaned areas.

Figure 87. Macro-photograph at slightly higher magnification of area in Figure 86. This again contrasts clean and uncleaned and uncleaned areas as described in the legend for Figure 86..

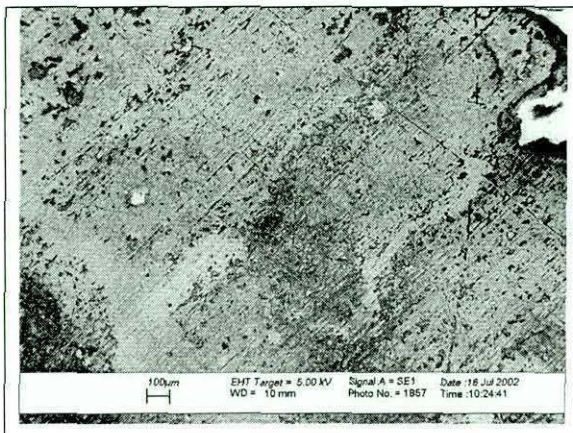

Figure 88. SEM of laser cleaned surface shown in Fig.87. Scale bar = 100 micrometres

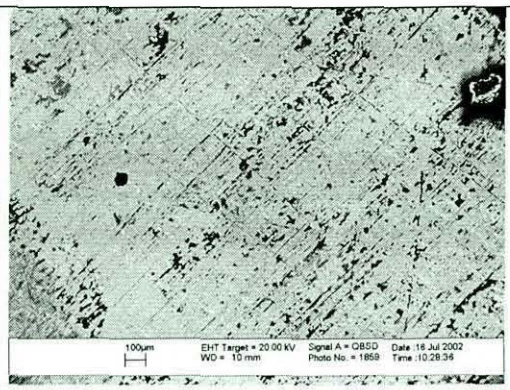

Figure 89. As figure 8.Scale bar = 100 micrometres

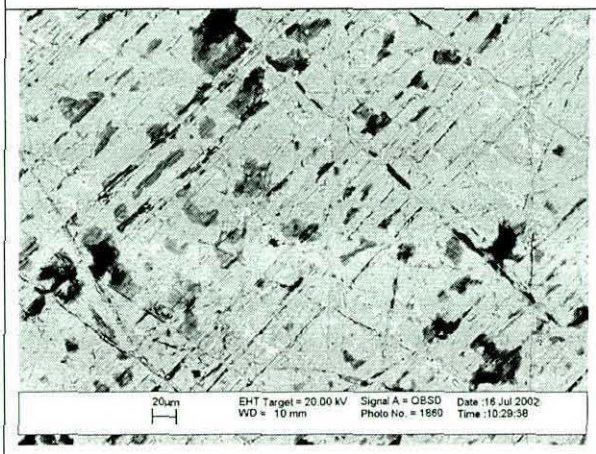

Figure 90. SEM of laser cleaned surface Scale bar = 20 micrometres.

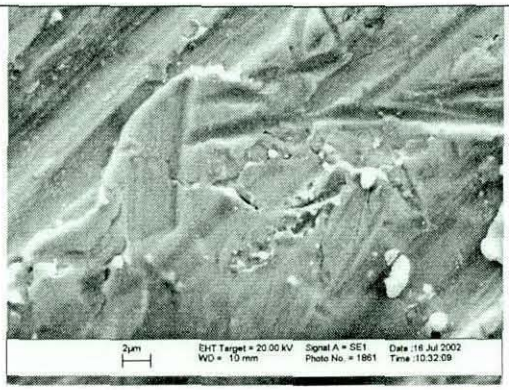

Figure 91. As figure 90.Scale bar = 2 micrometres.

Figures 86 and 87 show macro-photographs of TEA CO_2 laser treated resin bonded to a nickel substrate. The coupon dimensions were 50mm x 50mm x 5mm thickness. It is seen that the laser removes most of the brown resin but that it does not leave a bright metal surface. This is apparent when the surface is examined in the SEM (figures 88 to 90) where the dark features are resin residues. Only at high magnification where the area examined is very small, is the surface clean but here there is some evidence of thermal damage from the laser, implying that the fluence used was too high for a cleaning application (figure 91).

5.2.3.2.Resin coated mild steel coupon

See figures 92 – 97.

Treatment conditions: Larger removed area, F= 8 J.cm^{-2} Part of this area single scan, the remaining region (more complete removal) three scans.

Single line, F= 6.0 J.cm^{-2} single scan.

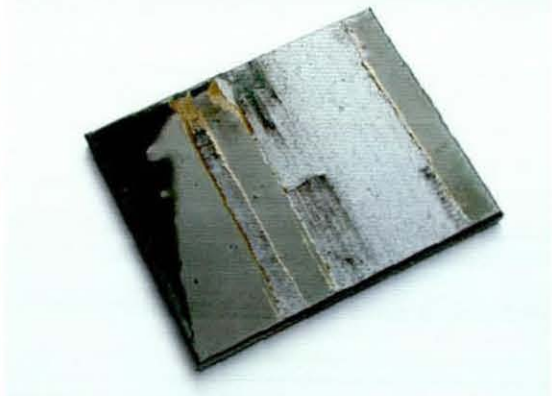

Figure 92. Macro-photograph showing the partial removal of epoxide resin bonded onto a mild steel test plate using a TEA CO_2 laser .

Figure 93. Macro-photograph at a slightly higher magnification of an area depicted in Figure 92. This more clearly contrasts cleaned and uncleaned areas (darker grey colouration with brown edges where the resin has been burnt during the laser cleaning.

Figure 94. This macro-photograph shows a area laser cleaned in figure 92 at a slightly higher magnification.

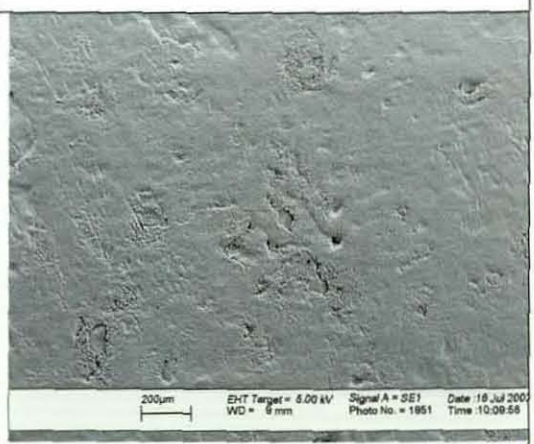

Figure 95. This figure shows an SEM image of the surface depicted in figure 94 from which it is seen that there is little obvious surface damage at low magnifications. Scale bar = 200 micrometres

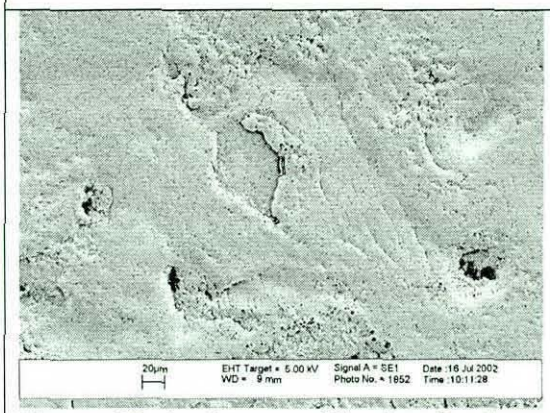

Figure 96. As the magnification for the area depicted in the previous figure is increased fine scale damage begins to be resolved by the SEM. Scale bar = 20 micrometres

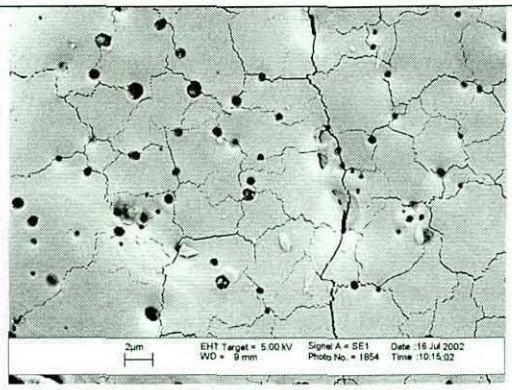

Figure 97. At fairly high magnification the SEM resolved a fine scale pitting of the oxide surface of the cleaned mild steel plate. Scale bar = 2 micrometres

Figures 92 to 94 show macro-photographs of resin bonded to the mild steel substrate that was cleaned using a TEA CO_2 laser. The SEM images of the cleaned surface, shown in figures 95 and 96, reveal a much cleaner surface than was seen for the nickel substrate. The difficulty in comparing these effects is that the absorption properties of mild steel surface are different to that of the nickel. The laser fluence for this sample may have been high enough to completely remove the bonded resin but the presence of the thick oxide layer on the surface of the mild steel has apparently resulting in an additional effect resulting from the laser treatment (figure 97). This shows that the substrate surface is pitted with numerous circular porosities suggestive of the release of trapped gas from the surface.

Similar effects were reported by Cottam [49] and are thought to arise from interaction of the laser-generated plasma with the substrate surface. When the surface is irradiated, the resin is vaporized and very hot plasma exists momentarily above the surface. The temperature of this plasma is believed to be several thousand degrees Celsius and heat from it re-radiates to the surface and is sufficient to cause the surface layers to melt. Gases trapped in the surface below this melt zone then migrate into it. At the cessation of laser treatment, the melt zone cools and solidifies causing micro-cracks to appear, as are seen in the above micrograph. Also gases present are trapped

giving the appearance of porosities although no similar surface features are seen in untreated surfaces. The effects are, of course, non-uniform and reflect the spatial distribution of the laser energy.

5.2.4.Laser cleaning using a Nd:YAG laser

5.2.4.1 Laser cleaning of contaminants from nickel and mild steel samples using a Spectron Nd:YAG laser

The Spectron 450 Nd:YAG laser was used for a number of experiments to study the efficiency of laser cleaning on selected samples. The following photographs illustrate some of the effects obtained. Figure 98 shows an untreated nickel coupon (50mm x 60 mm) cut from a used tool whose surface is uniformly covered with the slight brownish contamination typical of Bombardier used tooling and upon which the imprint from the weave pattern of mouldings can just be discerned. This adhered quite tenaciously to the nickel substrate and could not be removed using a cloth moistened with acetone.

The Nd:YAG laser was used to remove this contamination at a range of fluences and the results are shown in Figure 99. This coupon was then sputter coated with gold and examined in the SEM to determine the microstructural effects for the different areas treated.

As discussed, the Spectron laser output is not optimised for a cleaning application since the largest beam diameter than can be used is approximately 8 mm and cleaning is consequently slow. The brown resinous contamination is easily removed (figure 100) at a variety of fluences that cause no significant damage to the substrate. Figure 101 shows the effects for an RMT6 resin coated mild steel coupon of the same dimensions.

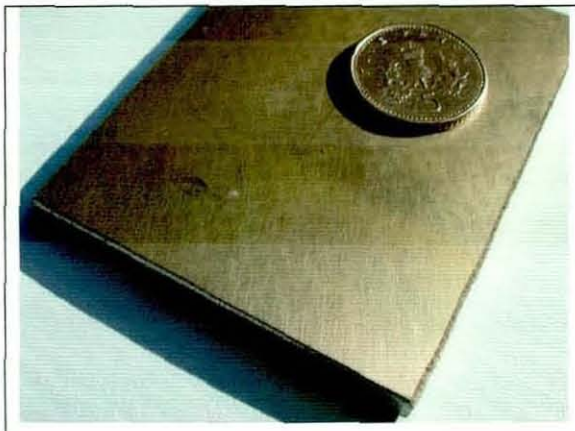

Figure 98. Macro-photograph showing the texture of the contamination present on used nickel tooling (ex-Bombardier)

Figure 99. This figure depicts the partial cleaning of selected areas of contamination (similar to that shown in the previous figure) using a Nd:YAG laser at different cleaning fluences.

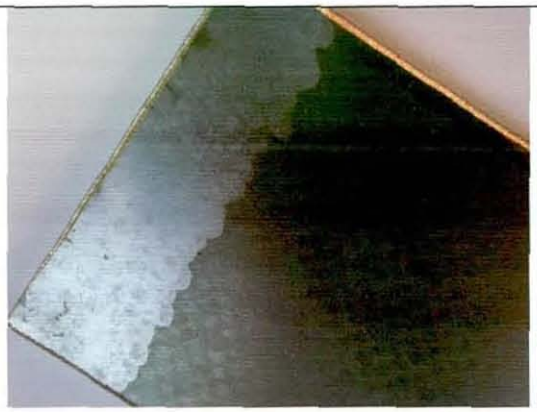

Figure 100. This figure is similar to figure 99 and shows removal of the particulate contamination depicted in figure 98.

Figure 101. This figure shows multiple impacts of a Nd:YAG laser on a mild steel sample which has been coated with a thin layer of epoxide resin. The resin is debonded at each point of impact.

The Nd:YAG laser was operated in Q-switched mode with the power level set at 850mJ and repletion rate at 1Hz in all the above figures. This allowed the test piece to be moved manually and an area cleaned. In an optimised laser cleaning application either the mould tool would be moved automatically in a controlled manner or else the laser would be mounted on a robot arm and automatic cleaning effected in that way. Manual cleaning is only generally used for restoration applications where cleaning speed is not an important factor.

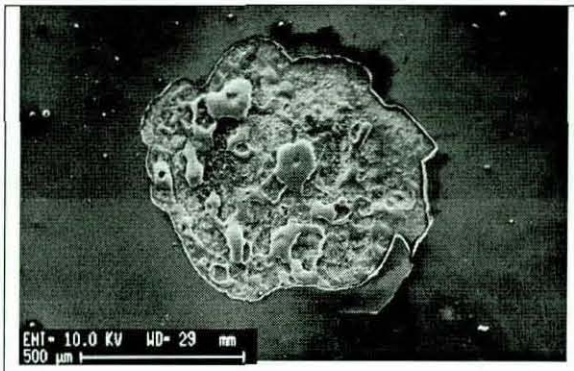

Figure 102. This figure shows an SEM image of bonded resin which has been attacked by a Nd:YAG laser which was focussed onto the resin surface at sufficiently high fluence to burn it.

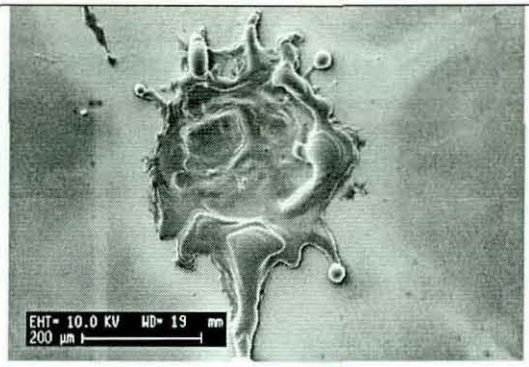

Figure 103. This figure shows how a focussed Nd:YAG laser will also damage a nickel surface unless a low cleaning fluence is used.

Figure 99 shows four areas where the Nd:YAG laser beam has been progressively defocused to reduce the energy density. It is necessary to recognise that without this degree of defocus, the laser beam can greatly damage the surface as shown in figure 103. Continued pulses would bore a hole in the metal surface quite easily. As discussed in Chapter 2, resin poorly absorbs light energy of 1.06 micrometre wavelength (the output of a Nd:YAG laser). However, when a sufficiently high fluence is used, the resin is attacked. Figure 102 for an RTM6 resin coating on mild steel illustrates this. These operating conditions have to be avoided for laser cleaning applications and by optimising the laser parameters, effective cleaning can be demonstrated which causes negligible surface damage.

5.2.4.2.Laser cleaning of contaminants from a nickel sample using a commercial Nd:YAG laser system at Quantel Inc., France.

A contaminated tooling plate (ex Bombardier) of dimensions 150 mm x 205 mm was divided into two and one half (figure 104) submitted to Quantel in Paris, France for laser cleaning using a 20W LaserBlast Nd:YAG laser which has been designed for commercial laser cleaning applications. The laser output energy was 330mJ per pulse at 1064nm. The other half was sent to the National Laser Centre in Pretoria, South Africa to be similarly treated using their laser facilities.

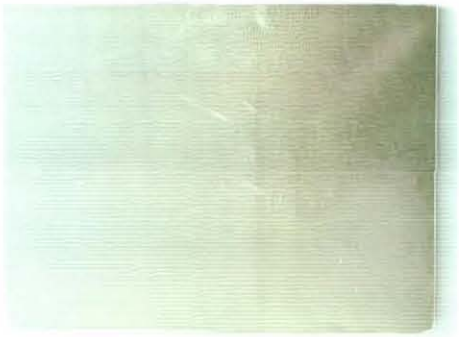

Figure 104. Nd:YAG cleaned nickel tooling plate (150 mm x 100 mm)

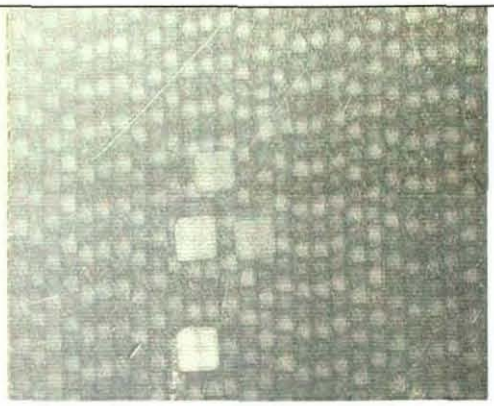

Figure 105. Close up photograph of area cleaned by laser in figure 104.

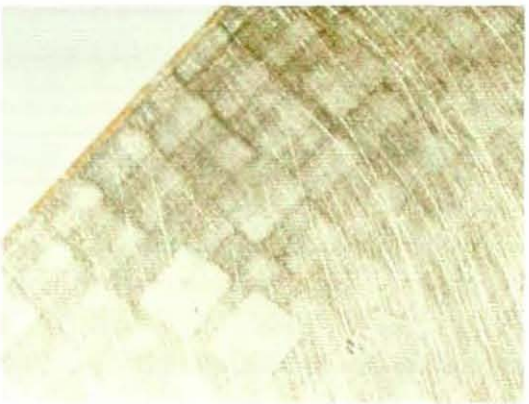

Figure 106. As figure 105.

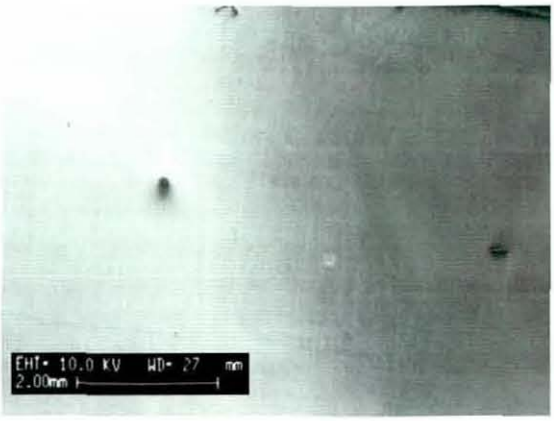

Figure 107. Low magnification SEM image of area in figure 106. Scale bar = 2.0 millmetres.

Different fluences were tried initially and it was found that a fluence of $2J.cm^{-2}$ attacked the resin but that the best results were obtained using a lower fluence of 1.0 $J.cm^{-2}$. The used nickel tooling plate was positioned on a platform, which was moved under computer control relative to a static laser beam, and this allowed cleaning at a speed of $10cm^2$ per second. This equates to approximately two and three quarter hours to clean an area of one square metre. The lines resulting from this scanning are evident on the cleaned face, which has a bright metallic lustre (figure 104). As is apparent from Figures 105 and 106, a regular patterning is discernable. The Nd:YAG laser used to clean the sample has a square beam profile. It is thought that overlap of this profile during mechanical scanning of the plate results in corners of successive profiles receiving an overdose of radiation and that this gives rise to the patterning

effect shown. Figure 107 shows that the surface is clean at low magnifications when viewed in the SEM.

The laser treatments discussed in sections 5.2.2 and 5.2.3.2 were performed in different laboratories and in both cases involved returning of samples by overseas mail. Consequently it was not possible to quantitatively measure cleanliness on the treated surfaces immediately following laser cleaning. Such measurements were restricted to laser treatments conducted at Loughborough where treated sample could be analysed relatively quickly and contact angle analysis was used. Such measurements, however, gave water contact angles in the order of 70°. It is very probable such angles reflect the fact that the samples absorbed atmospheric contamination very readily.

5.2.4.3.Laser cleaning of RTM6 resin coatings from nickel tooling

The previous discussion of the cleaning application of Nd:YAG lasers has been restricted to the removal of the relatively slight levels of resinous contamination present on the ex Bombardier tooling. The RTM6 resin coatings on both nickel and mild steel samples pose a more significant challenge. Figures 108 and 109 show the effect of cleaning using the Spectron 450 Nd:YAG laser for resin coatings on nickel and mild steel test coupons respectively. The laser beam diameter was approximately 5mm and the fluence ~ 1.0 $J.cm^{-2}$. The laser beam was very efficient at detaching resin from the area irradiated and only a single pulse was necessary to achieve this. The test coupon was moved manually in the laboratory and so there was some overlap of the treated areas to produce the area cleaning illustrated. This makes it difficult to estimate the precise amount of energy imparted to the sample during treatment. Resin coated samples were also submitted to the Quantel laboratories and the same effects were observed to those reported except in this case, the samples were mechanically scanned.

The resin itself does not appear to absorb the laser energy to any significant degree and this is, perhaps, not surprising in view of the data published by Stratoudaki [21], as discussed in Chapter 2. The laser treatment appears to destroy the adhesion of the resin and this is an important finding in the present study. As a consequence, effective

removal of resin bonded to metal substrates is not dependent on thermal degradation of the resin through absorption of the laser energy at a particular output wavelength.

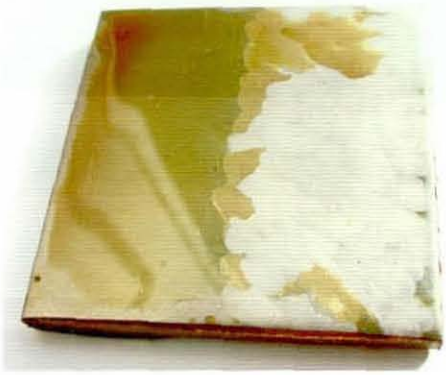

Figure 108. Photograph showing how bonded resin flakes away from Ni substrate after Nd:YAG laser cleaning.

Figure 109. Photograph showing how bonded resin flakes away from steel substrate after Nd:YAG laser cleaning.

SEM examination of the surface of the nickel coating in an area where the resin had been removed showed that at low and moderately high magnifications, there was no noticeable substrate damage. Only at higher magnification was there any evidence of thermal effects (figures 110 and 111). This is attributed to the fact that metal substrates do not reflect the incident laser energy at the shorter wavelengths used by Nd:YAG lasers (1.06 micrometres) as efficiently as occurs with CO_2 lasers (10.6 micrometre wavelength). The thermal damage is, however, relatively slight in comparison to the surface finish produced by abrasive cleaning of the tool surface so it is not thought to be deleterious to the cleaning application.

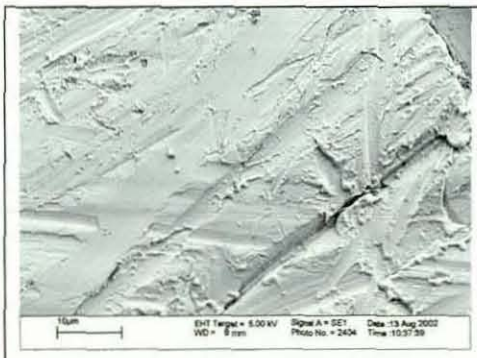

Figure 110. SEM of area of nickel tooling after removal of bonded resin by thermomechanical detachment as described. Scale bar = 10 micrometres

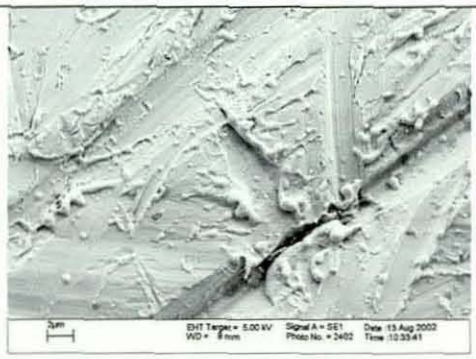

Figure 111. Higher magnification of area in Fig.110.Scale bar = 2 micrometres

SEM examination of the oxide layer underneath the detached resin on the mild steel sample (figure 109) revealed no surface porosities similar to the effects noted for CO_2 laser treatment shown in figure 97. To arrive at an explanation for the resin removal mechanism following laser treatment it is necessary to consider the structure of a typical oxide layer on a metal. The oxide at the surface of metal can have a complex structure as depicted schematically in figure 112. Only in the case of a noble metal such as gold or platinum is the layer non-existent or else comprises a monolayer of oxygen atoms. On common metals, oxygen atoms in the atmosphere react with the metal to form a surface oxide layer. There then exists a layer on top of this, which absorbs atmospheric gases and molecules of water vapour. On top of this is a hydrocarbon layer of contamination, which the surface attracts from contaminants present in most industrial and laboratory environments.

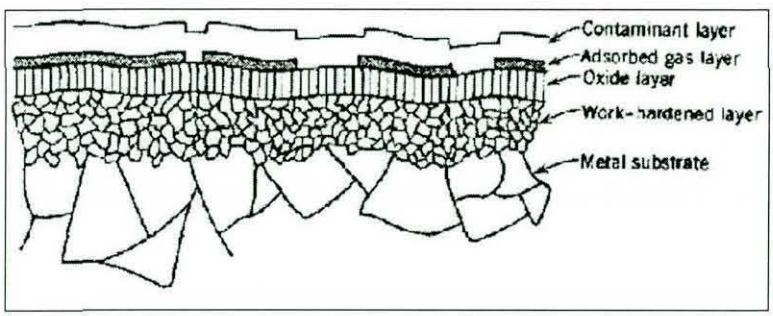

Figure 112. Structure of a typical metal surface. (After Rabinowicz [189])

It was conjectured that the Nd:YAG radiation might be preferentially absorbed by the surface oxide layer since the resin or indeed any hydrocarbon contamination has little propensity for absorption at this laser wavelength for low fluence levels of irradiation. The underside of a piece of the detached resin from figure 109 was examined by XPS to ascertain whether any metal oxide was present. If present this would suggest the locus of adhesive failure occurred at the oxide/resin interface. It was found that iron was present on the underside of the resin flake and that there was a small chemical shift in the binding energy of the oxygen peak from 531.0 eV to 530.5 eV. A shift to lower binding energies for the oxygen peak is associated with the presence of a metal oxide and since iron is present, it is reasonable to assume that cohesive failure of the oxide did occur in some measure. Similar measurements were not made on resin

detached from the nickel sample and in that case the oxide present is denser but also finer so that the substrate thus appears bright in reflected light.

As have been discussed in Chapter 2, laser interaction mechanisms are strongly dependent on the absorption properties of coatings and substrates and this makes it difficult to correlate effects observed on different samples. In all probability, in the case of bright metals with only fine oxide layers, absorption by the oxide may be less significant in comparison to removal caused solely by shock waves resulting from laser irradiation. Out of interest, one sample of the mild steel that possessed the thick grey oxide layer was ground down, removing most of the oxide to a bright finish. This was then coated with resin, which was cured. Laser cleaning under identical conditions had the same result – that the resin was mechanically detached and flaked off the treated surface.

Roberts [36] also reports that epoxide resin is weakly absorbed by laser energy and that the penetration depth (reciprocal of absorption coefficient) for 10600nm radiation is ~20 micrometres but is ~100 micrometres for radiation of 1064nm wavelength. Assuming the validity of these figures, in the present case of a resin coating of nominally 150 micrometres thickness, the fact that detachment rather than photothermal vaporization apparently dominates the laser cleaning using Nd:YAG lasers seems reasonable in view of the expected penetration depth and assumes preferential absorption of the radiation by a metal oxide layer is responsible for the a detachment mechanism. In this case the coating thickness is of the same order as the penetration depth.

Another possible explanation that concurs with the experimental observations is that the detachment of resin is due to thermally induced shockwaves resulting from the rapid expansion of the surface of the metal substrate following pulsed laser irradiation. This expansion creates a compressive wave that propagates through the substrate and is then reflected back from the other face. The reflected wave subjects the metal-resin interface to a tensional force and it is conjectured that the magnitude of this force is great enough to detach the resin, destroying its adhesive bonding to the substrate. In separating, the resin could remove with it fragments of metal oxide from the substrate.

Further, water, present either as a molecularly absorbed layer on the substrate prior to resin coating, or by ingress from the atmosphere after coating, may assist in the detachment process, since this will readily absorb laser energy and spontaneously vaporise. Thus mechanisms similar to those involved in laser particle removal (section 2.3.4) may be invoked.

It is argued that this thermo-mechanical detachment mechanism for contaminant coatings is superior in some ways to cleaning using pulsed CO_2 lasers because a cleaner surface is obtained with less opportunity for redeposition of thermally ejected material onto the surface or incomplete volatilisation of the coating as seen in some of the CO_2 laser treated samples in this study.

AES was used to determine the cleanliness of a nickel plate sample following Nd:YAG laser cleaning of a 150 micrometre thick resin coating. Figure 113 shows the concentration of carbon and oxygen from a hydrocarbon residue (assumed to be resin residue) as a function of etching time. The concentration of these elements approaches zero after 100 seconds of etching and so assuming an etching rate of 12nm/min (see section 3.8.5) the thickness of the residue is approximately 20 nm and this value suggests the surface is very clean following laser treatment.

The surface was protected from contamination after laser treatment by the resin itself since, although detached from the metal, this adhered at an untreated area and could then be broken off prior to preparation. Water contact angle measurements of 36° and 38° were obtained for freshly cleaned steel and nickel surfaces respectively following Nd:YAG laser removal of resin.

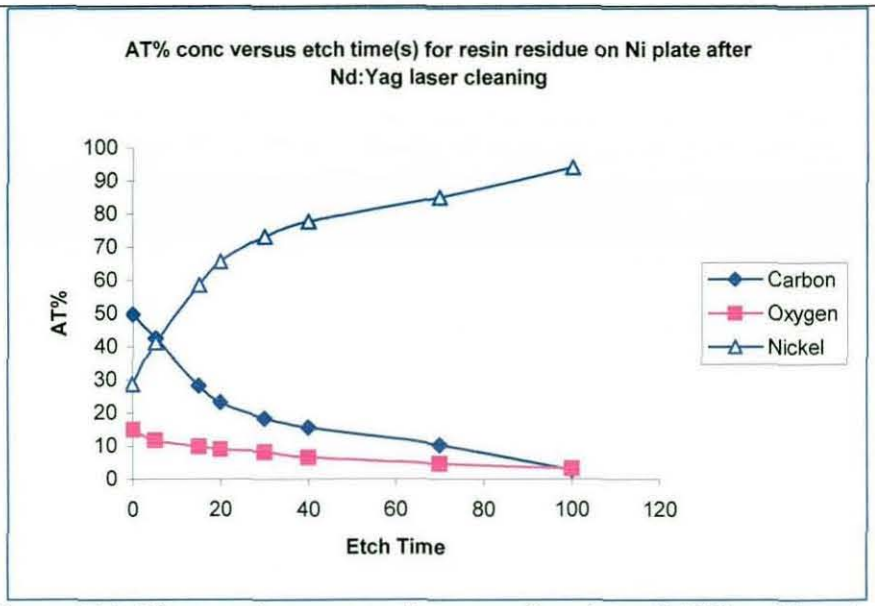

Figure 113. Elemental concentrations as a function of AES etching time

5.3 Laser Cleaning of Resin from Composite Mould Tooling

The application of lasers for the cleaning of composite tooling used for aerospace manufacturing processes was briefly discussed in Chapter 2. The principal difficulty for this application is that for lasers that offer efficient cleaning rates, such as pulsed TEA CO_2 or pulsed Nd:YAG lasers, fibre reinforced composite materials possess similar absorption coefficients to those of typical hydrocarbon contaminants. Unlike metal substrates, where laser cleaning is self-limiting due to the good reflectivity of metals once the contamination is removed, there is no similar discontinuity in the properties of contaminated composite tooling. Consequently, there exists a high probability that the laser will attack the resin rich surface layers of composite structures with the same vigour as the contamination unless a means is employed to distinguish between them. This can only be achieved in two ways, both of which reduce significantly the rate at which large surfaces areas can be cleaned and add substantial capital cost for setting up the laser cleaning process.

The first method involves using an efficient cleaning laser such as those mentioned and continuously monitoring the cleaning process using a technique that is sensitive to the discontinuity at the contaminant-substrate interface. One means to monitor the process is to spectroscopically detect the molecular fragments of the material being removed using techniques such as Laser Induced Breakdown Spectroscopy (LIBS) [190-192], as discussed in section 5.3.1. This technique will detect the small difference in chemical composition between the contamination and the resin rich composite surface.

A second method is to monitor the reflective properties of the surface between each applied laser pulse. This process is used by Dornier Wessling, Germany to strip paint from airbus fuselages and utilizes a 2kW pulsed TEA CO_2 laser. The automated computer controlled process claims ablation depth control to within a couple of micrometres [111]. Laser fluence control permits intensive cleaning where required and assist gases are used either to support selective combustion or else cool the surface. Using two laser systems it is claimed that 630m^2 of an A320 airbus fuselage can be stripped of paint in just less than 40 hours. Details of the calibration process are not given in the reference cited and one would envisage that some form of dynamic

calibration would be required since the reflective properties of a newly painted surface would change after subsequent paint removals. The first time the paint was stripped the calibration would use the reflection from the unpainted surface as a reference standard and this would simplify the process but this reference standard would change each time paint was stripped so that the process control would need to be related to the history of a particular airbus fuselage that was treated.

In the first method discussed ultra-violet wavelength light either in the form of a high intensity lamp or more commonly an Excimer laser is commonly used to remove the contamination. Ultra-violet excimer lasers are ten times as precise as infrared lasers at removing coatings, as discussed in Chapter 2. For reasons discussed previously, Excimer lasers tend to be used more in art restoration laser cleaning where cleaning rate and cleaning costs are less important than in a commercial manufacturing process.

Similar technical problems are encountered in art restoration. For example, in varnished paintings the underlying pigments are sensitive to photons transmitted through the resin so that removal of the varnish to effect any restoration has to be sensitively controlled as discussed by Zafiropulos [19]. For such resins of thickness in the range 10 – 100 micrometres, the penetration depth per pulse is typically ~ 0.1 micrometres for a laser wavelength of 193nm and ~1.0 micrometres for 248nm.

This author also sites the example of paint removal from an epoxide/carbon fibre composite painted with a silicon based polymeric paint which was stripped using a XeCl excimer laser at an operating fluence of 1.4 Jcm^{-2}. In this material a 3 micrometre thick epoxide primer had been used to treat the composite prior to painting and it was possible to control the laser ablation to strip the paint down to this primer without exposing the carbon fibres beneath. Similar effects were reported for polyurethane based paint removal from Kevlar composites using a KrF excimer laser operating at a fluence of 0.5 $J.cm^{-2}$.

Although photochemical (bond breaking) laser interaction mechanisms are involved in laser cleaning at ultra-violet wavelengths, Zafiropulos [19], investigating the photoablation of polyurethane films from delicate composite materials using pulsed

ultra-violet lasers, commented on the fact that the upper limit of the mean activation energy for the removal process was 3 to 15 times lower than the average energy required to break single covalent bonds suggesting that photophysical ablation mechanisms such as shock wave generation also play a part in the removal process and the evidence collected in the present study supports this.

5.3.1.Laser Induced Breakdown Spectroscopy

Laser-Induced Breakdown Spectroscopy (LIBS) is a form of atomic emission spectroscopy in which a pulsed laser is used as the excitation source.. The output of a pulsed laser, typically a Q-switched Nd:YAG, is focussed onto the surface of the material to be analysed. For the duration of the laser pulse, which is typically 10- 50 nanoseconds, the fluence is high enough to eject a microgramme quantity of the surface coating irradiated. Assuming the laser parameters are set to generate a microplasma, the ejected material will be dissociated into excited ionic and atomic species. At the end of the laser pulse, the plasma quickly cools as it expands outwards at supersonic speeds. During this time the excited ions and atoms emit characteristic optical radiation as they revert to lower energy states. Detection and spectral analysis of this optical radiation using a sensitive spectrograph can be used to yield information on the elemental composition of the material.

Time-gated detectors are employed which allow the optical emission from the laser plasma to be recorded at some time delay after the laser pulse. This is important since the characteristic atomic and ionic emission lines only start to appear after the plasma has expanded and cooled and the delay can be ~ 10 microseconds. The LIBS instrument would be calibrated to perform quantitative measurements of minor elements within a matrix material.

Since the laser may be used to remove surface coatings in a controlled manner, depth profiling of layered structures is possible with LIBS. Spectroscopic measurements may be performed as the laser "drills" into the material, providing information on the elemental composition of the material as a function of distance into the layered structure. Generally, this technique is effective only for materials that are relatively easy to ablate using laser powers typical of a LIBS instrument. Examples include

compositional analysis of zinc coatings on steel for process control during manufacture, detection of heavy metals (lead, uranium, plutonium) in paint and detection of elemental contamination in concrete. Commercial LIBS instruments come with their own laser but in a laser cleaning application the specific laser used for the application would be linked to the LIBS instrumentation. Problems envisaged in their use for laser cleaning would again relate to how to calibrate a system using this spectroscopic technique in such a way that the ablation depth could be controlled to cut off at the composite tooling surface. If the contamination possessed a markedly different composition to the substrate, such as in the case of a pigmented paint layer, then the spectral data would show a discontinuity once the non-pigmented composite surface was reached. However, if the composition of the contaminant were very similar to that of the resin composite, differentiation would still be difficult.

5.3.2 Laboratory study of the laser cleaning of composite tooling

It is apparent from the above discussion that considerable investment and resources are required to use lasers to clean composites in a controlled manner. Without these sophisticated means of monitoring the ablation depth, laboratory based investigations inevitably show that laser cleaning produces substrate damage. The simplest means of effecting control is to monitor the acoustic reports that are generated as each laser pulse ejects material. The intensity of the acoustic emissions fall off rapidly as the substrate, possessing different properties from those of the contamination, is approached. Cottam [49] discussed the use of this technique. However, it is not suitable to control the laser ablation of composites for the reasons already discussed.

5.3.2.1.Cleaning of composites using TEA CO_2 lasers

Use of the Laserbrand TEA CO_2 10.6 micrometre wavelength laser at Loughborough showed that a single laser pulse directed at virgin composite or used composite tooling caused significant surface damage. The fluence used was approximately 2 Jcm^{-2}. Identical damage resulted when the pulses were applied to resin coated onto virgin composite coupons. The resin was removed after several pulses but the underlying substrate was damaged since there was no means of controlling the process.

The polished reflective surface of the virgin composite tooling reflected some of the laser light for the first pulses as shown in figures 114 -116 but after two or more pulses or so carbon, ejected in the ablation as the underlying carbon fibres began to be exposed, initiated plasma formation and the intensity of the acoustic emissions increased as a result. The process created smoke from the combustion and was unstable.

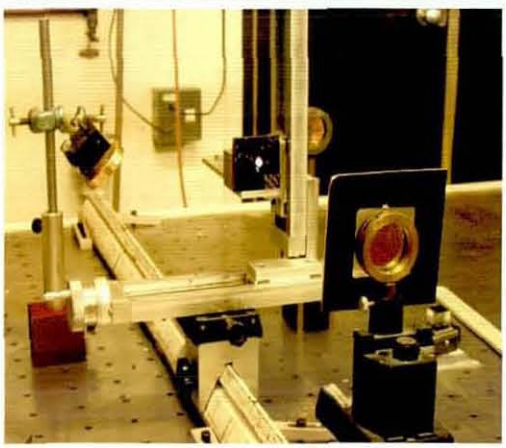

Figure 114. Macro-photograph showing TEA CO_2 laser focussed onto virgin composite tooling.

Figure 115. As Figure 114 showing a close up photograph of the laser focussed onto the composite tooling..

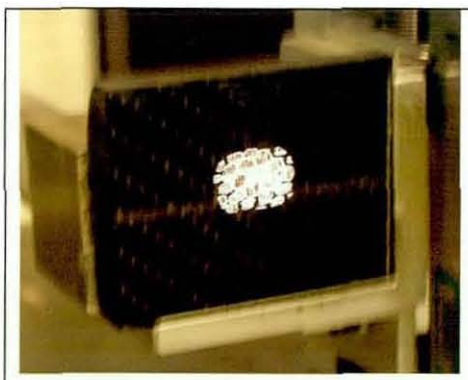

Figure116. In this macro-photograph of the laser focussed onto composite tooling it is possible to see the stronger absorption of the carbon fibre resin matrix..

Identical samples were treated using the facilities at the National Laser Centre, Pretoria, South Africa. These show that at higher fluences (7.6 Jcm^{-2}), using TEA CO_2

laser operating at the same output wavelength as the Loughborough laser, similar damage occurs on virgin composite tooling as shown in figures 117 and 118. The tested coupon in Figure 120 was 120mm x 100 mm in area. Figures 119 and 120 show the effect of the laser, using the same fluence, for RTM6 resin coated onto virgin composite tiles.

As expected these macro-photographs show how difficult it is to control the laser cleaning process such that it will remove a hydrocarbon based contaminant coating without exposing the fibres of the composite. The R_a roughness parameter for the gloss area of the tile shown in Figure 117 was 0.0418 micrometres. After laser treatment the surface was damaged and this increased the roughness value by two orders of magnitude to 4.5293 micrometres as measured using Talysurf profilometry.

Figure 117. Photograph showing effect of TEA CO_2 laser on virgin composite tile. The resin rich gel coat has been striped by the laser to expose the carbon fibre matrix.

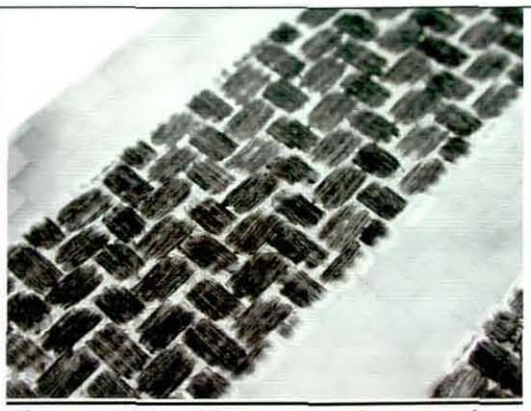

Figure 118. Close up photograph of effect shown in figure 117.

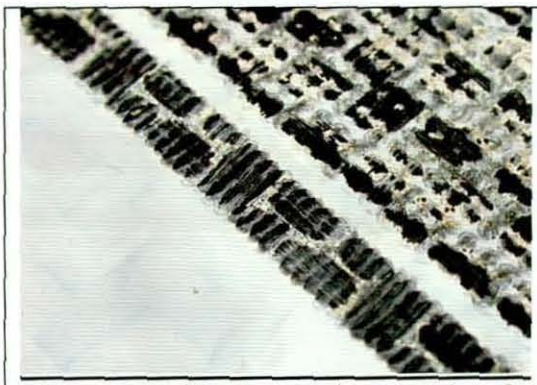

Figure 119.Close up photograph of the effect of TEA CO_2 laser on resin, which has been bonded onto the surface of a composite tile. The resin layer is striped away together with the resin rich gel coat and also exposes the carbon fibre matrix.

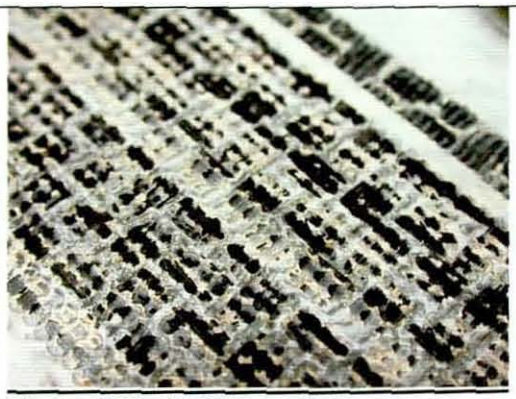

Figure 120. As Figure 119.

5.3.2.2.Cleaning of composites using Nd:YAG lasers

The Spectron 450 Nd:YAG Q-switched laser at Loughborough was used to study the effects of the 1.06 micometre radiation from this laser on similar virgin and resin coated composite tiles. Figure 121 shows the pronounced plasma plume, typical on composites treated with with lasers. Greater surface damage results when target-to-source distances used for metal substrates are tried with composites. With the beam diameter approximately 2mm, a single pulse penetrated the resin rich surface of a virgin composite tile to expose the carbon fibres beneath. This is shown in the low magnification SEM image in figure 122. The beam area was expanded to its maximum (about 8mm diameter) for subsequent tests though damage was still severe.

Figure 121. Photograph showing plasma effect when Nd:YAG laser focussed onto resin bonded to composite tile.

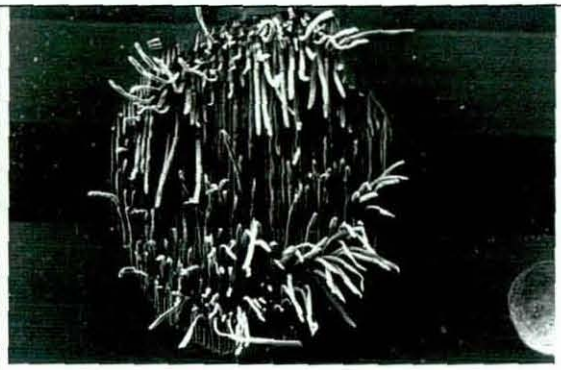

Figure 122. SEM image showing carbon fibre damage for area in figure 124. Diameter of hole approx.0.5mm.

Using a similar Q-switched Nd:YAG laser at the National Laser Centre, South Africa (with pulse duration 7ns) a single line scan was made on a resin coated composite tile as shown in figure 118. An area from this scan was examined using an SEM and the images shown in figures 123 – 125 were recorded which show the substrate damage at a range of magnifications.

Figure 123. Close up macro-photograph showing effect of Nd:YAG laser used to clean resin bonded onto composite tile.

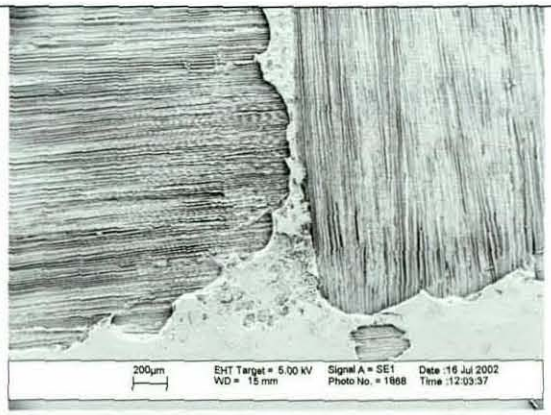

Figure 124. This figure shows an SEM image of a damaged area depicted in figure 123.

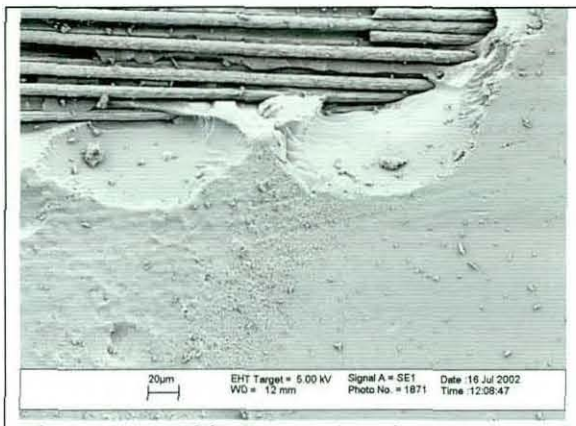

Figure 125. This figure also shows an SEM image of a damaged area of the composite tooling depicted in the macro-photograph (figure 123).

Figure 126 illustrates how absorption within the carbon fibre reinforcement of the composite tile causes the fibres to fracture. The energy dissipated disrupts the surrounding non-absorbing resin causing it to fracture extensively and this changes the scattering properties when the treated tile is viewed in visible light. Shockwaves associated with the energy release can cause fractured fragments of the overlying resin to be blown off exposing areas of fibre beneath (figure 125). The level of damage is similar to that found using TEA CO_2 lasers at Loughborough.

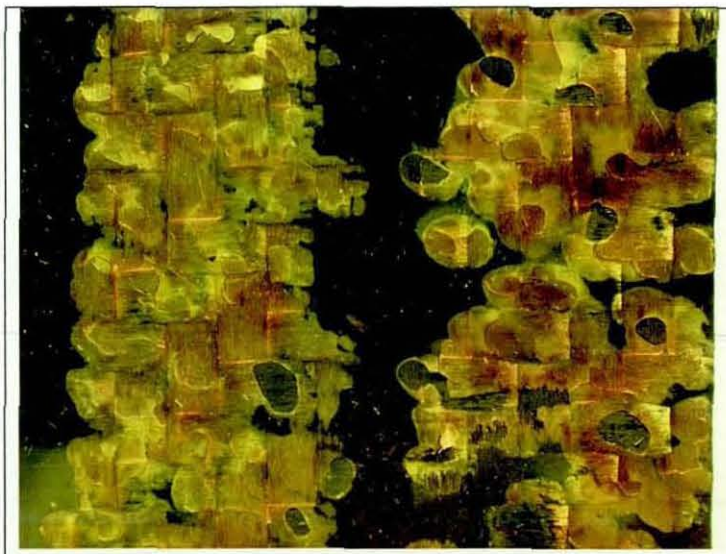

Figure 126. Close up photograph of composite tile where Nd:YAG laser beam was manually scanned across the surface.

5.3.3.Summary

The results presented illustrate the difficulties in removing resinous contamination from composite mould tooling possessing a very similar chemical composition. The potential to clean composite structures using lasers has, however, been established and the key to success is in controlling the process by continuous monitoring using techniques such as LIBS. This is a proven technology but constitutes a specialised cleaning application and the capital costs involved in setting up the technology may well render it uncompetitive as a general mould cleaning method when compared to different cleaning technologies which will be discussed in the following sections.

5.4. Dry ice Cleaning

The principles and technology associated with this cleaning method were discussed in Chapter 2 and in the present study cleaning was performed on selected resin coated metal and composite test coupons. Although coated metal samples were examined, the main reason for investigating this cleaning technology was to appraise its potential for cleaning composite tooling. Details of the results are shown in this section for a range of blasting pressures and treatment times as detailed in section 4.3.4.

No significant effect was observed using small, dry ice shavings except for very long treatment times. The addition of sodium bicarbonate as an abrasive medium also failed to have much significant effect on the cleaning produced. Most success was obtained using standard size dry-ice pellets, which are a few cubic millimetres in volume.

5.4.1. Resin coated composite samples

Macro-photographs were subsequently taken from areas of treated resin coated composite samples. Further quantification of surface damage was made using the SEM.

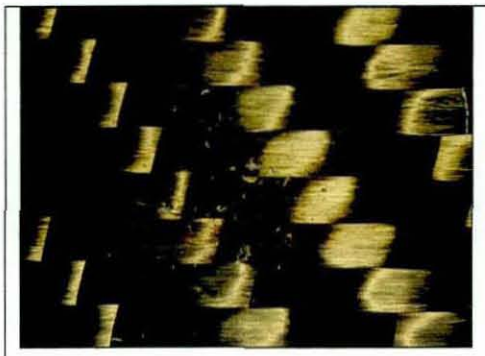

Figure 127. Dry ice blasting damage to resin on composite tile (see description in 5.4.1.1 below).

5.4.1.1.Sample treated at 3 bar (304kPa) for 20 seconds

Figure 127 above shows that very little dry ice blasting damage has occurred to resin bonded onto a composite tile at an operating pressure of 3 bar (304kPa) applied for 20 seconds.

5.4.1.2.Sample treated at 4 bar (405kPa) for 10 and 20 seconds

At 4 bar pressure, figures 128 – 132 on the next page show macro-photographs of the composite tiles for treatment times of 10 and 20 seconds respectively together with corresponding SEM images. These SEM images show that not only the resin contamination is removed but also the process continues and attacks the substrate exposing carbon fibres.

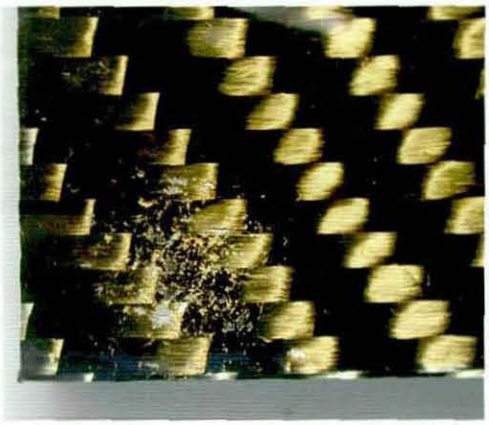

Figure 128. Close up photograph of dry ice blasted composite tile coated with resin (10 seconds treatment time at 4 bar).

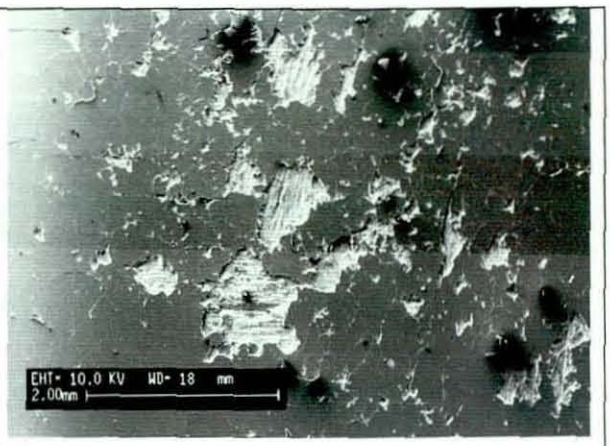

Figure 129. SEM image of area in figure128. Scale bar – 2 millimetres.

Figure 130. As figure 131 but treatment time increased to 20 seconds.

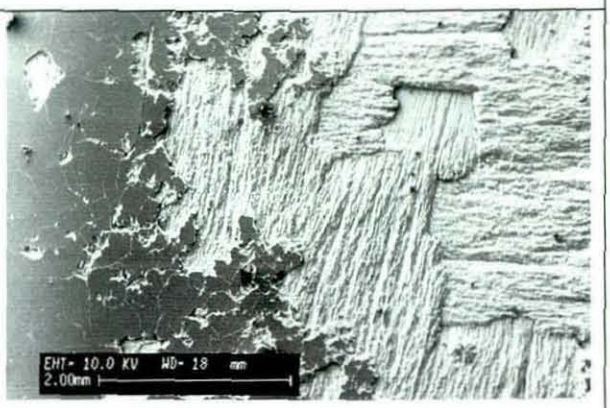

Figure 131. SEM image of area in figure 130. Scale bar = 2 millimetres

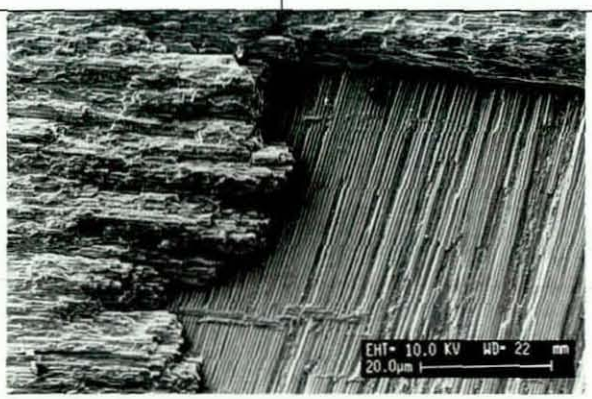

Figure 132. SEM image of area in Figure 131. Scale bar = 20 micrometres

5.4.1.3 Sample treated at 5bar (506kPa) for 10 and 15 seconds

Figures 133 - 136 show composite tooling tiles dry ice blasted treated at a constant pressure of 5 bar for 10 and 15 second intervals

Figure 133. Dry ice blasted composite tile coated with resin (10 seconds treatment time at 5 bar).

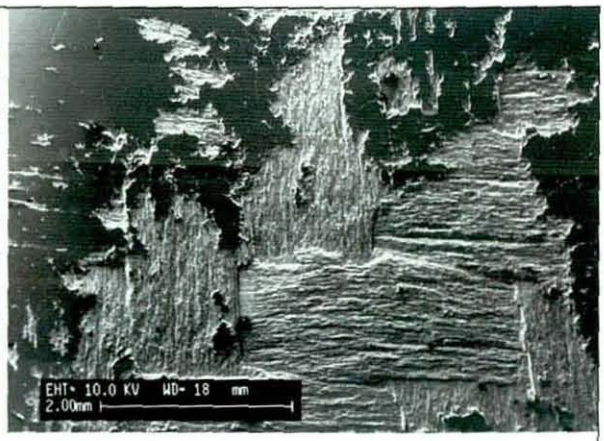

Figure 134. SEM image of area in Fig.133. Scale bar – 2 millimetres.

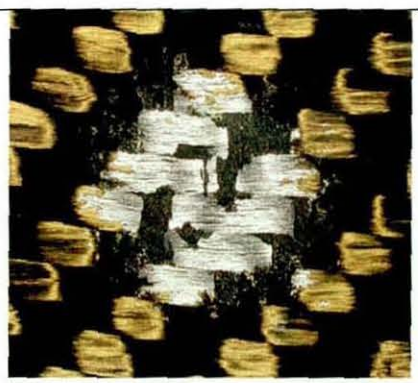

Figure 135. Treated 15 seconds

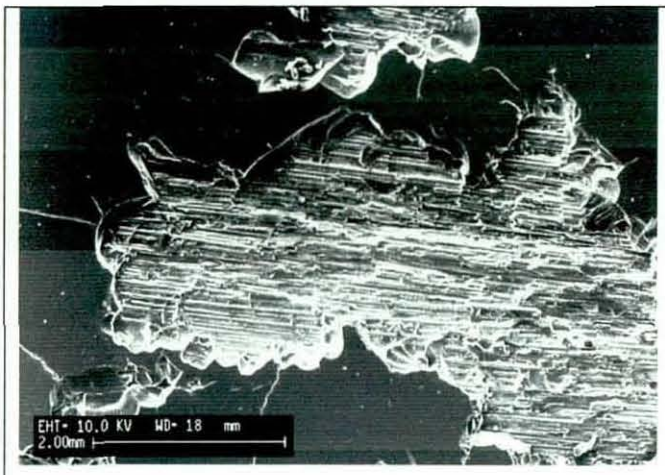

Figure 136. SEM image of area in figure 135.
Scale bar = 2 millimetres.

5.4.1.4.Sample treated at 7 bar (709kPa) and 10 bar (101MPa) for 15 and 30 seconds respectively.

Figures 137 and 138 show macro-photographs of resin coated composite tiles treated at 7 bar for 15 seconds and 10 bar for 30 sec respectively. No corresponding SEM images were recorded.

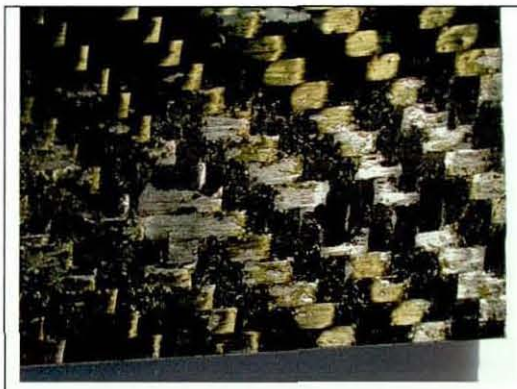

Figure 137. Close up photograph of dry ice blasted composite tile coated with resin (15 seconds treatment time at 7 bar).

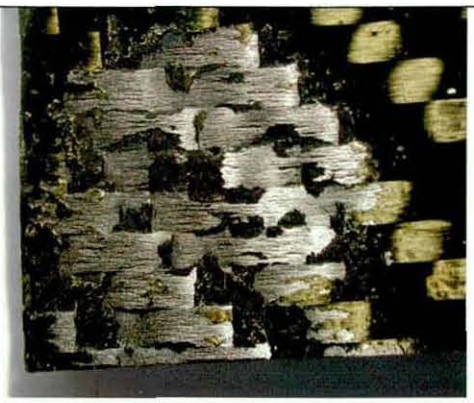

Figure 138. Close up photograph of dry ice blasted composite tile coated with resin (30 seconds treatment time at 10 bar).

5.4.2.Discussion of results

It became apparent when these dry ice blasting experiments were conducted that there existed a threshold pressure at which cracking of the resin contamination layer was

initiated, and further, that once this process had begun, the reverse fracturing effect discussed in Chapter 2 accelerated the removal of further material with continued treatment time.

The problem is that the choice of resin as a contamination layer that is cured onto a resin composite surface is just about the worst material combination possible. With laser cleaning, similarity of the chemistry and absorption properties of the resin contamination and resin matrix of the substrate posed the biggest problem in controlling the cleaning process. The same problem arises with dry ice blasting except that here is it similarity of the physical properties of the two materials that is the problem and since the bonding between the samples is so good, it is almost impossible for the process to remove the resin contamination without pitting the resin matrix of the substrate. The results using 3 bar pressure show that pitting of the contaminant layer is just occurring but at 4 bar pressure the resin matrix of the substrate is attacked. The macro and SEM images clearly show significant damage at 4 bar and higher pressures.

In real samples, however, there would exist a weak boundary layer comprising of degraded mould release between the substrate and any contaminant material and the reverse fracturing effect would then result in removal of the contaminant skin without necessarily causing the same degree of damage to the resin matrix of the substrate. Although this contamination may be resinous in nature, SEM analysis of typical metal mould tooling contamination shows that it comprises of fine beads of materials and not a continuous cohesive layer.

It was very difficult to simulate a weak boundary layer on composite substrates in the preparation of test samples in the laboratory because such a boundary layer possesses a low surface energy, which resists wetting by an applied adhesive resin. Consequently an applied resin beads up on the surface as its viscosity is reduced during oven curing and it is impossible to prepare an even coating of any resin that sits over such a boundary layer even with moderate pressure is applied during the curing process. In essence one is trying to make a coating stick to a good mould release agent and surface physics makes this difficult. Very similar conditions must exist to some extend when such tooling is used industrially except that in these

conditions a very high pressure is exerted which forces the resin against the tooling and which is maintained for the duration of a curing cycle that may last 8 hours or more.

Another problem with dry ice cleaning of composites is that the surface gets very cold and frosts up with ice condensed from the atmosphere as shown in figure 12, section 2.4.1. This also occurs with metal samples but the low thermal conductivity of composite tooling means that it takes longer for this ice to dissipate and in practice some form of heating would be required if large area tooling were cleaned.

5.4.3 RTM6 resin coated metal substrates

Resin coated ex-Bombardier nickel plate of dimensions 50mm x 50mm x 5mm was treated for 5 seconds at 3,4,5 7 & 10 bar pressure (304, 405, 506, 709, and 1013kPa). With reference to figure 139 below the central area shows damage at 10 bar. The area in the bottom left hand corner shows damage at 7 bar. Other corners treated at 3, 4 and 5 bar in clockwise order.

Figure 139. Resin coated nickel substrate dry ice blast treated for 5 seconds at 3,4,5,7 and 10 bar pressure.

In the next test a sample of resin coated mild steel was treated using a constant pressure of 10 bar (1.01MPa) for different treatment times. These are shown in figure

140 below where, in clockwise order from bottom right hand corner, the treatment times were 3, 7 and 10 seconds. The central area was treated for 20 seconds.

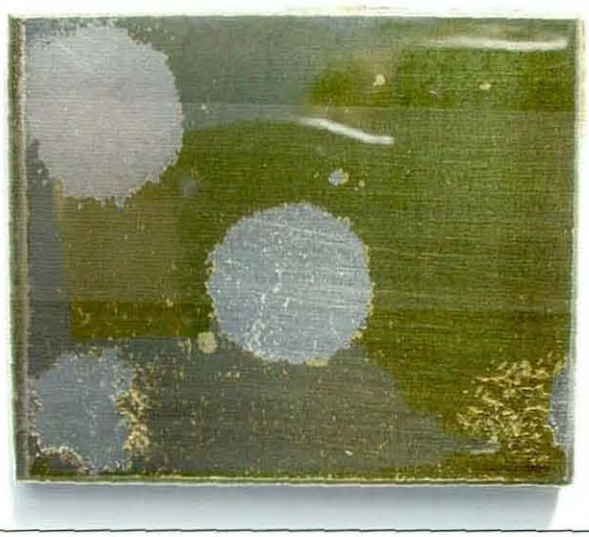

Figure 140 Resin coated steel dry ice blasted at 10 bar for 3,7,10 and 20 seconds.

Higher treatment pressures can be used to remove coatings from metal tooling substrates in comparison to those applicable to composite tooling. Pressures up to 10 bar (1.01MPa) were observed to have no detrimental effect on metal substrates and cleaning efficiency was greater at these higher pressures.

5.4.4 Summary

The results of the present study suggest that dry-ice pellet blasting would be effective for metal mould cleaning but that the low damage threshold of composite tooling might result in substrate damage unless low treatment pressures are used which reduce cleaning efficiency.

5.5 Sodium hydride cleaning process

5.5.1 Evaluation of the cleaning procedure

Details of this cleaning process were discussed in Chapter 2 and in this section the results from two test trials are presented together with analytical data.

Figure 141. Treatment of resin coated nickel using the sodium hydride process

Figure 141 above shows a photograph of a resin coated nickel sample (left) adjacent to one that has been treated using the sodium hydride process (centre). The high temperature process reduces any organic material to a black char which is easily removed using a water jet provided this is done immediately following treatment.
The result of washing after treatment is shown in the third image (right) and it is seen that a bright metal surface is revealed. Water contact angle measurements gave an average angle of 40° but the surface rapidly contaminated by absorption from the laboratory atmosphere.

On the first trial of the process the samples were not washed vigorously enough and although they looked cleaned, examination by SEM, (figure 142), show dendrite growths of carbonates formed through absorption of carbon dioxide from the atmosphere by sodium salt residues on the surface. These growths follow the scratch marks caused by mechanical polishing of the sample prior resin coating and subsequent sodium hydride cleaning.

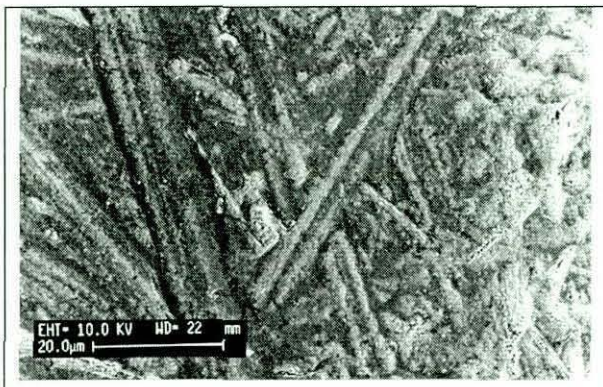

Figure 142. SEM image of sodium salt growths on poorly washed nickel substrate following sodium hydride cleaning. Scale bar = 20 micrometres

A second test trial was conducted later where the treated samples were first thoroughly washed before being stored under absolute ethanol to protect them until they could be examined in the laboratory. Examination by SEM reveals only the scratches from abrasive scouring prior to bonding of the resin (figures 143 and 144).

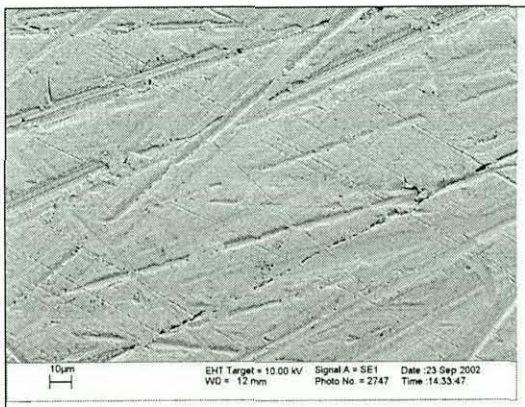

Figure 143. SEM image of nickel substrate following resin removal by sodium hydride process. Scale bar = 10 micrometres.

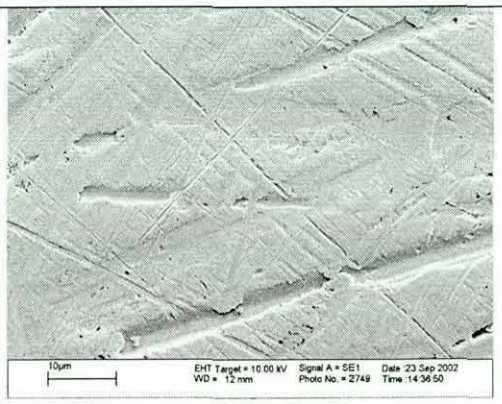

Figure 144. As Figure 143.

Using EDX microanalysis, the elemental composition of the cleaned surface is revealed (figure 145 below) and this shows only trace levels of elemental impurities

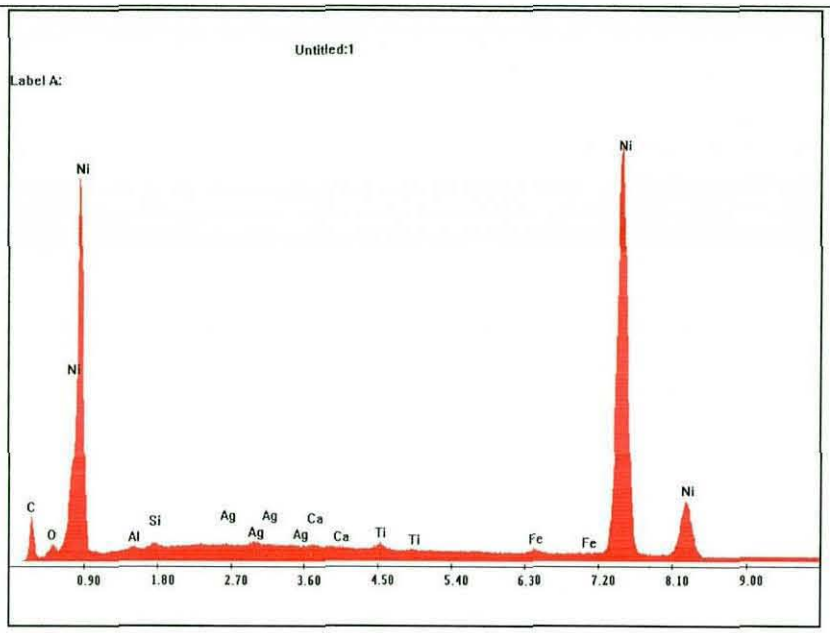

Figure 145. EDX spectrum from sodium hydride cleaned nickel tooling

below the main intense peaks associated with nickel. The most likely source of these impurities is from samples previously cleaned using the process since a commercial metal finishing bath was used.

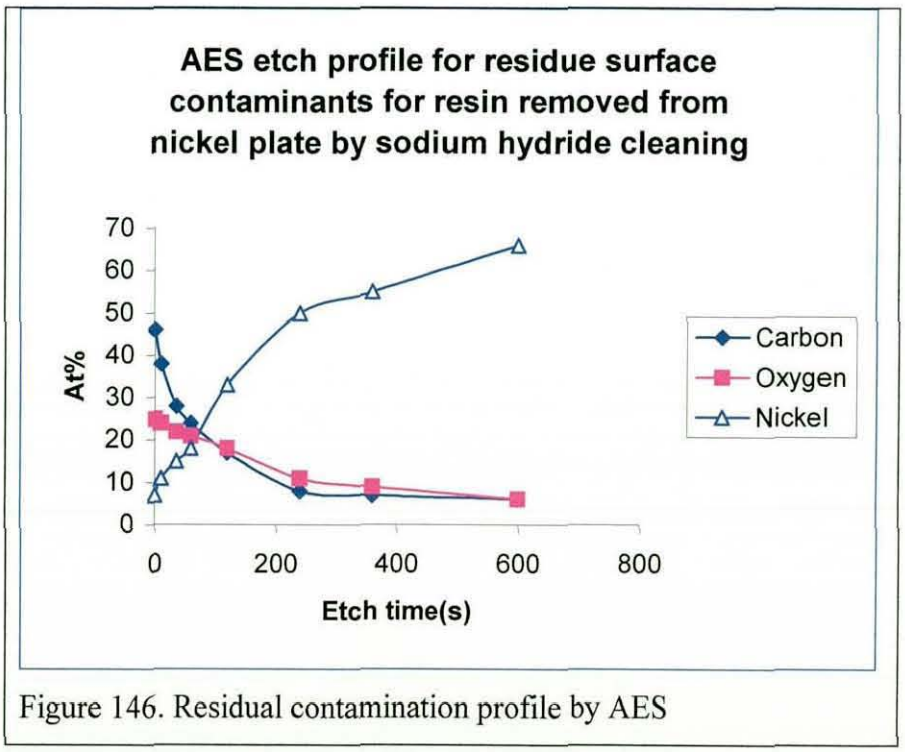

Figure 146. Residual contamination profile by AES

By using ion etching in an AES experiment the residual surface contamination (assumed to be solely hydrocarbons) was removed after 600 seconds of etching.

Assuming an etch rate of 12nm/minute (see section 3.8.5) this equates to a residue contamination thickness of approximately 120nm (see figure 146). Although considerably thicker than that obtained by laser cleaning the level of contamination is still slight and relatively inconsequential for industrial applications.

Water contact angle measurements showed an average value of 32° also indicating a reasonably clean surface. This average angle increased to 45° after the sample had been exposed to the atmosphere for 30 minutes.

5.5.2 Summary

The sodium hydride process has been demonstrated to be very effective at removing bonded epoxide resin from nickel tooling and would offer one solution to removing contamination quickly from complex shaped metal moulds. AES shows that a very clean surface is obtained after this chemical treatment.

Although the sodium hydride cleaning process was applied to resin coated steel samples, it was a measure of how efficient the cleaning process was that these samples rusted very quickly after treatment. The need to remove carbonised contamination using water jets immediately following treatment poses difficulties for the cleaning of steel tooling using this technique. Even samples of stainless steel were prone to rusting after the sodium hydride cleaning. It is concluded the process is unsuitable for cleaning ferrous metals.

Chapter 6 Results and Discussion of Coatings for Mould Release Applications

6.1. Fluoroalkylsilane coatings

6.1.1. Introduction

At the start of this experimental aspect of the research, one of the major aims was to evaluate surface coatings that offered potential as mould release agents. A number of candidate systems were selected using the criteria detailed in section 3.9. The premise initially adopted was that the mould release properties of a coating were dominated largely by its surface chemistry and the requirement to engineer an exceptionally low energy surface that would resist the adhesion of any liquid resin. The properties of fluoroalkylsilanes, discussed in Chapter 3, suggest these materials satisfy these requirements.

As the experimental data accumulated it became evident that creating a low surface energy alone was insufficient to engender good release properties and that commercial mould release products, developed over many years, functioned on a number of different levels and low surface energy was only one property that contributed to their success.

From the literature survey in Chapter 3, covering the many different facets of non-stick coatings, the functionality required for good release began to emerge and largely supports the above assumption. In the following sections, the stages by which these views were formulated are developed and supporting experimental evidence presented.

6.1.2. Dynasylan fluoroalkylsilane coating evaluation

The interesting properties of these coatings were discussed in Chapter 3 and a particular compound, Dynasylan F8261 (tridecafluoro-1,1,2,2-tetrahydrooctyl) triethoxysilane $C_{14}H_{19}F_{13}O_3Si$.) was identified as worthy of further study. A patent filed in America (6,544,466) in April 2003 discusses the use of fluoroalkylsilanes to provide non-stick moulds for use during semiconductor

fabrication and provides evidence that the surface modifying properties of these compounds are beginning to find industrial applications.

Stainless steel foil samples were coated with this chemical and cured according to the schedule discussed in section 4.4.3.

6.1.2.1 Surface energy measurements

Contact angles and surface energy calculations were made on stainless steel foil (model substrate) that was treated using different concentrations of the chemical and for different treatment times. These results are presented in Table 12 below.

fluoroalkylsilane conc% on SS foil substrate	Dipping time(min)	Contact angle in water (°)	Contact angle in DIM (°)	Calculated surface energy $mJ.m^{-2}$
0.1	10	104	94	14.0
0.1	30	114	97	10.6
0.1	60	114	96	10.9
0.5	0.5	112	97	11.0
0.5	1.0	116	95	10.2
0.5	2.0	118	95	10.6
0.5	5.0	111	97	10.1
0.5	10	111	97	11.1
0.5	20	112	99	10.5
0.5	60	119	106	7.4
1.0	0.5	118	98	10.0
1.0	1.0	117	100	9.5
1.0	2.0	116	98	10.1
1.0	5.0	114	95	11.5
1.0	10	116	100	9.6
1.0	30	117	99	9.6
1.0	60	118	96	10.8
5.0	1.0	119	101	8.3
5.0	2.0	119	106	7.5
5.0	60	122	103	7.6

Table 12 Contact angles and surface energies for different fluoroalkylsilane treatment times

Measurements were also made on a standard sample of PTFE. An average water contact angle of 116° was obtained although this value can vary depending on the surface roughness between 110° and 140°. Using diiodomethane an average contact angle of 82° was obtained. From these values a surface energy of 16.72

$mJ.m^{-2}$ was computed. The standard value is 18.5 $mJ.m^{-2}$ so the measured value is somewhat low. The reason for this is unknown but even assuming a systematic error of the same order applies to the values tabulated above, the surface energies measured for the coatings are very low and significantly lower than PTFE suggesting that they would constitute very effective coatings for release applications.

From the data in Table 12 it was concluded that a treatment time of 10 minutes for a concentration of 1% of the chemical was optimal for most applications and gave a surface energy ~10 $mJ.m^{-2}$. Improvements of surface energy using higher concentration were impractical for industrial samples because the chemical is expensive and would treat larger areas more economically at the lower concentration. Treatment times in excess of 10 minutes did not result in a proportionately enhanced surface energy but for practical reasons a treatment time of 30 minutes was more convenient when treating many samples. Subsequent laboratory samples were treated at concentrations and treatment times according to what specific information was sought from an analytical technique.

Because the stainless steel foil substrate for these coatings was being used as a surrogate material for limited supply of real mould tooling plate received, it was decided to apply the coating at 1% concentration for 10 minutes on a sample of clean nickel plate tooling. It was conjectured that the effectiveness of the coating might be a function of the surface area accessible for reaction and hence dependent on the surface roughness of the substrate (the surface roughness parameter for nickel plate was $R_a = 0.405$ micrometres whereas that for the steel foil was 0.1295 micrometres, as listed in Table 8).

Allowing a treatment time of 30 minutes using a 1% concentration of the chemical in ethanol, a water contact angle of 119° was obtained for a treated nickel tooling plate and a contact angle of 104° using DIM. A surface energy of 7.9 $mJ.^{-2}$ was calculated. This exceptionally low value could be due to the high packing density of the CF_2 and CF_3 groups on the Dynasylan treated surface.

The cured fluoroalkylsilane film was colourless and stable. It did not appear to be susceptible to moisture absorption even with exposure of several weeks to laboratory air. From published work on fluoroalkylsilanes [133], [137], [140], [141] and other silane metal treatments [186] it was believed that the cured coatings were very thin extending to a few nanometres and to investigate the surface morphology of the coating it was apparent that high resolution microscopy would be required. XPS was used to confirm the estimated coating thickness.

6.1.2.2 High Resolution SEM

As discussed in Chapter 4, samples of nickel sputtered onto glass slides to a thickness of 1.1 micrometres were prepared to be utilized for such investigations since the surface roughness values of real tooling or even the stainless steel surrogate material were too high to allow clear resolution of the coating. Initially, one of the sputtered nickel slides was treated in a 1% solution of Dynasylan for 30 minutes and the coating cured. The sample was then examined using high resolution SEM without any additional preparation and the images shown in figures 147 and 148 were recorded. These images appear to show the coating comprises discrete islands of the cured chemical with features up to about 40 nanometres in diameter.

There is a problem in knowing whether this structure is representative of a coating of the silane on a rough metal surface or merely an artefact of preparation reflecting poor wetting of the chemical on the very smooth substrate used. Other observations from the treatment of the smooth surfaces of virgin composite tooling suggested that smooth substrates are not conducive to the production of a uniform coating and that the chemical binds more effectively to rougher surfaces. Indeed the chemical is marketed as a surface treatment for textile fibres and these afford much greater surface areas over which the chemical can react and bind itself.

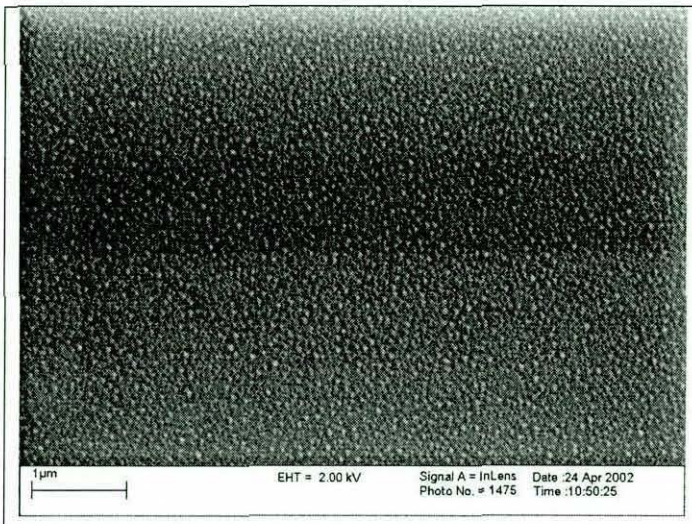

Figure 147. SEM image of fluoroalkylsilane coating on stainless steel foil. Scale bar = 1 micrometre

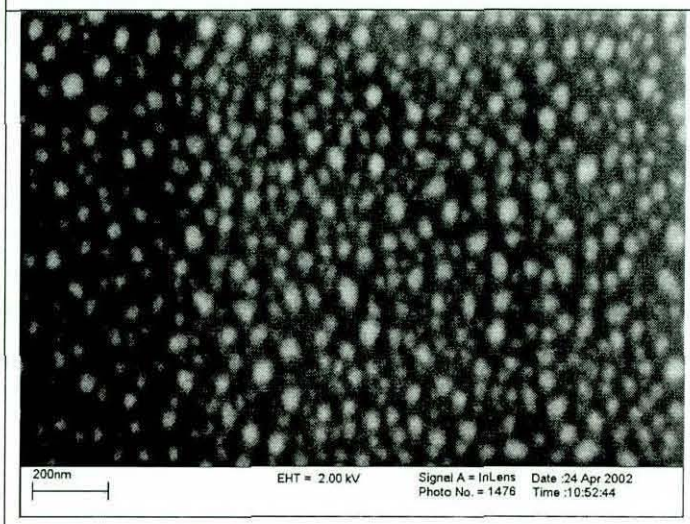

Figure 148. SEM image of fluoroalkylsilane coating on stainless steel foil. Scale bar = 200 nanometres

6.1.2.3 Analysis of coatings using XPS

A sample of stainless steel foil was treated with 5% Dynasylan for 60 minutes to fully react the chemical with the metal substrate and produce the lowest surface energy possible, as indicated by treatment table 12. Analysis using XPS was then performed to confirm the expected surface chemistry and obtain information about the coating thickness.

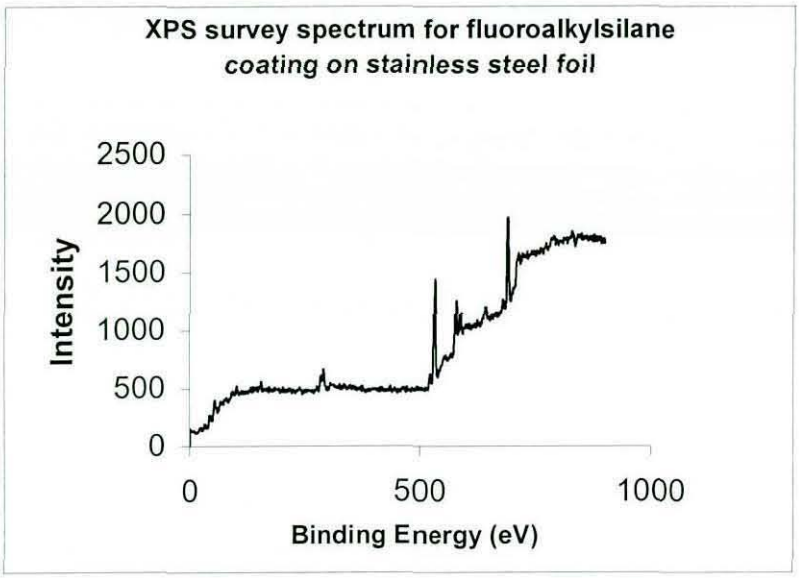

Figure 149.XPS survey spectrum of fluoroalkylsilane on steel.

A survey spectrum shown in figure 149 shows that the largest peaks in spectrum are for oxygen (531eV) and fluorine (698eV). Smaller peaks for carbon were also seen (285 eV and 291eV). Other elements detected are Si, Mn, Cr and Fe associated with the stainless steel substrate. The fact that these elements are detected is evidence that the fluoroalkylsilane coating is between 5 and 10 nanometre in thickness since this is the sampling depth for photoelectrons as previously discussed in section 3.8.4.

A higher energy resolution scan was performed for carbon to obtain more accurate information about chemical shifts in binding energy (figure 150). The binding energy shift between the two carbon peaks is 6.0eV. From XPS reference data the chemical shift in binding energy associated with a CF_2 functional group should be 5.90eV and for a CF_3 functional group the shift should be 7.69eV.

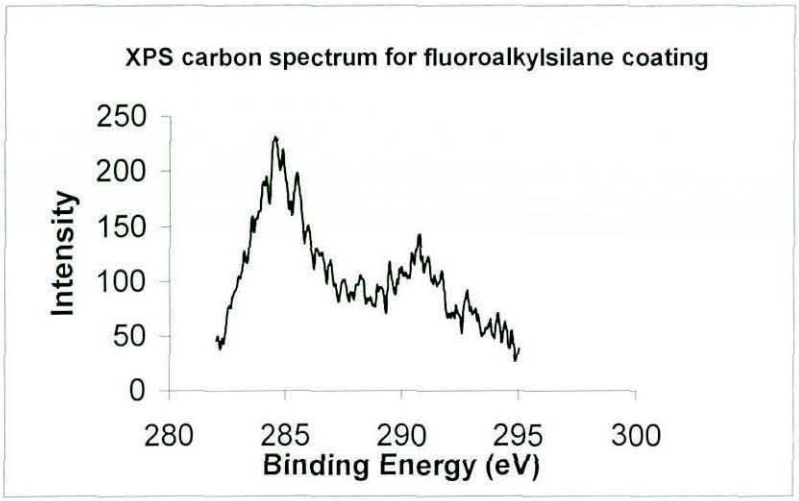

Figure 150. Chemical shift of carbon for fluoroalkylsilane coating

The molecular structure of the Dynasylan molecule is as shown in figure 151 and has five CF_2 functional groups terminated by a single CF_3 functional group and it is suggested that the 6.0eV shift seen in the high resolution scan for the carbon peak implies that the shift due to the CF_2 functional groups dominates and effectively masks the presence of the terminal CF_3 group.

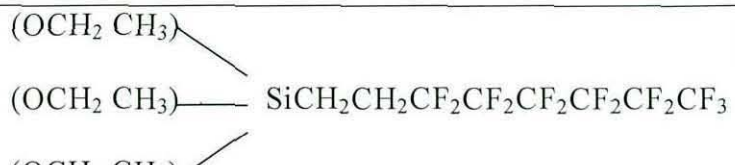

Figure 151. Molecular structure of Dynasylan F8621 molecule.

XPS spectra are usually collected at a take off angle of 90° so that the photoelectrons generated originate from the deeper layers of the sample (5 to 10 nm). By this means the best chemical shift data for an unknown sample is obtained. If the photoelectrons were collected at a grazing take off angle of a few degrees they would originate from the very surface layer, as discussed in Chapter 3. In practice it is possible to collect spectra at a range of take off angles and thus vary the sampling depth of the technique. By comparing the relative intensities of peaks of the same kinetic energy for different take off angles it is possible to calculate the thickness of a thin coating.

In Angle Resolved XPS experiments a very smooth substrate is really essential and the sputter coating nickel samples used for high resolution SEM were also used for this experiment. In this case the purpose of the proposed experiment was to obtain any information about how the fluoroalkylsilane molecules might be oriented on the nickel substrate.

The ion etching facility in the instrument used for these experiments had been disabled. In these experiments it was not appropriate to ion etch the samples since this would have destroyed the coating we wished to examine. However, all samples prepared in any laboratory environment (no matter how carefully prepared) attract a layer of hydrocarbon several monolayers thick and this is seen when they are examined in an XPS because of the extreme surface sensitivity of the technique.

In this experiment it was appropriate to attempt to produce a coating thickness of only a few monolayers and a low concentration solution of 0.1% Dynasylan was used to treat a nickel sputtered slide for a reaction time of one minute.

Data was collected using take off angles of 20°, 50°, 70° and 90°.

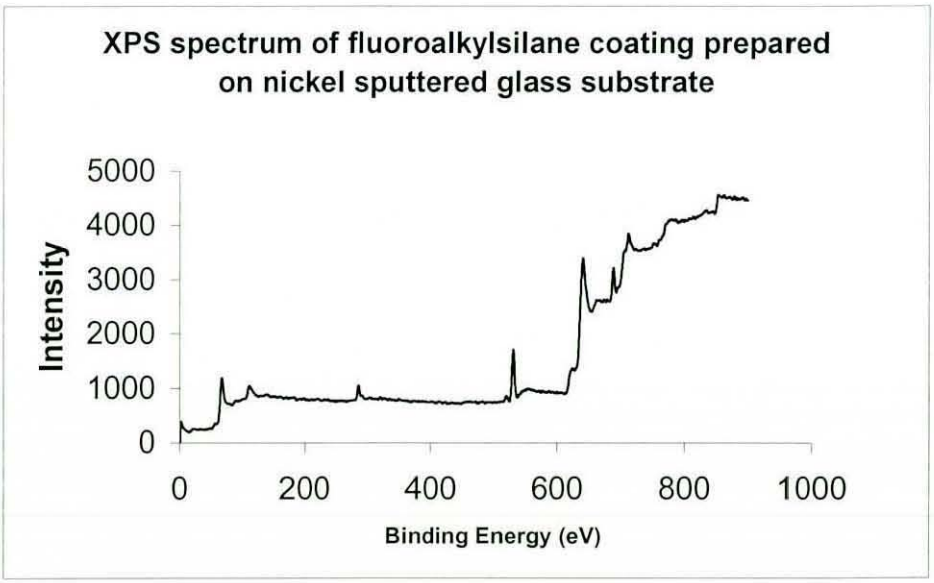

Figure 152.XPS survey spectrum for fluoroalkylsilane on nickel.

Figure 152 shows an XPS survey spectrum for the treated nickel slide and figure 153 below shows the atomic percentages for carbon, fluorine and nickel plotted as a function of take-off angle.

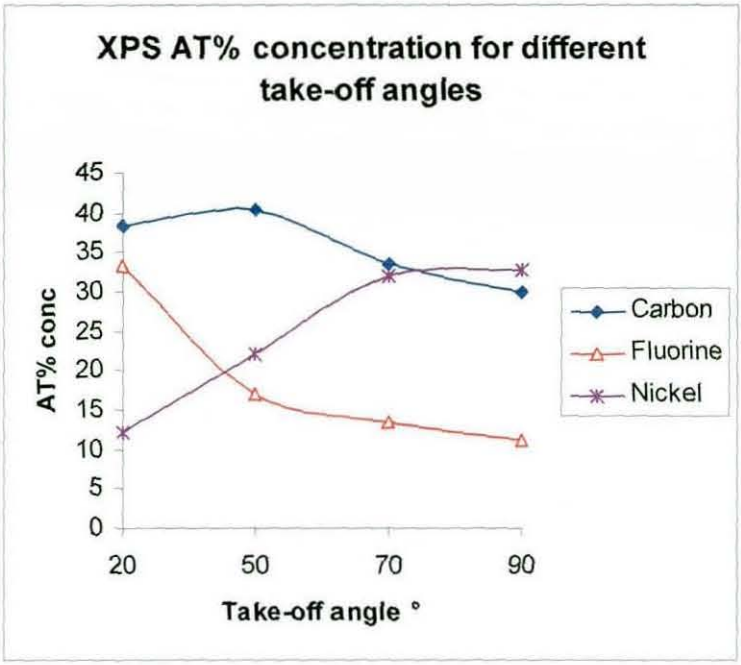

Figure 153. Carbon, Fluorine and Nickel concentrations for different XPS take-off angles.

The data can be interpreted either as suggesting an enrichment of fluorine at the surface consistent with the known molecular structure as depicted and comprising a CF_2 tail terminated by a CF_3 group in which the tail orients itself perpendicular to the surface or the data may simply show that defluorination is occurring over the time scale taken to collect the data in each case. Fluorine present on surface coatings examined using XPS is known to be sensitive to the X-ray irradiation experienced during XPS analysis. The fact that the fluorine to carbon ratio does not exceed unity is suggestive that defluorination is occurring since if CF_3 were present at the surface, one would expect the ratio to be greater than unity. Defluorination at the sample surfaces by irradiation over the duration of these experiments severely limits the interpretation of the data.

6.1.2.4 Atomic Force Microscopy (AFM)

Published literature [138], [193] suggests that AFM can provide useful topographic and functional images relating to the tribological properties of fluoroalkylsilanes. AFM images were collected from nickel sputtered coated glass slides following treatment with Dynasylan fluoroalkylsilane for varying concentrations and treatment times, referenced against an untreated control sample (figure 154). The images show the pull off force or "stickiness" of the surfaces represented in three-dimensional plots. One of the AFM images for the treated surface is shown in figure 155. Although the vertical scaling is different, the area examined is 2.5 x 2.5 micrometres in each case and the images suggest that there is not a great deal of difference in the surface stickiness between the treated and control surface, which is surprising, The patterning developing on the treated sample comprising circular blotches is difficult to interpret. The features are ~ 180 nm diameter and do not correlate with the islands shown in the high resolution SEM images which were only ~ 40 nm diameter. Similar structures attributed a phase separation effects have been reported in the literature.

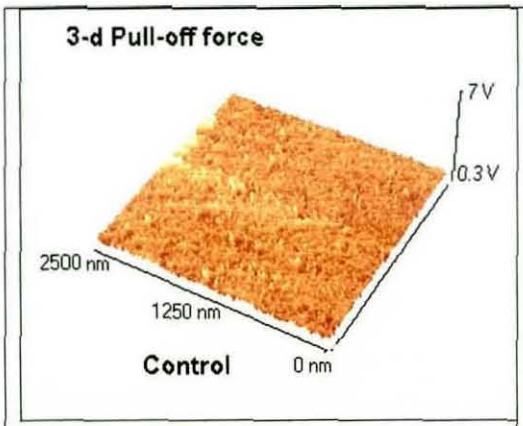

Figure 154.AFM image of untreated nickel sputter coated onto glass.

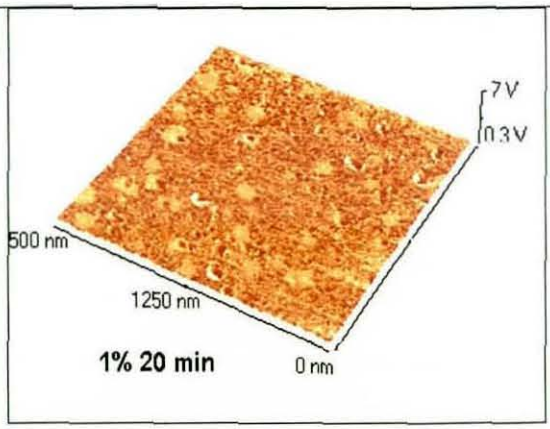

Figure 155.AFM image of surface in figure 154 following treatment with fluoroalkylsilane.

It was decided to repeat the AFM experiments at a later stage substituting polished nickel plate for the nickel sputtered glass slides since the Dynasylan fluoroalkylsilane was shown to coat rough nickel plate effectively and this would then reduce the variables that needed to be considered to surface roughness only.

6.1.2.5 Testing the release properties of Dynasylan

Following the analytical work discussed it was decided to use the blister tester developed, as discussed in Chapter 4, to evaluate the potential of this fluoroalkylsilane coating as a mould release agent. It was applied to pre-cleaned stainless steel discs (65 mm diameter) at 2% concentration and cured. A water contact angle measurement resulted in an average angle of 121° (over twenty measurements) implying a low surface energy coating had been created. Next FM300 Cytec resin sheets, cut to size, were laid on top and weighted in an oven set at 180°C. The FM300 resin was used for convenience and also since it comprised material used by Bombardier and represented a realistic material to test. It was oven cured for 3 hours.

Another stainless steel disc machined to fit the blister tester was similarly cleaned and then coated with Frekote mould release components comprising of surface sealer and mould release agent. The manufacturers recommendations for coating were followed. After curing of the Frekote, FM300 resin sheets were laid onto the disc and cured in exactly the same way as described previously.

After removal from the curing oven and cooling the two samples were compared. The FM300 resin disc had only to be touched lightly to affect its immediate release from the metal disc that had been Frekote treated. In comparison, the resin disc for the Dynasylan treated surface stuck tenaciously as shown in the left hand image in figure 156 below. The resin disc stuck so tenaciously to the metal that it had to be ground off mechanically back to before it was possible to begin to detach the resin at the edges of the metal disc using a razor blade. It was perplexing that despite possessing producing a low energy surface, the Dynasylan coating had so little effect in reducing adhesion of the resin.

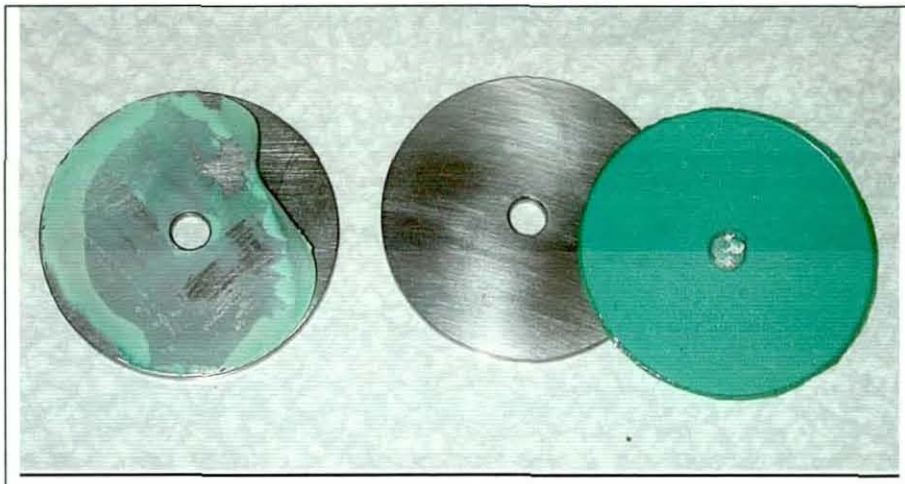

Figure 156.Comparison of poor release for fluoroalkylsilane coating (left disc) to excellent release obtained for Frekote (right).

It was suspected that to obtain good release properties it was necessary to fill in the asperities and porosities on a rough surface such that mechanical interlocking was denied as a mechanism for adhesion. It was clear that many widely used commercial mould releases used a sealing agent that was compatible with a mould release coating applied afterwards. In other words it was necessary to use a primer to treat the surface before producing a low energy surface.

One of the discs shown in figure 156 was subsequently hand polished to a mirror finish and then cleaned thoroughly before being and coated with 2% concentration fluoroalkylsilane, which was cured. An average water contact angle of 118°C was measured for the treated surface. FM300 epoxide adhesive was applied and cured under the same conditions as previously used. The purpose of this test was to see if the coating would produce better release properties if the starting substrate was relatively smooth. It was found that the epoxide resin stuck with almost equal vigour on this surface also. The problem with this test is that in creating a smooth polished substrate, the surface area over which the fluoroalkylsilane can react and bind to the metal is reduced significantly over that of a mechanically abraded substrate. Therefore rather than having a single variable of surface roughness, the reactivity of the surface has to be considered also which complicates interpretation of the result.

6.1.2.6 Other silane coatings

The use of Oxsilan AL-0501 silane as such a primer was discussed in Chapter 4 and this was used to coat a fresh, pre-cleaned blister test disc prior to application of a further coating Dynasylan fluoroalkylsilane. It was thought this combination might constitute a bifunctional coating where a weak boundary layer would exist between the Oxsilan and the Dynasylan coatings and thus engineer good release properties. Repeating the comparative test described previously, essentially the same result was obtained and it was concluded that the problem might be that the Dynasylan coating failed to react sufficiently to bind itself onto an already existing silane treated surface.

Element & Peak	Binding Energy eV	Atomic % present
Carbon C1s	285	34.8
Oxygen O1s	525.8	29.8
Silicon Si2p	102.5	33.8
Fluorine F1s	689.0	1.6

Table 13. XPS composition of Oxsilan coating

XPS analysis of Oxsilan (Table 13 above) shows it to be a fluorinated silane itself and this suggests it might be difficult to bind to another silane. It was apparent from these results that a far more detailed study of the physics and chemistry of mould releases was necessary in order to formulate new coatings that would perform better than the PDMS based products such as Frekote that were used commercially. The amount of work necessary is commensurate with a separate doctoral dissertation and it was considered that the time remaining for this research would be better spent in trying to understand why products such as Frekote or the water based Zyvax release, mentioned in Chapter 4, functioned so well as mould release agents and how conventional PTFE based polymers used for non-stick coatings would compare.

6.1.3.Summary

Whilst commercial fluoroalkylsilanes such as Dynasylan produce very low surface energy coatings with a surface energy value lower than Frekote release agent and even lower than PTFE, its weakness for mould release application lies in its propensity to form only a monolayer film thickness on the substrate surface. Although Dynasylan is an expensive material, the self-limiting thickness of the coating meant that a small amount diluted in a solvent would coat large surface areas economically. As has been argued, the weakness of this for release applications is that resin used for mouldings will be forced under pressure and temperature into the micro-cavities in a rough substrate providing many sites for mechanical interlocking. This does not apparently occur for Frekote. The evidence from contact angles and AFM (section 6.1.2) illustrates that a cured Dynasylan coating is less sticky than a Frekote coating but that, despite this fact, it is not suitable on its own as a release agent.

Mention has been made of the use of another material (Oxsilan) as a primer to treat surfaces prior to application of Dynasylan. Evidence from both ellipsometry (section 6.1.2) and SEM suggests this material forms a sufficiently thick coating to fill in many micro-cavities in a substrate surface. XPS analysis shows that it is a fluorinated compound and experiments with depositing Dynasylan onto an Oxsilan coating have not been successful. It is felt that the chemistries of the two materials are not sufficiently compatible to allow this and that use of Oxsilan alone is not appropriate as the chemical is not intended as a release agent and is not optimised for that application.

6.2.Frekote mould release coating

6.2.1. Analysis of the chemical and physical properties of Frekote

6.2.1.1.FTIR

The application of this commercial mould release product has been discussed in section 3.2.2. Semi-permanent mould release products in general comprise of a sealing material or surface primer, which is cured and then the mould release product is applied. Usually several coats of each are applied. In the Frekote products evaluated, B15 sealer was used with 710 NC mould release.

Using FTIR spectroscopy the absorption spectra for Frekote 710 mould release agent (figure 157) and Frekote B15 sealer (figure 158) were obtained as shown below. The most intense peaks occur at similar positions between 1500 and 500 wavenumbers (cm^{-1}) in both spectra but show a number of subtle differences in minor peaks and broadening of the absorption bands. Other peaks common to both samples are clustered close to 3000 wavenumbers.

Considering the spectrum for Frekote 710, the principal peaks occur at 2931, 2878,1261,1095,1020 and 807 cm^{-1}. Strong absorption peaks assigned to dimethyl- and trimethyl-substituted silicon atoms are reported to occur near 800 cm^{-1} [196] . Also a strong band at 1263 cm^{-1} is assigned to the bending mode for a silicon bonded methyl group [197]. Absorptions correlated with CH_2 and CH_3 stretching are observed at higher wavenumbers and overall the spectrum resembles that obtained for PDMS. Overall there appears to be a reasonable qualitative similarity between the spectrum for Frekote and the B15 sealing agent and since these are chemically compatible, it is reasonable to assume this may also be based on PDMS.

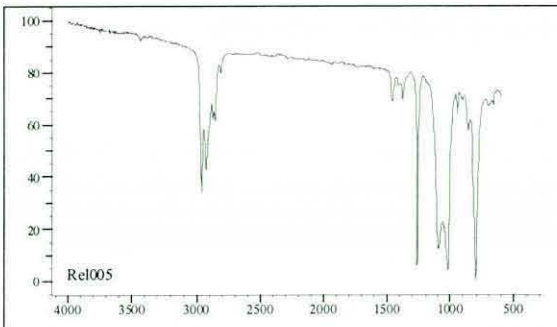

Figure 157. FTIR Spectrum of Frekote 710 mould release agent.

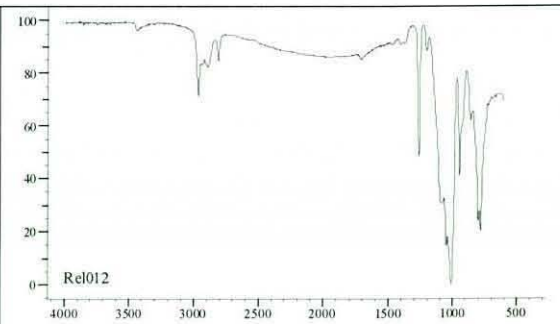

Figure 158. FTIR Spectrum of Frekote B15 sealer.

6.2.1.2. SIMS

Blanchard [49] used secondary ion mass spectrometry (SIMS) to determine that Frekote was based on polydimethylsiloxane (PDMS). The positive ion SIMS spectrum of PDMS [198] shows peaks at 73, 147, and 221 atomic mass units (a.m.u.) in order of intensity and attributed to $(CH_3)_3Si$, $(CH_3)_3SiOSi(CH_3)_2$ and $(CH_3)_3Si(OSi(CH_3)_2)_2$. Minor peaks also occur at 207 and 295 a.m.u.

SIMS spectra from Frekote cured onto nickel foil were acquired in this study and are shown in figures 159 to 161 below.

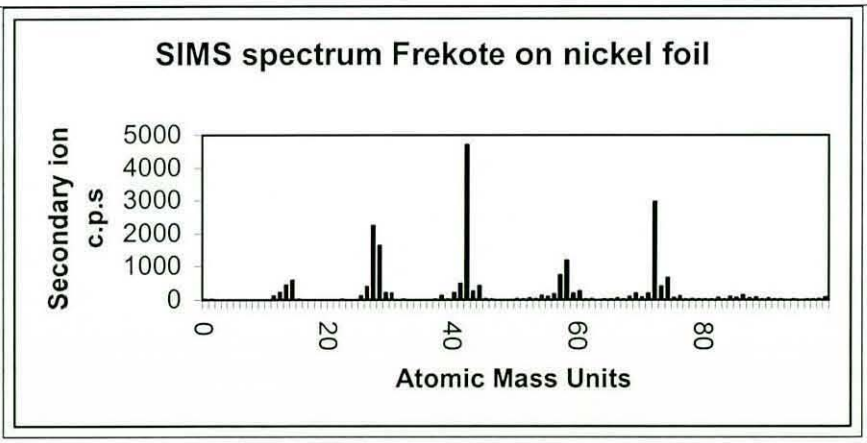

Figure 159. SIMS positive ion spectrum for Frekote on nickel foil. Range 0 – 100 a.m.u.

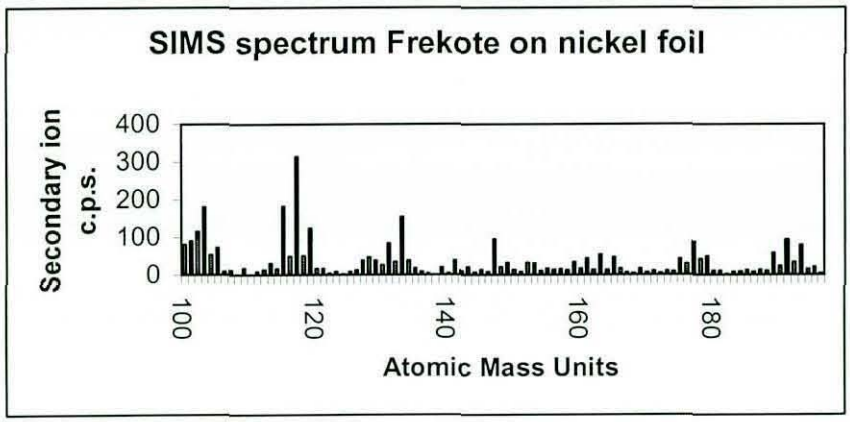

Figure 160. SIMS positive ion spectrum for Frekote on nickel foil. Range 100 – 200 a.m.u.

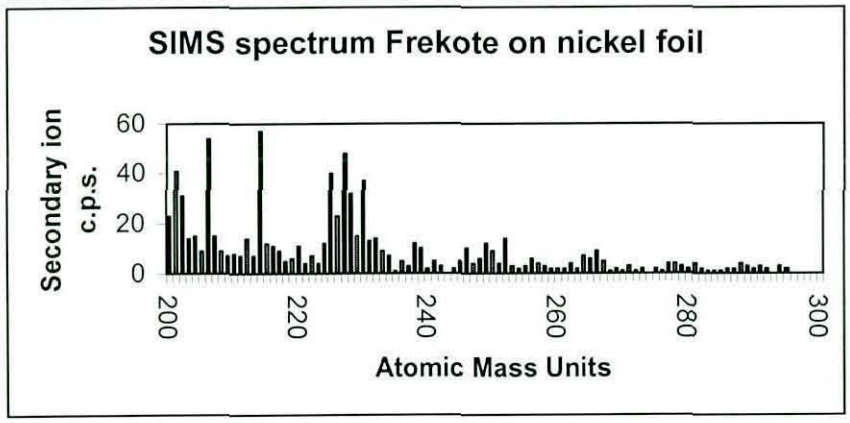

Figure 161. SIMS positive ion spectrum for Frekote on nickel foil. Range 200 – 300 a.m.u.

The main peaks at 73 and 147 a.m.u. are seen in the above spectra confirming the presence of PDMS although there are many other peaks which cannot be as easily assigned and are likely to be associated with the formulation of Frekote which is a complex product and not a single compound such as PDMS. These results are very similar to those published by Blanchard.

6.2.1.3. DSC and TGA

From simple evaporation experiments discussed in Chapter 3, it was apparent that Frekote mould release agent would condense down to a transparent, rubbery film once the dibutyl ether solvent had been driven off. This again was consistent with the physical properties of PDMS and an experiment was performed using differential

scanning calorimetry (DSC) to determine its glass transition temperature. The experimental details for these thermal measurements were discussed in section 4.5.10. The rubbery nature of solid Frekote at room temperature suggested a sub-ambient T_g and the calorimeter was cooled using liquid nitrogen to a temperature of –100° before the experiment was started. Despite these efforts no T_g was measured and it was concluded that the T_g must be very low and this is consistent with the known T_g for PDMS that has been measured as -127°C. Both figure 162 and a thermogravimetric analysis of the sample (figure 163) showed that it is a very thermally stable material. Sample weight losses of only 2.18% were measured from ambient to 300°C.

The significance of these measurements mean that films of the mould release agent will be very viscoelastic at the temperatures experienced by mould tooling during a typical heating cycle. Consequently the molecular mobility release molecules will tend to lubricate the moulding and the viscoelastic nature of the film will resist the pressures applied to the tool surface during the cure cycle. The desirability of these properties to obtain good release was discussed in Chapter 3 where other researchers cited had reached similar conclusions. These are very different properties to those of fluoroalkylsilanes that cure to form a scratch resistant very thin film on a surface that conforms to the surface topography without sealing porosities or roughness irregularities on the surface. In terms of release properties such cured films only possess low surface energy and this appears to be only one property that must be possessed by a good release agent.

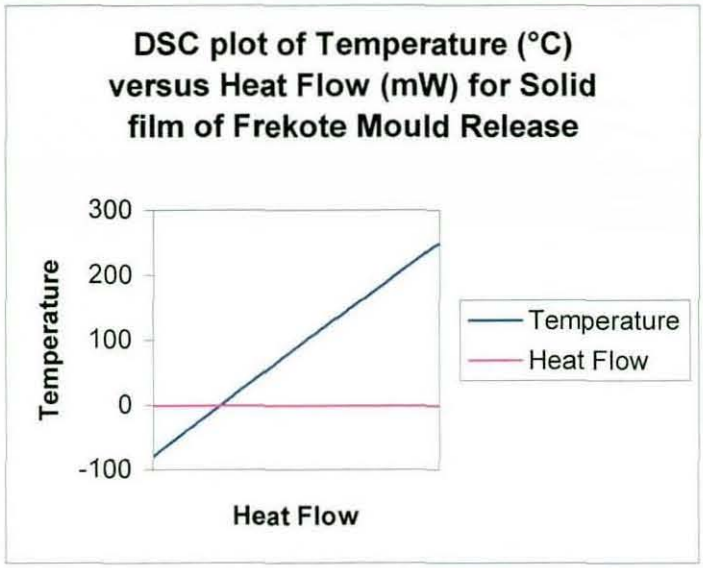

Figure 162. TA Instruments 2920 Modulated DSC data plot.

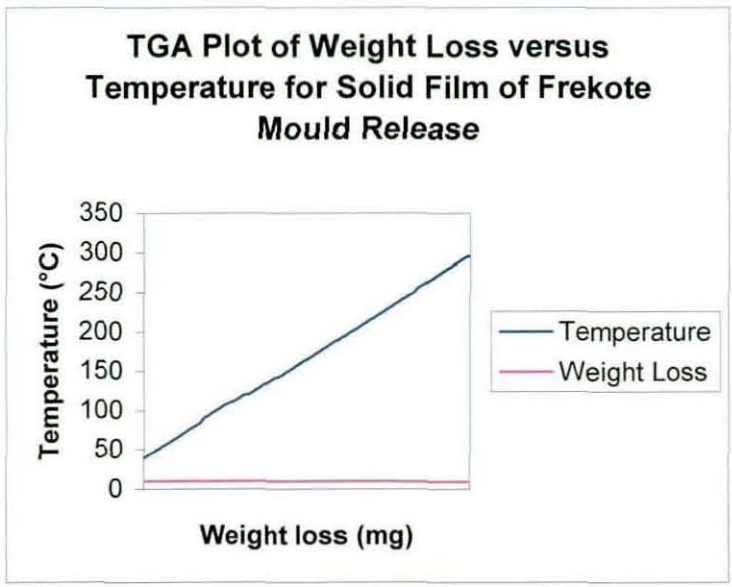

Figure 163. TA Instruments Auto TGA 2950HR data plot.

6.2.2.Coating thickness measurements using SEM, ellipsometry and interference microscopy

Conventional methods of preparing cross sections of materials by embedding samples in resin, curing the resin and then grinding and polishing cannot be used with mould releases since resin will not stick to them and an indirect method has to be used.

Frekote sealer and mould release agent were applied to nickel mould tooling according to the manufacturers instructions and the resulting film was stripped off and examined edge on in the SEM to obtain a thickness measurement (figure 164). This shows the thickness to be ~5 micrometres. The R_a surface roughness for the untreated substrate varies in the range 3.8 to 5.4 micrometres and consequently a typical application of the Frekote products must largely fill in most surface irregularities. (figure 165 shows an X-ray spectrum (EDX) for the sample shown in the previous figure.

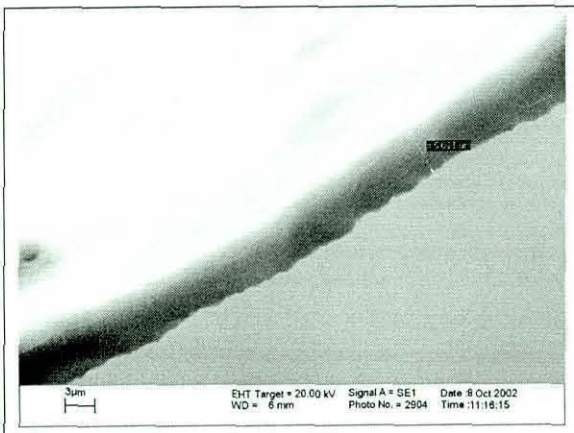

Figure 164. SEM thickness measurement of a flake of Frekote(and sealer) is shown and thickness measured as 5.033 micrometres.

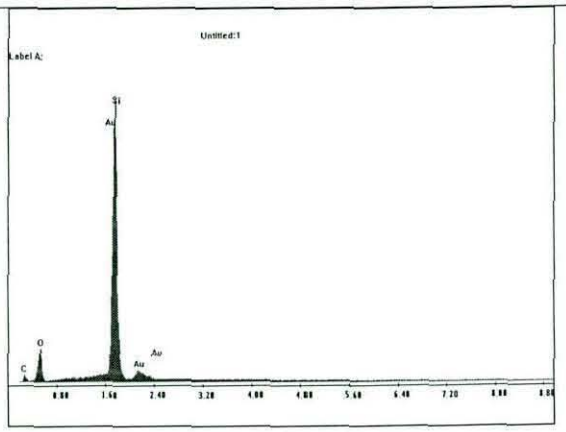

Figure 165. EDX spectrum of Frekote flake in figure 164 shows that that it is an organosilicon compound. The largest peak is for silicon.

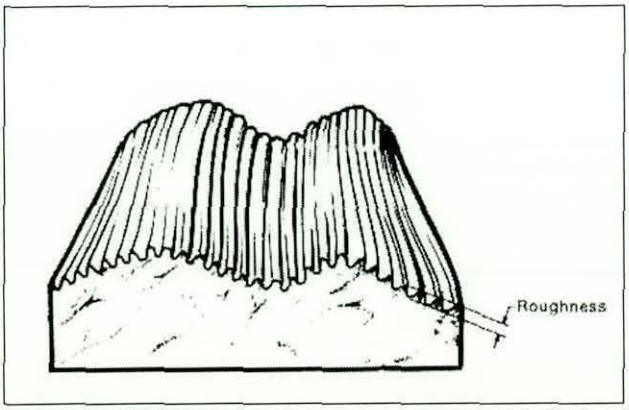

Figure 166 Diagram of rough surface undulations(After Dagnall [194])

Figure 166 shows a schematic representation of a rough surface and, as discussed, it is though that the Frekote products fill in the surface irregularities depicted. When a surface coated with these products is examined using SEM, it is seen that this is the

case. Figure 167 shows an area at the boundary between a Frekote treated and untreated substrate. The scratch marks from the abrasive cleaning of the substrate are clear on one half of the image but are clearly obscured on the other half by the Frekote coating. The coating shown was produced by dipping an abraded and cleaned metal coupon into a beaker of Frekote 710 NC mould release agent so that when it was withdrawn, half the area was coated. This coating was then cured.

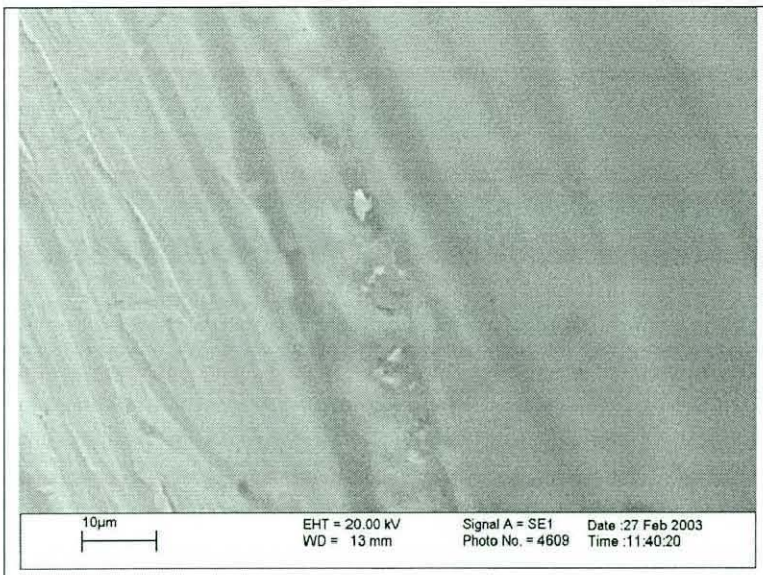

Figure 167. SEM image showing boundary between areas coated with Frekote (right) with uncoated surface (left). Scale bar = 10 micrometres

The Frekote sealer and mould release combination create a comparatively thick film when applied according to the manufacturers instructions. An attempt was made to quantify how the surface roughness varied on a model stainless steel substrate with and without a single coating of Frekote mould release agent. R_a and R_t roughness parameters were measured in two orthogonal directions as shown in Table 14 below.

	R_a(micrometres)	R_t(micrometres)	R_a(micrometres)	R_t(micrometres)
Uncoated	0.1703	1.6040	0.1610	1.5358
Coated	0.1318	1.0591	0.1678	1.3313

Table 14.Surface roughness comparison of uncoated and Frekote treated stainless steel foil.

These show an apparent reduction in surface roughness but only in one direction. An SEM image of the uncoated substrate (figure 72, section 5.1.1.4.2) shows that it possesses unidirectional surface features attributed to production of the foil by rolling. The surface roughness values seem consistent with this microstructure where depressions have been partially filled with the Frekote product. Both original samples were cut from the same area of steel foil so it would be expected that the roughness variation between each (prior to coating of one sample) would be small. Different areas though show significant differences in R_a. A measurement given in Table 8, section 5.1.1.2.3, for cleaned foil was $R_a = 0.1295$ micrometres and so some care is required in interpretation.

It is apparent though that for a full application of Frekote sealer and mould release on an industrially sourced substrate, many of the surface irregularities resulting from abrasive cleaning are at least partially filled. When one rubs ones finger over such a Frekote treated surface it does not, however, feel very smooth.. On closer inspection using an SEM it is apparent that this rubbing action dislodges platelets of cured mould release (figures 168 & 169). This would be expected since the Frekote functionality requires it to act as a weak boundary layer and the cohesive strength between separate applications of coatings must be poor. It is conjectured that under conditions of elevated temperature and applied pressure commensurate with moulding processes, the Frekote smears and flows over a surface filling in many microscopic substrate irregularities.

The following images show a full application of Frekote sealer and mould release applied to a steel substrate that was degreased and then grit blast cleaned prior to Frekote treatment.

Mould sticking is believed to be due to the build up of residues of degraded mould release after many mould cure cycles.

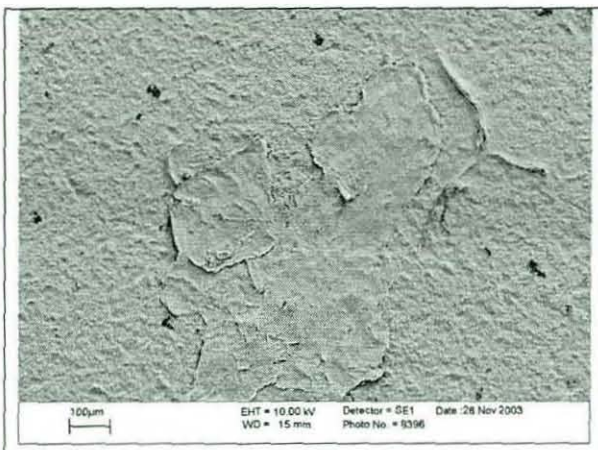

Figure 168.SEM image of full Frekote application on grit blasted steel surface. Scale bar = 100 micrometres.

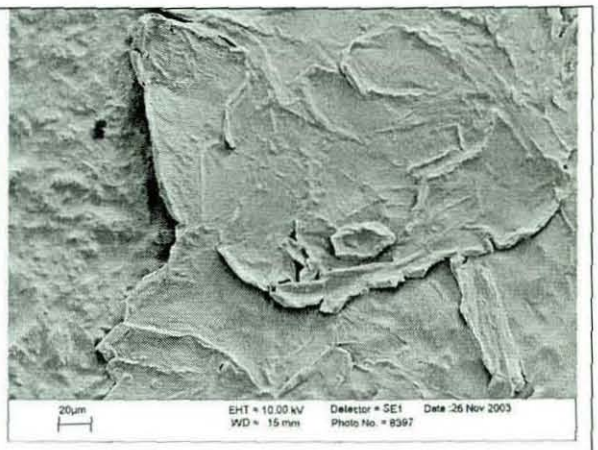

Figure 169. Higher magnification of Frekote layers shown in figure 168.Scale bar = 20 micrometres.

The thickness resulting from a single dip coating of a metal substrate in Frekote 710 mould release was measured using Ellipsometry and Interference Microscopy and compared to measurements from similar dip applications of Oxsilan. The following results were obtained using Ellipsometry:

Frekote on nickel (sputtered onto glass slide) 56 nm (nanometres)
Frekote on stainless steel foil 120nm
Oxsilan on nickel (sputtered onto glass slide) 421 nm
Oxsilan on stainless steel foil 219 nm

Since a film of Oxsilan shows interference colours when coated onto stainless steel foil, this implies a coating thickness equal to some fraction of the wavelength of visible light and so the ellipsometry value is of the correct magnitude.

Both ellipsometry and interference microscopy are best suited to measuring coatings on smooth substrates. No measurements were possible using interference microscopy for the coated stainless steel samples. For the Frekote coating a thickness of 68 nm was obtained which is in reasonable agreement with that obtained by ellipsometry.

Unfortunately, it is difficult to correlate these measurements made on smooth glassy surfaces (as required by the measurement techniques) to the film thickness that may exist on abrasively cleaned metal tooling. In that case the Frekote may be retained and fill porosities rather than spreading evenly to form a uniform film. The measurements suggest that the Frekote product itself has no propensity to form an intrinsically thick layer on a substrate. Since Frekote and similar PDMS products are always applied as multiple coats following surface sealing with a compatible product, it is probable that that thick coatings give the best results in terms of release. This can only be because they reduce the opportunity for adhesion by mechanical interlocking. The role of the sealing component in mould release products is also clearly important.

6.2.3.Comparative AFM study of adhesion differences between Frekote and other coatings

Nickel mould tooling substrate was hand polished and characterized as discussed in Chapter 4. Four samples were mounted for AFM study as shown in figure 170. These were identified: -

(i) Sample 1. Untreated clean surface control.

(ii) Sample 2. Zyvax water soluble semi-permanent mould release

(iii) Sample 3. Frekote mould release,

(iv) Sample 4. Dynasylan fluoroalkylsilane (5% solution)

Figure 170. Samples 1 – 4. A five pence coin is used as a scale reference.

Water contact angle tests were made to ensure surface cleanliness on the polished nickel substrates prior to coating and it was found that a drop of water would spread over the cleaned surfaces (average contact angle ~35°). For samples 2, 3 and 4 water contact angles of 110°,107° and 116° were measured.

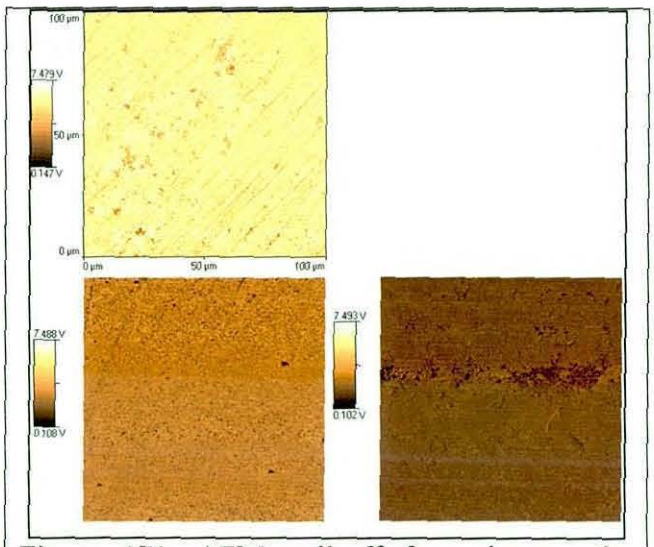

Figure 171. AFM pull-off force images for samples 1 – 4 shown in figure 171.

Figure 171 shows the pull-off force images for samples 1 – 4. The area examined was 100x100 micrometres. For sample 2 the signal was saturated due to the AFM tip being stuck to the surface. For this reason the top right image is absent. The darker colour indicates the lower pull-off force.

These AFM images imply that the fluoroalkylsilane coating produces the lowest pull-off force closely followed by the Frekote treated surface, both compared to the untreated surface. The result for sample 2 for the Zyvax treated surface was interesting. The surface energy of this coating was 24.4 $mJ.m^{-2}$. The AFM tip apparently stuck to the surface during AFM characterisation. This is interpreted as implying that this release coating is unstable by virtue of it being hygroscopic. It is suggested that a trace residue of the surfactant, used to aid emulsification of the silicon based release agent in an aqueous solvent, remains on a treated surface after the coating is cured and that over time this can attract moisture from the atmosphere. Confirmatory evidence for this was also obtained from water contact angle analysis where it was observed that a water droplet applied to a cured coating would gradually spread implying some component on the surface was changing the surface tension of

the water. The spreading was measured and is shown in figure 172. The initial water contact angle was 110° but reduced so rapidly that data collection could only be started once the angle had reached 105° as shown. Since this product gave this result it was decided to eliminate it from further study and restrict this to present samples already considered.

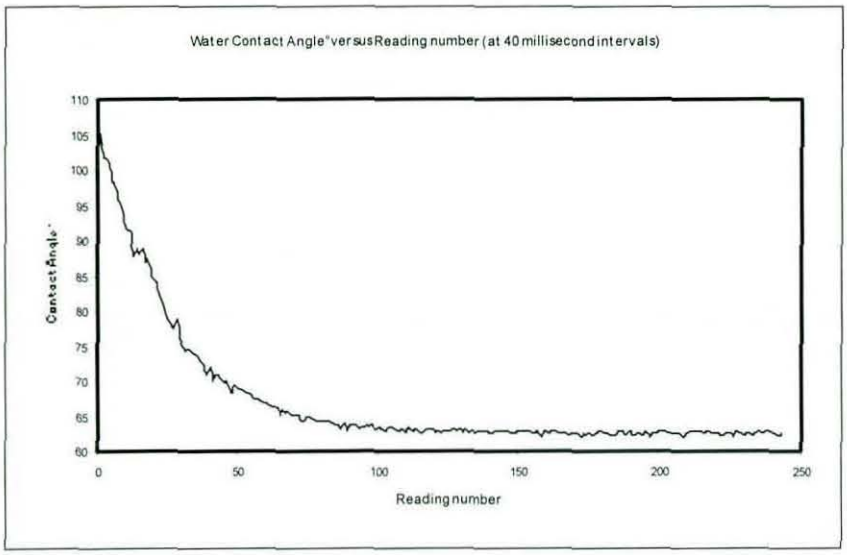

Figure 172. Spreading of water on Zyvax mould release coating showing contact angle reducing over 40 millisecond time period.

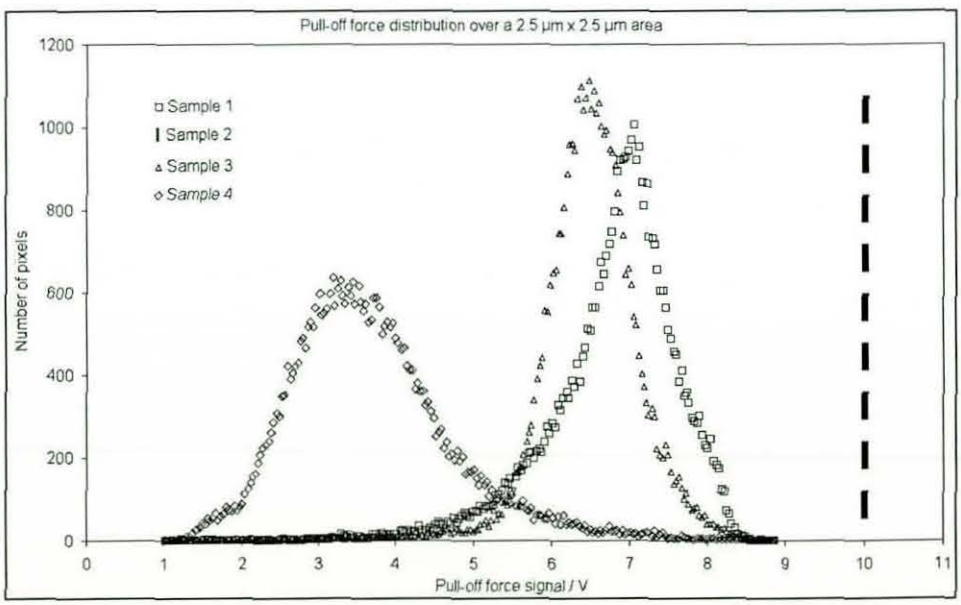

Figure 173. Pull-off force distributions for samples 1 –4 from a smaller area of 2.5 x 2.5 micrometres over which the adhesion was more uniform.

The pull-off force images (figure 171) can be converted into data point distributions that reflect the adhesion of the tip as it is retracted from the sample. As has been discussed in section 3.8.5, it is difficult to quantify this force since it depends on many AFM instrumental parameters such as the stiffness and spring constant of the probe. Presenting the data in this form more clearly illustrates the differences between the samples and it is that there exists a clear distinction between the fluoroalkylsilane coating and the Frekote with the distinction between Frekote and the untreated control not being as great as might have been expected.

6.3. Alternative fluoropolymer-based non-stick coatings

6.3.1 Sintered fluoropolymer coatings

The application of Whitford Xylan and Xylar PTFE based coatings, discussed in section 4.4.6, and the performance of these coatings sintered onto different steel substrates has been evaluated. The contact angles and surface energies of the prepared coatings were measured and tabulated in Table 8, section 5.1.2. The surface of the cured Xylar coating was examined using SEM and an EDX spectrum obtained (figures 174 and 175). Cytec Fiberite FM300 epoxide resin sheets were used as a test resin system and sheets were laid onto a 65 mm blister test disc upon which the Xylar coating had been prepared. The FM300 resin was cured under weighted loading in a laboratory oven maintained at 180°C for three hours.

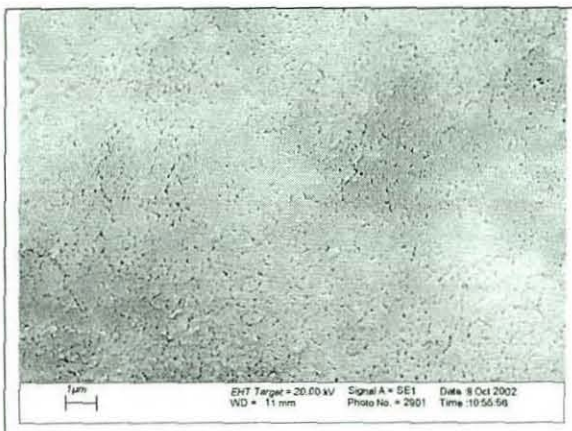

Figure174. SEM image of Xylar 2020 surface coating.

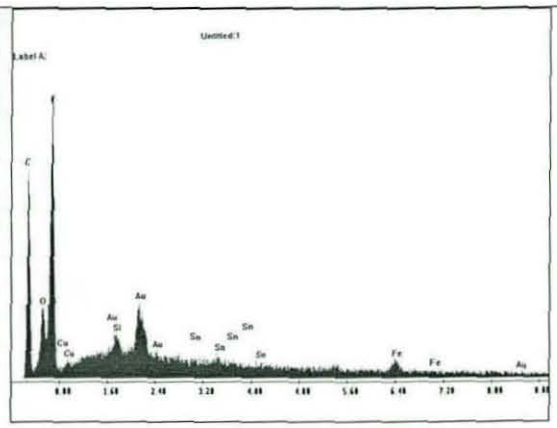

Figure 175. EDX spectrum of Xylar 2020. C,O,F,Si and Fe detected

It was found that the FM300 epoxy resin tenaciously adheres to the Xylar coating despite the fact that the Xylar coating possessed a low surface energy of 10.8 $mJ.m^{-2}$. This is shown in figure 176. The adhesion was so strong that a segment could be sawn from the disc as shown without releasing the epoxide resin or reducing its adhesion at all. The removed cross section was mounted in resin, ground and polished and then examined in the SEM. Using a backscattered electron detector, which is sensitive to differences in atomic number that exist in the structures resolved, enhanced the image contrast. The coatings are soft and smear easily during sample preparation resulting in an indistinct interface when examined using a secondary electron detector. Figures 176 and 177 show areas of the section. In figure 177 the white area on the right hand side of the image originates from the steel substrate that was very bright in the SEM

image. A polyethylene terepthalate (PET) support membrane is present in the FM300 resin sheet as a supporting binder and this is seen as the oval and round, darkened areas PET on the left hand side of the image (figure 177). The Xylar coating is sandwiched between the two and has sufficient contrast to be just discernable. It is seen to be approximately 50 micrometres thick.

Figure 176. Photograph showing adhesion of FM300 resin to Xylar 2020 coating on steel blister test disc.

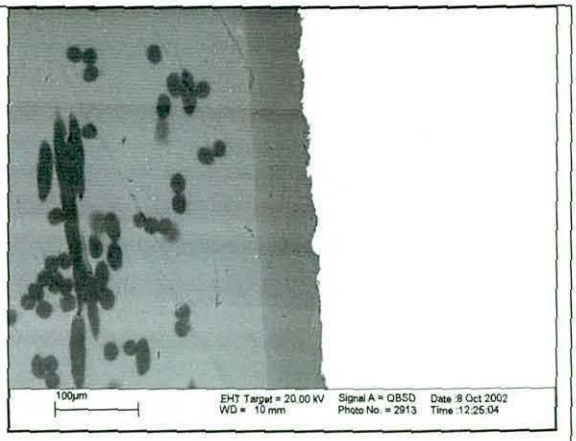

Figure 177. SEM cross section of Xylar 2020 from area removed in figure 176. Steel substrate on right with Xylar coating in centre.

Figure 178. SEM cross-section of Xylar 2020 at interface with FM300 resin.

A higher magnification image of the interface between the Xylar coating and the resin is shown in figure 178. It is interesting to note there is a particulate phase present in

the resin, which is uniformly dispersed and appears as white specs. There are also dark specs. An EDX analysis using spot mode was made of these white particles and the spectrum collected is shown in figure 179.

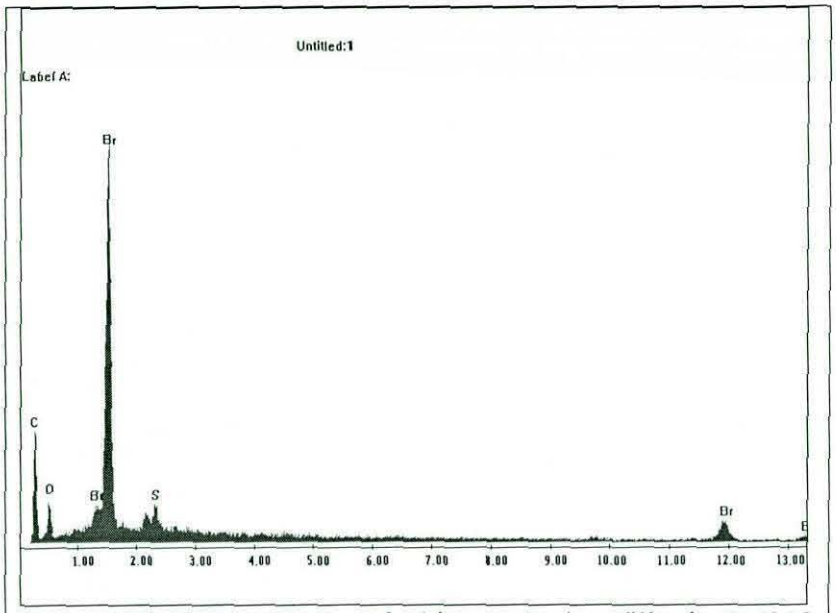

Figure 179.EDX spectrum of white particulate filler in FM300 resin shown in figure 181.

It is apparent from figure 179 that the resin contains a brominated compound. This is possibly a fire retardant. It is difficult to know how a resin system such as this, with one or more unsuspected components, will react at temperature and pressure with a substrate coating of different chemistry. It is possible that quite complex reactions occur which may in some part account for the sticking observed. The number of variables in the combined system makes it difficult to formulate a strategy for investigating the effects more fully in the time available. Ideally it would have been desirable to work with a monocomponent resin system rather than a proprietary resin whose chemistry was not divulged. The FM 300 resin was chosen because this resin was that used by Bombardier and is therefore closer to the intended application being investigated. Shrinkage of the resin during cure has not been quantified (thought to be several percent) but does not seem to decrease the tenacity of its adhesion to the substrates.

When the surface of non-stick Xylan 8080 is examined (figure 180 below) a different morphology again is resolved. When examined at higher magnification the porous structure of PTFE is clearly resolved (figure 181). It is these porosities combined with the pressure and temperature applied to the resin system that causes mechanical interlocking and adhesion despite the low surface energy of the PTFE surface. Again it is seen that a low energy surface does not by itself prevent sticking. This fact is well known in the marine coatings industry. The key point about this application is the applied pressure and high temperature (180°C). Other non-stick applications of the Whitford coatings are unlikely to have to contend with relatively high-pressure conditions and therefore the coatings almost certainly satisfy their intended function.

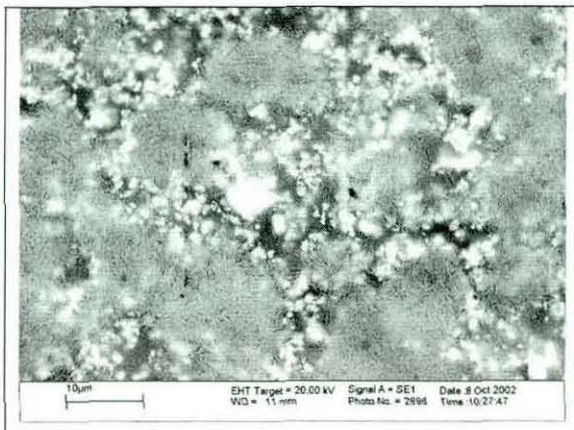

Figure180.Xylan 8080 surface topography using SEM.Scale bar = 10 micrometres.

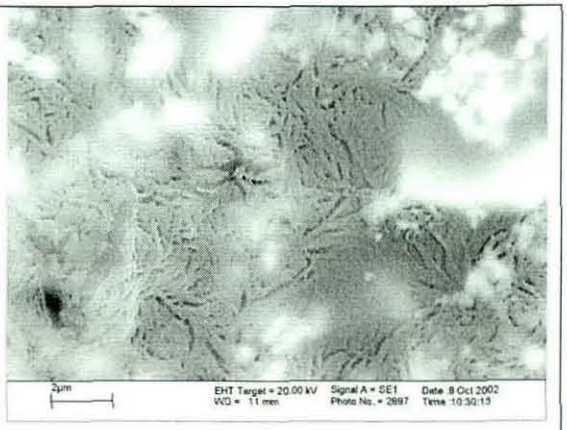

Figure181. Higher magnification of area in figure 183. Scale bar = 2 micrometres.

Figure 182 shows an EDX spectrum for the Xylan 8080 coating from which it is seen that the coating composition is different to that of the previous Xylar 2020 coating with possible barium sulphate and copper chromate present as additives. The role of these additives is unknown and again emphasises the difficulty in understanding adhesion when the chemistry of both adhesive and adherent are unknown.

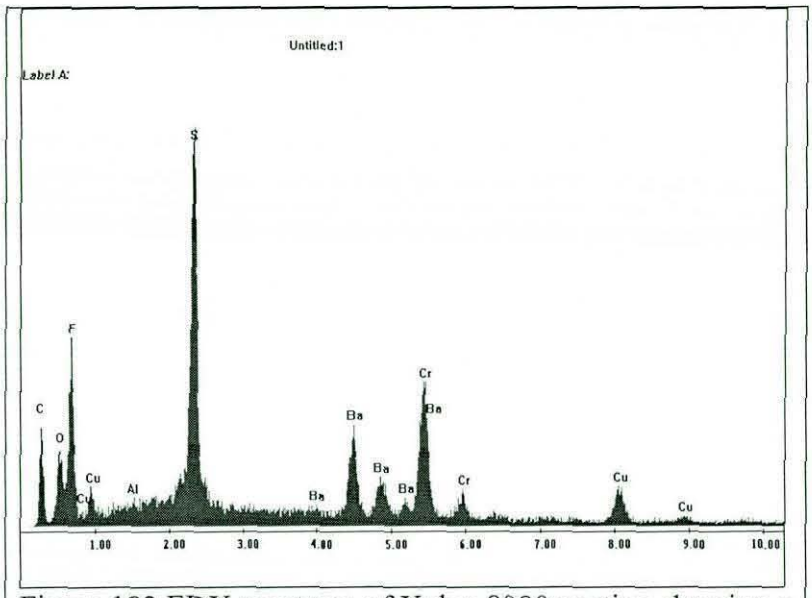

Figure 182.EDX spectrum of Xylan 8080 coating showing a different filler composition to that for Xylar 2020 (fig.179).

6.3.2 Interpretation of the findings for the Xylar/Xylan coatings

These Whitford coatings are commercial products and assumed to perform as non-stick coatings as claimed by the manufacturers. Therefore their apparent failure in these tests suggests that either

(i) the coatings have not been prepared properly or

(ii) they react in some way with additives present in the FM300 epoxide resin adhesive

(iii) they are not being used as intended by the manufacturers

There is no evidence to suggest that coatings used for testing were unsatisfactory although some experimental difficulty was encountered in their preparation. The coatings used were visibly smooth over the areas used and yielded low energy surfaces. PTFE is a major additive in the coating formulation and this is very unreactive so although the second cause listed cannot be eliminated, it is highly unlikely.

The intended applications of these coatings are most often as non-stick coatings for bakeware and whilst these items will be used at high temperatures commensurate with cooking food, substances are unlikely to be squeezed against the coated surfaces under considerable pressure, and the latter condition is that under which the coatings gave poor results in these tests.

Further tests were made on the Xylan 8080 coating. This PTFE coating was sintered onto a piece of stainless steel foil and Cytec FM300 epoxide resin sheets were laid up and cured onto the coating under weighted loading in an oven. It was found that the resin could be peeled away from the metal foil substrate with only slight difficulty on this occasion (figure 183 below). This is attributed to the flexibility of the thin substrate, which allowed the materials to be more easily pulled apart. It was thus possible to remove the epoxide resin from an area where it had been in contact with the Xylan coating and examine the surface using SEM (figures 184 & 185).

Figure 183. Xylan 8080 coating sintered onto stainless steel foil (black coating). FM300 resin (green) was then cured onto the Xylan coating.

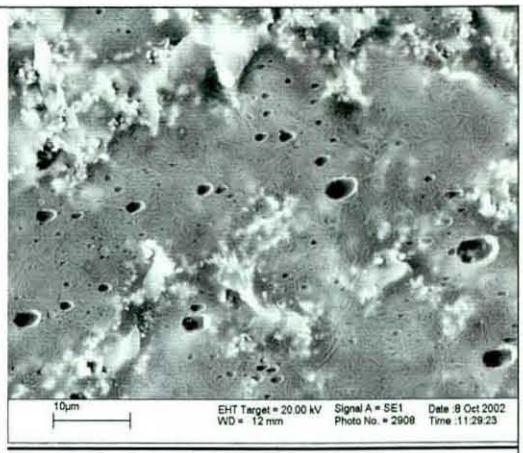

Figure 184. SEM image of Xylan 8080 coating following removal of green FM 300 resin in figure 183. Scale = 10 micrometres

Figure 185. Higher magnification of area in figure 184. Scale = 3 micrometres

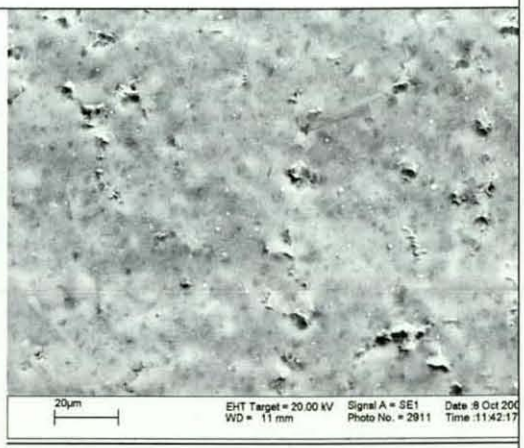

Figure 186. SEM image of underside surface of FM300 resin shown in figure 183. Scale = 20 micrometres.

Figure 186 shows an image of the underside on the resin where it has been in contact with the Xylan coating. It is suggested that the asperities seen on this surface may be points where mechanical interlocking has occurred with the Xylan coating giving rise to a level of adhesion making it difficult to separate the two surfaces. The virgin Xylan coating surface possesses fine structural porosites typical of PTFE (figure 181) but does not normally possess the pits seen in figures 184 and 185. It is suggested that the Xylan coating resists wetting from the resin in its liquid phase, but that the pressure applied overcomes the surface tension forces and forces the resin into the porosities in the soft PTFE structure and opens them up at the elevated cure temperatures. In other words the conditions prevailing in an unrestrained system where surface tension forces are dominant do not exist in a system constrained by pressure and temperature. When the liquid resin crosslinks and cools, a mechanical interlock has occurred and the surfaces become difficult to separate. It would be fortuitous if a single prepared cross section, such as that shown in figures 177 or 178, would show one of these sites of mechanical interlocking, and, although this cross-section was thoroughly examined at a range of magnification no features resembling an "ink-pot" feature were found. It would be necessary to many cross sections to find evidence of features commensurate with sites of possible interlocking.

6.3.3. Electroless Ni/PTFE non-stick coatings

Stevens[147] has claimed that the Apticote coatings already described offer a good solution to the problems of mould users. They possess many of the good attributes of PTFE coatings but offer greater toughness and durability for industrial applications. As has been shown the microstructure of the PTFE particle phase is very fine (figure 79) and the surface does not contain the same deficiencies of surface porosity seen in figure 180 above.

The FM300 epoxide resin sheets, which stuck tenaciously to the other coatings as discussed, did not stick to an Apticote 450 coating when cured under weighted loading in exactly the same way as for the other coatings. The cured epoxide resin sheet released with ease from the Apticote coating and behaved similarly to a Frekote treated substrate. This release is shown in figures 187 and 188.

Figure 187. FM300 epoxide resin sheet cured onto Apticote 450 coated nickel substrate.

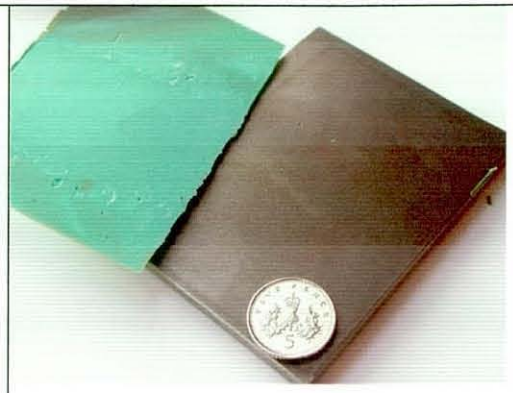

Figure 188. Ease of release of cured epoxide.

This release behaviour is not perhaps surprising in view of the very low friction coefficient measured for the Apticote 450 coating. This surface was characterised in section 5.1.4.3 for 5N and 10N loadings. The Apticote 450 coating was used in preference to the Apticote 460 coating, despite its slightly lower friction coefficient, because 450 is temperature hardened.

The desirable properties of mould releases have been discussed previously. Two of these were that the release coating should possess molecular mobility and cohesively weak boundary layers. Clearly the Apticote coating does not meet these particular properties and yet it appears to be successful at ensuring easy release of parts moulded against it. This emphasises an important fact, namely that whilst mould releases may possess a number of desirable properties, one or more of those properties may only be required in a particular environment with a given set of moulding processes. For example the Apticote coating might perform badly as an antifouling coating for marine applications but appears to perform well as a mould release for bakeware and similar industrial applications.

In discussing the non-stick properties of these coatings it is necessary to distinguish between "release" and "low friction" as depicted in figure 189. Friction results from two surfaces sliding across each other and is measured by a number that describes the reduction of drag (drag force) between the sliding parts. Release is different because the separating force is normal to the two surfaces involved and relates to the material properties of the surfaces such as, though not exclusively, surface energy.

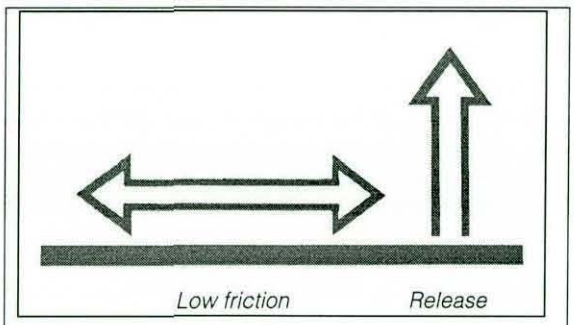

Figure 189. Diagram showing the difference between friction and release forces.

6.3.4. Mechanical testing

The blister test method proposed failed to generate useful data on the mould release properties of the coatings discussed. The epoxide adhesive either releases from a test surface with such ease that the release force is too small to measure, as occurs with Frekote treated surfaces and Apticote 450 coatings, or else it adheres so strongly that the separation force likely exceeds that required to fracture the resin at the point where the gas presses against the resin disc in the test geometry. Figure 176 illustrates this latter case obtained for the Xylar 2020 coating. For that test the blister tester was connected to a small gas cylinder that applied pressures up to 6 bar (608kPa) but application of the maximum pressure failed to produce a blister or show any sign that the resin disc was separating from the coating. The fact that the resin has to be physically ground away to remove it testifies to the fact that it adhered quite strongly to the coating.

An alternative means of testing is required and various designs have been cited in the literature, as discussed in chapters 3 and 4. The different subject areas studied in this dissertation were so broad and encompassed many different technologies and materials that there has been insufficient time to develop alternative testing methods that could yield this quantitative data.

6.3.5 Comparative AFM studies

In this respect the qualitative data provided from the pull-off forces determined from AFM studies of different coating surfaces is encouraging. Pull-off force comprises a

histogram of contact measurements and the force is a function of the spring constant of the cantilever and area of contact, though the latter is unknown for the particular instrument that was used. This technique has been used to rank the performance of Apticote 450 coating in relation to Frekote.

Figure 191 and 192 show AFM topographic images at different scales for the Apticote 450 coating surface. It is seen that the surface topography correlates well with the images obtained from SEM (figures 78 and 79, section 5.1.5.3). Figure 192 shows both a topography image and pull-off force image for the same area examined.

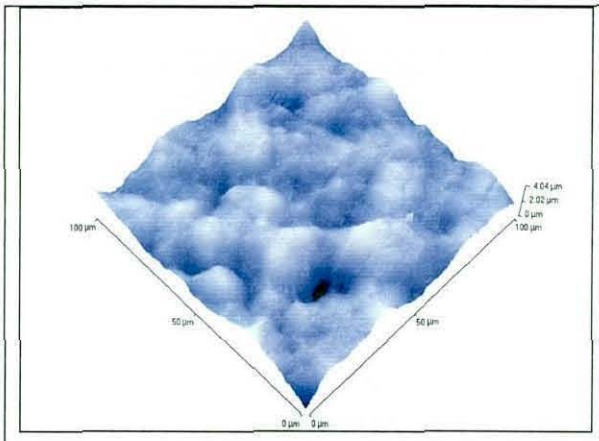

Figure 190. AFM Topographic 3D image for Apticote 450. Area 100x100 micrometres.

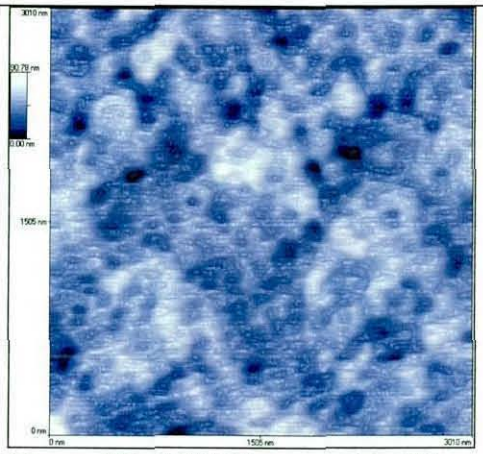

Figure 191.AFM Topographic 2D image for Apticote 450.Area 3x3 micrometres.

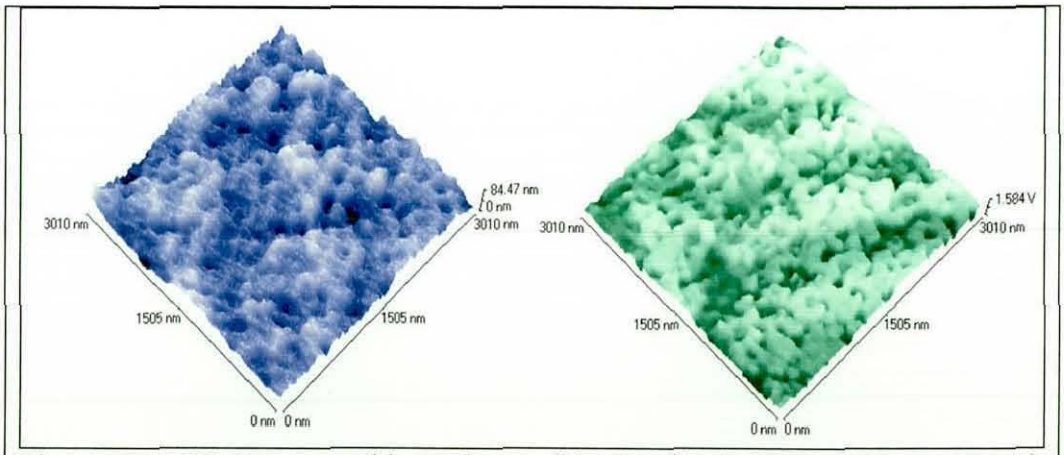

Figure 192. AFM Topographic 3D image (blue) and pull-off force image (green) for Apticote 450. Area 3x3 micrometres.

The pull-off force, as discussed previously, is a mixture of the elastic, frictional and adhesive properties of the surface [160]. The adhesion component can be separated using the AFM software and allows images showing differences in adhesion to be displayed (figures 193 and 194). The dark areas in these images represent points where the adhesion is low and conversely the bright areas are those where the adhesion is greatest. The scale of the dark areas in figures 193 and 194 suggest a correlation exists between these and the dispersed PTFE particles in the Apticote 450 coating as shown using SEM (figure 79).

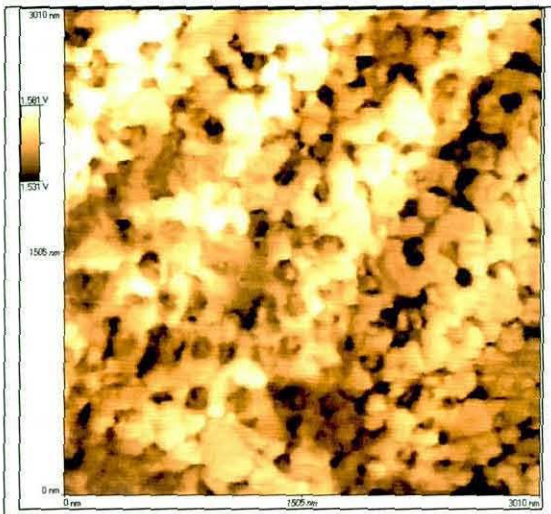

Figure 193. AFM Adhesion image for Apticote 450. Area 3x3 micrometres.

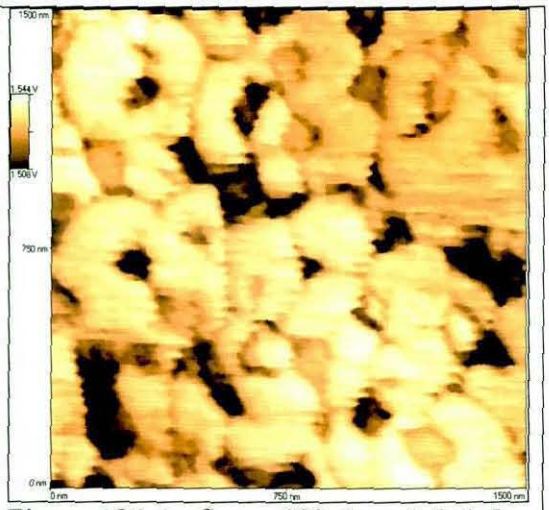

Figure 194.As figure 193.Area 1.5x1.5 micrometres.

Four different surfaces were compared using AFM and the pull-off force data is presented in figure 195.

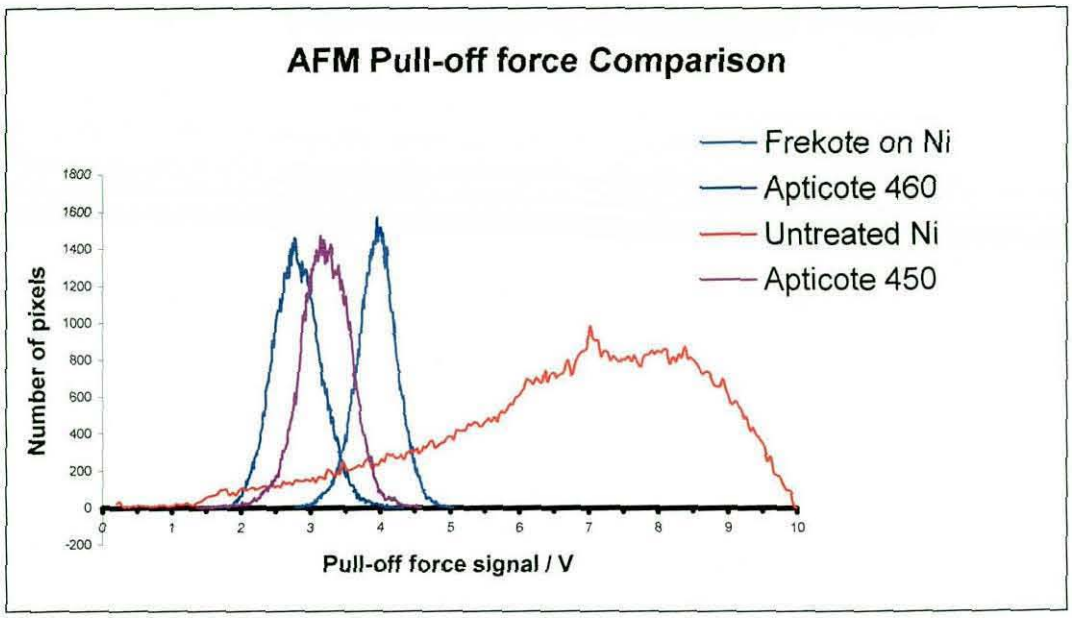

Figure 195. AFM pull-off force comparison for different surfaces.

The data in figure 195 shows clear differences between the adhesive nature of both Frekote and Apticote coatings relative to the control sample comprising an untreated sample of abrasively cleaned nickel tooling. The data suggests that the Apticote coatings are least as good as the Frekote treated surfaces allowing for the closeness between the peak distributions.

6.3.6 Summary

The requirements of mould users in the aerospace industry are such that few coatings will be as widely applicable as Frekote, not least because it can be easily applied from an aerosol spray and this allows surfaces to be touched up easily as and when required.

Sintered fluoropolymer coatings based on PTFE perform well in food industry applications but do not perform as well when subjected to crosslinking epoxide adhesives cured against their surfaces at elevated temperatures and pressures.
Apticote coatings in contrast offer good release properties and are tough enough to withstand the aggressive moulding conditions prevalent in the aerospace industry. They may find application in niche areas in the fabrication of composite products that currently use existing solvent based chemicals as mould releases.

Chapter 7. General Discussion

7.1.Mould cleaning procedures

This first part of this thesis has considered the use of several procedures for cleaning metal and composite tooling that are used in the aerospace industry. Throughout the experimental investigation an emphasis has been placed on evaluating the merits of the different procedures by appraisal of the surfaces of treated substrates using a broad range of analytical techniques. The link between substrate cleanliness and the effective performance of a semi-permanent mould release agent is very important since such mould releases must adhere strongly to a substrate if they are perform well for many moulding cycles.

7.1.1. Laser cleaning

A significant finding of the present work was the importance of thermomechanical effects that contribute to efficient laser removal of bonded epoxide resin at low energy densities.

The pure epoxide resin will absorb the laser energy relatively weakly but this energy will be strongly absorbed in the electromagnetic skin layer of the metal (5 – 10 nm) causing it to heat up and this surface heating will be influenced by the thermal time constants of metals for very short duration pulses (section 2.2.3.2).

The heated skin layer will expand rapidly along the plane of the interface creating a shear stress between itself and the epoxide resin layer bonded to it. The expansion will also exert a powerful compressive force directed into the bulk of the substrate and the rapidity of the event will thus generate a compressive shockwave that will propagate through the thickness of the tooling plate and be reflected back from the non-contaminated face. This reflected wave will in turn generate a tensile force within the epoxide contaminant layer of sufficient magnitude to completely detach it from the metal surface at the interface (figure 109, section 5.2.3.3).

If the laser fluence is increased, a level will be reached when any surface material, even one that weakly absorbs at a given wavelength, will be heated sufficiently to

melt or vaporise. In the case of very short duration, high power laser pulses these effects can be so rapid that the surface layer is effectively detonated explosively, ejecting material at high velocities. The resulting recoil force exerted by this material, and from any expanding plasma of vaporised material, will also generate a powerful ultrasonic shockwave in the substrate. Two energy regimes are thus identified as capable of generating powerful debonding forces which assist in coating removal through the absorption of high power laser pulses of very short duration. This absorption is dependent on many variables but particularly on the wavelength of the laser radiation, as described in this thesis.

Significant heating effects can also be observed at sub-plasma fluences, as reported by Cottam[49] and these are influenced by the absorptive and reflective properties of any surface contamination and substrate as discussed in detail in section 2.2.3.1.
The experimental results for TEA CO_2 and Nd:YAG lasers will now be interpreted.

7.1.1.1. Laser cleaning using TEA CO_2 laser (output wavelength 10600nm).

These lasers are currently used to remove thick paint layers (typically > 500 micrometres) on aircraft. Typical paint formulations comprise of inorganic pigments and fillers dispersed in a resin binding matrix. Pure epoxide resin absorbs the far infrared output wavelength from this laser such that the reported optical penetration depth is in the order of 100 micrometres and is thus a relatively weak absorber. However, inorganic pigments in the paint absorb the radiation much more strongly and this absorption at many sites within the resin binder initiates a pyrolysis reaction. In an air atmosphere this will lead to the formation of carbon char that will further enhance absorption, and the gas pressure resulting from the pyrolysis will fragment and crack the surrounding resin matrix and assist in breakdown of the contaminant layer under the action of the laser pulse. Absorption of laser radiation is thus efficient for thick layers of pigmented paint and gives rise to combustion conditions such that a few laser pulses are usually sufficient to ablate paint layers or, as observed in the present work, to ablate a 150 micrometre thickness of pigmented resin sheet (figure 83 section 5.2.1). The energy density in the beam from a commercial 2kW TEA CO_2 laser is such that thermal vaporisation will also occur. Paint stripping of thick layers of paint from aircraft can thus be achieved at impressive removal rates.

For an epoxide resin contaminant thickness less than 100 micrometres and where there is little or no inorganic pigmentation present, absorption of the laser radiation is much weaker such that repeated laser pulses are required to achieve a significant removal and where the poor spatial homogeneity of the laser beam becomes significant (figure 84 section 5.2.1). However, despite the use of repeated pulses to remove such weakly absorbing layers, the high reflectivity of metal substrates for far infrared radiation results in no observable microstructural changes to the metal or changes in its surface roughness (figure 85 section 5.2.2).

If the fluence is increased then although the resin is a weak absorber, the energy density in the radiation is such that thermal vaporisation becomes the dominant ablation mechanism and the results obtained (figures 87 and 93 section 5.2.3) show that the laser can effectively clean epoxide resin. Whilst most of the contamination is removed, remaining residues are detectable by electron microscopy (figure 90 section 5.2.3) and contribute to a significantly higher surface energy than might be expected.

The presence of a thick oxide layer on a metal substrate, however, significantly changes the absorption characteristics for 10600nm radiation. The effect of this combined with the lower thermal conductivity and diffusivity of the oxide layer causes significant surface heating. The experimental results obtained support this conclusion (figure 97, section 5.2.3.2). A plausible explanation of the features shown in the latter figure is that significant absorption occurred for this sample within the thickness of the epoxide resin resulting in vaporisation of material. The poor thermal properties of the oxide prevented any dissipation of the heat and energy re-radiated from the plasma, momentarily confined above the surface, resulted in melting of the surface layer of the oxide. Gases present in the porous oxide would then have migrated through the melt zone to the surface and burst. Once the vaporised material dissipated, the surface would rapidly cool and surfaces stresses concentrated at the frozen gas bubbles would cause localised surface fractures radiating between the microporosities, as seen in figure 97. The scale of these effects is small such that they can only be seen using an electron microscope. Consequently the effects are below the resolution of profilometry techniques and no significant difference in surface roughness is detected from the untreated oxide surface. Resin residues as depicted in figure 90 (for the case of cleaned nickel tooling) were not seen on the mild steel

sample and it is conjectured that the different absorption properties of the oxide present on the surface of the steel, combined with the fluence used, created greater vaporisation temperatures that completely removed all the resin. Similar effects to those shown in figure 97 were not observed for Nd:YAG lasers and this is attributed to the fact that the wavelength for this laser is an order of magnitude lower at 1064nm and it is concluded that oxides are not as strongly absorbing at this lower wavelength.

In the case of the industrially-sourced contamination on nickel tooling from Bombardier, this is seen to be very thin and possesses a discontinuous texture (figures 63 and 64 section 5.1.1.4.1), and its reflection and absorption properties are very different from the homogeneous model resin contamination used to assess laser cleaning. This disparity has complicated evaluation of cleaning procedures generally but was unavoidable for the reasons given in Chapter 1. Experiments show that repeated pulses at moderately high fluences were required to remove this material using a TEA CO_2 laser and that the cleaning efficiency was not very great on account of the very small thickness of material. No damage to the substrate was apparent (figure 85 section 5.2.2).

When a TEA CO_2 laser is focussed at typical cleaning fluences ($0.5 - 2.0\ J.cm^{-2}$) on a piece of virgin carbon fibre reinforced composite tooling, it is observed that absorption is greatest in the carbon fibres that lie just below the resin rich surface. The resin at this level usually is discoloured as the carbon fibres fracture and the fracture energy dissipates in the surrounding resin matrix, creating multiple fractures. These scatter incident light differently to the untreated composite and give rise to perceivable damage. As more pulses are applied the resin rich surface layer is disrupted and the carbon fibres are exposed (figures 117 –120 section 5.3.2.1). This exposure of the fibres increases the surface roughness by two orders of magnitude over that of the untreated surface. When the virgin composite is coated with a model epoxide resin at a thickness of approximately 150 micrometres, this is greater than the optical penetration depth of this material for 10600nm radiation and so the laser energy is absorbed below this depth but continues to extend within the bulk of the composite with repeated pulses. The overall effect is usually exposure of the carbon fibres as before. Laser cleaning is thus destructive.

With hindsight the model resin system applied to composite tooling fails as a realistic contamination since resin flash contamination on real used composite tooling would be overlaid upon residues of silicone based mould release agents at the surface (figure 68, section 5.1.1.4.2). This system could not be reproduced in the laboratory because of the low surface energy of the mould release residues that prevented adhesion of a subsequently applied resin layer of uniform thickness.

The literature cites examples of successful applications of TEA CO_2 lasers for paint stripping from composite structures. It is the author's view that this can only be achieved using a technique such as LIBS (section 5.3.1) that allows continuous spectroscopic analysis of the molecular fragments of the ablated contamination. This must slow the cleaning process appreciably. In the aforementioned case of removing of epoxide resin flash from used composite tooling, the different chemical composition of mould residues underlying the contamination would allow easy differentiation of the contamination from the composite substrate despite their similarity in composition of the latter materials. Thus the laser cleaning could be controlled precisely and the technique would not damage the tooling.

TEA CO_2 laser cleaning solutions are usually bespoke and designed around specific high technology applications with the consequence that cleaning systems are currently very expensive in terms of hardware and total running costs.

7.1.1.2 Laser cleaning using Nd:YAG laser (output wavelength 1064nm).

The application of Nd:YAG laser cleaning for the removal of epoxide resin is dominated by the optical penetration of the radiation in this material which has been reported as several millimetres. The model resin contaminant is thus virtually transparent at typical cleaning fluences. Where the resin coats a metal substrate, removal of the coating was found to be very good due to thermomechanical ablation as previously described in section 7.1.1.1. Further the detachment of resin by this mechanism leaves no residue behind and the surface is very clean as determined using AES. The same mechanism ejects resinous particulate contamination such as that found on the nickel tooling received from Bombardier (figure 100, section 5.2.4.1) but here lack of efficient extraction of the ablated material can cause it to redeposit back

onto the surface. Highly efficient extraction is required for all laser cleaning. In the case of composite tooling, only the carbon fibres absorb the laser energy and these fracture (figure 126 section 5.3.2.2) and give rise to similar effects as discussed for TEA CO_2 laser cleaning. Shockwaves can be generated with both types of laser that can cause fragments of the fractured resin above the fibres to be blown off exposing the fibres (figure 125 section 5.3.2.2). Only if the fluence is increased near to or at the level where plasma formation occurs (figure 47, section 4.3.2) will the resin absorb sufficient energy to degrade. Overall the net effect is still one of destructive cleaning since the carbon fibre reinforcement is attacked and fibres exposed on the laser cleaned surface.

Commercial Nd:YAG laser cleaning systems are already available and are reasonably priced, offering affordable solutions for industrial applications. Such systems are very flexible because the laser energy can be transmitted to the work piece using optical glass fibre technology thus avoiding the need for expensive robotics, and working units are compact making them ideal for industry (figure 196).

Figure 196. Commercial Nd:YAG laser cleaning system.

Their disadvantage, compared to a TEA CO_2 laser system, is that cleaning is slower where ablation by vaporization processes are involved, since the peak power per pulse is lower for Nd:YAG lasers, and the operating lower wavelength of the laser is less efficient in coupling to the absorption properties of a contaminant layer of comparable thickness. However Nd:YAG laser ablation using shockwaves has been demonstrated

to be very effective and may be a better method of producing clean substrate surfaces under certain circumstances.

Experimentally, determining the best set of laser operating parameters for ablation of contaminant coatings on metal substrates is dependent on knowledge of the absorption characteristics and texture of the materials to be irradiated, both of the contaminant and underlying substrate. Metal oxides have different absorption properties from the parent metals and these may be attacked by laser radiation even in cases where an organic coating over the oxide does not appear to interact with the laser. A secondary effect may occur where the oxide acts as a weak boundary layer and fails cohesively aiding the removal of the overlying contaminant layer.

Cleaning parameters are generally much more controllable using solid state lasers and the direction of the present research has been biased towards studying the effects of Nd:YAG lasers on different substrates. There is some evidence that a tiny amount of thermal damage to the substrate occurs with cleaning using Nd:YAG lasers (figure 110 section 5.2.3.3). Such damage is insignificant in comparison to existing abrasive cleaning methods used by Bombardier (figure 61 section 5.1.1.4.1). The effects very likely reflect non-optimised processing conditions with the target being too close to the laser source or the laser beam not being sufficiently defocused.

7.1.2. Dry ice blasting

The experimental evaluation presented in section 5.4.3 shows that this cleaning procedure is effective at removing resin that is cured onto metal tooling. The resin is removed without any detrimental effect to the substrate at blasting pressures up to 10 bar (101MPa).

The apparent failure of the procedure to clean composite samples without substrate damage (except at very low pressures) occurs for the same reasons as discussed in section 7.1.1 above, i.e., that there is no appreciable discontinuity of properties at the interface between the resin contaminant and the composite substrate. Again the model RTM6 resin contaminant cured onto virgin composite is a very severe test and in reality mould release present at the interface would greatly assist this cleaning procedure. Thermal differentials, discussed in section 2.4.1, associated with this low

temperature process would embrittle and dislodge resin flash and act in an analogous role to thermomechanical cleaning invoked by laser ablation.

It is believed that dry ice blasting offers an acceptable means of cleaning composite and metal tooling but suffers from the practical disadvantage that the tool that is cleaned becomes very cold and moisture from the surrounding air condenses as ice onto the surface. This has to be removed by heating for industrial tooling and this adds additional cost to the process and can be detrimental to metal tooling which may rust quickly when cleaned.

7.1.3. Sodium hydride cleaning

This procedure is very effective at removing any organic or inorganic contamination from a metal surface and results in a very clean surface. Because it is a high temperature process it cannot be used to clean composite tooling. The most obvious disadvantage of the procedure is that it cannot be applied on site and aerospace tooling would have to be shipped to a treatment works. The process uses hazardous materials and can only accommodate tooling of moderate dimensions. Another disadvantage is that freshly cleaned parts must be pressure washed with water jets to remove reduced organic material. Unless rapid and thorough drying can follow this post cleaning operation immediately, there is a high probability that steel tooling would rust. Consequently this restricts the practical application to non-ferrous metal tooling such as nickel. There may exist a niche application for this procedure where a complex shaped non-ferrous tool needs to be cleaned.

7.1.4 Summary

Of the three cleaning procedures investigated, the advantages of laser cleaning appear to outweigh its disadvantages. The literature suggests it can be successfully applied to composite tooling though with this latter substrate, dry ice blasting comes a close second as an acceptable cleaning procedure. The sodium hydride cleaning procedure is novel and very effective but limited to metal tooling and cannot be used on site in the aerospace industry.

7.2. Alternative mould release coatings

The second part of this thesis considered some aspects of the chemistry and physics of non-stick coatings and the role of polydimethylsiloxane in some mould release agents that are widely used in the aerospace industry. Following a detailed literature survey several coatings capable of producing a low surface energy were identified and investigated, with a view to evaluating their performance under similar conditions of use to existing mould release agents used in the aerospace industry. As a consequence of this study the essential properties of a successful mould release agent have been identified and one commercial coating found that offers good release properties has been found and evaluated.

7.2.1. Fluoroalkylsilane coatings

With hindsight it was naïve to suppose that simply engineering a low energy surface would be sufficient to give good release properties. If that were the case the discovery of PTFE many years ago would have solved many mould release problems. The fact that marine organisms can stick with apparent impunity to such low energy fluoropolymer surfaces is evidence that abhesion, like its counterpart adhesion, is not a simple phenomenon.

The fluoroalkylsilane compound investigated in this research has been successfully applied to enamelled surfaces to prevent the sticking of food and has also been used successfully as a water repellent coating for textiles. In both these applications high applied pressure against the coated substrate appears to be a common system variable that is absent. It is claimed that it is effective in mould release for semiconductor fabrications but in such applications only moderate moulding pressures are used. The molecular structure of fluoroalkylsilanes makes it difficult to develop a thick coating on any surface. In fact the coating thickness is usually only a few monolayers and this is assumed to conform to any substrate topography. The surface energy of the coating is lower than that of PTFE.

A water droplet applied to such a coating cured onto a rough surface will not wet the surface but instead roll off the surface if the surface is tilted. If the water droplet is applied to such a horizontal coated surface and then deformed by the application

pressure, in such a way that it is trapped on the surface, it is argued that the droplet will deform itself to the contour of the surface. It will not intimately wet the surface because the low surface energy resists this but it may well fill some of the larger irregularities on the surface. Once the pressure is released the water droplet will return to a roughly spherical bead on the surface because this shape is thermodynamically favoured. If instead of water, a drop of liquid thermosetting resin is applied to the coated surface and deformed by pressure, this will behave similarly to the water droplet. However if the system is now heated so that the deformed resin crosslinks and hardens, then it will still grip the surface once the pressure is released. In essence this corresponds to mechanical interlocking which is one mechanism believed to be responsible for adhesion.

The above scenario is presented as a plausible explanation of the observed facts that despite engineering a low energy surface, liquid resin applied to such a fluoroalkylsilane coated surface and cured by heat, whilst being vigorously pressed against the surface as, for example, under autoclave conditions, results in apparent adhesion. It is unlikely, however, that this simplistic explanation fully explains the observation. It is implied that the resin whilst still liquid would fill an "ink pot" shaped micro-porosity in the surface in such a manner as to provide a mechanical keying point once the resin set. No evidence has been found to show the extent of pore penetration as a function of applied pressure to support this argument. Microscopic evidence of mechanical interlocking has been presented in the case of fluoropolymer coatings but the extreme thinness of the fluoroalkylsilane coating makes it difficult to study by SEM. Evidence from high resolution SEM of fluoroalkylsilane treated surfaces suggest that deposition conditions may be critical to prevent aggregation of the polymer. The fine scale of aggregates (figure 148, section 6.1.2.2) may have negligible effects on surface energies calculated derived from contact angle measurements but any uncoated metal surface area would provide sites for chemical bonding of a resin under circumstances where it was pressed hard against the surface.

Comparing the behaviour of fluoroalkylsilane coatings against Frekote, the commercially successful PDMS based mould release agent, evidence has been presented to show that Frekote largely satisfies the criteria required for a non-stick coating (outlined in section 3.9).

Frekote provides: -

- a low surface energy
- thermal stability (and chemically inertness)
- durability and will last for at least twenty releases
- mobility at a molecular level, associated with low glass transition temperature
- a coating that will cover and fill major surface irregularities resulting from abrasive finishing.
- a coating that creates weak boundary layers assisting the separation of a moulded part.

These properties derive from the formulation of Frekote developed over many years and it is the combination of these properties that renders it such a useful product.

For rough surfaces such as industrially sourced metal substrates, although several coatings of mould sealing agent and mould release agent are applied, these do not necessarily fill in all the rough contours and irregularities on the surface. Grit-blasted metal surfaces for example, that have been treated with Frekote can still feel slightly rough and it may be that a degree of roughness assists separation of a moulding since this will trap air pockets. On rough surfaces, thin layers of Frekote are easily parted and SEM shows the presence of irregularly shaped platelets overlying surface asperities arising from the grit blasting treatment. These must act are weak boundary layers and assist in mould release.

The Dynasylan fluoroalkylsilane product evaluated in the present work satisfies the first two criteria and is also durable but it does satisfy the last two requirements and it appears that these are important. It cannot be coincidental that other rival products to Frekote all use a compatible sealing compounds explicitly designed to fill in surface micro-porosties and this seems to be a crucial factor. Fluoroakylsilanes such as Dynasylan , by virtue of their chemistry, cannot be deposited as thick coatings and this appears to make them unsuitable as mould release agents when used on their own to modify a surface. Commercial products providing non-stick coatings with very low surface energy have found application in low temperature environments where ice

build up is a problem. Such ice repellent coatings combine the properties of fluoropolymers (fluoropolyurethane and PTFE) with both fluoroalkylsilane and PDMS.

7.2.2. Fluoropolymer coatings

It has been shown that sintered fluoropolymer coatings containing a high proportion of PTFE, whilst effective as non-stick coatings for bakeware applications, do not apparently function well under the rigours of temperature and high pressure that are utilized in the present application. High pressure applied to a mobile adhesive in conjunction with moderately high temperatures commensurate with curing appears to open up the micro porosities present in the PTFE structure and when the resin crosslinks and sets, a degree of mechanical interlocking has occurred which makes it difficult to separate the resin from the coating.

7.2.3 Electroless Ni/PTFE composite coating

In the case of the Apticote 450 release coatings, very tiny PTFE particles are uniformly dispersed in a strong nickel matrix that resists the application of pressure applied to a curing resin system. The porosities present in a PTFE film of continuous coating are not manifest in the ~200nm diameter PTFE particle phase present in the Apticote 450 coating. Thus the coating combines a low surface energy, derived from the PTFE, with the toughness of a nickel matrix and it is conjectured that these qualities account for its apparent success as a release coating as demonstrated in the present work. The FM300 resin system used for these tests is the same resin system used by Bombardier Aerospace and therefore the results are very relevant to the proposed industrial application. The ease of release of cured FM300 resin from repeated application and curing of the resin on the same area of coating was assessed and five test applications were made. The resin removed easily from the substrate and in this sense performed equally as well as the PDMS based Frekote mould release agent. The results from the AFM pull-off force measurements concur with this finding (figure 195). The Frekote coating does however have the advantage that it is applied as a spray coating and coatings can be easily and quickly repaired on site in an industrial application. This advantage is not available for the Apticote 450 coating, which has to be applied off-site, and this might limit its usefulness to small moulds

that can be easily shipped for coating repair. Another advantage of Frekote is that it can be applied to composite moulds whilst the Apticote 450 process can only be applied to metals at present.

Taken collectively the results of the evaluations of different potential mould release coatings show that the problems associated with achieving a successful mould release are not simply restricted to engineering a low energy surface. This is only one of several desirable properties and the success of commercial products such as Frekote testify to the fact that considerable formulation expertise is required to achieve these optimum properties. The present work has highlighted these difficulties and attempted to explain the observations recorded. The study has concluded with an example of a commercially available coating (Apticite 450) that rivals the performance of the Frekote and offers some potentially useful applications for aerospace mould tooling. Despite the difficulties encountered in obtaining a quantitative measure of mould release performance, the study was able to show, qualitatively, that an electroless nickel/PTFE coating offered the best compromise of properties and durability for an industrial application.

Chapter 8. Conclusions

8.1. Laser Cleaning

This research has demonstrated that a Nd:YAG laser has the potential to clean fully bonded epoxide resin contamination from metal surfaces and that this is achieved primarily through thermomechanical effects associated with concussive shockwaves reflected back from the metal surface, which cleanly detaches resinous contamination. The TEA CO_2 laser is also effective at removing resinous contamination from metal surfaces and has the capability to achieve this at impressive cleaning speeds. This type of laser ablation is dominated by thermal rather than thermomechanical processes.

Very fine scale artefacts can be associated with the TEA CO_2 laser when it interacts with thick oxide layers present on steel surfaces. Plasmas can be created during laser cleaning under certain conditions and these plasmas can be very hot. Thermal energy can be re-radiated to the surfaces below and can induce surface melting when the surface strongly absorbs the laser energy. The artefacts, comprising porosities created at the oxide surface, are believed to arise from the migration of gases absorbed into the bulk oxide layer which are released when the oxide melts under the plasma layer. In contrast, cleaning of metal surfaces using Nd:YAG lasers does not produce any similar artefacts even when a thick oxide is present, though at high magnifications some slight thermal damage is apparent on bright, cleaned surfaces.

Laser cleaning of resinous contamination from composite tooling is difficult using either Nd:YAG or TEA CO_2 laser technology. This is because the absorption properties of the matrix match so closely those of typical resinous contamination, which leads to significant substrate damage with carbon fibres being exposed in the matrix of the composite tooling following laser cleaning. Monitoring of this process by the technique of laser induced breakdown Spectroscopy has been discussed and is one method which might successfully enable such composite tooling to be cleaned by lasers though this might reduce cleaning speeds considerably.

The most cost effective overall laser cleaning technology utilises Nd:YAG lasers. The cost saving arising from using this technology over a bespoke TEA CO_2 laser system

is significant despite the fact that these lasers can remove contamination at impressive cleaning rates . The cost saving achieved using Nd:YAG lasers is made at the expense of cleaning speed although the solid state technology is more reliable for an industrial application and this is another factor that has to be considered.

8.2. Dry ice blasting

This is an effective method of cleaning resinous contamination from metal tooling surfaces, as has been demonstrated. One disadvantage is that the tooling becomes very cold in the process and this causes condensation of moisture from the atmosphere onto the treated surface. For an industrial process environment, this would require post cleaning treatment to dry the tooling thoroughly before use and this would incur extra costs.

Dry ice blasting for the removal of contamination from composite tooling would be an effective cleaning technology provided a physical discontinuity such as a weak boundary layer existed on the surface due to degraded mould release residues. Such residues would be expected on used composite tooling. In cases where resinous contamination has adhered to virgin tooling, dry ice blasting cannot differentiate easily between the physical properties of the resin contamination and the resin component in the tooling with the result that the tooling surface is damaged.

8.3. Sodium hydride cleaning

This technology can only be used on metal tooling and is best suited to non-ferrous metals. It can clean complex shapes very thoroughly provided these can be lowered into a treatment bath. As such its application is restricted to modest sized tooling. As it is a high temperature process it cannot b used for cleaning composite tooling.

8.4.Mould Release Coatings

Bombardier currently use Frekote mould release agent which is available as an aerosol spray. It is based on PDMS and is a semi permanent release agent. It is extremely effective as such, and, when used in conjunction with a chemically compatible sealant, it can be applied to clean metal tooling and allows many moulding

cycles to be completed before any mould fouling problems are experienced. It has proved difficult to find an alternative release that is as effective and offers the same versatility as Frekote.

8.4.1 Fluoroalkylsilane coatings

The work presented in this thesis suggests that careful preparation of these coatings is required to ensure to optimise their properties. They produce very thin coatings which conform any existing surface topography. As such, whilst they provide a low energy surface, they do not seal any surface porosities present on a substrate and adhesion through mechanical interlocking can occur without any significant impediment. Whilst there are undoubtedly some specialised applications of these materials, especially in the microelectronics industry, it is considered that they are not suitable for the proposed industrial application in an aggressive environment.

8.4.2 Fluoropolymer coatings

The commercial formulations investigated in this thesis were PTFE based and produced low energy coatings on metal substrates which were claimed to provide good release properties for applications such as bakeware.
Two examples of these coatings were evaluated for use with metal tooling materials. It was found that when adhesive contaminants were cured under elevated pressure and temperature whilst in contact with the coatings, subsequent release was poor or impossible. It is conjectured that the porosities present in PTFE surfaces allow penetration of the resin and, after curing, these bond by partial mechanical interlocking. The formulations were considered not to be suitable mould release coatings for the intended application.

8.4.3. Electroless Ni/PTFE composite coatings.

These specialised coatings have been evaluated. They can only be applied to metal tooling and produce a hard coating comprising a nickel phosphorus matrix containing a very fine dispersion of PTFE particles. The nickel matrix is robust and hard and is considered suitable for industrial applications, and the low friction coefficient and low

surface energy of the embedded PTFE particles ensure an efficient mould release. The electroless coating is thick enough to completely fill any substrate porosities. In conclusion these coatings provide the best mould release found in this research that satisfies the particular requirements for tooling used by Bombardier.

Chapter 9. Further Work

The present study has covered two relatively broad subject areas to address the original aims of the project discussed in Chapter 1. The research content has been strongly influenced by the need to identify cost effective solutions that are robust enough for industrial applications.

8.1 Cleaning technologies

Laser generated shockwaves have been shown to possess the potential to clean fully cured epoxide resin from a metal substrate at relatively low fluences that do not damage the substrate itself. This enables modestly priced laser technology to be used to implement an efficient cleaning process that is environmentally benign. It would be useful to be able to specify the laser operating conditions conducive to industrial scale cleaning requirements and to be able to determine cleaning rates over large substrate areas. This would require close liaison between a chosen laser manufacturer and an industrial partner. Such a collaboration would demonstrate the viability of this method of laser cleaning over the predominantly photothermal cleaning afforded by more powerful but expensive carbon dioxide gas lasers.

This research has highlighted the importance of having realistic examples, covering the full range of contaminants, that such a cleaning technology is expected to remove. The presence of thick oxide layers on surrogate substrates generates artefacts arising from laser cleaning that would probably not be encountered on real aerospace tooling. Given an appropriate range of samples, it would be useful to measure the amount of material removed per laser pulse (possibly using a sensitive mass balance) and try to optimise the laser operating variables to achieve the greatest cleaning rate. The influence of thin oxide layers on common metals in relation to laser cleaning would also be a useful extension of the work.

In respect of composite tooling, the presence of partially degraded mould release on the surface of used tooling provides a surface discontinuity (both chemical and physical) would provides a means of controlling either laser ablation or dry ice

blasting. There is considerable scope to investigate how laser induced breakdown spectroscopy can be employed to limit substrate damage in laser cleaning. The scope of the present work has limited the time available to adequately address the problems of composite cleaning. The solvent properties of carbon dioxide for typical aerospace tooling contaminants is another area that could be investigated in relation to dry ice cleaning.

8.2.Mould Releases

This research has highlighted some of the properties of these materials that make commercial products successful. The research has described the problems encountered when seeking to find alternative release coatings and has been successful in identifying electroless nickel/PTFE coatings as being a durable and effective for mould release applications in industry. There is a real need to obtain quantitative measurements of mould release efficiency and the two mechanical test methods reported in this research have proved inadequate in providing this data. The testing geometry is critical and since mould release forces are small, especially in laboratory sized apparatus, a sensitive method is sought.

The real need in the aerospace industry is to find a solvent based replacement for Frekote that is environmentally benign. Insufficient time has been devoted to studying the properties of water soluble semi-permanent mould release formulations and this is an obvious area where further work could be done. This work would be most productive if organised as a collaborative project with an existing mould release manufacturer since any student working alone is disadvantaged by the scarcity of useful information published in the area.

References

[1].Phipps.C. Laser applications overview:The state of the art and the future trend in the United States. RIKEN Review No.50 (January 2003):Focussed on Laser Precision Microfabrication (LPM 2002)

[2].Asmus J.F. Studies in the interaction of laser radiation with art and artefacts..Proceeedings of SPIE 41,(1973),p19-27.

[3].Asmus, J.F. Light Cleaning – Laser Technology for Surface Preparation in the Arts. Technology and Conservation 13,14 (1978).

[4].Asmus, J.F More Light for Art Conservation. IEEE Circuits and Devices Magazine.March,6-15 (1986)

[5].Asmus, J.F Light for Art Conservation. Interdisciplinary Science Reviews 12,171 (1987).

[6].Cooper.M. Laser Cleaning in Conservation. Butterworth Heinemann 1998.

[7] Agapaki.P. (1994). Physical Aspects of Conservation. M.Phil.Thesis. Loughborough University.

[8].Lu,Y.F., Song,W.D., Ye,K.D., Hong,M.H., Lui,D.M., Chan,D.S.H., Removal of submicron particles from nickel phosphorus surfaces by pulsed laser radiation', Applied Surface Science,120(3-4),(1997),317-322.

[9].Bewley,D., Spotless with lasers, New Scientist.(5th July 1997),20-21

[10]Luk'yanchuk.B.(Editor). Laser Cleaning. World Scientific.2002

[11] Manz C. and Zafiropulos V. Laser ablation strips thin layers of paint. Opto and Laser Europe. 1997 Pt 45 pp27-30

[12].Schulz O.G., SLCR Laser Paint Stripping Process – Process Qualification Based on SAE A4872. 2001 Aerospace Coatings Removal and Coatings Conference.San Antonio Texas USA May 22-24th 2001.

[13].A.Tsunemi, A.Endo and D.Ichishima. Paint Removal from Aluminium and Composite Substrate of Aircraft by Laser Ablation Using TEA CO Lasers SPIE Conference on High Power Laser Ablation. Santa Fe, New Mexico April 1998

[14].Schweizer G.;Werner L. Industrial 2KW CO2 laser for paint stripping of aircraft. Proc.SPIE Vol 2502 pp57-62 Published 9/1995

[15].Walters C.T, Dulaney J.L and Campbell B.E. Advanced Technology Cleaning Methods for High-Precision Cleaning of Guidance System Components .
Battelle Memorial Institute, Columbus Ohio. Report prepared for Department of the Air Force, Aerospace Guidance and Metrology Centre, Newark Ohio on September 1993.

[16].Patel J.N., The Use of Nd:YAG LASER as a Complimentary Tool for Removing Paint From Aircraft Structures. 2001 Aerospace Coatings Removal and Coatings Conference.San Antonio Texas USA May 22-24th 2001.

[17].Slife R., The Use of FlashJet for Stripping Ramomes and Composites at Warner Robins Air Logistic Center. 2001 Aerospace Coatings Removal and Coatings Conference.San Antonio Texas USA May 22-24th 2001.

[18].Engelsberg A.C., Laser Assisted Cleaning of Contaminated Surfaces, Flammability and Sensitivity of Materials in Oxygen-Enriched Atmpsheres:7th Volume,ASTM STP 1267, Dwight D Janoff, William T Royals and Mohan V.Gunaji, Eds. American Society for Testing and Materials, Philadelphia 1995.

[19].Zafiropulos V. Laser-assisted removal of paint from composite materials in Laser Cleaning Edited by B.S.Luk'yanchuk.World Scientific .2002

[20].Pantelakis Sp.G.,.Despotopoulos Al.Ch,.Lentzos G.An and.Kermanidis Th.B Influence of the laser paint stripping process on the mechanical behaviour of fibre reinforced composites by.Advanced Materials and Processes – 4th European Conference –Padua. Sept 1995 pp345-348

[21]Stratoudaki. T;Edwards C.;Dixon.S;Palmer S.B.Advances in Laser Based Ultrasound in Carbon Fibre Reinforced Composites For Aircraft Inspection.NDT.net February 2003, Vol 8 No.2. Paper presented at the 8th ECNDT, Barcelona, Hune 2002.

[22].Scruby C.B, Drain L.E. Laser Ultrasonics. Adam Hilger 1990

[23].Srinivasan R. Interaction of Laser Radiation with Organic Polymers. Chapter 5 in Laser Ablation: Principles & Applications Edired by John C. Miller. Springer-Verlag 1994.

[24].Buchter.E. Mould Cleaning with Laser Radiation . Kunstoffe Plast Europe Vol 89 (1999) 11.

[25].Durrani M. Lasers clear leaves on the line. .Physics in Action. May 2002.

[26].Watkins K.G. Mechanisms of Laser Cleaning .Proceedings of SPIE Vol3888 pp165-174 (2000).

[27].Stein W.M. Laser Material Processing. Springer, London 1998. p60.

[28] Aden M, Beyer E and Herziger G. Laser-induced vaporisation of metal as a Riemann Problem. J.Appl Phy D23 (1990) pp655-661

[29].Knight C. Theoretical Modelling of Rapid Vaporisation with Back Pressure. AIAA Journal 17 (1979) pp519-523.

[30] Chan C.L. and Mazumder J. One-dimensional steady state model for damage by vaporisation and liquid expulsion due to laser-material interaction.J Applied Physics 62 (1987) pp4579-4596.

[31] Phipps C.R., Turner T.P, Harrison R.F, York G.W., Osbourne W Z, Anderson G.K., Corlisd X.F., Hayes L.C., Steele H.S and Spiochi K.C. Impulse Coupling to Tagets in Vacuum by KrF, HF and CO_2 Single-pulse Lasers. J. Applied Physics 64 (1988) pp1083-1096.

[32] Bleaney. B.I. and Bleaney. B Electricity and Magnetism. 3rd End. Oxford University Press.1989.

[33].Wilson J., Hawkes J.F.B. Lasers:Principles and Applications.Prentice Hall.1987

[34].Kaye & Laby. Tables of Physical and Chemical Constants.16th Edn.Longman 1985

[35].Prokorov A.M.,Konov V.I.,Milailescu I.N., Laser heating of metals. Adam Hilger Series on Optics and Optoelectronics, Bristol,(1990),30-35.

[36].Roberts E. National Laser Centre of South Africa. Private Communication

[37].Carslaw H.S., Jaeger J. Conduction of Heat in Solids. Oxford University Press 1959.

[38].Zhou X.,Imasaki K., Furukawa H, Umino H *et al.* Simulation study and experiment on laser-ablation surface cleaning . Optics & Laser Technology 33 (2001) 189-194

[39].Autric M. Thermomechanical effects in Laser-Matter Interaction. SPIE Conference on High-Power Laser Ablation. Santa Fe. New Mexico.1998.Vol.3343.

[40].Obata M., Sano Y, Mukai N., Yoda M., Shima S., Kanno M.. Effect of Laser Peening on Residual Stress and Stress Corrosion Cracking For Type 304 Stainless Steel.The 7th International Conference on Shot Peening. 1999. p387-394

[41].Gupta. V, Yuan.J, Pronin. A. Recent developments in the laser spallation technique to measure the interface strength and its relationship to interface toughness with applications to metal/ceramic, ceramic/ceramic and ceramic/polymer interfaces. In Adhesion Measurement of Films and Coatings.pp 367-401, K.L.Mittal(Ed.) .Published VSP 1995.

[42] Israelachvili. Ya., Intermolecular and Surface Forces, 2nd.Ed.Academic Press 1991.

[43] Tam A.C., Leung W.P., Zapka W. and Ziemlich W.,' Laser-cleaning Techniques for Removal of Surface Particulates', Journal of Applied Physics, Volume 71 (7) 1 April 1992, pp 3515 – 3523

[44].Lee J.M., Watkins K.G. Laser removal of oxides and particles from copper surfaces for microelectronic fabrication. Optics Express 68 .17th July 2000/Vol.7, No.2.

[45].Stokes.R.J., Fennell Evans.D., Fundamentals of Interfacial Engineering. Wiley-vch.1996.

[46].Hamaker.H.C. The London-Van der Waals attraction between spherical particles. PhysicaIV, No.10 pp1058-1072 (1937)

[47].Garbassi.F., Morra.M., Occhiello.E. Polymer Surfaces.Wiley.1994.

[48].Grigoropoulos C.P., Kim D. Liquid-Assisted Pulsed Laser Cleaning with Near-Infrared and Ultraviolet Pulsed Lasers. Chapter 5 in Laser Cleaning Edited by B.S.Luk'yanchuk. World Scientific .2002.

[49].Cottam C.A. TEA CO2 Laser Treatment of Coated and Corroded Metals. PhD thesis. Loughborough University .1998.

[50].Walters C.T., Campbell B.E., Hull R.J. Laser cleaning of metal surfaces Proceedings of SPIE.1998 Vol 3343 pp 859-865.

[51].Randall P., Williams D. Guide to Cleaner Technologies – Alternatives to Chlorinated Solvents for Cleaning and Degreasing. Washington,DC:US EPA, February 1994 (EPA report number EPA/625/R-93/016).

[52].Hill.L. Carbon Dioxide Cleaning: Going through Phases .CleanTech 99 International Cleaning Technology Exposition. July/August 1999. p27-34

[53].Bryan C.J, Gebert-Thompson K. Alternatives to Chlorofluorocarbon Fluids in the Cleaning of Oxygen and Aerospace Systems and Components. ASTM Publication 04-011810-31.(1993).

[54] 2002 December. Removing fouling residue from moulds in-the-press with CO2 pellet blasting. Rubber World Vol 227, no.3.

[55].Rex J. A Review of Recent Developments in Surface Preparation Methods. Journal of Protective Coatings and Linings.Oct.1990 p50-58.

[56].Spur.G., Uhlmann E., Elbing F. Dry-ice blasting for cleaning:process, optimisation and application . 9th International Conference on Erosion by Liquid and Solid Impact.Wear of Materials.ICEAWE.Cambridge, UK.13th-17th Sept 1998.pp402-411

[57].Kimura W.D. and Kim G.H. Comparison of laser and CO2 snow cleaning of astronomical mirror samples. Proceedings of SPIE.1994 Vol 2199 pp 1164-1171.

[58].McHardy J and Sawan S.P (Editors). Supercritical Fluid Cleaning Fundamentals, Technology and Applications. Noyes Publications. 1998.

[59].Deffeyes J.E., Lilenfeld H.V and Reilly J.J. Dry ice –ultra-violet light process for metal cleaning. SAMPE Journal Vol 33 No.1 Jan/Feb 1997.

[60].Rich M.J., Pschigoda. S and Lawrence T.D. Surface Cleaning of Mould Release Compounds From Metals and Non-Metallic Materials. Proc of 60th SPE Annual Technical Conf.San Francisco, CA. 5th-9th May 2002.Vol 1 pp640-644

[61].Lightfoot I.P. Reductive Destruction of Chlorinated Organics in Molten Salts. PhD Thesis 2000 De Montfort University

[62].DuPont Patent Specification Oct 16th 1942 no 14502/42 (565,567) Improvements in and relating to the Removal of Surface Impurities from metals by fused alkali baths.

[63].Kern, W., ed. Handbook of Semiconductor Wafer Cleaning Technology. Park Ridge, N.J.: Noyes Publications; 1993.

[64].Paciej R., Jansen F., Krommenhoek S. Evaluation of Plasma Cleaning, An Environmentally Friendly Process, For Removing Lubricants From Metallic Surfaces. pp124-140 in Bryan C.J, Gebert-Thompson K. 'Alternatives to Chlorofluorocarbon.

[65].Shenton M.J., Stevens G.C. Atmospheric Pressure Non-Equilibrium Plasma Processing of Polymers .1998 ICPP 25th EPS Conf.on Contrr.Fusion and Plasma Physics, Praha 29 June – 3 July. ECA Vol 22C(1998) pp2587-2590.

[66].Ward P.P. Plasma Cleaning Techniques and Future Applications in Environmentally Conscious Manufacturing. Sandia National Laboratories, Albuquerque, New Mexico.Published through auspices of US Dept of Energy Pollution Prevention Information.

[67].Pinson S.J.M., Collins J., Thompson G.E., Alexander M.R. Atmospheric Pressure Plasma Cleaning of Aluminium. Finishing. March 2002

[68].Hicks R.F.;Selwyn G S. Atmospheric-Pressure Plasma Cleaning of Contaminated Surfaces. Final Report US Department of Energy. Project No.54914.1996 –1999. (http://emsp.em.doe.gov/EMSPprojects1996_2002/ completed/54914.pdf).41 refs given.

[69].Zisman W.A.Constitutional Effects on Adhesion and Abhesion, p176 in Adhesion And Cohesion Edited by P.Weiss. Elsevier 1962

[70].Miller A., A Slippery Business. Chemistry & Industry;No.4,15th Feb 1988, p102

[71].Mould Fouling and Mould Cleaning. Rapra Published Search Number 33. October 2002

[72].Packham D.E. Mould Sticking, Fouling and Cleaning. Rapra Report 150. Vol 13, Number 6, 2002

[73].Mann J.B. Mould Release Agents: A Different View.142nd Meeting Fall 1992 Conf.Proc.Nashville.Tn.3rd-6th Nov.1992.Paper 34 pp15.012

[76].Axel F. Axel Laboratories (Mould Release Manufacturer). Private communication.

[75] R.K.Champaneria, M.Lotfipour, D.E.Packham, D.Brister and D.M.Turner Adhesion of Nitrile and Ethylene-propylene rubber to mould materials. Adhesion 12.25th Annual Conference on Adhesion and Adhesives.London 1987.

[76] Reeves L.A.and Packham D.E. Effect of compounding on the adhesion of rubber to medium carbon steel. J.Phys D:Appl.Physics,25,(1992) A14-A19.

[77] Yokoyama T. Mechanisms of Mould Fouling .International Polymer Science & Technology. 1985 Vol 12,Part 9 pp pt 40-6

[78] Yamaguchi K. and Yukawa A. Mould fouling and countermeasures. International Polymer Science & Technology, Vol 2,No.4,1994

[79].Reeves L.A., Kiroski D., Packham D.E.. Weak boundary layers in rubber moulding .Adhesion '93 – 5th Adhesion Conference Sept 1993,York pp 277-282.

[80].Comyn J., Non-stick Applications to Polymers. High Performance Plastics.1988 Vol 5 Pt 6 pp7-9.

[81] Reinforced Plastics October 1996. Wax releases: a thing of the past?

[82] Fleig P.F., Schwab S.T.,.Beauchamp W.A & Brown J. Durable Release Coatings for Polymer Composite Processing. 31st International SAMPE Technical Conference Oct.26-30,1999.

[83].Clarke C., Mergenhagen T., and Just.B. Semi-permanent release agents – theory and application .Rubberchem 2001.Proceedings of a conference held Brussels, 3rd-4th April 2001.Shawbury,Rapra Technology Ltd.,2001,Paper 15,pp4.012

[84].Utz.R, Hensel.M, and Sprenger.S. Minimal Mould Fouling – a Miracle or Know-how? .KGK Kautschuk Gummi Kunststoffe 48, Jahrgang,Nr.2/95

[85].Briscoe B.J and Panesar S.S. The effect of surface topography on the adhesion of poly(urethane)-metal contacts. J.Phys D: Appl. Phys. 25,(1992) A20-A27

[86].Blanchard. P.J. High Speed Resin Moulding of Composite Structures. PhD Thesis Nottingham University 1995.

[87].Werner.J.J., The Use of Perfluorinated Polyethers as Mould Release Agents for High Temperature Thermoset Resins. 43rd Annual Conference, Composites Institute, The Society of the Plastics Industry,Inc,February 1-5,1988.

[88].Allen K.W. Formation and failure of adhesive bonds .Surface Coatings International 2000 (1).

[89].Guthrie J.T Pretreatments and their effect on the adhesion of coatings. Surface Coatings International Part B:Coatings Transactions Vol 85,B1,1-78,March 2002.

[90].Voyutskii S.S, Autohesion and Adhesion of High Polymers. English translation Interscience 1963

[91].Vasenin R.M. RAPRA Translations 1005,1006,1010,1960,1961

[92].Venables J.D, Adhesion 7. Ed.KW Allen.Applied Science Publishers 87,1983, .J.Adhesion,39,79,1992

[93].Deryaguin B.V, Adhesion:Fundamentals and Practice.McLaren 1969

[94].Plunkett R..J., U.S.Patent 2,230,654 (February 4,1941).

[95].Roberts R.M., Serendipity:Accidental Discoveries in Science John Wiley 1989.

[96].Bradrup,J., Immergut,E.H.(1989).Physical Constants of Fluoropolymers. Polymer Handbook.3rd Edn.

[97].Drobny J.G. Technology of Fluoropolymers.CRC Press 2000

[98] Desimone J.M., Guan Z. Elsberned C.S. Science 1992,257,945.

[99].Morita,M.., Ogisu,H., Kubo.M. J.App.Polym.Sci 1999,73,1741

[100].Schmidt D.L., Coburn C.E., DeKoven B.M., Potter G.E., Meyers.G.F., Fisher.D.A. Nature 1994,368,39

[101].Takahashi,S., Kasemura,T., Asano K. Polymer 1997,38,2107

[102].Perutz. S., Wang J, Kramer E.J, Ober C.K, Ellis. K Macromolecules 1998,31,4272

[103] .Kobayashi H., Owens M.J., Trends Polym Sci 1995,3,10

[104].Blanchet G.B. Deposition of amorphous fluoropolymer thin films by laser ablation. Appl.Phys.Lett.62(5),1 February 1993

[105] Bailey. T. Step and Flash Imprint Lithography: Template Surface Treatment and Defect Analysis J. Vac. Sci. Technol. B, Vol. 18, No. 6, p. 3572.

[106].Douglas J., Resnick and David P. Mancini, Motorola Labs, Tempe, Ariz. S.V. Sreenivasan and C. Grant Willson, University of Texas, Austin, Texas -- Release Layers for Contact and Imprint Lithography Semiconductor International, 6/1/2002

[107].Scheirs J. (Ed). Modern Fluoropolymers .Wiley.1997

[108].Kipping F.S., J.Chem.Soc.,1912,101,2125

[109].Arkles B. Look what you can make out of silicones. Chemtech 13 pp542-555 (1983).

[110].Thomas.P. The use of fluoropolymers for non-stick cooking utensils. Surface Coatings Internatiional 1998(12)

[111].Herber J.,Reucker K.J. New non-stick coatings for culinary utensils. Surface Coatings International Part B:Coatings Transactions Vol 84,B1,1-90,January 2001

[112].Waite J.H., Reverse engineering of bioadhesion in marine mussels. Ann N Y Acad Sci. 1999 Jun 18;875:301-9.

[113].Autumn.K. Evidence for van der Waals attachment by Gecko foot hairs inspires design of synthetic adhesive. Nature 2002

[114].Autumn.K. Adhesive force of a single gecko foot hair. Nature Vol 405,pp681-685, June 8 ,2000

[115].Beier R. E, Meyer A. E and King R. W. Canadian J.Chem.Eng.66,55-62,1988.

[116].Bonafede S.F and Brady R F Jr Compositional Effects on the Fouling Resistance of Fluorourethane Coatings. Surface Coatings International 4, p181-185 (1998)

[117].Andrade J.D, Hlady V and Jeon S. I Hydrophillic Polymers (Ed Glass JE).Advances in Chemistry Series 248, Washington:American Chemical Society,51-59,1996.

[118].Brady R..F.Jr., In search of non-stick coatings .Chemistry & Industry 17th March 1997, pp219-222.

[119].Owen M..J. Surface Properties of Silicone Release Coatings. Surface Coatings International. (9) 1996 pp 400-405

[120].Ho,T., Wynne K.J.,Nissan.R.A., Macromolecules,26,7029,1993.

[121]. Bey. A.E. New Developments in Silicone Release Coatings for Pressure-Sensitive Adhesives. Adhesives Age,October 1972

[122].Gordon D.J. and Colquhoun. J.A. Surface Properties of Silicone Release Coatings.Adhesives Age, June 1976.

[123] Packham D.E. Work of adhesion:contact angles and contact mechanics .Int.J.Adhesion and Adhesives 16 (1996),121-128.

[124].Johnson K.L., Kendall K.and Roberts A.D. Proc.Roy.Soc.1971,A324,301

[125].Harkins.W.D. J.Chem.Physics,9,552,1941

[126].Andrews E.H.and Kinloch. A. J.Proc.Roy.Soc.1973,A332,385

[127].Meyer, H. Masonry Protection with Silanes,Siloxanes and Silicone Resins. Surface Coatings International 1998 (2)

[128].Meyer H., The chemistry and properties of silicone resins. Surface Coatings International (2), p77-83 (1999).

[129] Pocius A.V., Adhesion and Adhesives Technology 2nd Edn Hanser 2002

[130].Packham D.E., in Adhesion Aspects of Polymeric Coatings, Mittal K.L., (Ed),(1983),Plenum Press, New York.

[131].Schonhorn H., Frish H.L.and Kwei T.K. J.Appl.Phys.37,(1966) p4967.

[132].Newman S. J.Colloid.Inferace Sci.26,(1968),p209

[133].Kojio K., Takahara A., & Kajiyama T. Aggregation Structure and Surface Properties of Immobilized Fluoroalkylsilanes and their mixed monolayers in Fluorinated Surfaces, Coatings and Films. ACS Symposium Series 787 editered by Castner D.G. & Grainger D.W. American Chemical Society.200

[134].Sugimura H, Ushivama K, Hozumi A, Takai O. Lateral force on fluoroalkylsilane self assembled monolayers dependent on molecular ordering.J.Vac.Sci Technol B.Microelectronic Nanometer Struct. Vol 20,No1, pp393-395.2002

[135] Pittman A G, Wasley W L, Roitman J N. Fluorosiloxane copolymers as soil release agents. Textile Chemist and Colourist;4, No.12,Dec 1972, p278-82

[136].Narita M, Kasuga T, Kivotani A. Super water repellent aluminium by electrolytic etching and chemical adsorption. Journal of Japan Institute of Light Metals 50,(11),p594-597,Nov 2000

[137].Mayer T.M, de Boer M.P , Shin N.D , Clewis P.J & Michalske T.A. Chemical vapor deposition of fluoroalkylsilane monolayer films for adhesion control in microelectromechanical systems. J.Vac.Sci.Technology.B 18(5), Sep/Oct 2000.

[138].Burns A.R. et al. Molecular Level Friction As Revealed with a Novel Scanning Probe.. Langmuir 1999, 15, 2922 – 2930

[139].Tadanaga,T *et al.* Superhydrophobic-Superhydrophillic Micropatterning on Flowerlike Alumina Coating Film by the Sol-Gel Methods .Chemistry of Materials 12,590-592(2000).

[140].Shanahan M.E.R. *et al* . Fluoroalkylsilanes as non-stick coatings: adhesion of glucose and its thermal byproducts. International Journal of Adhesion and Adhesives 18 (1998) 273 – 281

[141].Shanahan M.E.R *et al* . Use of fluoroalkylsilanes as non-stick coatings for thermal by-products of linoleic acid. International Journal of Adhesion & Adhesives 20 (2000) 257-261

[142] Ikeda K., Okuno M., Yukawa A., Kakuda.K and Yamaguchi K. Evaluation of mould fouling with fine particles of polytetrafluoroethylene included in nickel or chromium coatings. International Polymer Science and Technology, Vol 20,No6,1993.

[143]. Feldstein M.D. Composite Electroless Nickel Coatings For The Aerospace & Airline Industries. Plating And Surface Finishing 85(11), page248 (Nov1998)

[144].Metzger W. Galvanotechnik 63(8) page 722 (1972)

[145].Simmons M. Zinc based composite coatings as an alternative to electrodeposited cadmium. PhD Thesis 2002.Loughborough University.

[146].Ebdon P. R. Electroless Nickel/PTFE Composites – The Niflor Process International Journal of Vehicle Design 6(4/5) page466(1985)

[147] Stevens K. Non-stick coatings are a better option for mould release. British Plastics and Rubber. 2002 Pt Nov pp38.

[148].Percell K.S., Tomlinson H.H., Walp L.E. Non-metallic Fatty Acids as Internal Mould Release Agents in Polymers .ANTEC'87,45th Annual Conference, Society of Plastic Engineers, Los Angeles,USA,4th-7th May 1987,pp1289-1293

[149].Wilkomm W.R., Jennings R.M., Macosko C.W. Quantitative Evaluation of Internal Mould Release Agents for Polyurea RIM by Measurement of Release Forces'.Plastics, Rubber and Composites Processing and Applications Vol 19,1993,pp69-76

[150].Clayfield T.E. and Berry J.P. Measurement of Adhesion to External Semi-Permanent Mould Release Agents Using The Tapered Double Cantilever Beam. Adhesion 87' 3rd International Conference, York Vol 9 A/1-A/5. 1987

[151].Dannenburg.H. Measurement of adhesion by a blister method . J.App.Polymer Sci.5 (1961) p125

[152.Parry T.V. and Wronski. A.S. A technique for measurement of adhesive fracture energy by the blister method J.Adhesion.1992 Vol 37 p251 –260

[153].Kinloch.A.J and Fernando.M. Use of the inverted blister test to study adhesion of photopolymers Int.J.Adhesion & Adhesives Vol 10.No2 April 1990.

[154].de Laat.Ir A.L.M., Bancken E.L.J. Advanced Adhesion Measurements: A new instrumental development for the quantitative evaluation of coatings. 5th Nuremberg Congress:Creative Advances in Coatings Technology 12-14th April 1999.

[155].Bennet S.J., DeVries K.L. and Williams M.L. Int.J.Fract.10,33 (1974)

[156].Briscoe B.J and Panesar S.S. The application of the blister test to all elastomeric adhesive. Proc.R.Soc.London Ser A (1991) 433,23-43

[157].Briscoe B.J.and Panesar S.S. The adhesion of poly(urethane) to rough countersurfaces: the influence of weak boundary layers. J.Adhesion Sci.Technol.Vol 8.No.12.pp 1485 – 1504 (1994)

[158].Shields K.S., Beck R., Scott M., Shook A.. The Evaluation of Release Agents Using a New Test Method.151st ACS Rubber Division Meeting.Spring.Anaheim,CA, 6th-9th May 1997.Paper 91, pp14.012

[159].Feast W.J, Munro H.S, Richards R.W. Polymer Surfaces and Interfaces II. Wiley 1993

[160].Sheiko S. New Developments in Polymer Analytics II Edited by Schmidt. M. Springer-Verlag 2000.

[161].Johnson K.L, Kendall K., Roberts A.D. Proc.R.Soc.London,Ser A 1971,324,301

[162]. Rochow, T. and Tucker, P. Interference microscopy., in Introduction to Microscopy by Means of Light, Electrons, X Rays, or Acoustics, Plenum Press, New York, pages 221-231 (1994).

[163]. Richards, O. An introduction to the theory of interference microscopy., in Introduction to Quantitative Cytochemistry, Wied, G. (ed), Academic Press, New York, pages 43-61 (1966).

[164]. Francon, M. Interference microscopy in transmitted light., in Progress in Microscopy, Row, Peterson, and Company, New York, pages 94-128 (1961).

[165].Riedling K. Ellipsometry for Industrial Applications. Springer-Verlag Wien. New York.1988

[166].Tompkins H.G. A User's Guide to Ellipsometry. Academic Press.San Diego.1993.

[167].Press.W.H., Flannery B.P., Teukolsky S.A., Vetterling W.T. Numerical Recipes. Cambridge University Press (1986)

[168]. Briggs D. and.Seah M.P (editors). Practical Surface Analysis Volume 1 Auger and X-ray Photoelectron Spectroscopy .2nd Edition.Wiley.1990

[169].Tanuma,S., Powell,C.J, ;Penn,D.R. Surf.Interface Anal.1994,21,165.

[170] XPS Handbook. Physical Electronics

[171] (1980).Fowkes.F.W., McCarthy D.C., Mostafa.M.A., J.Colloid Interface Sci.78,200.

[172].T.Young, Phil.Trans.Roy.Soc(London),95:65(1805)

[173].Comyn J. Adhesion Science. Royal Society of Chemistry.1997.

[174].Rance. D.G., Thermodynamic Approach to Adhesion Problems in Industrial Adhesion Problems Edited by Brewis.D.M. and Briggs.D. Orbital Press.1985.

[175].Shanahan M.E.R. Surface characterisation by contact angles – polymers, in Handbook of Adhesion Edited by Packham D.E. Polymer Science & Technology Series.Longman.1992

[176].Dupre A., Theorie Mechanique de la Chaleur, Gauthier-Villars (1869) Paris, p369

[177].Fox H.W. & Zisman W.A. J.Coll.Sci 5 (1950) 514

[178].Fowkes F.M. J.Phys.Chem 66 (1962) 382

[179].Owens D.K. & Wendt R.C. J.App.Polym.Sci 13 (1969) 1741.Also Kaelble, D.H. J.Adhesion 1970,2,50.

[180].Kwok, D.Y., Neumann, A.W. Adv.Colloid Interface Sci.1999,81,176.

[181].Wu,S. Polymer Interface and Adhesion Marcel Dekker: New York,1982.

[182].Good R.J., van Oss C.J. Modern Approaches to Wettability Edited by Schrader M.E. and Loeb G I. Plenum Press 1992.

[183] Socrates.G. Infrared Characteristic Group Frequencies, Tables and Charts. 2nd Edn. Wiley 1994.

[184] Chalmers J.M. and Dent G. Industrial Analysis with Vibrational Spectroscopy. RSC Spectroscopy Monograph.1997

[185] Turi.E.A. (Editor). Thermal Characterisation of Polymeric Materials.Volume 2. Academic Press.1997.

[186].Van Ooij W.J. The potential of organofunctional silane as chromate replacements on aluminium alloys SINTEF Seminar on Chromium free Pretreatments, Holmenkollen,Norway,March 18-19,2002.

[187] Fowkes. F.M. Attractive Forces at Interfaces. Ind.Eng.Chem. Vol 56, no.12 December 1964 pp 40-52

[188]. Tabor.D The Hardness of Metals. Oxford University Press 1951, page 112.

[189].Rabinowicz E . Friction and Wear of Materials 1st Edn. 1965 John Wiley

[190].Gobernado-Mitre.I , Prieto A. C., Zafiropulos V., Spetsidou Y., and C. Fotakis C., On-line monitoring of Laser cleaning of limestone by Laser induced breakdown spectroscopy, Applied Spectroscopy 51, 1125-1129 ,1997

[191]. Laser cleaning of paper and parchment (LACLEPA) , EUREKA project (1999-2001)

[192].Non-intrusive Laser Measurement Techniques for Diagnostics of the State of Conservation of Frescoes, Paintings and Wooden Icons , E.U. Standards, Measurements & Testing (SMT) Programme (1996-1999)

[193] Eaton.P, Smith J.R., Graham.P, Smart.J.D, Nevell T.G., Tsibouklis J. Adhesion Force Mapping of Polymer Surfaces: Factors Influencing Force of Adhesion. Langmuir 2002,18,pp 3387-3389.

[194] Dagnall.H. Exploring Surface Texture. Published Rank Taylor Hobson 1986.

[195] Hecht.J. Understanding Lasers.IEEE Press 2nd Edn 1990

[196}Kriegsmann H. Advances in Molecular Spectroscopy:Proceedindings of the IVth International Meeting on Molecular Spectroscopy,Bologna and Rome, Italy,1962;p 1000-1014.

[197] Belamy,L.J. The Infrared Spectra of Complex Molecules, 2nd ed.,John Wiley.1958.

[198] Briggs.D. Surface Interface Anal. 5,113,(1983).

[199] Dow Corning Technical Bulletin 1999. Silicone Chemistry: Polydimethylsiloxane.

[200] Ready.J.F. Effects of High-Power Laser Radiation.Academic Press 1971

[201] Hatakeyama.T., Quinn F.X. Thermal Analysis. Wiley 1994.

[202] Van Zeghbroeck.B., The Ellipsometer. University of Colorado.1997

[203] Southworth H.N., Introduction to Modern Microscopy. Wykeham Science Series. 1975.

[204] Mathieson. I. PhD Thesis Loughborough University 1995.

[205] Goodhew P.J. Electron Microscopy and Analysis. Wykeham Science Series. 1975.

[206] Zettlemoyer A.C. Hydrophobic Surfaces .Journal of Colloid anfd Interface Science, Vol. 28, No.3/4, November-December 1968, p343.

[207] Wu. S. Interfacial and Surface Tensions of Polymers. Journal of Macromolecular Science .Part C 10, 1, 1974.